



UNIVERSIDADE DE BRASÍLIA
INSTITUTO DE GEOCIÊNCIAS

BALANÇO ESPAÇO-TEMPORAL DO CICLO DOS
ISÓTOPOS DE Fe NO MATERIAL EM SUSPENSÃO DE
ÁGUAS DA BACIA INTERTROPICAL DO RIO
AMAZONAS E DE SEUS AFLUENTES

Giana Márcia dos Santos Pinheiro

TESE DE DOUTORADO NÚMERO 110,
APRESENTADA AO INSTITUTO DE
GEOCIÊNCIAS DA UNIVERSIDADE DE
BRASÍLIA PARA OBTENÇÃO DO TÍTULO
DE DOUTOR EM GEOLOGIA, NA ÁREA DE
GEOLOGIA REGIONAL

ESTE EXEMPLAR CORRESPONDE
À VERSÃO FINAL DA TESE, DEFENDIDA
PELA ALUNA E ORIENTADA PELOS
PROF. DR. MÁRCIO MARTINS PIMENTEL
(BRASIL) E DR. FRANCK POITRASSON (FRANÇA)

TESE DE DOUTORADO

Nº 110

Giana Márcia dos Santos Pinheiro

**BALANÇO ESPAÇO-TEMPORAL DO CICLO DOS ISÓTOPOS DE Fe
NO MATERIAL EM SUSPENSÃO DE ÁGUAS DA BACIA
INTERTROPICAL DO RIO AMAZONAS E DE SEUS AFLUENTES**

Orientador: Prof. Dr. Márcio Martins Pimentel

Co-Orientador: Dr. Franck Poitrasson

Banca Examinadora

Prof. Dr. Márcio Martins Pimentel (Orientador, presidente)

Prof. Dr. Ari Roisenberg (relator, UFRGS, Brasil)

Prof. Dr. José Elói Guimarães Campos (UnB, Brasil)

Prof. Dr. David Labat (Universidade de Toulouse III - UPS, França)

Prof. Dr. Thierry Allard (relator, Universidade de Paris 6, França)

Relatores (exigência da Universidade Paul Sabatier, Toulouse III, França)

Prof. Dr. Thierry Allard (Universidade de Paris 6, França)

Prof. Dr. Ari Roisenberg (URFGS, Brasil)

Brasília, Março de 2013

AGRADECIMENTOS

Aos meus orientadores, Franck Xavier Alain Poitrasson (França) e Márcio Martins Pimentel (Brasil), pela enorme liberdade que me foi concedida durante o período de desenvolvimento deste Doutorado. Aprendi duras e importantes lições, principal e especialmente em relação à conduta humana, que só vocês poderiam ter lecionado e que com certeza vou levar para toda a vida.

Ao Conselho Nacional de Desenvolvimento Científico e Tecnológico (CNPq), por minha bolsa brasileira; à Coordenação de Aperfeiçoamento de Pessoal de Nível Superior / Comité Français d'Évaluation de la Coopération Universitaire et Scientifique avec le Brésil (CAPES-COFECUB), por minha bolsa enquanto estive na França; à Agencia Nacional de Águas (ANA) e à Companhia de Pesquisa de Recursos Minerais (CPRM), pela logística das viagens de campo; Ao Instituto de Geociências da Universidade de Brasília (IG-UnB), Institut de Recherche pour le Développement (IRD) e Centre National de la Recherche Scientifique (CNRS), pelo apoio em viagens para participação em eventos e congressos. Ao projeto ORE-HYBAm (Observatoire de Recherche en Environnement - Contrôles géodynamique, hydrologique, climatologique et biogéochimique de l'érosion/altération et des transferts de matière dans le bassin de l'Amazone), pelas amostras cedidas para meu trabalho. Aos laboratórios de geocronologia e geoquímica da Universidade de Brasília (UnB) e Géosciences Environnement Toulouse (GET, França), pela oportunidade de analisar minhas amostras.

Aos técnicos que me ajudaram com os equipamentos que utilizei para fazer diversas análises nos laboratórios mencionados, da UnB e do GET : Alain Plenecassagne, Bárbara Lima, Fernando Souza Cavalcante, Myller Sousa, Rafael Grudka Barroso (Brasil); Aurélie Lanzanova, Carole Caussérand, Christelle Lagane, Damien Guillaume, Jérôme Chmeleff, Jonathan Prunier, Manuel Henry, Michel Thibaut, Philippe Besson, Stéphanie Mounic, Thierry Aigouy (França).

Aos funcionários e técnicos do IG e da Geocronologia da UnB, supercompetentes, que estão presentes em minha vida há vários anos (ou não!) e que me ajudaram com as burocracias do nosso Brasil de hoje e sempre: Alice Maria Falquetto, Dione Moreira de Souza, Jaqueline Oliveira Rodrigues, Maristela Menezes de Araújo, Ricardo Lívio Santos Marques, Rômulo Franco de Melo e, apesar de eu não ter descrito nenhuma lâmina neste trabalho, às queridas da laminação do IG-UnB, Adalgisa Ferreira dos Santos e Francisca das Chagas Morais, pela eterna simpatia.

Aos membros de meu comitê de acompanhamento, que também foram membros em minha qualificação: Lucieth Cruz Vieira e Bernhard Bühn. À Geraldo Boaventura e Patrick Seyler pelo apoio. Aos membros de minha banca de defesa, Ari Roisenberg (UFRGS), Thierry Allard (Université de Paris 6), David Labat (Université de Toulouse III), pelo tempo dispensado na leitura de meu trabalho e pelas idéias e comentários. Muito grata!

Aos colegas franceses do laboratório de Toulouse, que conheci tanto em Brasília – antes de partir para meu estágio no GET – quanto por lá mesmo: Alisson Akerman, Guillaume Tessier, Jean-Sebastien Moquet, Mathieu Benoît, Sophie Demoy, Tristan Rousseau. Aos brasileiros que estiveram em Toulouse na mesma época que eu, Daniel Santos e Rodrigo Paiva. Todas as pessoas mencionadas neste parágrafo me ensinaram que nem sempre seres humanos são o que parecem ser, outra lição que pretendo levar por toda a vida.

Aos colegas de diversas nacionalidades que também estavam fazendo seus estudos em Toulouse, e que fizeram grande diferença na vida diária por lá: Gérman Velásquez (Venezuela),

Joaquín Cortéz (Chile), Olga Drozdova e Svetlana Ilina (Rússia). Aos queridíssimos e sorridentes vietnamitas, Cam Chi Nguyen, Thi Nguyet Minh Nguyen (as meninas!) e Anh Tuan Nguyen, Van Bai Nguyen (os meninos!). Ainda, aos temporários Ana Pantano (Argentina) e Chaima Djebbi (Tunísia).

À francesa mais querida, competente e preocupada com o próximo (além de gentil e bem humorada!) que conheci na Universidade de Toulouse: Catherine Stasiulis. Grata por toda a ajuda (e foi muita!), pela paciência, pela sabedoria, pelo apoio... sem palavras para te descrever, você é incrível!!!

À pessoa mais linda que conheci no laboratório de Toulouse, Rawaa Ammar (Libano!). Se não fosse por você, Rawaa, e por seus amigos que não tive a oportunidade de conhecer pessoalmente (Ahmad Sharanek e Elaine El Hayek, também libaneses), tudo seria muito diferente e mais complicado para mim. Muito grata pela sua companhia diária (enquanto estivemos juntas por lá!), Rawaa!

Aos meus amigos franceses (os “de rocha”!) que fizeram toda a diferença em minha vida em Toulouse, em inúmeros sentidos: Elodie Sammut, Frédéric Satgé, Laure Joaquim, Mathieu Tecles e companhia ltda..! Obrigada por terem existido no mesmo tempo-espacô, cada instante com vocês foi precioso e renovador!

Aos companheiros nas viagens pelos rios amazônicos (são muitos, da UnB, da ANA, do IRD, da UFAM, da CPRM...): Ana Strava, André Santos, Alessandro Ferreira Silva, Cristina Arantes Miranda, Dhalton Tosetto Ventura, Eldis Camargo, Elisa Armijos, Eurides de Oliveira, Gwenaël Abril, Jean-Michel Martinez, Jean-Michel Mortillaro, João Bosco Alfenas, Jorge Carranza, Marie-Paule Bonnet, Matheus Marinho de Faria, Maurrem Ramon Vieira, Pauliane Sampaio, Raimundo Glauber Lima Cunha (muitas risadas!), Stéphane Calmant, Rubens Kenup, Taise Bresolin, Valdemar Santos Guimarães... Daqui em diante, perdoem-me, não sei os sobrenomes (só alguns apelidos!), mas e espero que valha a lembrança: Aos capitães dos barcos (Franciney, Eraldo, Zé), aos ajudantes da tripulação (Aldair – Baixinho, Antunes, Gilberto - Nil!, Gleison - Cojac, Jackson - Branco, João e sua voadeira!) e às cozinheiras das missões, Giolaine - Laine, Heloísa, Viula Macedo – Loirinha. A presença de cada um de vocês, entre outros que porventura não estão citados aqui, fez com que a Amazônia fosse ainda mais encantadora do que já é!

À Francis Sondag, que me ajudou em muitos cálculos de química quando da preparação de amostras para análises. À duas pessoas em especial, que sempre arranjaram tempo e disposição, onde quer que estivessem, para me “socorrer” com o que quer que fosse relacionado à Tese: Gérard Cochonneau e Paulo Henrique Junker Menezes (Doutor & Professor, parabéns, amigo!). Muito grata mesmo, vocês também me dão esperanças de que existem pessoas muito do bem e sensíveis ao próximo neste mundo!

A todos os professores do IG que contribuíram para minha formação, sem exceção. Entre eles, Catarina Labouré Benfica Toledo, Tati Almeida e José Oswaldo de Araújo Filho, pelo apoio, pelas conversas e pelos cafés tão necessários em vários momentos. Agradeço em especial aos professores que mais admiro desde o primeiro contato, ainda na graduação (e que continuam sendo muito admirados até hoje!): José Elói Guimarães Campos (também ilustre membro de minha banca de defesa!) e Nilson Francisquini Botelho (membro de minha qualificação). Vocês são um grande exemplo e a esperança para o ensino universitário no nosso Brasil brasileiro. Obrigada por mostrarem todos os dias, sem pretensões, a inúmeros alunos e pessoas que passam pela UnB que, quando uma pessoa gosta do que faz, ela faz muito mais bem feito. Grata pelas ajudas, pela compreensão e pelos ensinamentos, desde 2000 (!) até hoje, 2013, ano em que encerro minha carreira acadêmica (ao menos por um bom tempo!).

Aos meus amigos da vida, que espero estejam comigo mais muitos e muitos anos: Ana Gabriela Pulchério de Medeiros Campos, Daniela & Letícia Cureau (e obviamente, à toda a linda família Cureau!), Fabiana Soares, Felipe Liparelli Tironi, Felipe Silverwood-Cope, Fernanda Iglesias, Fernanda Miziara, Getúlio Brasil, Jussara Costa e Sinara Bertholdo de Andrade.

Aos amigos sempre presentes, ainda que por vezes fisicamente distantes, da Geologia (e igualmente da vida!): André Sabóia (Dardenninho), Dângelo Victor Gonçalves Silva, Fabiana de Souza Pereira, Federico Cuadros, Josineuza Brilhante, Lara Nigro, Lindaray Sousa da Costa, Liz Matos Cunha, Marcos Alberto Vasconcelos, Marcos Flávio Nogueira Chiarini, Murilo Bastos, Tiago Rabelo, Rafaela Andraus Portugal, Ricardo Carlos de Oliveira (Mestre) e Stella Bijos Guimarães.

E por último, salvo os mais importantes, sinceros e necessários agradecimentos, às duas pessoas mais extraordinárias e admiráveis de meu mundo (meus verdadeiros e inigualáveis amores, para todo o sempre!): Celeida Márcia dos Santos (minha maínha linda!) e Tiago Eli de Lima Passos (meu marido maravilhoso!). Sem vocês ao meu lado, eu não teria terminado doutorado nenhum, muito menos este. E minha vida seria tão desinteressante quanto a vida de várias das pessoas que, nesta fase, cruzaram meu caminho... como disse meu poeta preferido, Mário Quintana, “eles passarão, eu passarinho!”

Obrigada UNIVERSO, uma vez mais, pela fluidez de sempre!

Zahlreich sind die Lehrkanzeln, aber selten die weisen und edlen Lehrer. Zahlreich und groß sind die Hörsäle, doch wenig zahlreich die jungen Menschen, die ehrlich nach Wahrheit und Gerechtigkeit dürsten. Zahlreich spendet die Natur ihre Dutzendware, aber das Feinere erzeugt sie selten.

Albert Einstein, 1953.

*Mein Weltbild: Von der Freiheit der
Lehre*

Para Celeida Márcia e Tiago Eli

SUMÁRIO

SUMÁRIO	I
LISTA DE FIGURAS	V
LISTA DE TABELAS	VIII
LISTA DE ABREVIACÕES.....	IX
EXTENDED ABSTRACT.....	1
RÉSUMÉ ÉTENDU.....	4
RESUMO EXPANDIDO.....	7
APRESENTAÇÃO	
1. ABORDAGEM	10
2. ESTRUTURA DA TESE.....	10
CAPÍTULO UM	
INTRODUÇÃO GERAL.....	13
1. ABORDAGEM	13
2. OBJETIVOS.....	16
3. MÉTODOS	16
CAPÍTULO DOIS	
THE AMAZON BASIN AND THE DISTRIBUTION OF IRON	18
1. INTRODUCTION	18
2. SOURCES OF IRON IN RIVERS	19
3. THE AMAZON BASIN AND ITS RIVERS	20
4. IRON IN SUSPENDED MATTER AT THE AMAZON BASIN	23
5. FINAL REMARKS ON THE STUDY AREA AND THE SCOPE OF THIS THESIS	24
CAPÍTULO TRÊS	
IRON ISOTOPES – A REVIEW.....	26
1. INTRODUCTION	26
2. DATA PRESENTATION	27
3. AVAILABLE DATA ON THE VARIABILITY AND IRON ISOTOPE FRACTIONATION OF NATURAL MATERIALS	28
3.1 High Temperature Processes.....	29
3.1.1 Extraterrestrial Materials.....	29
3.1.2 Terrestrial Igneous Rocks	30
3.1.2.1 Inter-mineral fractionation	33
3.2 Low Temperature Processes.....	34
3.2.1 Soil and Aqueous Systems.....	35
3.2.2 Porewaters, Oceans and Rivers	37
3.2.2.1 Dissolved and Particulate Matter in Rivers	39
4. PANORAMA AND PERSPECTIVES	41

CAPÍTULO QUATRO

ANALITICAL METHODS FOR IRON ISOTOPIC DATA ACQUISITION	43
1. INTRODUCTION	43
2. MULTI-COLLECTOR INDUCTIVELY COUPLED PLASMA MASS SPECTROMETER (MC-ICP-MS)	44
3. POSSIBLE CAUSES FOR FRACTIONATIONS IN THE LABORATORY	48
4. MOST COMMON CORRECTION METHODS: A REVIEW	50
<i>4.1 Standard bracketing methods</i>	<i>50</i>
<i>4.2 Ni doping technique.....</i>	<i>51</i>
<i>4.3 Reproducibility issues.....</i>	<i>51</i>
<i>4.4 Correction of the non-mass dependent instrumental bias in static mode.....</i>	<i>52</i>
5. FINAL CONSIDERATIONS	52

CAPÍTULO CINCO

IRON ISOTOPE COMPOSITION OF THE SUSPENDED MATTER ALONG DEPTH AND LATERAL PROFILES IN THE AMAZON RIVER AND ITS TRIBUTARIES.....	54
---	-----------

ABSTRACT.....	54
1. INTRODUCTION	55
2. STUDY AREA, SAMPLING AND METHODS	57
<i>2.1 Study area</i>	<i>57</i>
<i>2.2 Sampling</i>	<i>58</i>
<i>2.2.1 Depth Profiles (DP).....</i>	<i>58</i>
<i>2.2.2 Lateral Profiles (LP).....</i>	<i>59</i>
<i>2.3 Methods.....</i>	<i>60</i>
<i>2.3.1 Sample collection and preparation.....</i>	<i>60</i>
<i>2.3.2 Sample dissolution and iron purification</i>	<i>60</i>
<i>2.3.3 Iron isotope analyses by mass spectrometry</i>	<i>62</i>
3. RESULTS	63
<i>3.1 Environmental parameters</i>	<i>63</i>
<i>3.1.1 Depth profiles.....</i>	<i>63</i>
<i>3.1.2 Lateral profiles</i>	<i>64</i>
<i>3.2 Comparison between the suspended matter of the rivers studied.....</i>	<i>65</i>
<i>3.3 Iron content and isotope composition of suspended matter in the Amazon River and its tributaries</i>	<i>67</i>
4. DISCUSSION	70
5. CONCLUSIONS	72

ACKNOWLEDGEMENTS.....	73
------------------------------	-----------

CAPÍTULO SEIS

PRELIMINARY IRON ISOTOPIC DATA ON SUSPENDED AND DISSOLVED MATERIAL FROM DISTINCT WATER NATURES IN THE PERUVIAN AND BRAZILIAN AMAZON.....	78
---	-----------

1. INTRODUCTION	78
2. METHODS	78
3. RESULTS	79

3.1 Suspended Matter from White, Black and Clear water rivers.....	79
3.2 Suspended Matter from Várzeas.....	81
3.3 Negro River Dissolved Fraction.....	82
4. BRIEF DISCUSSION ON THE PRELIMINARY DATA.....	82
5. CONCLUDING REMARKS.....	83
CAPÍTULO SETE	
CONTRASTED TEMPORAL IRON ISOTOPIC EVOLUTION OF THE SUSPENDED MATTER FROM THE AMAZON AND NEGRO RIVERS.....	87
1. INTRODUCTION	88
2. STUDY AREA AND SAMPLE COLLECTION	90
3. ANALYTICAL METHODS	92
3.1 Sample collection and preparation.....	92
3.2 Sample dissolution and iron purification	93
3.3 Iron isotope analyses by Mass Spectrometry.....	94
4. RESULTS	95
4.1 Characterization of mineral phases and environmental parameters	95
4.2 Iron Isotopes	99
5. DISCUSSION	101
5.1 Comparison to previous $\delta^{57}\text{Fe}$ data on the Amazonian rivers	101
5.2 Possible sources of iron in the Negro River Basin.....	103
5.3 The role of weathering and organic substances on the transport of iron	104
5.4 Seasonal variations and comparison of suspended matter iron isotopic compositions in boreal, temperate and tropical regions	105
ACKNOWLEDGEMENTS.....	108
CAPÍTULO OITO	
CONCLUSÕES GERAIS.....	113
HOMOGENEIDADE DE PERFIS EM PROFUNDIDADE E LATERAIS.....	114
VARIABILIDADES TEMPORAIS CONTRASTADAS	115
INFLUÊNCIA DA NATUREZA DA ÁGUA	116
FONTES DE FERRO PARA OS RIOS AMAZÔNICOS	118
CAPÍTULO NOVE	
PERSPECTIVAS	121
CAPÍTULO DEZ	
REFERÊNCIAS	123
MATERIAL ONLINE	136
ANEXOS	137
Parâmetros físico-químicos e localização de amostras não analisadas coletadas na região amazônica.....	138
Protocolos para tratamento e análise de amostras – Laboratório de Geocronologia – UnB	141
LIMPEZA DE SAVILEX	142

LIMPEZA DE TUBOS DE CENTRÍFUGA.....	142
ABERTURA DOS FILTROS DE MATERIAL EM SUSPENSÃO OU MATERIAL DISSOLVIDO	143
PURIFICAÇÃO DE FERRO EM COLUNAS CROMATOGRÁFICAS	144
LIMPEZA DAS COLUNAS APÓS SUA UTILIZAÇÃO PARA PURIFICAÇÃO DE FERRO	145
MATRIZ DAS AMOSTRAS PARA LEITURA NO MC-ICP-MS	145
MATRIZ DE FILTROS DE MATERIAL EM SUSPENSÃO:	145
MATRIZ DE MATERIAL EM SUSPENSÃO:	145
MATRIZ DE BRANCOS DE LABORATÓRIO E BRANCOS DE CAMPO:.....	145
Lista de Comunicações, Artigos Submetidos e Publicados	146

LISTA DE FIGURAS

Fig. 1 – Variações na composição isotópica de ferro no período de um ano no Rio Kalix, Suíça (Ingrı et al., 2006). _____ 14

Fig. 2 – Contrastes nas variações da composição isotópica de ferro em diferentes tipos de solo (Poitrasson et al., 2008). _____ 15

Fig. 3 – Estações da rede HYBAm na Bacia Amazônica (www.ore-hybam.org). _____ 17

Fig. 4 – Sketch map of the Amazon Basin and its main tributaries, showing sample locations. _____ 22

Fig. 5 - The Fe isotopes. Relative abundances are recommended average values from IUPAC (Taylor et al., 1992). _____ 26

Fig. 6 - Fe isotope compositions of mantle minerals, xenoliths, and basalts (from Zhao et al., 2009). The solid and dashed lines give the weighted mean of all the available data for mantle xenoliths and basalts, respectively. The gray bands represent 2 standard error uncertainties of the representative mean mantle xenoliths and basalts. Data from Zhu et al. (2002); Rouxel et al. (2003); Beard et al. (2003b); Poitrasson et al. (2004); Williams et al., (2004); Beard and Johnson (2004a); Williams et al. (2005); Weyer et al. (2005); Schoenberg and von Blanckenburg (2006); Weyer and Ionov (2007); Teng et al. (2008); Schuessler et al. (2009); Zhao et al. (2009). Ol olivine; Opx orthopyroxene; Cpx clinopyroxene; Sp spinel; Amp amphibole; Phl phlogopite; Sp Lher Sp Lherzolite. The horizontal dashed and solid lines with gray bands represent the weighted average values and two standard deviation of mantle xenoliths and basalts, respectively. Data from Beard et al. (2003b); Beard and Johnson (2004a) are recalculated to a common Fe isotope composition for the IRMM-014 standard through $\delta^{57}\text{Fe}_{\text{IRMM-014}} = \delta^{57}\text{Fe}_{\text{igneous rocks}} + 0.11$. Data from Weyer et al. (2005); Weyer and Ionov (2007) are recalculated to $\delta^{57}\text{Fe}$ through $\delta^{57}\text{Fe}_{\text{IRMM-014}} = 1.5 \times \delta^{56}\text{Fe}_{\text{igneous rocks}}$. _____ 31

Fig. 7 - Comparison of $\delta^{56}\text{Fe}$ values for bulk igneous rocks, suspended river loads and individual minerals from volcanic rocks (right panel). Left panel shows the fraction of Fe that exists as oxides (data for igneous rocks arbitrarily plotted as 0.02). Right panel shows $\delta^{56}\text{Fe}$ values for coexisting magnetite, olivine, hornblende and biotite in four volcanic rocks. Data from Canfield (1997); Beard and Johnson (2004a); Beard and Johnson (2004b). _____ 40

Fig. 8 - Efficiency of ionization as described by Saha's law as a function of the ionization potential for a representative electronic density of 1021 m^{-3} . The ionization potentials of some elements for which the isotopic composition is commonly analyzed are shown at the top (from Albarède and Beard, 2004). _____ 45

Fig. 9 - Mass scan performed with the Neptune's "medium resolution" entrance slit and "low resolution collector slits" showing all Fe isotopes and their respective molecular interferences. All Fe signals are normalized to the signal of ^{56}Fe . Since the Fe isotopes have a lower mass, they enter the detector first in a scan and form the left plateau. The center plateau consists of polyatomic interferences added to the Fe isotopes. The right plateau is formed by the polyatomic interferences only. Fe isotope ratios can be measured interference-free on left plateau. The scan was performed on a 1 ppm Fe solution, using the SIS (wet plasma) and standard (H) cones (from Weyer and Schwieters, 2003). _____ 46

Fig. 10 - Fassel type torch that is typically used in MC-ICP-MS. Approximate Ar flow rates for the different plasma gasses are shown and the relative spatial relationships between the intermediate and sample lines relative to the RF-coil where the Ar plasma is generated are shown (from Albarède and Beard, 2004). _____ 46

Fig. 11 - The inductively-coupled plasma source (inspired in Niu and Houk, 1996). The original figure has been modified by Albarède and Beard (2004) to show the electrical potentials, the vacuum cascade (top), and the distribution of ions and neutral (bottom) in an MC-ICP-MS similar to the VG Plasma 54. The zone with incipient voltage

acceleration right behind the skimmer show maximum space-charge effect with the lighter ions being most efficiently driven off by the strong axial current of positive ions (adapted from [Albarède and Beard, 2004](#)). 47

Fig. 12 - Deviations of the $^{56}\text{Fe}/^{54}\text{Fe}$ ratios (right axis) and $^{57}\text{Fe}/^{54}\text{Fe}$ (left axis) in parts per 10.000 of the IRMM-14 Fe standard with respect to an in-house reference solution for a series of 37 runs determined by the standard bracketing technique ([Zhu et al., 2002](#)). A reproducibility of 0.04‰ and 0.06‰ is obtained on each ratio, respectively. 51

Fig. 13 – Map of sample locations. 56

Fig. 14 – SPOT Image showing the collecting strategy for the lateral profile samples at Manacapuru Station. White triangles represent the location of samples collected during the dry season, and white circles, superimposed to white triangles, represent the location of samples collected during the flood season. RM stands for right margin and LM for left margin. 59

Fig. 15 – The mean $\delta^{57}\text{Fe}$ value of individual measurements (black circles) for the Milhas hematite is $0.758 \pm 0.143\text{‰}$ (2SD, N=115), whereas pooled data by groups of 6 (red circles) yield a $\delta^{57}\text{Fe}$ of $0.757 \pm 0.067\text{‰}$ (2SD, N=20). 63

Fig. 16 – Suspended matter concentration in depths profiles - Negro, Madeira, Amazon and Solimões rivers. 66

Fig. 17 – Suspended matter concentration in lateral profiles - Negro and Solimões rivers. 66

Fig. 18 – Iron concentration variations in suspended matter according to depth (measured with MC-ICP-MS). Negro, Madeira, Amazon and Solimões rivers. 68

Fig. 19 – Iron concentration variations in suspended matter according to lateral profiles (measured with MC-ICP-MS). Negro and Solimões rivers. 68

Fig. 20 – $\delta^{57}\text{Fe}$ variations in suspended matter along depth profiles. The average isotopic composition of the continental crust ($\delta^{57}\text{Fe} \sim 0.1 \pm 0.03\text{‰}$; [Poitrasson, 2006](#)) is shown for reference. 69

Fig. 21 – $\delta^{57}\text{Fe}$ variations in suspended matter along lateral profiles in the Negro and Solimões rivers. The average isotopic composition of the continental crust ($\delta^{57}\text{Fe} \sim 0.1 \pm 0.03\text{‰}$; [Poitrasson, 2006](#)) is shown for reference. 69

Fig. 22 – Map of sample locations in the Amazon River Basin. 79

Fig. 23 – $\delta^{57}\text{Fe}$ values from white water rivers in Peru and Brazil. Values in the abscissa represent the average distance (km in straight line) from the collecting station to the Óbidos Station. 80

Fig. 24 – $\delta^{57}\text{Fe}$ values from black, clear and differentiated white water rivers in Brazil. Values in the abscissa represent the average distance (km in straight line) from the collecting station to the Óbidos Station (Amazon River). 81

Fig. 25 – $\delta^{57}\text{Fe}$ variations in dissolved fraction along depth profile. The average isotopic composition of the continental crust ($\delta^{57}\text{Fe} \sim 0.1 \pm 0.03\text{‰}$; [Poitrasson, 2006](#)) is shown for reference. Negro River at Paricatuba Station. 82

Fig. 26 – Map of temporal series samples locations (circles: Negro River at the Serrinha Station and Amazon River at the Óbidos Station). X-Ray Diffraction and Scanning Electron Microscope studies of the suspended matter were performed in the following locations (squares): Negro River at the Paricatuba Station and Amazon River at the Parintins Station. Precipitation data (available from the INMET - National Institute of Meteorology, Brazil, website in the references list): Negro River at the Barcelos Station (square) and Amazon River at the Óbidos Station (circle). 91

Fig. 27 – Average monthly precipitation along the Negro River area (Barcelos Station) and the Amazon River area (Óbidos Station). Both locations are shown in **Fig. 26**. Data downloaded from the Brazilian Institute of Meteorology (INMET, <http://www.inmet.gov.br/portal/index.php?r=bdmep/bdmep>). _____ 96

Fig. 28 – Monthly water discharge, suspended matter concentration and precipitation in the Amazon River (Óbidos Station) during the periods studied. _____ 97

Fig. 29 – Negro River - suspended matter concentration (*20), dissolved organic carbon contents (*10), monthly water discharge (Serrinha Station) and precipitation (Barcelos Station) during the periods studied. _____ 98

Fig. 30 – Iron concentration variations in suspended matter (SPM), measured with MC-ICP-MS, versus suspended matter (SPM) concentration – Amazon River at Óbidos Station (samples from November and December 2009 were taken out of the binary plot) and Negro River at Serrinha Station. _____ 99

Fig. 31 – $\delta^{57}\text{Fe}$ temporal variations in suspended matter (SPM) along time series in the Amazon River at the Óbidos Station. The average isotopic composition of the continental crust ($\delta^{57}\text{Fe} \sim 0.1 \pm 0.03 \text{ ‰}$; Poitrasson, 2006) is shown for reference. _____ 100

Fig. 32 – $\delta^{57}\text{Fe}$ temporal variations in suspended matter (SPM) along time series in the Negro River at the Serrinha Station. The average isotopic composition of the continental crust ($\delta^{57}\text{Fe} \sim 0.1 \pm 0.03 \text{ ‰}$; Poitrasson, 2006) is shown for reference. Additional data added for comparison: SPM Negro River (circle) from Bergquist and Boyle (2006); average (avr) SPM Negro River (Paricatuba Station) from dos Santos Pinheiro et al. (2013), where DP – depth profile; LP – lateral profile). _____ 100

Fig. 33 – Comparison between $\delta^{57}\text{Fe}$ temporal variations in suspended matter along time series in three different rivers: boreal Kalix (Sweden, Ingri et al., 2006), tropical Amazon River at Óbidos and tropical Negro River at Serrinha Station. The average isotopic composition of the continental crust ($\delta^{57}\text{Fe} \sim 0.1 \pm 0.03 \text{ ‰}$; Poitrasson, 2006) is shown for reference. _____ 106

Fig. 34 – Variability on the iron isotopic composition of suspended matter from rivers around the world. Data from Table I. _____ 107

LISTA DE TABELAS

Tabela 1 - Physico-chemical parameters of the Amazonian rivers studied. _____ 74

Tabela 2 - Suspended matter concentrations and their iron isotope compositions $\delta^{57}\text{Fe}_{\text{IRMM-14}}$ for the Negro, Madeira, Amazon and Solimões rivers lateral and depth profiles. _____ 76

Tabela 3 - Physico-chemical parameters, along with suspended matter concentrations and iron isotope compositions $\delta^{57}\text{Fe}_{\text{IRMM-14}}$. Surface samples from Amazonian rivers in Peru and Brazil, Várzeas (Solimões and Juruá rivers) and dissolved matter (Negro River depth profile). _____ 85

Tabela 4 - Physico-chemical parameters, along with suspended matter concentrations and their iron isotope compositions $\delta^{57}\text{Fe}_{\text{IRMM-14}}$ for the Negro and Amazon rivers time series. Additional (non-refined) data on surface suspended matter samples from variable Amazonian waters are also provided. _____ 109

LISTA DE ABREVIACÕES

aq	Aqueous
ADCP	Acoustic Doppler Current Profiler
Ar	argon
avr	average
BIF	Banded Iron Formation
BMOOS	Standard of soft water lake sample from up-state New York, available by the National Water Research Institute, Canada
C	carbon
CAI	Calcium Aluminum Inclusions (meteorites)
<i>cf.</i>	Latin: <i>confer</i> (<i>i.e.</i> , compare)
CNRS	Centre National de la Recherche Scientifique
CO ₂	carbon dioxide
C _(org)	Organic Carbon
CPS	Counts Per Second
DP	Depth Profile
EDS	Energy Dispersive Spectrometry
<i>e.g.</i>	Latin: <i>exempli gratia</i> (<i>i.e.</i> , for instance)
<i>et al.</i>	Latin: <i>et alii</i> (<i>i.e.</i> , and co-workers)
eV	electron volt
Fe	iron
FeOM	Iron bound to organic matter
GET	Laboratoire Géosciences Environnement Toulouse
GGA mode	Global Positioning System Fix Data
GPS	Global Positioning System
H	hydrogen
HED	Howardite-Eucrite-Diogenite meteorite group
HTCO	high temperature catalytic oxidation
HYBAm	HYdrology of the AMazon Basin
<i>i.e.</i>	Latin: <i>id est</i> (<i>i.e.</i> , in other words)
IAB	Island Arc Basalts
ICP-OES (or ICP-AES)	Inductively Coupled Plasma Optical Emission Spectrometry (or Atomic Emission Spectroscopy)
INMET	Instituto Nacional de Meteorologia - Brazil
INSU	Institut National des Sciences de l'Univers - France
IRD	Institut de Recherche pour le Développement - France
IRMM-14	Institute for Reference Materials and Measurements – reference material for iron
km	Kilometers
LP	Lateral Profile
kDa	Kilodaltons
m	meters
MC-ICP-MS	Multi-Collector Inductively Coupled Plasma Mass Spectrometer
meq	milliequivalent
mg	milligram
μg	microgram
ml	milliliter
μm	micrometer
MORB	Mid Ocean Ridge Basalt

MT	Mega Tons
n	number of analyzes
N	nitrogen
ng/g	Nanogram per gram (~ ppb, parts per billion)
NTA-resin	NitriloTriacetic Acid resin
OIB	Ocean Island Basalt
$p\text{CO}_2$	Carbon Dioxide (CO_2) Partial Pressure
PGT	Princeton-Gamma-Tech (part of the Thermo Scientific group)
pH	potential of Hydrogen
ppb	parts per billion
ppm	parts per mil
SD	Standard Deviation
SDD	Silicon Drift Detector
SE	Standard Error
SEM	scanning electron microscope
SIMS	Secondary ion mass spectrometry
SIS	stable introduction system
SNC	Shergottite-Nakhlite-Chassigny meteorite group
SPM	Suspended Matter Content (~ MES)
TIMS	Thermal Ionization Mass Spectrometry
UFAM	Federal University of Amazonas, Manaus, Brazil
UnB	University of Brasília – Brasília, Brazil
UPS	Université Paul Sabatier – Toulouse III, France
wt.%	weight percent

EXTENDED ABSTRACT

DOS SANTOS PINHEIRO, Giana Márcia. **Space and time variations on the iron isotopic composition of water suspended matter from the intertropical Amazon River and its main tributaries.** 163 pp. PhD Thesis (Doctorate in Geology) – Geosciences Institute, University of Brasília (UnB), Brasília, Brazil and Universe, Environment and Space Sciences (SDU2E), Paul Sabatier University (Toulouse III), Toulouse, France.

Suspended matter samples were collected during field campaigns on the Amazon River and three of its main tributaries: the Negro, Solimões and Madeira Rivers. They were investigated for their iron isotope composition in order to verify the possible sources of iron and relate them to different physico-chemical parameters, such as the water pH, the suspended matter content and the percentage of iron in the suspended matter. The samples were collected in different locations and seasons, along depth and lateral profiles. The main objective was to validate the hypothesis that, even though there are a number of processes that can affect the distribution and transport of iron in these rivers, their iron isotopic composition would remain unchanged, unlike other isotopic tracers like Strontium, which have been reported to change according to these parameters (e.g., depth).

Temporal variations in the iron isotopic composition of suspended river loads have already been reported in boreal rivers. Therefore, samples from two temporal series, collected monthly by the observers of the HYdrology of the AMazon Basin (HYBAm) network over at least one year, were also studied. This comprehensive approach, along complete hydrological cycles, intended to search for possible shifts in the iron isotopic signature of suspended matter from intertropical rivers with relation to the seasons, and verify a possible correlation of this parameter with a water level increase / decrease, since related iron sources may be different in these periods.

In situ parameters were measured in the field with a multiparametric probe and water discharge values, water velocity and section profiles were obtained in field campaigns with the Acoustic Doppler Current Profiler (ADCP). These data was used to calculate the sampling steps of depth profiles, which intended to be equally distributed along each river water column.

The laboratory methodology applied included samples dissolution followed by purification of iron by anion exchange chromatography. Concentrations of iron were measured by Inductively Coupled Plasma Optical Emission Spectrometry (ICP-OES) before chromatography, to check for possible iron losses during this procedure. Recoveries were between 80 and 100%, and since iron was collected with 0.05N HCl, iron fractionation during the chromatography step was discarded.

X-ray Diffraction and Scanning Electron Microscopy analyses were performed in some of the samples at the Laboratory *Géosciences Environnement Toulouse* (GET, France), to verify the presence of iron mineral phases that could be related to the iron isotopic signature found. Iron isotopes were measured with a Thermo Finnigan Neptune Multi-Collector Inductive Coupled Plasma Mass Spectrometer (MC-ICP-MS) at both the University of Brasília (UnB) Geochronology Laboratory, Brazil, and the GET (Toulouse, France). Data here presented are reported as $\delta^{57}\text{Fe}$ (in ‰) relative to the international reference material IRMM-14. The performance of the instruments used was assessed by repetitive measurements of an internal standard (hematite from Milhas, Pyrenees, also known as ETH hematite) relative to the IRMM-14. The long-term external reproducibility for the method applied at the University of Brasília was estimated from replicate analyses of this hematite in every session and the results obtained agree with previously published values from several laboratories around the world. International rock standards were also dissolved, purified and analyzed at the Geochronology Laboratory of Brasilia to validate the methodology used, and include the IF-G ($\delta^{57}\text{Fe}_{\text{IRMM-14}} = 0.931 \pm 0.082\text{‰}$), in agreement with previously published values.

Results obtained for the suspended matter of white water rivers, such as the Amazon, Solimões and Madeira, contrast with results observed for the black and clear water rivers analyzed in this work. The first group shows positive homogeneous values according to all the parameters studied, with results that are similar to the calculated mean value for the continental crust ($\delta^{57}\text{Fe}_{\text{IRMM-14}} = 0.1 \pm 0.03\%$). Results for the black / clear water rivers studied, however, are mainly negative and display variable $\delta^{57}\text{Fe}$ through time.

For all the rivers studied, the suspended matter iron isotopic compositions do not display any relation with depth or lateral profiles, in contrast to other parameters, such as Fe concentrations. Also, white water rivers, within analytical uncertainties, keep their isotopic composition constant, even in different seasons, as observed for the Solimões River lateral profiles (Manacapuru Station) collected at two different water stages, and for the Óbidos Station temporal series, over two years (Amazon River). Both sets of samples display homogeneous $\delta^{57}\text{Fe}$ values in either the flood and the dry seasons.

On the other hand, the Negro River is an interesting case to study the variations in iron isotopic composition of suspended matter. Although there are no changes of this parameter along depth and lateral profiles, there are variations during the hydrological cycle. Organic carbon contents vary along the seasons and have an important effect on the active weathering of materials that come from podzols, one of the main sources of iron to the Negro river area. This particular weathering has an influence on the oscillation of the suspended matter iron isotopic signatures along the year. It was also found that precipitation values have an essential role on the supply and transport of iron in this river, also contributing to the distinct iron isotopic compositions observed.

All the results point to a very important distinction related to the transport and nature of river-born suspended material in white and black water rivers: in the white water Solimões, Madeira and Amazon rivers, which have organic-poor neutral waters, little or no fractionation occurs during the transport of iron from clastic sources (rock fragments) to the mainstream of these rivers. Suspended matter is then represented mostly by oxy-hydroxides and silicates, which have a continental crust-like positive $\delta^{57}\text{Fe}$ value. On the other hand, in black water rivers, such as the Negro River, characterized by acidic organic-rich waters, the heavy iron preferentially bounds to organic matter, mostly in the form of colloids, which will be responsible for the heavy iron isotopic composition of the dissolved fraction. The main source of organic matter and reduced iron for the Negro River Basin are podzols that occur in this area. The light iron, probably fractionated during pedogenesis, is associated with the suspended matter, and kinetic processes may also have an important role on the fractionation of iron in this river.

Flood seasons, as well as heavy precipitations, allow the water column to reach the upper organic rich horizons of highly degraded podzols, which will therefore contribute with lighter iron during these periods. These parameters have also an influence on the water pH (favors the stability of Fe^{2+} in the surroundings) and on the dissolved organic carbon contents, which increases the rates of weathering – one of the major processes that release iron in the environment – of silicates and oxides.

In the case of the white water rivers, which drain an area of geological igneous basement or sediments instead of soils, the iron isotopic signatures reflect the composition of detrital particles eroded from the Andes, which have an isotopic composition similar to that of the continental crust. These results confirm the prediction that bulk water from rivers with large amounts of suspended matter presents an iron isotopic composition similar to continental crust.

The Negro River results seem to confirm the opposite relation, *i.e.*, bulk water from rivers with small amounts of suspended loads has lighter iron isotopic signatures compared to the continental crust. They also show the important role of biologic activity and organic compounds, which seem to have a much stronger control on the iron isotopic fractionation than climatic contexts themselves to the suspended matter iron isotopic composition of rivers.

The Amazon River results, which are similar to the continental crust values, indicate that the influence of suspended matter with continental crust-like iron isotopic composition from the Solimões and the Madeira rivers to the Amazon River is much stronger than the contribution of negative, organic-rich,

suspended matter iron isotopic composition from the Negro River, which is organic-rich. This is in accordance with the fact that the input of the Solimões and Madeira rivers to the suspended fraction of the Amazon River is much more important than the input of the Negro River, which is characterized by a very low suspended matter content. It is inferred, on the basis of this study, that the Amazon River delivers to the Atlantic Ocean a slightly heavy, similar to the continental crust, suspended matter iron isotopic composition.

Keywords: iron isotopes, suspended matter, Amazonian rivers, intertropical zones, Amazon River.

RÉSUMÉ ÉTENDU

DOS SANTOS PINHEIRO, Giana Márcia. **Bilan spatio-temporel du cycle du fer dans un grand bassin intertropical: Étude isotopique de la matière en suspension des eaux du fleuve Amazone et de ses grands affluents.** 163 pp. Thèse (Doctorat en Géologie) – Sciences de l'Univers, de l'Environnement et de l'Espace (SDU2E), Université Paul Sabatier (Toulouse III), Toulouse, France.

Des échantillons de matières en suspension ont été collectés lors des campagnes de terrain sur le fleuve Amazone et trois de ses principaux affluents: le Negro, le Solimões et le Madeira. Leurs compositions isotopiques du fer ont été étudiées pour les relier aux différents paramètres physico-chimiques, tels que le pH de l'eau, la teneur en matières en suspension et le pourcentage de fer dans les matières en suspension, et vérifier les possibles sources du fer. Les échantillons ont été prélevés en différents endroits et saisons, le long de profils verticaux et transversaux. L'objectif principal consistait à valider l'hypothèse selon laquelle, même si il y a des nombreux processus qui peuvent affecter la distribution et le transport du fer dans ces cours d'eau, la composition isotopique du fer resterait inchangée, contrairement à d'autres traceurs isotopiques comme le Strontium, dont la composition isotopique change en fonction de ces paramètres (*e.g.*, profondeur).

Des variations temporelles sur la composition isotopique du fer des matières en suspension fluviales ont déjà été signalées pour des rivières boréales. Par conséquent, les échantillons provenant de deux séries temporelles, collectées mensuellement par les observateurs du réseau *HYdrology of the Amazon Basin* (HYBAm) sur au moins un an, ont aussi été étudiés. Cette approche globale, sur des cycles hydrologiques complets, était destinée à rechercher des possibles changements de la signature isotopique du fer de la matière en suspension dans les cours d'eau intertropicaux en relation avec les saisons, et vérifier une éventuelle corrélation de cette signature avec une augmentation / diminution du niveau d'eau, puisque les sources de fer peuvent être différentes au cours de ces périodes.

Des paramètres *in situ* ont été mesurés au cours des campagnes de terrain avec une sonde multiparamétrique et des valeurs de débit liquide, de champ de vitesse et des profils de la section ont été obtenus avec un *Acoustic Doppler Current Profiler* (ADCP). Ces informations ont permis de définir les intervalles d'échantillonnage des profils verticaux, qui doivent être également répartis le long de la colonne d'eau.

La méthodologie de laboratoire appliquée comprenait la dissolution des échantillons suivie de la purification du fer par chromatographie d'échange d'anions. Les concentrations de fer ont été mesurées par *Inductively Coupled Plasma Optical Emission Spectrometry* (ICP-OES) avant la chromatographie, pour vérifier une possible perte de fer au cours de cette procédure. Les taux de récupération se situent entre 80 et 100% et, le fer ayant été collecté avec HCl 0.05 N, un fractionnement au cours de l'étape de chromatographie a été écarté.

Des analyses par diffraction des rayons-X et microscopie électronique à balayage ont été effectuées dans certains des échantillons au Laboratoire Géosciences Environnement Toulouse (GET, France), pour vérifier la présence de phases minérales qui pourraient être liées à la signature isotopique de fer trouvée. Des isotopes de fer ont été mesurés avec un *Thermo Finnigan Neptune Multi-Collector Inductive Coupled Plasma Mass Spectrometer* (MC-ICP-MS) au Laboratoire de Géochronologie de l'Université de Brasilia (UnB), au Brésil, et au GET, à Toulouse. Les données ici présentées sont exprimées en $\delta^{57}\text{Fe}$ (en ‰) par rapport au matériel de référence international IRMM-14. La performance des instruments utilisés a été évaluée par des mesures répétitives d'un étalon interne (hématite de Milhas, Pyrénées, aussi connu comme hématite ETH) par rapport à l'IRMM-14. La reproductibilité externe à long terme pour la méthode appliquée à l'Université de Brasilia a été estimée à partir des analyses répétées de cette hématite dans chaque session et les résultats obtenus sont en accord avec les valeurs publiées antérieurement dans plusieurs laboratoires autour du monde. Des étalons internationaux de roche ont aussi été dissous, purifiés et analysés au Laboratoire de

géochronologie de Brasília pour valider la méthodologie utilisée, et notamment l'IF-G ($\delta^{57}\text{Fe}_{\text{IRMM-14}} = 0.931 \pm 0.082 \text{‰}$), qui est également en accord avec des valeurs publiées antérieurement.

Les résultats obtenus pour les matières en suspension des rivières d'eau blanche, comme l'Amazone, le Solimões et le Madeira, sont en opposition avec ceux observés pour les rivières d'eaux noire et claire analysées dans ce travail. Le premier groupe montre des valeurs positives homogènes en fonction de tous les paramètres étudiés, avec des résultats qui sont similaires à la valeur moyenne calculée pour la croûte continentale ($\delta^{57}\text{Fe}_{\text{IRMM-14}} = 0.1 \pm 0.03 \text{‰}$), alors que les résultats pour les rivières noires / claires étudiées sont essentiellement négatifs et affichent des valeurs $\delta^{57}\text{Fe}$ variables dans le temps.

Pour tous les cours d'eau étudiés, les compositions isotopiques de fer des matières en suspension ne présentent pas de relation avec les profils verticaux ou transversaux, contrairement à d'autres paramètres, comme les concentrations de fer. En outre, les rivières d'eau blanche, dans la limite des incertitudes analytiques, gardent leur composition isotopique constante, même en différentes époques, comme observé pour les profils transversaux du Solimões (Station de Manacapuru), échantillonnés à deux saisons différentes, et pour la série temporelle de la Station d'Óbidos (fleuve Amazone) sur deux ans. Les deux séries d'échantillons affichent des valeurs $\delta^{57}\text{Fe}$ homogènes en périodes d'inondation ou en périodes de basses eaux.

Par ailleurs, la rivière Negro est un cas intéressant pour étudier les variations de la composition isotopique du fer dans la matière en suspension. Bien qu'il n'y ait aucune modification de ce paramètre au long de profils en verticaux et transversaux, des variations se produisent au cours du cycle hydrologique. Les teneurs en carbone organique dissous varient selon les saisons et ont un effet important sur l'altération des matériaux qui proviennent des podzols, une des principales sources de fer pour le bassin du Negro. Cette particulière altération a une influence sur l'oscillation des signatures isotopiques du fer de la matière en suspension au long de l'année. Il a aussi été constaté que les valeurs des précipitations ont un rôle essentiel sur la fourniture et le transport du fer dans cette rivière, contribuant également à des compositions isotopiques de fer distinctes observées.

Tous les résultats montrent une différence très importante liée au transport et à la nature de la matière en suspension des rivières d'eaux blanches et celles d'eaux noires: dans les rivières d'eaux blanches comme le Solimões, le Madeira et l'Amazone, qui ont des eaux neutres, pauvres en matière organique, peu ou pas de fractionnement se produit pendant le transport du fer à partir de sources clastiques (fragments de roche) jusqu'au lit de ces rivières. La matière en suspension est donc représentée principalement par des oxy-hydroxydes et des silicates, qui montrent une valeur positive de $\delta^{57}\text{Fe}$, similaire à celle de la croûte continentale. D'autre part, dans les rivières d'eaux noires, comme le Negro, caractérisées par des eaux acides et riches en matières organiques, le fer lourd est préférentiellement lié à la matière organique, principalement sous la forme de colloïdes, qui seront responsables d'une composition isotopique lourde du fer dans la fraction dissoute. Les principales sources de matière organique et de fer réduit pour le bassin du Rio Negro sont les podzols qui se rencontrent dans cette région. Le fer léger, probablement fractionné au cours de la pédogenèse, est associé à la matière en suspension et des processus cinétiques peuvent également avoir un rôle important sur le fractionnement du fer dans cette rivière.

Saisons des crues, ainsi que des précipitations abondantes, permettent la colonne d'eau d'atteindre les horizons supérieurs, riches en matières organiques, des podzols fortement dégradés qui contribuent alors avec un fer plus léger à cette période. Le niveau d'eau, ainsi que les fortes précipitations, ont également une influence sur le pH de l'eau (favorise la stabilité de Fe^{2+} dans le milieu) et sur la teneur en carbone organique, qui augmente les taux d'altération – un des principaux processus qui libèrent du fer dans l'environnement – des silicates et des oxydes.

Dans le cas des rivières d'eau blanche, qui drainent une superficie de sous-sol géologique igné ou sédimentaire au lieu de sols, les signatures isotopiques du fer reflètent la composition des particules détritiques érodées des Andes, qui ont une composition isotopique semblable à celle de la croûte continentale. Ces résultats confirment la prédiction que l'eau totale (*i.e.*, échantillon non filtré)

provenant des rivières avec des grandes quantités de matière en suspension présente une composition de fer isotopique similaire à la croûte continentale.

Les résultats pour le Negro semblent confirmer la relation inverse, à savoir, que l'eau totale des rivières avec une faible quantité de matière en suspension présente des signatures isotopiques de fer plus légers que la croûte continentale. Ils montrent également le rôle important joué, sur la composition isotopique du fer des matières en suspension des fleuves, par les composés organiques et par l'activité biologique, qui semblent avoir un contrôle beaucoup plus fort sur le fractionnement isotopique de fer que les contextes climatiques eux-mêmes.

Les résultats pour le fleuve Amazone, similaires aux valeurs de la croûte continentale, indiquent que l'influence des matières en suspension avec une composition isotopique du fer semblable à la croûte continentale des rivières Solimões et Madeira, est beaucoup plus forte que la contribution isotopique légère et négative du fer de la matière en suspension du Negro, qui est riche en matière organique. Ceci est en accord avec le fait que l'apport de matières en suspension du Solimões et du Madeira pour l'Amazone est beaucoup plus important que celui du Negro, qui est caractérisé par une teneur en matières en suspension très faible. Il est déduit, sur la base de cette étude, que le fleuve Amazone fournit à l'Océan Atlantique une matière en suspension dont la composition isotopique de fer est légèrement lourde, semblable à celle de la croûte continentale.

Mots-clés: isotopes du fer, matières en suspension, rivières amazoniennes, zones intertropicales, Amazone.

RESUMO EXPANDIDO

DOS SANTOS PINHEIRO, Giana Márcia. **Balanço espaço-temporal do ciclo dos isótopos de Fe no material em suspensão de águas da Bacia Intertropical do Rio Amazonas e de seus afluentes.** 163 pp. Tese (Doutorado em Geologia) – Instituto de Geociências, Universidade de Brasília (UnB), Brasília - DF, BRASIL.

Amostras de material em suspensão foram coletadas em campanhas de campo no Rio Amazonas e em três de seus principais afluentes: o Negro, o Solimões e o Madeira. Estes rios foram investigados quanto à composição isotópica de ferro, a fim de verificar as possíveis fontes deste elemento e relacioná-las com diferentes parâmetros físico-químicos, tais como o pH da água, o teor de material suspenso e a porcentagem de ferro no material em suspensão. As amostras foram coletadas em diferentes locais e estações climáticas, ao longo de perfis em profundidade e laterais. Tal abordagem teve em vista validar a hipótese de que, ainda que existam certos processos que podem afetar a distribuição e transporte de ferro nestes rios, as composições isotópicas de ferro se mantêm inalteradas, ao contrário de outros sistemas de traçadores isotópicos, como Estrôncio, para o qual foram relatadas modificações de acordo com estes parâmetros (e.g., profundidade).

Variações temporais na composição isotópica de ferro de materiais fluviais em suspensão já foram relatadas em rios boreais. Desta maneira, amostras de duas séries temporais, coletadas mensalmente por observadores da rede *HYdrology of the AMazon Basin* (HYBAm) durante ao menos um ano, também foram estudadas. Esta abordagem mais abrangente, ao longo de ciclos hidrológicos completos, foi destinada a analisar possíveis mudanças na assinatura isotópica de ferro do material em suspensão de rios intertropicais com relação às estações do ano, além de verificar se há correlação deste parâmetro com o aumento / redução do nível de água, uma vez que as fontes de ferro podem ser diferentes nestes períodos.

Parâmetros *in situ* foram obtidos em campo com uma sonda multiparamétrica e valores de vazão e velocidade da água, além de perfis das seções, foram medidos em campanhas de campo com *Acoustic Doppler Current Profiler* (ADCP). Estes últimos dados foram utilizados para calcular os intervalos de amostragem relativos aos perfis em profundidade, os quais deveriam ser igualmente distribuídos ao longo da coluna de água de cada rio.

A metodologia aplicada em laboratório incluiu a dissolução das amostras, seguida da purificação de ferro por cromatografia aniônica. Concentrações de ferro foram medidas com *Inductively Coupled Plasma Optical Emission Spectrometry* (ICP-OES) antes da cromatografia, para verificar possíveis perdas de ferro durante este procedimento. As recuperações estão entre 80 e 100% e, uma vez que o ferro foi coletado com HCl 0,05 N, o fracionamento deste elemento durante a etapa de cromatografia foi descartado.

Análises por Difração de raios-X e microscopia eletrônica de varredura foram realizadas em algumas das amostras no Laboratório *Géosciences Environnement Toulouse* (GET, França), para verificar a presença de fases minerais que poderiam estar relacionadas à assinatura isotópica de ferro observada. Dados de isótopos de ferro foram adquiridos com *Thermo Finnigan Neptune Multi-Collector Inductive Coupled Plasma Mass Spectrometer* (MC-ICP-MS) no Laboratório de Geocronologia da Universidade de Brasília (UnB) e no GET, França. Os resultados de isótopos de ferro aqui apresentados são relatados em $\delta^{57}\text{Fe}$ (em ‰), tendo por base o material de referência internacional IRMM-14. O desempenho dos instrumentos utilizados foi avaliado através de medições repetidas de um padrão interno (hematita de Milhas, Pirineus, também conhecida como hematita ETH) em relação ao IRMM-14. A reproduzibilidade externa a longo prazo para o método aplicado na Universidade de Brasília foi estimada a partir de análises replicadas desta hematita em cada sessão, e os resultados obtidos estão de acordo com valores previamente publicados por vários laboratórios ao redor do mundo. Padrões

internacionais de rochas também foram dissolvidos, purificados e analisados no Laboratório de Geocronologia de Brasília, para validar a metodologia utilizada, e incluem o padrão IF-G ($\delta^{57}\text{Fe}_{\text{IRMM-14}} = 0,931 \pm 0,082 \text{‰}$), que também está de acordo com valores anteriormente publicados.

Os resultados obtidos para o material em suspensão de rios de águas brancas, tais como o Amazonas, Solimões e Madeira, contrastam com os resultados observados para rios de águas pretas e claras analisados neste trabalho. O primeiro grupo mostra valores positivos homogêneos em relação a todos os parâmetros estudados, com resultados semelhantes ao valor médio calculado para a crosta continental ($\delta^{57}\text{Fe}_{\text{IRMM-14}} = 0,1 \pm 0,03 \text{‰}$). Por outro lado, resultados obtidos para o material em suspensão de rios de águas pretas / claras são principalmente negativos e exibem $\delta^{57}\text{Fe}$ variável ao longo do tempo.

Para todos os rios estudados, as composições isotópicas de ferro do material em suspensão não apresentam nenhuma relação com os perfis em profundidade ou laterais, em contraste com os outros parâmetros, tais como a concentração de Fe. Além disso, rios de águas brancas, dentro das incertezas analíticas, mantêm sua composição isotópica constante, mesmo em diferentes épocas do ano, como observado para os perfis laterais coletados em dois diferentes níveis de água no Rio Solimões (Estação de Manacapuru) e para a série temporal da Estação de Óbidos (Rio Amazonas), ao longo de dois anos. Ambos os conjuntos de amostras apresentam valores de $\delta^{57}\text{Fe}$ homogêneos nos períodos de inundação e seca.

Por outro lado, o Rio Negro é um caso interessante para o estudo de variações na composição isotópica de ferro do material em suspensão. Apesar de não existirem alterações deste parâmetro ao longo de perfis em profundidade e laterais, existem variações durante o ciclo hidrológico. Teores de carbono orgânico dissolvido e pH da água variam ao longo das estações e têm um importante efeito sobre o intemperismo ativo de materiais provenientes de espodossolos, uma das principais fontes de ferro para a área do Rio Negro. Este particular intemperismo influencia na oscilação das assinaturas de ferro do material em suspensão ao longo do ano. Foi verificado que valores de precipitação têm papel essencial no fornecimento e no transporte de ferro neste rio, o que também contribui para as distintas composições isotópicas de ferro observadas.

Todos os resultados apontam para uma distinção muito importante com relação ao transporte e a natureza do material em suspensão de rios de águas brancas e águas pretas: em rios de água branca, como o Solimões, Madeira e Amazonas, que possuem águas neutras e pobres em matéria orgânica, pouco ou nenhum fracionamento ocorre durante o transporte de ferro de fontes clásticas (fragmentos de rocha) para a corrente principal destes rios. O material em suspensão é, neste caso, representado principalmente por oxi-hidróxidos e silicatos, que têm valor de $\delta^{57}\text{Fe}$ positivo e similar ao valor da crosta continental. Por outro lado, em rios de água preta, como o Rio Negro, caracterizado águas ácidas e ricas em matéria orgânica, o ferro pesado se liga preferencialmente à matéria orgânica, principalmente sob a forma de colóides, que serão responsáveis pela composição isotópica pesada de ferro na fração dissolvida. A principal fonte de matéria orgânica e ferro reduzido para Bacia do Rio Negro são espodossolos que ocorrem nesta área. O ferro leve, provavelmente fracionado durante processos pedogenéticos, está associado ao material em suspensão, e processos cinéticos podem também exercer um papel importante no fracionamento de ferro neste rio.

Estações de inundação, bem como fortes precipitações, permitem que a coluna de água alcance os horizontes superiores ricos em matéria orgânica de espodossolos bastante degradados, os quais contribuem com ferro leve durante estes períodos. Estes parâmetros possuem ainda influência sobre o pH da água (que favorece a estabilidade de Fe^{2+} nas imediações) e sobre o teor de carbono orgânico, que aumenta a taxa de intemperismo – um dos principais processos que liberam ferro no ambiente – de silicatos e óxidos.

No caso dos rios de água branca, que – ao invés de carrearem elementos de solos – drenam uma área de embasamento geológico ígneo ou sedimentar, as assinaturas isotópicas de ferro refletem a composição de partículas detriticas erodidas dos Andes, que têm a composição isotópica semelhante à da crosta continental. Estes resultados confirmam a previsão de que a água bruta (*i.e.*, amostra não

filtrada) de rios com grandes quantidades de material em suspensão apresenta composição isotópica de ferro semelhante ao valor da crosta continental.

Os resultados para o Rio Negro parecem confirmar a relação oposta, ou seja, a água bruta de rios com pequenas quantidades de material em suspensão apresenta assinaturas isotópicas de ferro mais leves em comparação com a crosta continental. Eles também demonstram o importante papel de compostos orgânicos e da atividade biológica, os quais parecem ter um controle muito maior sobre o fracionamento isotópico de ferro do que os contextos climáticos em si para a composição isotópica de ferro de material em suspensão de rios.

Os resultados do Rio Amazonas, semelhantes aos valores de crosta continental, indicam que a influência do material em suspensão com composição isotópica semelhante à da crosta continental dos rios Solimões e Madeira para o Rio Amazonas é muito mais forte do que a contribuição do material em suspensão com composição isotópica de ferro negativa, leve, proveniente do Rio Negro, rico em matéria orgânica. Isto está de acordo com o fato de que o aporte dos rios Solimões e Madeira para a fração suspensa do Rio Amazonas é muito mais importante do que o aporte do Rio Negro, que é caracterizado por baixo teor de material em suspensão. Infere-se, com base neste estudo, que o Rio Amazonas descarrega no Oceano Atlântico material em suspensão com composição isotópica de ferro levemente pesada, semelhante à da crosta continental.

Palavras-chave: isótopos de ferro, material em suspensão, rios amazônicos, zonas intertropicais, Rio Amazonas.

APRESENTAÇÃO

1. ABORDAGEM

A presente Tese discute os resultados da pesquisa realizada por Giana Márcia dos Santos Pinheiro, de 2009 à 2013, e atende a um dos requisitos necessários à obtenção do título de Doutora em Geologia. O trabalho, intitulado “BALANÇO ESPAÇO-TEMPORAL DO CICLO DOS ISÓTOPOS DE Fe NO MATERIAL EM SUSPENSÃO DAS ÁGUAS DA BACIA INTERTROPICAL DO RIO AMAZONAS E DE SEUS AFLUENTES”, foi desenvolvido simultaneamente no Brasil (Universidade de Brasília, Laboratório de Geocronologia) e na França (Universidade de Toulouse III – Paul Sabatier –, Laboratoire Géosciences Environnement Toulouse, GET). Desta maneira, para facilitar a comunicação e a troca de informações, os textos são aqui apresentados em Inglês.

A Tese aborda o ciclo biogeoquímico de isótopos de ferro na Bacia Amazônica. O estudo é baseado na quantificação e análise de isótopos de ferro e investiga o comportamento deste elemento no material em suspensão de águas do Rio Amazonas e de seus principais afluentes. Este trabalho resultou, até o momento, em um artigo publicado e um segundo artigo submetido, ambos encaminhados à revistas internacionais especializadas. Ademais, seis comunicações, que representam resumos publicados, foram apresentadas em conferências nacionais / internacionais. Todos os referidos trabalhos contam com a autora da presente Tese como primeira autora, o que totaliza oito divulgações que estiveram diretamente ligadas à referida pesquisa.

2. ESTRUTURA DA TESE

A Tese foi organizada sob a forma de publicações, de acordo com as regras do Programa de Pós-Graduação do Departamento de Geologia (Instituto de Geociências) da Universidade de Brasília. Os capítulos 1 (Introdução Geral) e oito (Conclusões Gerais) apresentam considerações atinentes ao conjunto da Tese. O segundo, terceiro e quarto

capítulos consistem em compilação bibliográfica, delineiam o estado da arte do tópico em estudo e, desta forma, não foram submetidos à revistas. O capítulo seis é focado em dados preliminares, não refinados, sobre a composição isotópica de ferro no material dissolvido e em suspensão de águas da região amazônica, de sorte que também não foi submetido à publicação – a inclusão dele se justifica, contudo, em razão da pertinência de se compartilhar dados que possam ser de interesse para futuras pesquisas. O capítulo 5 corresponde ao artigo original publicado, enquanto o capítulo 7, em apreciação, consiste em artigo submetido à revista científica especializada, de maneira que poderá passar por algumas alterações no que se refere à sua versão final. Ambos são baseados nos dados adquiridos durante os quatro anos de desenvolvimento desta Tese. Finalmente, o capítulo 9 (Perspectivas) consiste na síntese das principais discussões e sugestões aportadas pelos membros da banca quando da defesa de Tese. As figuras foram numeradas de forma contínua ao longo do documento, da **Fig. 1** à **Fig. 37**. Os formatos dos números em todos os textos em inglês são dados em formato americano (separador de milhares = vírgula (“,”) – *i.e.*, um mil = 1,000). Além disso, no final deste documento, são apresentados anexos (locais de coleta e parâmetros físico-químicos de amostras não analisadas obtidas na Amazônia, diversos protocolos de laboratório utilizados no Laboratório de Geocronologia da Universidade de Brasília e lista de publicações decorrentes deste trabalho).

Os capítulos são apresentados da seguinte maneira:

1. Introdução Geral;
2. A Bacia Amazônica e a distribuição de ferro;
3. Isótopos de Ferro - uma revisão;
4. Métodos analíticos para a aquisição de dados de isótopos de ferro;
5. IRON ISOTOPE COMPOSITION OF THE SUSPENDED MATTER ALONG DEPTH AND LATERAL PROFILES IN THE AMAZON RIVER AND ITS TRIBUTARIES – *Artigo aceito, Journal of South American Earth Sciences, disponível online desde 27 de agosto de 2012*;
6. Dados preliminares sobre a composição isotópica de ferro de material dissolvido e em suspensão provenientes de distintas naturezas de água na Amazônia Peruana e Brasileira;

7. CONTRASTED SUSPENDED MATTER IRON ISOTOPE COMPOSITIONS:
COMPARISON OF THE AMAZON AND NEGRO RIVERS TEMPORAL SERIES –
submetido à revista Earth and Planetary Science Letters, Fevereiro 2013;

8. Conclusões Gerais;
9. Perspectivas;
10. Referências (e materiais para consulta *on-line*).

==> Anexos

CAPÍTULO UM

INTRODUÇÃO GERAL

1. ABORDAGEM

O ferro é o quarto elemento mais abundante na crosta na Terra. Desta forma, desempenha papel-chave em grande variedade de processos, que incluem a evolução do solo, a co-precipitação de metais em rios através de efeitos redox e o fluxo de água de superfície. Além disso, é utilizado por quase todos os organismos vivos na planeta. Por estas razões, as reações de troca envolvendo ferro em solos, águas e organismos têm sido estudadas há vários anos e, como resultado, existe conhecimento significativo sobre sua distribuição em rochas e solos formadores de minerais, bem como sobre sua especiação em solução aquosa e sobre a termodinâmica de fases minerais ricas neste elemento, como hematita ou goethita.

Isótopos estáveis de ferro são utilizados como traçadores de diferentes reservatórios, os quais podem compor a mistura de ferros isotopicamente distintos, presentes tanto em rios (de afluentes, solos, vegetação), quanto em oceanos (de rios, aerosóis, fluidos em poros de sedimentos de margens oceânicas). Além disso, assinaturas isotópicas de ferro são particularmente sensíveis à alterações no estado redox do ferro e sua especiação ([Johnson et al., 2004](#)).

A transferência de ferro de águas de rios para oceanos tem se mostrado de difícil quantificação devido ao seu comportamento não conservador e às limitações analíticas associadas ao estudo deste elemento ([Benedetti et al., 2003a](#)). Estudos publicados acerca da composição isotópica de Fe das águas de rios são baseados em coleta limitada de amostras ([Beard et al., 2003a; Fantle e DePaolo, 2004; Bergquist e Boyle, 2006](#)). Contudo, a amostragem mais sistemática de [Ingri et al. \(2006\)](#) mostra dois pontos fundamentais: 1) isótopos Fe são um indicador sensível de mudanças em sistemas dinâmicos *solos-rios*, os quais são induzidos por processos críticos, tais como inundações. Tanto o desmatamento antrópico quanto a seca de zonas pantanosas são fortes fatores que convergem para o aumento dos riscos de inundaçāo, de maneira que isótopos de Fe podem ser utilizados como monitor sensível das vulnerabilidades dos sistemas *vegetação-solos-rios* e dos efeitos da pressão antrópica sobre eles; 2) a resposta dos isótopos de Fe ocorre em escala anual, fator importante

para a compreensão e previsão do comportamento e vulnerabilidade do sistema *vegetação-solos-rios*.

[Ingri et al. \(2006\)](#) mostraram que as composições isotópicas de ferro variam de acordo com as estações nas águas do Rio Kalix (norte da Suécia – **Fig. 1**). Esta variabilidade sazonal foi atribuída à mistura de duas fontes distintas de solos que contêm reservatórios de Fe em diferentes estados de oxidação e, portanto, diferentes composições isotópicas. Além disto, comparações de estudos de solo em diferentes contextos climáticos ([Fantle e DePaolo, 2004](#); [Emmanuel et al., 2005](#); [Thompson et al., 2007](#); [Wiederhold et al., 2007a](#); [Poitrasson et al., 2008](#)) mostram quão sensível são os isótopos de Fe a este parâmetro (**Fig. 2**).

O estudo de [Bergquist e Boyle \(2006\)](#) sobre isótopos de ferro na região amazônica mostrou fracionamento isotópico deste elemento entre material em suspensão e dissolvido no Rio Negro. Entretanto, não se verificou o mesmo fenômeno com relação ao Rio Solimões, o que indica que as assinaturas isotópicas de Fe variam de acordo com a química das águas dos rios e ainda, com relação à natureza dos solos e da vegetação drenados por diferentes tributários do Rio Amazonas.

O estudo destes autores foi baseado em poucas amostras de água do sistema do Rio Amazonas. Os primeiros dados reportados para solos lateríticos ([Poitrasson et al., 2008](#)) sugerem que em zonas intertropicais a transferência de ferro total do solo para as águas do rio, e em seguida para o oceano, deve acontecer sem fracionamento isotópico, o que diverge dos resultados reportados por [Bergquist e Boyle \(2006\)](#).

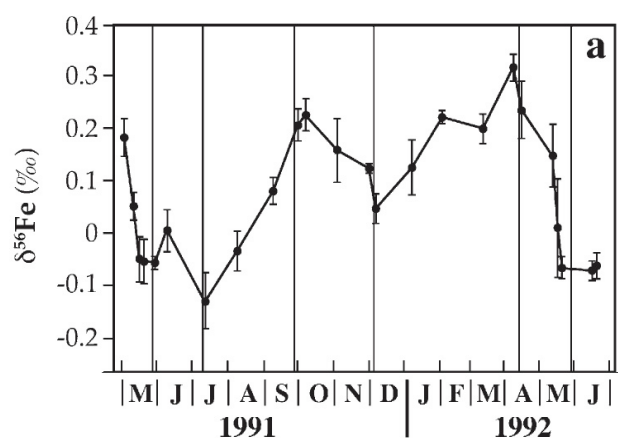


Fig. 1 – Variações na composição isotópica de ferro no período de um ano no Rio Kalix, Suíça ([Ingri et al., 2006](#)).

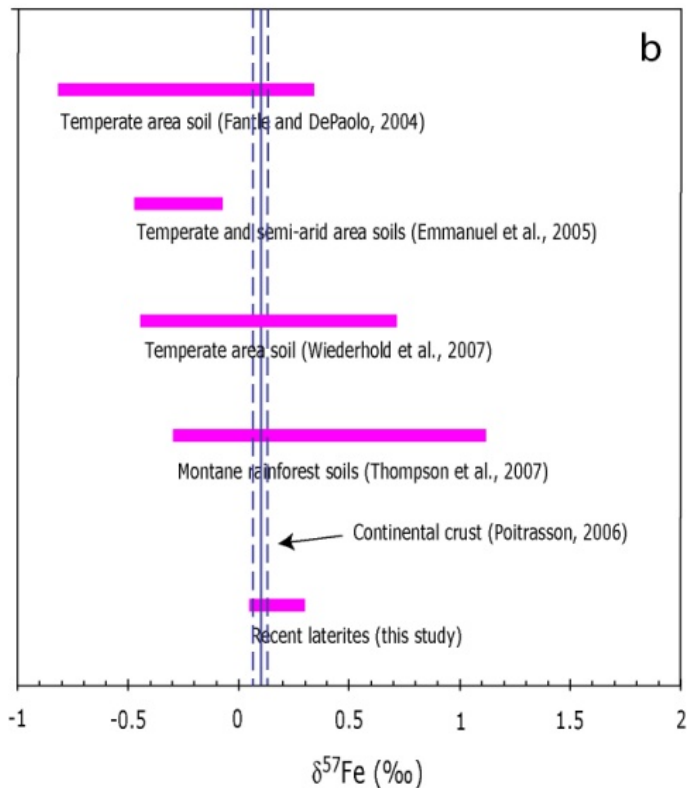


Fig. 2 – Contrastos nas variações da composição isotópica de ferro em diferentes tipos de solo ([Poitrasson et al., 2008](#)).

Todos os estudos mencionados indicam que isótopos de ferro podem ser utilizados para inferir a transferência de material dos continentes para o oceano. Eles ainda demonstram que assinaturas isotópicas de Fe são sensíveis à parâmetros críticos, tais como clima, solos e tipo de vegetação existente, que podem variar com o aumento da média da temperatura atmosférica ou com mudança da cobertura vegetal em resposta à diversos fatores, entre os quais a pressão antrópica.

O Rio Amazonas representa mais de 20% das águas continentais mundiais descarregadas nos oceanos. Assim, a bacia amazônica constitui local privilegiado para o estudo da transferência do ferro em zonas tropicais, onde processos de alteração e erosão são particularmente relevantes. Faz parte do escopo deste trabalho avaliar e compreender estes e outros processos que ocorrem durante o transporte de ferro na região, bem como os efeitos que eles têm na partição de ferro entre as diferentes fases (ou compartimentos) presentes nestes rios.

2. OBJETIVOS

Um estudo abrangente de Fe elementar e isotópico foi conduzido em águas e material em suspensão de rios na bacia amazônica, de forma a estimar corretamente o fluxo de ferro particulado nesta área. Este estudo objetivou responder a várias questões sobre o comportamento de ferro elementar e de seus isótopos. Para tanto, o material suspenso foi coletado de acordo com:

- Diferentes localidades;
- Diferentes estações (ou ciclos hidrológicos);
- Diferentes profundidades na coluna de água (perfis em profundidade);
- Diferentes distâncias entre as margens dos rios (perfis laterais);
- Diferentes tipos de águas (Brancas, Pretas e Claras).

Os resultados obtidos foram comparados com estudos em sistemas de rios localizados em áreas intertropicais, boreais e subárticas, para compreensão dos processos que controlam a concentração, a composição isotópica e a especiação de isótopos de Fe nestes sistemas fluviais.

3. MÉTODOS

Como mencionado anteriormente, a amostragem foi realizada em diversos locais da Bacia Amazônica, ao longo de seções aproximadamente perpendiculares ao fluxo do rio, e ao longo de perfis em profundidade e temporais. O objetivo foi avaliar a heterogeneidade dos rios com respeito às composições química e isotópica. Análises de difração de raios-X e microscopia eletrônica de varredura (MEV) foram realizadas para qualificar a mineralogia do material em suspensão retido nos filtros (membranas) estudados. *Inductively Coupled Plasma Atomic Emission Spectrometer* (ICP-OES) foi utilizado para analisar as amostras antes da

cromatografia, no intuito de verificar possíveis perdas de ferro após a etapa de separação química. Outras informações sobre os equipamentos utilizados podem ser encontrados nos capítulos 5 e 7.

Para determinação da composição isotópica de ferro, as amostras foram dissolvidas e em seguida purificadas por cromatografia aniónica. Resultados de composição isotópica são dados em $\delta^{57}\text{Fe}$, em relação ao padrão internacional IRMM-14, e a unidade utilizada é per mil (\textperthousand). Os dados foram adquiridos em *Multi-Collector Inductively Coupled Plasma Mass Spectrometer* (MC-ICP-MS), conforme protocolo utilizado no GET ([Poitrasson & Freydier, 2005](#)). O método, que visa estabelecer adequada abordagem para análises de isótopos de ferro, foi implementado no Laboratório de Geocronologia da Universidade de Brasília. Outras informações sobre este assunto podem ser encontradas neste volume, na seção “Métodos” dos capítulos 5 e 7.

Parâmetros químicos *in situ*, tais como pH da água, condutividade elétrica e temperatura, entre outros, são determinados no momento da coleta da amostra com uma sonda multiparamétrica. Este estudo é baseado na análise de: 1) amostras coletadas durante as campanhas de campo realizadas anualmente pelo programa de cooperação entre Brasil e França e; 2) dados adquiridos em amostras coletadas pelo projeto HYBAm (*HYdrology of the AMazon Basin*, **Fig. 3**) em diferentes períodos.



Fig. 3 – Estações da rede HYBAm na Bacia Amazônica (www.ore-hybam.org).

CAPÍTULO DOIS

THE AMAZON BASIN AND THE DISTRIBUTION OF IRON

1. INTRODUCTION

In an era of increasing interest in the interface between geosciences and life sciences, iron is an element of central importance (Anbar, 2004). It is of great relevance in all kinds of environments (Gibbs, 1972; Gibbs, 1977; Benedetti *et al.*, 2003a) and organisms. Iron is the most abundant element (by mass) in the Earth, forming much of its inner core, as well as the inner core of many other planets, accounting for approximately 35% of their total masses. It is the second most abundant metal on Earth (behind aluminum) and fourth most abundant element in the Earth's crust (~ 5,1%). It is found in almost all rocks, soils and hundreds of minerals (Nielsen, 1960) and it also forms the nucleus of red giant stars, representing, therefore, one of the most abundant elements in the Universe.

Iron is one of the last products generated before a supernova collapse. It is formed by nuclear fusion in high mass stars, at temperatures higher than 3 billion K, in an exothermic process known as silicon burning. In this process, unstable elements are generated, fuse with other elements and form denser atoms until the last possible reaction, the one that creates the stable nuclide of ^{56}Fe .

As previously stated, iron compounds are of fundamental importance to living organisms, both animal and vegetal, being mainly required to promote oxidation and photosynthesis. They are also important catalysts for chemical processes, especially oxidation-reduction reactions (Nielsen, 1960), as well as an important constituent of blood: once bonded with molecular oxygen, iron forms hemoglobin and myoglobin proteins.

The most common iron redox states at the surface of Earth are ferrous iron (Fe^{2+}) and ferric iron (Fe^{3+}), but iron can also exhibit oxidation states of +4 and +6 in unstable salts, such as ferrite (FeO_2^-), perfferrite (FeO_3^-) and ferrate (FeO_4^-) compounds (Nielsen, 1960). In the presence of free oxygen, iron is under the oxidized form Fe^{3+} , which has a very low solubility at neutral pH (Curie and Briat, 2003) and therefore is mostly present in the form of iron (hydr)oxides such as ferrihydrite (Fe(OH)_3), goethite (FeOOH), hematite (Fe_2O_3), maghemite

(γ -Fe₂O₃) and magnetite (Fe₃O₄, formed by both Fe²⁺ and Fe³⁺) (Cornell and Schwertmann, 2003).

The ferrous iron (Fe²⁺) is stable under reductive conditions and is present either as dissolved species or in the form of Fe²⁺ minerals such as Fe-carbonate (*e.g.*, siderite, FeCO₃) or Fe-phosphate (*e.g.*, vivianite, Fe₃(PO₄)₂). Abiotic pathways of Fe redox cycling include chemical reduction of Fe³⁺ (*e.g.*, by sulfide) and chemical oxidation of Fe²⁺ (*e.g.*, by O₂) (Kappler *et al.*, 2010). Iron redox cycling may also be driven by biologically catalyzed processes (*e.g.* Kappler and Straub, 2005; Weber *et al.*, 2006), such as microbial iron reduction.

2. SOURCES OF IRON IN RIVERS

There are a variety of sources of iron in rivers, such as tributary inputs, autochthonous material (formed during primary production and mineralization), weathering products, soils, atmospheric deposition, continental run-off, re-suspended sediments, diagenetic pore fluids, underground waters, vegetation and hydrothermal fonts, among others (Hakanson and Peters, 1995; Wells *et al.*, 1995; Elderfield and Schultz, 1996; Johnson *et al.*, 1999; Beard *et al.*, 2003b; Malmaeus and Hakanson, 2003; Elrod *et al.*, 2004; Jickells *et al.*, 2005; Severmann *et al.*, 2006; Bennett *et al.*, 2008; Rouxel *et al.*, 2008a; Rouxel *et al.*, 2008b; Escoube *et al.*, 2009).

The composition of river particles results from the interaction of a number of parameters, such as the crustal bedrock type, weathering and sediment sorting processes (hence, hydrodynamic and geomorphologic properties of the area – Bouchez *et al.*, 2010). Also, the possible variety of iron sources contribute to the chemical composition of materials in rivers, and the fate and transport of iron strongly depends on the reactions involving this element, which include biological and abiotic processes that make its biogeochemical cycling complicated (Song *et al.*, 2011).

Tropical regions generally undergo important modifications, such as natural weathering (Benedetti *et al.*, 2003a). Continental weathering involves the breakdown of rocks and minerals by mechanical and chemical means, with subsequent development of soils, and the transport of these weathering products to oceans and rivers (Fantle and DePaolo, 2004).

Chemical weathering is a key process in the cycle of the elements at the Earth's surface, where, within the different reservoirs (continent, ocean and atmosphere) it provides a major source of elements delivered by rivers to oceans ([Martin and Whitfield, 1983](#)).

Weathering reactions of most silicate minerals in soils proceed incongruently ([White and Brantley, 1995](#), and references therein). The most mobile elements (*e.g.*, Na and Ca) tend to be removed in the dissolved form by soil solutions; immobile elements such as Al or Fe are incorporated into stable secondary products such as clays (*e.g.*, kaolinite) and metallic oxy-hydroxides (*e.g.*, goethite), which accumulate in soils ([Viers *et al.*, 2007a](#), and references therein). It is important to recognize that the dissolved material in rivers generally represents the products of chemical weathering, whereas the particulate phase corresponds to the transport of particles produced during chemical weathering (*i.e.*, production of secondary minerals) and physical weathering (*i.e.*, mechanical breakdown of rocks - [Viers *et al.*, 2007b](#)).

A large diversity of iron-rich particles have been described in aquatic systems using transmission electron microscopy (*e.g.*, [Leppard, 1992](#)) and their association to organic matter appears to be widespread in freshwaters from various origins ([Buffle *et al.*, 1998](#); [Perret *et al.*, 2000](#); [Ingri *et al.*, 2006](#)). The presence of organic compounds affects the conditions of environments and may strongly influence the redox state of iron, which would implicate in a partitioning of this element into distinct reservoirs. In the case of rivers, these reservoirs consist, in a broad sense, on the particulate (defined in this work as the material that is retained in the 0.45 μm membrane filter), colloidal and dissolved phases (here considered together and defined as the material that passes through the 0.45 μm membrane filter).

3. THE AMAZON BASIN AND ITS RIVERS

The Amazon River is the largest river of the world and represents approximately 20% of the world fresh water flux from land to ocean ([Molinier *et al.*, 1996](#)), a proportion which is greater than the combined annual discharge of the Earth's next eight largest rivers ([Seyler and Boaventura, 2001](#)). It drains ~ 6.4 million km^2 and has an average discharge of $209,000 \text{ m}^3 \text{ s}^{-1}$ ([Aucour *et al.*, 2003](#)). The flux of solid discharged to the ocean by the Amazon is between 500 and 1,200 MT yr^{-1} ([Meade *et al.*, 1979](#); [Dunne *et al.*, 1998](#); [Maurice-Bourgoin *et al.*, 2007](#)).

The source of the Amazon River is the Lauricocha Lake, located in the Peruvian Andes, where the Amazon River starts. It passes through Peru, Colombia and Brazil. The Amazon River mainstream is formed by the confluence of the Ucayali and Marañon rivers, which come from the Peruvian Andes. Therefore, the length of the Amazon is measured from the source of the Ucayali River. When it crosses to Brazil, it is called Solimões River, and when its waters combine with the Negro River waters, near Manaus, it is once again recognized as the Amazon River. The five main inflowing tributary rivers in Brazil are the Negro, Solimões, Madeira, Tapajós and Xingu, where most samples here studied were collected ([Fig. 4](#)).

The majority of the Brazilian part of the river exceeds 40 meters in depth, although in some parts near the mouth, depth may reach 100 meters. The width of the river ranges from 1 to 8 km. Annual precipitation varies significantly with time and space throughout the basin ([McClain, 2001](#)), with an average of 1,500 – 3,000 mm / yr, while temperatures are generally uniform, ranging annually from 24 to 26 °C ([Seyler and Boaventura, 2001](#)), except in the Andean Amazon ([McClain, 2001](#)). Between 1940 and 2003, the real evapotranspiration calculated for the Amazonian Basin until the Óbidos Station (further discussed) is 1,112 mm ([Callède et al., 2008](#)). Between Óbidos and the ocean, the average real evapotranspiration vary from 1,200 and 1,501 mm ([Callède et al., 2010](#)).

In the early 70's, the whole Amazon basin was covered by tropical rainforest (71%) and savannas (29%, [Sioli, 1984](#)). Nowadays, estimates indicate that around 20% of the original area is deforested, mostly for pasture or to cultivate agricultural commodities.

The Amazon River basin can be geologically and morphologically divided into four main units: the Andean Cordillera (11% of the basin area), the two shields (Brazilian and Guyana shields – 44% of the basin area), and the Amazon plain (45% of the basin area) ([Seyler and Boaventura, 2001](#)).

At Óbidos, the last gauging station where the river is still channelized upstream the delta, about 90% of the sedimentary budget of the Amazon River is accounted for the two main tributaries in terms of sediment discharge of the Amazon River: the Solimões and Madeira rivers ([Gibbs, 1967](#); [Meade et al., 1985](#)), which drain the northern and southern part of the Andean Cordillera respectively ([Martinez et al., 2009](#)).

From the left bank, the Solimões River receives the Içá and Japurá tributaries, which originate in the Andes, and from the right bank it receives the Javari, Itaquai, Jutaí, Juruá and

Purus tributaries (**Fig. 4**). Two hundred kilometers downstream, the Amazon River receives the Madeira River waters, which come from the Bolivian Andes ([Seyler and Boaventura, 2001](#)).

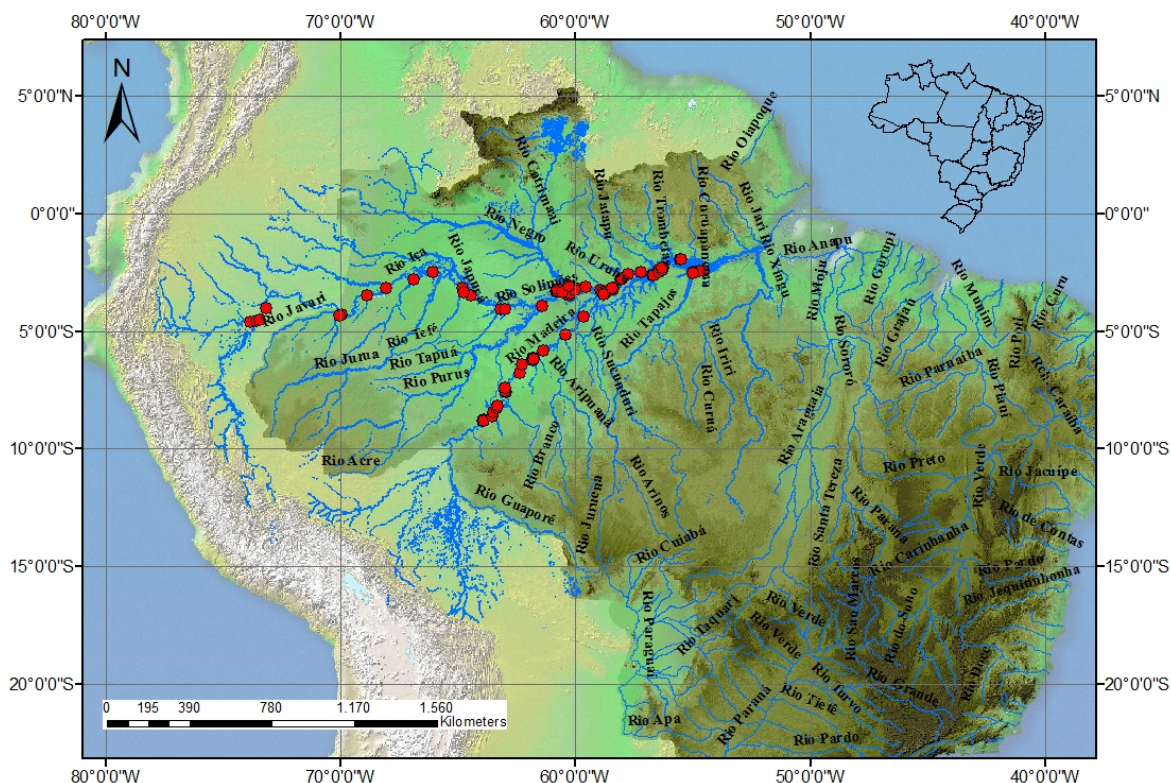


Fig. 4 – Sketch map of the Amazon Basin and its main tributaries, showing sample locations.

The Madeira River basin is essentially constituted of old crystalline and sedimentary rocks of various stratigraphic ages derived from these old terrains, while the Solimões River basin incorporates young subduction-related arc plutonic and volcanic rocks, mixed with older terrains similar to those of the Madeira River ([Basu *et al.*, 1990](#)).

The different rivers from the Amazon Basin account for a variety of physical and chemical characters that have long been recognized, and different classifications have been proposed to account for the white, clear, and black waters (Fittkau, 1971; Gibbs, 1972; Sioli, 1984; Lewis *et al.*, 1995). Schematically, clear and black waters are mostly related to chemical erosion, whereas white waters contain much higher sediment content inherited from mechanical erosion (Allard *et al.*, 2004).

The Negro River is a black water river with low pH (< 5), low mineral content and high bulk organic carbon concentration (*i.e.*, bulk water, not filtered). The Madeira and

Solimões rivers are white waters with higher pH, higher mineral content and lower bulk organic carbon concentration ([Benedetti et al., 2003a](#)). The Tapajós River is an example of clear water, and has similar properties to black waters rivers, depending on the location and time of the year ([Sioli, 1967](#)).

4. IRON IN SUSPENDED MATTER AT THE AMAZON BASIN

The flow of water, solutes and particulate matter in the Amazon River is the product of integrated hydrological, biological, physical and geochemical processes across the basin ([McClain, 2001](#)). Concentrations of most metals in the Amazon are comparable to those of other major rivers of the world and the Andes stand out as the dominant source area for the majority of the metals transported by this river. In the Amazon mainstream, iron is transported primarily in particulate form. Transport as a dissolved phase is predominant only in the Negro River, where metals are bonded to dissolved organic matter, due to the acidic reductive waters ([McClain, 2001](#)).

Worldwide comparison of river suspended matter shows a large variability, controlled by various parameters, such as climate conditions, tectonic and geomorphologic features, water discharge and the composition of the continental crust, which is submitted to chemical weathering and erosion ([Bouchez et al., 2010](#)). Nonetheless, [Martinez et al. \(2009\)](#), in a 12-year study in the Central Amazonian plain, at the Óbidos Station, showed the independence of river discharge and suspended sediment concentration.

According to [Bergquist and Boyle \(2006\)](#), the trace element budget (including Fe) of the Amazon River is not well constrained, and many trace elements are decoupled from major dissolved ion chemistry because of organic complexation, stabilization, and adsorption/desorption reactions. It has been reported that Fe contents are higher in tributaries that have high levels of organic material and lower pH (e.g., Negro River, pH ~ 4.8) compared with higher pH tributaries like the Solimões (pH > 6.8) ([Stallard, 1980](#)) and this has been interpreted as a result of strong Fe-organic matter interaction (e.g., [Eyrolle et al., 1996](#); [Viers et al., 1997](#); [Allard et al., 2011](#)).

Organic complexation of Fe^{2+} is minor when compared to that of Fe^{3+} (e.g., [Weber et al., 2006](#); [Allard et al., 2011](#)). The latter authors determined the Fe concentration (in % dry

weight) complexed to organic matter (FeOM) in the Negro River area and showed FeOM was relatively low in soil porewaters and related brooks (podzolic areas), whereas in the main corresponding black water rivers it was several times higher. Also, the Fe^{3+} complexed to organic matter concentrations were also correlated with $\text{Fe}^{2+}/\text{Fe}^{3+}$ ratios in solution, and these ratios were high in podzol porewaters and low in the rivers.

The export rates of iron from the Amazon River to the ocean are very large. On a global scale, the quantity of dissolved Fe from riverine sources is minor ([Beard et al., 2003b](#)) and a dominant part of iron (> 95%) is transported in the particulate fraction (> 0.2 μm), where it may occur mainly as oxide and oxy-hydroxide phases inherited from eroded soils and sediments from various rivers of the basin ([Allard et al., 2004](#)). The remaining Fe in the colloidal fraction is also minor relative to the iron found in the suspended matter ([Allard et al., 2002](#); [Benedetti et al., 2003a](#); [Allard et al., 2004](#)). According to the estimates of [Gibbs \(1973\)](#), performed using chemical selective extraction methods, most iron (~ 90%) in the Amazon River occurs almost equally as oxides and incorporated in silicate detrital grains, with a minor contribution from organic forms (~ 6,5%).

Iron concentration in river particulate matter is normally at the percent level in the Amazonian rivers ([Allard et al., 2004](#)). According to these authors, iron in the mineral form (ferrihydrite) dominates in most rivers except the Negro River where the organic form is dominant due to low pH and high organic matter concentration. Also, there are strong seasonal variations on the iron speciation in this river, with the amount of iron bound to organic matter (FeOM) varying from 10 to 50% for samples taken at the Moura Station in different hydrological seasons (July 1996 and October 1998).

5. FINAL REMARKS ON THE STUDY AREA AND THE SCOPE OF THIS THESIS

The Solimões River is estimated to supply ~ 40 to 60% of the major dissolved ion load, roughly 60% of the suspended sediment load, and more than 50% of the water load of the Amazon River ([Stallard, 1980](#)). This river drains the Peruvian Andes, is relatively cool, has a high suspended sediment load, and a high pH (> 6.8). In contrast, the Negro River drains lowlands that include the most weathered terrains in the Amazon ([Stallard, 1980](#)). It is

warmer than the Solimões River by 1–2°C, has a high concentration of organic matter, a low suspended load and a low pH of ~4.8 ([Bergquist and Boyle, 2006](#)).

The Solimões and the Negro rivers represent two extreme water types in the Amazon system, and they join each other at Manaus to form the unique Amazon River. The Amazon River drains a variety of geological regions that are subject to distinct kinds of weathering and therefore, may present iron from different sources and in different forms, which can contribute to varied iron isotope compositions.

Measurement of relative abundances of the iron isotopes in natural materials represent a relatively “new” technique, and until now, there are only two published articles of aqueous iron isotopic composition in the Amazon region: [Bergquist and Boyle, 2006](#) and [dos Santos Pinheiro et al., 2013](#), the latter being a result of this research project. A few more studies have been conducted in other natural and artificial aqueous systems (*e.g.*, [Ingrin et al., 2006](#); [Escoube et al., 2009](#); [Song et al., 2011](#)) and they will all be discussed in more detail in chapter three.

There is evidence suggesting that dissolved Fe in river waters is isotopically depleted relative to igneous rock sources: total Fe from unfiltered river samples (*i.e.*, bulk water) was observed to be isotopically light ($\delta^{57}\text{Fe}_{\text{IRMM}-14} \sim -1.35\text{\textperthousand}$ – [Fantle and DePaolo, 2004](#) – notation described in detail in chapter three). Also, exchangeable Fe and the more mobile phases of Fe in soils (an important source of Fe to rivers) are, as well, isotopically light ([Brantley et al., 2001](#); [Fantle and DePaolo, 2004](#); [Brantley et al., 2004](#); [Bergquist and Boyle, 2006](#)). These studies indicate that, in general, dissolved and biological Fe are isotopically light compared with igneous sources. The present work intends to investigate and characterize the iron isotopic signatures of river-born particulate matter in the Amazon Basin rivers, in order to understand the contribution of the different iron varieties to the iron isotopic signatures of these materials and, therefore, attribute possible iron sources for the suspended matter. It is expected that the new data will allow a better understanding of the isotopic signature delivered by the particulate phase of the Amazon River to the Atlantic Ocean, as well as constrain the processes, both organic and inorganic, that can have an effect on the results.

CAPÍTULO TRÊS

IRON ISOTOPES – A REVIEW

1. INTRODUCTION

Iron ($Z = 26$) occurs as four natural stable isotopes (^{54}Fe , ^{56}Fe , ^{57}Fe and ^{58}Fe), iron 56 being the most stable nuclide. Their natural abundances are shown in **Fig. 5**. As discussed in chapter two, Fe is the final product of nuclear fusion in stars and hence, the most abundant transition element. It figures as the fourth most abundant element in the Earth's crust and the dominant constituent of the Earth's core, due to the high density of metallic Fe. The magnetic properties of this element make Fe-bearing minerals dominate rock magnetism in the crust. It is, therefore, an element of great importance and interest in all research fields, and its mobility / solubility on Earth's surface is strongly affected by the redox potential of aqueous systems, resulting in the variation in Fe abundance according to the environment (Anbar, 2004).

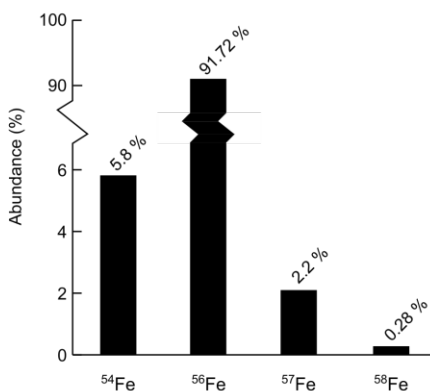


Fig. 5 - The Fe isotopes. Relative abundances are recommended average values from IUPAC (Taylor *et al.*, 1992).

In neutral pH, oxic environments or fluids, significant transport of aqueous Fe is excluded because of the very low solubility of Fe^{3+} in this kind of environment (Curie and Briat, 2003; Beard and Johnson, 2004a). Often, a reduction step is needed for its transport, for instance, for living organisms that require the Fe^{2+} reduced form (Briat and Lobreaux, 1997; Curie and Briat, 2003).

Reductive processes include bacterial iron reduction, interaction with H₂S or other reducing agents. If iron is fractionated into isotopically distinct reservoirs, variations in its signature may be recorded in bulk samples. For example, Fe²⁺_(aq) in equilibrium with Fe³⁺_(aq) show low δ⁵⁷Fe values (Johnson *et al.*, 2002; Welch *et al.*, 2003), whereas bacterial iron reduction also produces Fe²⁺_(aq) with low δ⁵⁷Fe values (Johnson *et al.*, 2004).

The interest in iron stable isotopes research first came from geosciences, but there are important applications in many other areas, such as ecology and biomedical research (Anbar, 2004), where the iron redox chemistry and speciation are also very important. Variations in δ⁵⁷Fe have been already reported in the food chain and in blood plasma (Zhu *et al.*, 2002; Walczyk and von Blanckenburg, 2002). A study of iron isotopes in blood and tissues (liver and muscle – Walczyk and von Blanckenburg, 2002) reveals that each individual bears a long-term iron isotope signature in the blood – compared to dietary Fe, the isotopic composition of these materials is depleted by up to 3.9‰ in δ⁵⁷Fe. Also, the same authors showed that the δ⁵⁷Fe in the blood of man is, on average, lower by 0.3‰ than that of women.

According to the study of Krayenbuehl *et al.* (2005), patients with hereditary hemochromatosis have their blood characterized by a higher δ⁵⁷Fe than the blood of healthy persons. Iron isotopes (both stable and radioactive) can also be used for diagnosis of hematopoietic disorders (Shreeve, 2007). Hence, research on Fe isotope fractionation has proven to be very useful in biomedicine (Anbar, 2004), as well as in environmental research.

The importance of biogenic and non-biogenic effects in the fractionation between organic and inorganic compounds has always been in debate for isotope systems (Craig, 1954) and it is not different with the iron isotopic system. The investigation of this parameter in natural systems can help to access the contribution of different sources and processes involved during the transport of this element between the different reservoirs. A significant target of this study is to contribute to the available knowledge on this isotopic tracer by enhancing the database available up to the date, which is discussed in this chapter.

2. DATA PRESENTATION

Iron isotope data have been reported in the literature as a standard δ notation (parts per 10³), either relative to terrestrial igneous rocks, or to the IRMM-14 standard (⁵⁷Fe/⁵⁴Fe =

0.36325, available from the Institute of Reference Materials and Measurements, Belgium, Taylor *et al.*, 1992; Taylor *et al.*, 1993):

$$\delta^{57}\text{Fe}/^{54}\text{Fe} = ((^{57}\text{Fe}/^{54}\text{Fe})_{\text{sample}} / (^{57}\text{Fe}/^{54}\text{Fe})_{\text{IRMM-14}}) - 1) * 1000$$

The delta notation may be reported in terms of $\delta^{57}\text{Fe}/^{54}\text{Fe}$ or $\delta^{56}\text{Fe}/^{54}\text{Fe}$ ratios. Data reported in $\delta^{57}\text{Fe}/^{54}\text{Fe}$ values can be converted to $\delta^{56}\text{Fe}/^{54}\text{Fe}$ by multiplying the $\delta^{57}\text{Fe}$ value by 0.667. For data reported relative to average igneous rocks, conversion to IRMM-014 is made by subtracting 0.09 from the $\delta^{56}\text{Fe}$ value or 0.11 from the $\delta^{57}\text{Fe}$ (Johnson *et al.*, 2003; Beard *et al.*, 2003b).

3. AVAILABLE DATA ON THE VARIABILITY AND IRON ISOTOPE FRACTIONATION OF NATURAL MATERIALS

Iron isotopes are naturally fractionated as a result of a number of processes, specially oxy-reduction and organic complexation (Bullen *et al.*, 2001; Johnson *et al.*, 2002; Dideriksen *et al.*, 2008). Improvements in mass spectrometric methods lead to a reproducibility better than 0.1‰ at two standard deviations and allowed the detection and quantification of the natural mass dependent variations in the iron isotopic system (Belshaw *et al.*, 2000; Zhu *et al.*, 2000; Zhu *et al.*, 2001; Zhu *et al.*, 2002; Beard and Johnson, 2004a; Anbar, 2004; Johnson *et al.*, 2004; Johnson *et al.*, 2008). These variations are small compared to other isotope systems, covering a range of approximately 11‰ in $\delta^{57}\text{Fe}$ relative to IRMM-014 (e.g., Anbar, 2004; Beard and Johnson, 2004a; Fantle and DePaolo, 2004; Bergquist and Boyle, 2006; Dauphas and Rouxel, 2006; Ingri *et al.*, 2006; Johnson and Beard, 2006; Anbar and Rouxel, 2007; Rouxel *et al.*, 2008b; Escoube *et al.*, 2009; dos Santos Pinheiro *et al.*, 2013; Ilina *et al.*, 2013), but they may record important shifts on the natural conditions of the environment, such as abiotic and biological redox processes, which are known to produce some of the most significant Fe isotope variations in nature (Johnson *et al.*, 2004; Beard and Johnson, 2004a).

3.1 High Temperature Processes

3.1.1 Extraterrestrial Materials

Vaporization and condensation of Fe can produce significant variability in the Fe isotope composition of extraterrestrial samples. Chondrules, as well as the lunar regolith, define an average $\delta^{57}\text{Fe}$ value of 3.75‰ (Zhu *et al.*, 2001; Mullane *et al.*, 2003a; Kehm *et al.*, 2003; Wiesli *et al.*, 2003). Hezel *et al.* (2010) studied 35 bulk chondrules from three different meteorites and found a different range of Fe isotopic composition for each of them, with the largest variation on $\delta^{57}\text{Fe}$ being from –1.2 to +0.55‰. According to these authors, Fe isotope composition of many chondrules is dominated by the Fe isotope composition of their opaque phases and the Fe isotope variation observed is the result of evaporation and re-condensation processes in a nebula setting with high dust densities.

Poitrasson *et al.* (2005) studied seven bulk chondrites and eleven bulk iron meteorites and showed that their $\delta^{57}\text{Fe}$ values relative to IRMM-14 are slightly different, the former between –0.1‰ and zero and the latter between 0.04‰ and 0.2‰. The same authors also analyzed pallasites (stony iron meteorites) and confirmed what was previously observed in other studies of the same material (Zhu *et al.*, 2001; Mullane *et al.*, 2002; Zhu *et al.*, 2002; Kehm *et al.*, 2003): the iron isotope composition of the metal fraction is isotopically heavier than coexisting olivines. The observed range of $\delta^{57}\text{Fe}$ values, from 0.32‰ to 0.07‰, is, however, larger than that originally reported by Zhu *et al.* (2002).

Lunar rocks define a range of Fe isotope compositions that is similar to those of terrestrial igneous rocks, although slightly higher ($\delta^{57}\text{Fe}$ is 0.09‰ greater than terrestrial rocks). In contrast, the lunar regolith sample has higher $\delta^{57}\text{Fe}$ values compared to those of crystalline lunar rocks, which probably reflect, once again, space weathering processes and Fe loss during vaporization (Wiesli *et al.*, 2003; Poitrasson *et al.*, 2003; Poitrasson *et al.*, 2005).

Bulk-rock analyses of achondrites (*i.e.*, meteorites originated from differentiated planetary bodies) and terrestrial igneous rocks define a relative narrow range of Fe isotope composition (Kehm *et al.*, 2003), whereas bulk calcium aluminum inclusions (CAIs) measured in chondrites have similar Fe isotope compositions to the matrix material analyzed in the same meteorites (Mullane *et al.*, 2003a; Mullane *et al.*, 2003b).

[Poitrasson et al. \(2005\)](#) reported light isotopic composition, depleted by 0.1‰ in $\delta^{57}\text{Fe}$ compared to the average of terrestrial mantle-derived rocks, in samples from Mars and Vesta. On the other hand, the average of fourteen lunar basalts and highland plutonic rocks is heavier by 0.1‰ in $\delta^{57}\text{Fe}$ relative to estimates for the Earth's mantle, and therefore $\sim 0.2\%$ heavier than howardite-eucrite-diogenite (HED) and shergottite-nakhelite-chassigny (SNC) achondritic meteorites. Although the differences are close to the limit of detection, the similarity between SNC and HED and the average of chondritic meteorites, added to the slightly higher $\delta^{57}\text{Fe}$ of the Earth-Moon system, are interpreted as evidence for vaporization, which lead to kinetic iron isotope fractionation, and loss of Fe from the Earth-Moon system during formation of the moon by a giant impactor ([Poitrasson et al., 2004](#); [Poitrasson et al., 2005](#)).

Nevertheless, different explanations for the abundance of heavy iron isotopes of lunar and Earth mantle samples can be found in literature, where other mechanisms of iron isotope fractionation are discussed (*cf.* [Weyer et al., 2005](#); [Beard and Johnson, 2007](#); [Poitrasson, 2007](#); [Weyer et al., 2007](#)). Anyhow, the mass-dependent Fe isotope differences found between planetary bodies are likely to be associated with Fe vaporization during planetary accretion ([Poitrasson et al., 2003](#); [Poitrasson et al., 2005](#)).

3.1.2 Terrestrial Igneous Rocks

The isotopic variability of iron in high-temperature environments is rarely seen in bulk crustal rocks: with the exception of more differentiated granites, the iron isotopic composition of a large variety of igneous rocks is rather constant ($\delta^{57}\text{Fe} = 0.1 \pm 0.03\%$, 1σ – **Fig. 6**, [Beard et al., 2003b](#); [Poitrasson et al., 2004](#); [Poitrasson and Freydier, 2005](#); [Poitrasson et al., 2005](#); [Poitrasson, 2006](#)). This was shown by the identical $\delta^{57}\text{Fe}$ in the average of 43 igneous rocks that range in composition from peridotite to high-silica rhyolite ([Beard and Johnson, 2004a](#)) and these data most likely reflect homogenization during magma generation, although there may be other possible explanations.

Carbonatites record significant isotopic fractionation between carbonate, oxide, and silicate minerals, defining the largest range in Fe isotope compositions yet measured for igneous rocks. For instance, calcite from carbonatites have $\delta^{57}\text{Fe}$ values between -1.5 and $+1.2\%$, a range that is similar to the range defined by whole-rock samples of carbonatites. These differences probably took place during generation in the mantle and subsequent

differentiation and therefore, iron isotopic measurements in these environments are a valuable tracer of redox conditions (Johnson *et al.*, 2009).

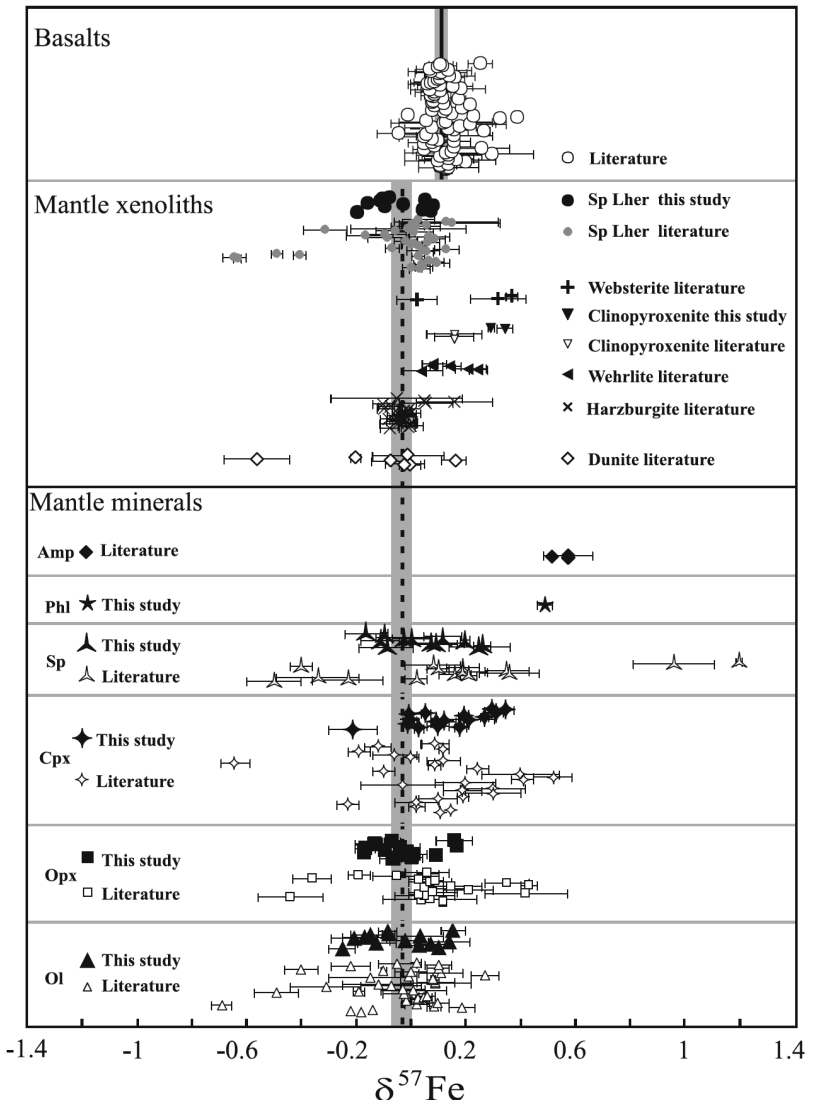


Fig. 6 - Fe isotope compositions of mantle minerals, xenoliths, and basalts (from Zhao *et al.*, 2009). The solid and dashed lines give the weighted mean of all the available data for mantle xenoliths and basalts, respectively. The gray bands represent 2 standard error uncertainties of the representative mean mantle xenoliths and basalts. Data from Zhu *et al.* (2002); Rouxel *et al.* (2003); Beard *et al.* (2003b); Poitrasson *et al.* (2004); Williams *et al.*, (2004); Beard and Johnson (2004a); Williams *et al.* (2005); Weyer *et al.* (2005); Schoenberg and von Blanckenburg (2006); Weyer and Ionov (2007); Teng *et al.* (2008); Schuessler *et al.* (2009); Zhao *et al.* (2009). Ol olivine; Opx orthopyroxene; Cpx clinopyroxene; Sp spinel; Amp amphibole; Phl phlogopite; Sp Lher Sp Lherzolite. The horizontal dashed and solid lines with gray bands represent the weighted average values and two standard deviation of mantle xenoliths and basalts, respectively. Data from Beard *et al.* (2003b); Beard and Johnson (2004a) are recalculated to a common Fe isotope composition for the IRMM-014 standard through $\delta^{57}\text{Fe}_{\text{IRMM-014}} = \delta^{57}\text{Fe}_{\text{igneous rocks}} + 0.11$. Data from Weyer *et al.* (2005); Weyer and Ionov (2007) are recalculated to $\delta^{57}\text{Fe}$ through $\delta^{57}\text{Fe}_{\text{IRMM-014}} = 1.5 \times \delta^{56}\text{Fe}_{\text{igneous rocks}}$.

Well preserved komatiites from Alexo (Canada), representatives of high-degree of mantle partial melting (50%), were studied by Dauphas *et al.* (2010), who observed that the

bulk flow of these materials shows positive $\delta^{57}\text{Fe}$ values ($+0.059 \pm 0.044\text{\textperthousand}$), a result that is consistent with minor fractionation during komatiite magma genesis.

The study conducted by [Dauphas et al. \(2009\)](#) shows that mid-ocean ridge and oceanic-island basalts (MORBs and OIBs) have slight, but distinctly higher $\delta^{57}\text{Fe}$ ratios ($\sim +0.09\text{\textperthousand}$) than both modern and Eoarchean boninites and many island arc basalts (IABs). Additionally, boninites and many IABs have iron isotopic compositions similar to chondrites and fertile mantle peridotites, Eoarchean mantle peridotites, and basalts from Mars and Vesta. According to [Dauphas et al. \(2009\)](#), the best explanation for the observed variations is that there is a preferential extraction of isotopically heavier and incompatible Fe^{3+} during mantle melting to form oceanic crust (represented by MORBs and OIBs), and therefore, the iron isotopic composition of the bulk silicate Earth shows $\sim +0.3\text{\textperthousand}$ equilibrium isotope fractionation between Fe^{3+} and Fe^{2+} .

[Poitrasson and Freydier \(2005\)](#) analyzed bulk granitic rocks and found that those with MgO contents below 0.6 wt.% and SiO_2 above 71 wt.% have $\delta^{57}\text{Fe}$ values significantly heavier than the bulk mafic Earth. They also showed that there is a positive correlation between the Fe isotope composition and decreasing MgO or increasing SiO_2 contents of the granitoids, fact that was interpreted as a result of late magmatic aqueous fluid exsolution from the granitic melt, with a preferential removal of the lighter iron isotopes, which lead to the enrichment of heavier isotopes in the residual magma.

Iron isotopes can also be helpful to determine rocks protoliths. [Dauphas et al. \(2004a\)](#) and [Dauphas et al. \(2007a\)](#) found that early Archean banded rocks from Isua, Akilia, and Innersuartuut, Greenland, which experienced granulite facies metamorphism in the early Archean, were enriched in heavy iron isotopes relative to igneous rocks worldwide. According to the authors, those signatures are compatible with transport, oxidation, and subsequent precipitation of ferrous iron emanating from hydrothermal vents, what suggest that the original rocks were banded iron formations (BIFs), and therefore, the Akilia banded rocks would have a sedimentary origin.

Metamorphic rocks (amphibolites, quartz-biotite and pelitic schists, orthogneisses, and banded quartz-magnetite-amphibole/pyroxene rocks) were studied by [Dauphas et al. \(2007b\)](#), who concluded that these metasedimentary rocks from Quebec (Canada) are enriched in heavy Fe isotopes. These authors used iron isotope signatures to constrain the protolith of these rocks and showed that, at least the quartz-magnetite-amphibole / pyroxene rocks analyzed are chemical sediments (*i.e.*, BIFs), formed by precipitation of dissolved ferrous iron

in a marine environment. They interpreted the dispersion in Fe isotope compositions, at a bulk sample scale in these BIFs, as a product of binary mixing between Fe-oxides and carbonates.

3.1.2.1 Inter-mineral fractionation

The partitioning of iron between mantle minerals at high temperatures also fractionates iron isotopes. Inter-mineral fractionations are very common in natural materials and represent the largest records reported, suggesting that Fe isotopes can be used to constrain conditions and processes such as magmatic differentiation, partial melting and metasomatism (Zhu *et al.*, 2002; Beard and Johnson, 2003; Weyer *et al.*, 2005; Williams *et al.*, 2005; Weyer and Ionov, 2007; Teng *et al.*, 2008; Dauphas *et al.*, 2009; Craddock *et al.*, 2010). Significant Fe isotope variability ($\sim 0.75\text{\textperthousand}$ in $\delta^{57}\text{Fe}$) is reported in some mantle-derived rocks, where inter-mineral differences in Fe isotope compositions appear to reflect an open-system behavior for olivine, orthopyroxene, and clinopyroxene from spinel peridotites (Beard and Johnson, 2004a; Beard and Johnson, 2004b).

Studies of iron isotopic composition carried out on mantle peridotites (Zhu *et al.*, 2002; Poitrasson *et al.*, 2004; Beard and Johnson, 2004a; Williams *et al.*, 2004; Weyer *et al.*, 2005; Williams *et al.*, 2005; Schoenberg and von Blanckenburg, 2006; Weyer and Ionov, 2007; Zhao *et al.*, 2009; Dauphas *et al.*, 2009) show that the Fe isotope variations exist between minerals within a single sample and between mantle xenoliths. This confirms that the lithosphere mantle has distinguishable and heterogeneous iron isotopic compositions at the xenolith scale. For all these authors, mantle metasomatism is the most likely cause of iron isotope variations in mantle peridotites.

The study conducted by Zhao *et al.* (2009) reports overall variations in $\delta^{57}\text{Fe}$ ranges from: -0.25 to $+0.14\text{\textperthousand}$ for olivine, -0.17 to $+0.17\text{\textperthousand}$ for orthopyroxene, -0.21 to $+0.27\text{\textperthousand}$ for clinopyroxene, and -0.16 to $+0.26\text{\textperthousand}$ for spinel. Within individual samples, clinopyroxene presents the heaviest iron isotopic ratio and olivine the lightest.

Dauphas *et al.* (2010) observed that the olivine separated from a cumulate sample presents light $\delta^{57}\text{Fe}$ and slightly heavy $\delta^{26}\text{Mg}$ values relative to the bulk flow of well-preserved komatiites from Canada. The authors suggest that kinetic isotope fractionation associated with Fe-Mg inter-diffusion in olivine is responsible for the effect observed.

Other reports of small (typically $< 0.75\text{\textperthousand}$) variations in $\delta^{57}\text{Fe}$ between igneous minerals were made by [Zhu et al. \(2002\)](#); [Poitrasson et al. \(2003\)](#); [Beard and Johnson \(2003\)](#), and these include $\delta^{57}\text{Fe}$ variations of $\sim 0.3\text{\textperthousand}$ between Fe metal and olivine in pallasite meteorites and $\sim 0.6\text{\textperthousand}$ between amphibole and olivine in terrestrial mantle xenoliths.

3.2 Low Temperature Processes

According to [Beard and Johnson \(2004b\)](#), calculated fractionation factors in low temperatures (0 to 250°C) indicate that ferric Fe-bearing phases (aqueous or solid, e.g., $[\text{Fe}^{3+}(\text{H}_2\text{O})_6]^{3+}$, $[\text{Fe}^{3+}(\text{H}_2\text{O})_4\text{Cl}_2]^+$, $[\text{Fe}^{3+}\text{Cl}_4]^-$ or magnetite, hematite, goethite, and lepidocrocite) will have higher $\delta^{57}\text{Fe}$ values than ferrous Fe-bearing phases (e.g., $[\text{Fe}^{2+}(\text{H}_2\text{O})_6]^{2+}$ or siderite, ankerite, and silicates such as olivine – [Schauble, 2004](#); [Beard and Johnson, 2004b](#)). On the other hand, [Skulan et al. \(2002\)](#) found no significant isotopic contrast between hematite and Fe^{3+} during slow precipitation of hematite in aqueous Fe^{3+} , what may suggest that flocculation of Fe particles in estuaries does not produce significant Fe isotope fractionation.

Low- C_{org} clastic sedimentary materials deposited in oxic environments, such as loess, turbidites and grey shales, display very homogenous Fe isotope compositions, indicating the conservative behavior of Fe during weathering under oxygenated surface conditions. On the other hand, organic-C rich sedimentary rocks, for which diagenesis occurred under anoxic conditions, like black shales ([Yamaguchi et al., 2003](#); [Matthews et al., 2004](#)) and chemically precipitated sediments, have varied $\delta^{57}\text{Fe}$ values, which is interpreted as a result of partitioning between minerals and Fe^{2+} -rich fluids ([Beard and Johnson, 2004a](#); [Beard and Johnson, 2004b](#)).

The largest variations in Fe isotope compositions in low temperature environments are associated with chemically precipitated sediments such as Pliocene to recent Fe-Mn crusts ([Zhu et al., 2000](#)) and Archean/Proterozoic age banded iron formations (BIFs; [Johnson et al., 2003](#)). Marine ferromanganese nodules and Precambrian BIFs show variations in $\delta^{57}\text{Fe}$ that range from -2.4 to $+1.35\text{\textperthousand}$, respectively, relative to the mean of approximately 30 terrestrial and lunar basalts ([Anbar, 2004](#)).

A high-precision iron isotope time series analysis made by [Zhu et al. \(2000\)](#) for a ferromanganese crust demonstrates that the iron isotope composition of the North Atlantic Deep Water has changed substantially over the past 6 million years. They observed a close

correlation of iron and lead isotope compositions in hydrogenous ferromanganese crusts, suggesting that the observed iron isotope variations predominantly reflect an iron input from terrigenous sources, providing no evidence for biologically induced mass fractionation in the North Atlantic Deep Water. Their study shows a range of variation of $\sim 2.2\text{\textperthousand}$, with layers that span an age from 6 to 1.7 Ma showing a constant Fe isotope composition ($\delta^{57}\text{Fe} = -1.55 \pm 0.75\text{\textperthousand}$), while layers younger than 1.7 Ma have increasing $\delta^{57}\text{Fe}$ values with decreasing age, up to a value of $+0.06\text{\textperthousand}$ at 0.15 Ma. The authors suggested that the variations reflect isotopic variability in the continental sources of Fe fluxes to the oceans. However, [Levasseur et al. \(2004\)](#) found no evidence that the observed oceanic Fe isotopic heterogeneity in marine hydrogenetic ferromanganese deposits is controlled by variations in continental sources.

Individual layers in Late Archean to paleoproterozoic BIFs have variable Fe isotope compositions correlated with mineralogy, where the $\delta^{57}\text{Fe}$ values increase in the following order: pyrite - Fe carbonates - hematite - magnetite ([Johnson et al., 2003](#)). Also, [Vieira et al. \(2010\)](#) found considerable variations in paleoproterozoic BIFs from the Quadrilátero Ferrífero (Brazil), with $\delta^{57}\text{Fe}$ values ranging from $-1.493 \pm 0.034\text{\textperthousand}$ and $-0.061 \pm 0.050\text{\textperthousand}$ relative to IRMM-14. These results refer to BIF samples with different mineralogical associations, where siliceous BIFs would be isotopically lighter than BIFs intermingled with carbonates.

3.2.1 Soil and Aqueous Systems

Some studies have been carried out on the compositional variations and fractionation of iron isotopes in rivers, oceans, lakes, aquifers and soil systems ([Zhu et al., 2000](#); [Rouxel et al., 2005](#); [Teutsch et al., 2005](#); [Emmanuel et al., 2005](#); [Staubwasser et al., 2006](#); [Severmann et al., 2006](#); [Ingri et al., 2006](#); [Bergquist and Boyle, 2006](#); [Wiederhold et al., 2007a](#); [Wiederhold et al., 2007b](#); [Poitrasson et al., 2008](#); [Fehr et al., 2008](#); [Severmann et al., 2008](#); [Rouxel et al., 2008b](#); [Escoube et al., 2009](#); [Severmann et al., 2010](#); [Song et al., 2011](#); [dos Santos Pinheiro et al., 2013](#); [Ilina et al., 2013](#)) but there are still many open questions about the biogeochemical cycle of iron ([Song et al., 2011](#)).

According to [Fantle and DePaolo \(2004\)](#), reactions within soils produce both isotopically light and heavy Fe, where biological processes, such as the growth of surface vegetation and synthesis of organic ligands, produce a source of isotopically light, relatively mobile Fe, that can be transported to streams via soil pore waters.

[von Blanckenburg \(2000\)](#) investigated Fe isotopes in a podzol formed in an alluvial soil sequence that consists of 95% of Fe-coated detrital quartz (Maas catchment, the Netherlands). They found $\delta^{57}\text{Fe}$ variations in the podzol sequence, of approximately 1.5‰ between the surface (Ah layer) and the C-horizon, which has the highest measured values within the area of the dark alluvial horizon. On the other hand, [Poitrasson et al. \(2008\)](#) showed that lateritic soils from Southern Cameroon, that have typically $\geq 96\%$ of its iron held in nanocrystalline hematite and goethite, display iron isotope signatures very close to the mean crustal value, with a maximum range of 0.2‰ in $\delta^{57}\text{Fe}$.

[Guelke et al. \(2010\)](#) studied the Fe isotopic composition of different soil mineral pools (exchangeable iron, iron of poorly-crystalline (oxy-hydr)oxides, iron in organic matter, iron of crystalline oxides and silicate bound iron) and found variations of about 1.5‰ in $\delta^{57}\text{Fe}$ between these different pools. In the water-extractable- and exchangeable iron fractions, iron in organic matter and iron of poorly-crystalline (oxy-hydr)oxides are about 0.45‰ lighter than bulk soils. Silicates have a $\delta^{57}\text{Fe}$ of up to 0.6‰, what suggests preferential loss of light Fe during weathering. As the studied pools contribute to plant nutrition, they may as well record the Fe isotope composition of plant-available iron in soils.

Iron isotopes were used to investigate iron transformation processes during an *in situ* field experiment for removal of dissolved Fe from reduced groundwater ([Teutsch et al., 2005](#)). The experiment consisted of injecting oxygen-bearing water at a test well into an aquifer containing Fe^{2+} -rich reduced water, what would lead to oxidation of Fe^{2+} and precipitation of Fe^{3+} (hydr)oxides. A series of injection-extraction (push-pull) cycles were performed at the same well. The authors showed that the $\delta^{57}\text{Fe}$ of the background groundwater ($- 0.6 \text{ ‰}$) is lighter by 0.3 ‰ from the aquifer material leach, what they attributed to microbial mediated reductive dissolution of Fe^{3+} (hydr)oxides.

The volcanic Lake Nyos (Cameroon) was studied by [Teutsch et al. \(2009\)](#), who observed an increase in $\delta^{57}\text{Fe}$ from the surface to the bottom of the lake, across the oxic-anoxic boundary. They showed that at 55 m depth, iron concentration and $\delta^{57}\text{Fe}$ are, respectively, $\sim 1 \text{ mg.L}^{-1}$ and $- 1.88\text{ ‰}$, whereas at the bottom of the lake (over 200 m depth), the same parameters are 3.44 mg.L^{-1} and $+ 0.83\text{ ‰}$. The strong shift in $\delta^{57}\text{Fe}$ was attributed to isotopic fractionation via dissimilatory Fe reduction across the oxic-anoxic boundary of the lake, whereas the shift towards more positive values below the oxic-anoxic interface was attributed to vertical mixing of a heavier component from the bottom of the lake.

Iron isotope compositions of suspended particulate matter from the Aha Lake, an artificial lake in southern China (karst area of Yun-Gui Plateau) and its tributaries were investigated during summer and winter (Song *et al.*, 2011). These authors showed there is a seasonal variation in the $\delta^{57}\text{Fe}$ values of suspended matter from both the lake and the rivers studied. Lake's samples display a range from $-2.04\text{\textperthousand}$ to $-0.15\text{\textperthousand}$ in the summer and from $-0.45\text{\textperthousand}$ to $-0.105\text{\textperthousand}$ in the winter, while river's samples vary from $-1.32\text{\textperthousand}$ to $0.105\text{\textperthousand}$ during the summer and from $-0.525\text{\textperthousand}$ to $-0.045\text{\textperthousand}$ in the winter. They also found a good negative correlation between $\delta^{57}\text{Fe}$ values and Fe/Al ratios for one station, and suggest that these parameters together can be used as good indicators of the redox-driven Fe transformations.

3.2.2 Porewaters, Oceans and Rivers

Redox cycling of Fe in reduced sediments and subterranean estuaries show negative signatures in surface porewaters, with $\delta^{57}\text{Fe}$ values down to $-7.5\text{\textperthousand}$ (Severmann *et al.*, 2006; Rouxel *et al.*, 2008b). Dissolved Fe concentrations in subterranean estuaries, like their river-seawater counterparts, are strongly controlled by non-conservative behavior during mixing of groundwater and seawater in coastal aquifers (Rouxel *et al.*, 2008b). The groundwater source has high Fe^{2+} concentration, consistent with anoxic conditions, and yield $\delta^{57}\text{Fe}$ values between 0.45 and $-1.95\text{\textperthousand}$. In contrast, sediment porewaters occurring in the mixing zone of the subterranean estuary have very low $\delta^{57}\text{Fe}$ values down to $\sim -7.5\text{\textperthousand}$. The low $\delta^{57}\text{Fe}$ values reflect Fe-redox cycling and result from the preferential retention of heavy Fe-isotopes onto newly formed Fe-oxy-hydroxides (Rouxel *et al.*, 2008b). Porewaters were also studied by Severmann *et al.* (2006), who observed a large range in dissolved Fe isotope compositions for $\text{Fe}^{2+}_{(\text{aq})}$: generally, the lowest $\delta^{57}\text{Fe}$ values are near the sediment surface (minimum of $-4.5\text{\textperthousand}$), and they increase with burial depth, what they interpret as an open-system behavior that involves extensive recycling of Fe.

In open modern oxic oceans, Fe contents are extremely low, typically between 0.1 and 1.0 nanomolar (*e.g.*, Martin and Gordon, 1988; Bruland *et al.*, 1991; Martin, 1992; Johnson *et al.*, 1997). Fluxes of dissolved or colloidal riverine iron to open oceans are $\sim 3 \times 10^9 \text{ mol yr}^{-1}$, whereas iron as detrital or suspended load is approximately 1.2 to $1.8 \times 10^{13} \text{ mol yr}^{-1}$ (Poulton and Raiswell, 2002). Also, it is recognized that marine productivity is Fe-limited in parts of the open oceans (*e.g.*, Martin and Fitzwater, 1988; Martin *et al.*, 1989; Martin *et al.*, 1994).

The Fe isotopic composition of seawater may rapidly change if the iron isotopic signature of the material delivered to the oceans varies, or if relative fluxes of Fe that have distinct Fe isotope compositions changes (Beard *et al.*, 2003a), specially due to the short residence time of Fe in seawater (Johnson *et al.*, 1997). Anyhow, sources and sinks of iron, as well as redox and/or biological cycles, can also be investigated for materials that have very small contents of iron, like oceanic dissolved matter. The study of the oceanic Fe cycle is possible thanks to the techniques available nowadays, which allow the detection of very small variations in the isotopic composition of iron.

Lacan *et al.* (2008) found isotopic variations of 0.51‰ in modern open oceans, with values from – 0.19 to + 0.32%. For these authors, the light $\delta^{57}\text{Fe}$ found in the dissolved fraction reflects the remineralization of organic matter. In a later study, Lacan *et al.* (2010) measured dissolved iron isotopic ratios with a MC-ICP-MS Neptune, coupled with a desolvator (Aridus II or Apex-Q), using the ^{57}Fe - ^{58}Fe double spike to correct the mass bias. They showed that the range of variation observed in the ocean is about 2.5‰, while their measurement precision is only about 3% of this range.

Following Lacan *et al.* (2008), John and Adkins (2010) developed analytical procedures to optimize $\delta^{57}\text{Fe}$ isotopic analysis by MC-ICP-MS in iron from seawater. They employ bulk extraction of Fe from seawater with an NTA-resin and use miniaturized columns for anion exchange chromatography. The authors state that this method has sufficiently high recovery, low blanks and no isotopic fractionation during processing, so it is possible to measure the iron isotopic composition of dissolved seawater from typical open oceans, with a good predicted accuracy for measurements ranging from 0.3‰ to 0.075‰ (2σ , $\delta^{57}\text{Fe}$).

Rouxel and Auro (2009) studied the iron isotope variation in coastal seawater and stated that dissolved Fe displayed a non-conservative behavior due to colloid flocculation, what is in opposition to the study conducted by Escoube *et al.* (2009) for the North River, Massachusetts (described in more detail in section 3.2.2.1). Preliminary results obtained by Rouxel and Auro (2009) show that iron in coastal seawater, derived from benthic diagenesis and/or groundwater, have light isotope signatures down to – 1.35‰, which are distinct from other iron sources, such as atmospheric deposition and rivers.

As one of the major fluxes of Fe that are delivered to the oceans comes from riverine iron (Beard *et al.*, 2003a), it is very important to determine the Fe isotope composition in these environments, as they provide information on the several sources available, such as soils and vegetation. According to Rouxel and Auro (2009), riverine inputs to the ocean have a

range of $\delta^{57}\text{Fe}$ values between -1.5 and $0.9\text{\textperthousand}$ (Fantle and DePaolo, 2004; Bergquist and Boyle, 2006; Ingri *et al.*, 2006; Escoube *et al.*, 2009; Song *et al.*, 2011; dos Santos Pinheiro *et al.*, 2013; Ilina *et al.*, 2013 and data further presented in this study) while non-anthropogenic atmospheric input yield $\delta^{57}\text{Fe}$ values similar to crustal values (Beard *et al.*, 2003a). This variability may reflect leaching of mobile Fe components from soils during weathering.

Isotope fractionation of Fe in rivers may take place by equilibrium speciation, precipitation of colloidal Fe^{3+} , and sorption of dissolved Fe onto particle surfaces (Fantle and DePaolo, 2004). Recent studies have suggested that rivers may present an isotopically light Fe source to the oceans, but according to Escoube *et al.* (2009) the global riverine source into the ocean can display both heavier and lighter $\delta^{57}\text{Fe}$ values. Indeed, Fe reaching the oceans in the form of detrital particles may be relatively unfractionated (Beard *et al.*, 2003a; dos Santos Pinheiro *et al.*, 2013), while dissolved Fe entering via rivers may exhibit isotopic variability related to weathering (Fantle and DePaolo, 2004; Bergquist and Boyle, 2006).

3.2.2.1 Dissolved and Particulate Matter in Rivers

The iron isotopic composition of the particulate matter in fresh waters is reported to be correlated with the percentage of Fe flocculation and characterized by lighter $\delta^{57}\text{Fe}$ values than for dissolved Fe, which, in their turn, are characterized by higher $\delta^{57}\text{Fe}$ values (up to $0.65\text{\textperthousand}$, Escoube *et al.*, 2009). In this work, iron isotopic composition in the North River (Massachusetts, USA) was studied, and particulate $\delta^{57}\text{Fe}$ values vary from $\sim -0.135\text{\textperthousand}$ at no flocculation to $\sim 0.15\text{\textperthousand}$ at the flocculation maximum, which reflect mixing effects between river-borne particles, lithogenic particles derived from coastal seawaters and newly precipitated colloids.

On the other hand, dissolved iron in the North River has an average $\delta^{57}\text{Fe}$ value of $0.65 \pm 0.06\text{\textperthousand}$ relative to the IRMM-14, and these values do not display any relationship with percentage of colloid flocculation. It was therefore suggested that the pristine iron isotope composition of fresh water is preserved during estuarine mixing and that the value of the global riverine source into the ocean can be identified from the fresh water values (Escoube *et al.*, 2009).

Results for igneous rocks and suspended river loads are compared, although in $\delta^{56}\text{Fe}$ values ($\delta^{57}\text{Fe} = 1.5 \times \delta^{56}\text{Fe}$), to the modal fraction of ferric oxide/hydroxide in suspended river loads (Fig. 7, Beard and Johnson, 2004b). Bulk water from rivers with large suspended

loads also has $\delta^{57}\text{Fe}$ values close to zero ([Fantle and DePaolo, 2004](#)). These authors suggest that the net effect of continental weathering under modern oxidizing surface conditions is to mobilize small amounts of isotopically lighter $\delta^{57}\text{Fe}$ in an exchangeable, or dissolved, form, which is transported in and from rivers in solution to the oceans, leaving behind continental residues which are isotopically similar to or slightly heavier than the parent material.

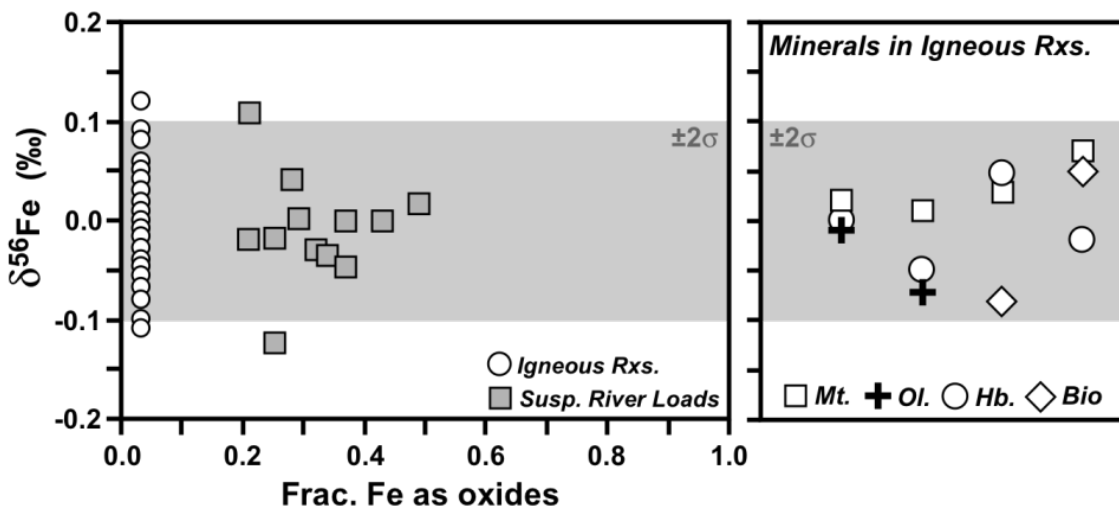


Fig. 7 - Comparison of $\delta^{56}\text{Fe}$ values for bulk igneous rocks, suspended river loads and individual minerals from volcanic rocks (right panel). Left panel shows the fraction of Fe that exists as oxides (data for igneous rocks arbitrarily plotted as 0.02). Right panel shows $\delta^{56}\text{Fe}$ values for coexisting magnetite, olivine, hornblende and biotite in four volcanic rocks. Data from [Canfield \(1997\)](#); [Beard and Johnson \(2004a\)](#); [Beard and Johnson \(2004b\)](#).

According to [Beard and Johnson \(2004b\)](#), as there are no large differences in the isotopic compositions of oxides and various silicate minerals in igneous rocks, differential weathering is unlikely to produce significant Fe isotope variability. Anyhow, it is possible that weathering in the presence of organic ligands produces Fe isotope fractionations ([Brantley *et al.*, 2001](#)).

As previously mentioned, temporal variations in iron isotopic composition of a boreal river (Kalix River, Northern Sweden) were investigated by [Ingrı *et al.* \(2006\)](#). They measured $\delta^{57}\text{Fe}$ in the suspended fraction, which ranged between $-0.195\text{\textperthousand}$ and $0.465\text{\textperthousand}$, along one complete hydrological cycle. They attributed the differences to the presence and variable influence of two types of materials with different hydrogeochemical origin and, therefore, different Fe-isotope compositions: the Fe-C material has a negative $\delta^{57}\text{Fe}$ value whereas the Fe-oxy-hydroxide material is enriched in $\delta^{57}\text{Fe}$.

Nevertheless, isotopic variations of around 2.25‰ in $\delta^{57}\text{Fe}$ were also reported by Bergquist and Boyle (2006) between different types of tributaries of the Amazon River. Dissolved and suspended loads of Fe from the mouth of the Amazon River at Macapá and upstream of Manaus, at the Solimões River, were isotopically similar (~ -0.15 to $-0.45\text{\textperthousand}$), whereas for the Negro River, these fractions show distinct values, with the dissolved load slightly isotopically heavy (+0.45‰) and the suspended load isotopically light ($-1.35\text{\textperthousand}$).

4. PANORAMA AND PERSPECTIVES

Equilibrium isotope fractionation between organic and inorganic Fe complexes, as well as kinetic isotope effects are significant, and therefore, should be investigated in all possible natural systems. It has been shown that there is a $\delta^{57}\text{Fe}$ fractionation of $\sim 1.5\text{\textperthousand}$ during rapid, out of equilibrium, precipitation of hematite from dissolved Fe^{3+} (Skulan *et al.*, 2002), which favors light isotopes onto the precipitate. Equilibrium isotope fractionation is the explanation given for a fractionation of $\sim 0.9\text{\textperthousand}$ during abiotic leaching of Fe from hornblende in the presence of strong chelating ligands (Brantley *et al.*, 2001). Experimental fractionation is also reported during anion exchange chromatography of Fe in HCl media (Anbar *et al.*, 2000; Roe *et al.*, 2003), where variations of $\delta^{57}\text{Fe}$ may be as high as $\sim 10\text{\textperthousand}$ and are also attributed to equilibrium fractionation between coexisting Fe^{3+} chloro-aquo complexes.

The studies available on iron isotopes in different materials indicate that, despite important controversies (e.g., cf. Skulan *et al.*, 2002; Escoube *et al.*, 2009; Rouxel and Auro, 2009), environmental chemistry and biochemistry in nature can produce significant variations in $\delta^{57}\text{Fe}$. Redox reactions are particularly important, as it was shown that equilibrium fractionation between $\text{Fe}(\text{H}_2\text{O})_6^{2+}$ and $\text{Fe}(\text{H}_2\text{O})_6^{3+}$ include the entire range of observed natural variations (Anbar, 2004).

The study of iron isotopes in river systems can be useful to constrain if Fe in poorly crystalline or labile components in the suspended river loads is isotopically variable, or if the dissolved load of Fe is isotopically distinct from bulk crustal sources (Beard and Johnson, 2004a). As iron isotopic composition of distinct reservoirs are different (Beard and Johnson, 2004a; Severmann *et al.*, 2006), this tool can be used to investigate the different iron sources

that are involved in the transport mechanisms of this element to the oceans ([Zhu et al., 2000](#); [Beard et al., 2003a](#)).

The ability to understand measured variations of iron isotope in nature is still limited, but the studies conducted in the past few years are helping to improve the database of well-constrained Fe isotope fractionation factors. Additionally to laboratory experiments, it is very important to investigate and determine the iron isotope signatures of natural samples (both aqueous phases and minerals). Analyses of materials that have low Fe contents, such as pore fluids or seawater, is challenging. Nevertheless, techniques are evolving and necessary precision was already achieved (e.g., [Lacan et al., 2008](#); [Lacan et al., 2010](#)). Iron isotopic signatures have proven to be useful to constrain the oxygenation of the ocean and atmosphere ([Johnson et al., 2003](#); [Dauphas et al., 2004a](#); [Rouxel et al., 2005](#); [Frei and Polat, 2007](#); [Tangalos et al., 2010](#)) and many more applications for this tool are to come in the next few years. As stated by [Lacan et al. \(2008\)](#), insights into the Fe cycle, such as iron speciation, dissolved/particulate fluxes or biological processes, can be accessed and unraveled as the ability to understand measured Fe isotope variations continues to improve.

Iron isotope measurements are in routine at the Geochronology Laboratory of the UnB, Brazil, along with some two-dozen other laboratories around the world ([Johnson et al., 2008](#)). A study of suspended matter iron isotopes in waters of the Amazon River and its major tributaries was carried out in an international cooperation project between this laboratory, the GET Laboratory (France) and the ORE-HYBAm (IRD and INSU environmental stations network, which covers most of the Amazon Basin).

Suspended matter samples of the Amazon River Basin rivers were collected in order to investigate the variability of this parameter according to geography, depth, lateral and temporal profiles, as well as hydrology and geochemistry related to these waters. The isotopic approach will help to provide a better understanding of the iron mass balance in the Amazonian Basin and its mechanisms of chemical transfer from continent to rivers and oceans, as well as enhance the database on the isotopic variability of natural materials.

CAPÍTULO QUATRO

ANALITICAL METHODS FOR IRON ISOTOPIC DATA ACQUISITION

1. INTRODUCTION

Non-traditional isotopes analyses are generally made using three main types of mass spectrometers: *i*) Gas Source Mass Spectrometer, when elements that can easily be introduced as gases, such as Cl or Br and *ii*) Thermal-Ionization Mass Spectrometer (TIMS) or *iii*) Multi-Collector Inductively Coupled Plasma Mass Spectrometer (MC-ICP-MS), when the elements to be analyzed are metals ([Albarède and Beard, 2004](#)).

The main difference between these instruments is the sample introduction and ionization. The analyzer part of each instrument, on the other hand, is similar. The three types of instruments are composed by a stack of lenses with variable potential to focus the ion beam, a magnet to separate the ion beam into different masses, and a series of collectors to measure ion currents of different isotopes simultaneously ([Albarède and Beard, 2004](#)).

The first studies of Fe isotope composition were made using SIMS ([Hutcheon *et al.*, 1987](#)) and multi or single collection TIMS (*e.g.* [Turnlund and Keyes, 1990](#); [Taylor *et al.*, 1992](#); [Walczyk, 1997](#); [Johnson and Beard, 1999](#); [Nabelek *et al.*, 1992](#); [Dixon *et al.*, 1993](#)). At that time, the double-spike method with TIMS was usual (*e.g.*, [Johnson and Beard, 1999](#); [Beard and Johnson, 1999](#); [Beard *et al.*, 1999](#); [Mandernack, 1999](#); [Bullen *et al.*, 2001](#)). Nowadays the most common technique is the Multi-Collector Inductively Coupled Plasma Mass Spectrometer (MC-ICP-MS - *e.g.* [Belshaw *et al.*, 2000](#); [Sharma *et al.*, 2001](#); [Kehm *et al.*, 2003](#); [Beard *et al.*, 2003a](#); [Beard *et al.*, 2003b](#); [Lacan *et al.*, 2008](#); [Lacan *et al.*, 2010](#), among others).

TIMS-based double-spike analyses were useful because there are relatively few isobaric interferences associated with this technique, except for elemental isobars from ^{54}Cr on ^{54}Fe and ^{58}Ni on ^{58}Fe ([Albarède and Beard, 2004](#)). Thus, to measure iron isotope composition of natural materials, the advantages were considerable: instrumental mass fractionation were not difficult to correct, memory effects associated with the instrument were

low, and the relatively small interferences could be resolved from the sample signal ([Fantle and Bullen, 2009](#)).

On the other hand, the difficulty to ionize Fe in a thermal ionization source, which necessitates relatively large sample sizes, made the scientific community embrace the MC-ICP-MS for measuring iron isotopes, which is an equipment that requires a relatively small sample size compared to the TIMS ([Fantle and Bullen, 2009](#)).

Despite a large mass bias in ICP systems (1-2% / amu, [Anbar, 2004](#)), a number of advantages apply to the study of stable isotopes by MC-ICP-MS ([Halliday et al., 1995](#); [Anbar, 2004](#)), and methods that avoid the use of a double spike for Fe and other systems have simplified analytical procedures ([Anbar et al., 2000](#); [Belshaw et al., 2000](#); [Beard et al., 2003a](#); [Beard et al., 2003b](#); [Poitrasson and Freydier, 2006](#); [Poitrasson et al., 2008](#), among others). More information on primary advantages and disadvantages of TIMS and MC-ICP-MS are detailed in [Walczuk \(2004\)](#) and references therein.

2. MULTI-COLLECTOR INDUCTIVELY COUPLED PLASMA MASS SPECTROMETER (MC-ICP-MS)

A mass spectrometer is an instrument designed to separate charged atoms and molecules on the basis of their masses motions in electrical and/or magnetic fields, and these instruments employ electronic methods for detection of the separated ions ([Faure, 1986](#)).

The ICP source produces precise isotopic compositions even for poorly ionizing elements, such as Fe, Cu, Zr, Hf and W, due to its ability to ionize nearly all elements in the periodic table. Essentially all MC-ICP-MS instruments are run in the static mode, a condition where the transmission of an ion beam depends on both the trajectory and the collection device associated with each individual isotope ([Albarède et al., 2004](#)).

The only elements that are poorly ionized by the Ar source are the ones that have an ionization potential greater than Ar (15.76 eV – **Fig. 8**), whereas elements with an ionization potential less than 7 eV are completely ionized. Mass-dependent fractionation in the torch can happen, but they are rather associated with vaporization and atomization processes in the Ar plasma, than a result of ionization ([Albarède and Beard, 2004](#)).

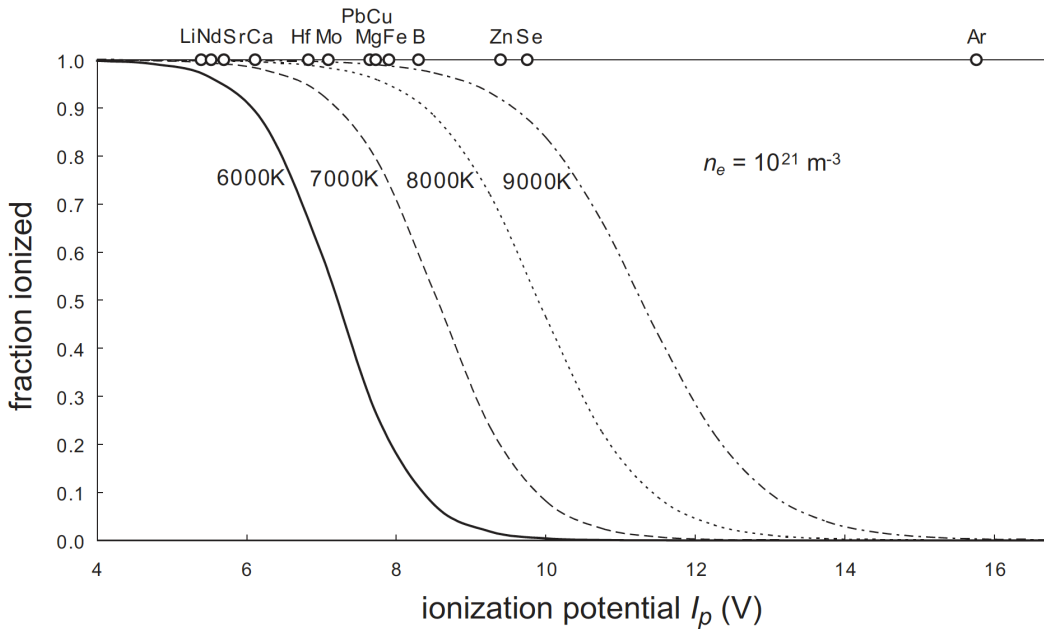


Fig. 8 - Efficiency of ionization as described by Saha's law as a function of the ionization potential for a representative electronic density of 10^{21} m^{-3} . The ionization potentials of some elements for which the isotopic composition is commonly analyzed are shown at the top (from Albarède and Beard, 2004).

The efficiency of Ar plasma ionization in the MC-ICP-MS can produce double ionized elements, ionization of atmospheric and Ar plasma gases, and formation of molecular ions such as metal oxides, which may introduce some unwanted isobars (Albarède and Beard, 2004). For iron analyses, such unwanted molecular interferences produced by the Ar plasma include ${}^{40}\text{Ar}{}^{14}\text{N}$ on ${}^{54}\text{Fe}$, ${}^{40}\text{Ar}{}^{16}\text{O}$ on ${}^{56}\text{Fe}$, and ${}^{40}\text{Ar}{}^{16}\text{OH}$ on ${}^{57}\text{Fe}$ (Fig. 9).

Anyhow, a number of solutions to this kind of problem (Anbar, 2004) were developed, and they include sample desolvation (Anbar *et al.*, 2000; Belshaw *et al.*, 2000), collision cells (Johnson *et al.*, 2002; Beard *et al.*, 2003a; Beard *et al.*, 2003b) and high-resolution multi-collection mass-spectrometry (*e.g.*, Weyer and Schwieters, 2003; Arnold *et al.*, 2004; Poitrasson *et al.*, 2004; Poitrasson and Freydier, 2005; Poitrasson *et al.*, 2005; Poitrasson and Freydier, 2006; Poitrasson *et al.*, 2006).

The MC-ICP-MS consists of four main parts (Fig. 10 and Fig. 11): 1) a sample introduction system, to inlet samples into the instrument in liquid, gas, or solid forms (*e.g.*, laser ablation); 2) an inductively coupled Ar plasma, where the sample is evaporated, vaporized, atomized, and ionized; 3) an ion transfer mechanism (the mass spectrometer interface), which separates the atmospheric pressure of the plasma from the vacuum of the analyzer and 4) a mass analyzer that resolves the ion kinetic energy spread and produces a

mass spectrum with flat topped peaks that are suitable for isotope ratio measurements ([Albarède and Beard, 2004](#)).

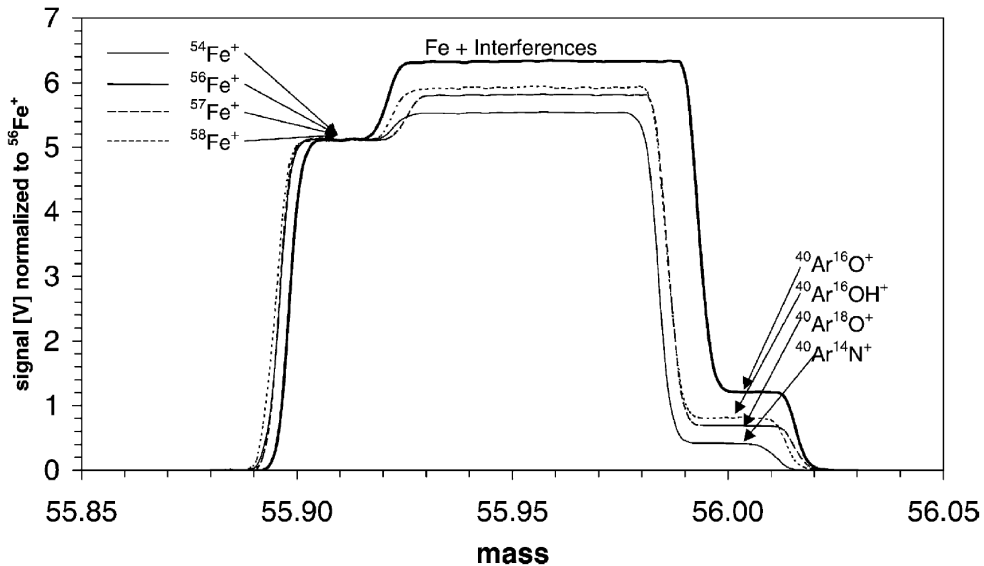


Fig. 9 - Mass scan performed with the Neptune's “medium resolution” entrance slit and “low resolution collector slits” showing all Fe isotopes and their respective molecular interferences. All Fe signals are normalized to the signal of ^{56}Fe . Since the Fe isotopes have a lower mass, they enter the detector first in a scan and form the left plateau. The center plateau consists of polyatomic interferences added to the Fe isotopes. The right plateau is formed by the polyatomic interferences only. Fe isotope ratios can be measured interference-free on left plateau. The scan was performed on a 1 ppm Fe solution, using the SIS (wet plasma) and standard (H) cones (from [Weyer and Schwieters, 2003](#)).

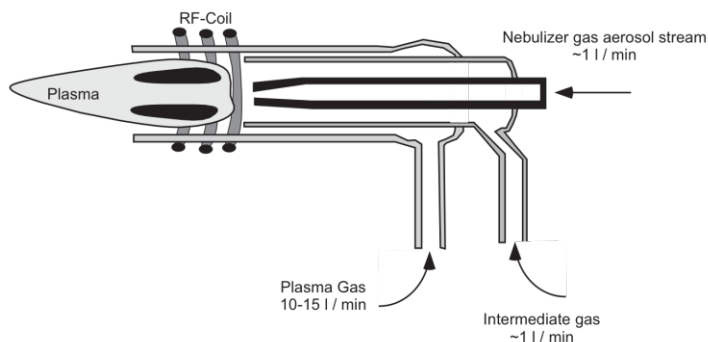


Fig. 10 - Fassel type torch that is typically used in MC-ICP-MS. Approximate Ar flow rates for the different plasma gasses are shown and the relative spatial relationships between the intermediate and sample lines relative to the RF-coil where the Ar plasma is generated are shown (from [Albarède and Beard, 2004](#)).

The most common method for introduction of sample into a MC-ICP-MS is by aspiration of a liquid as an aerosol into the plasma ([Albarède and Beard, 2004](#)). Generally,

only 2% of an aspirated sample by a pneumatic nebulizer has the correct aerosol size to be ionized in the plasma source (Platzner, 1997). A review of the nebulizers types and spray chambers commonly used and the critical aspects of aerosol formation can be found in Montaser *et al.* (1998a) and Montaser *et al.* (1998b).

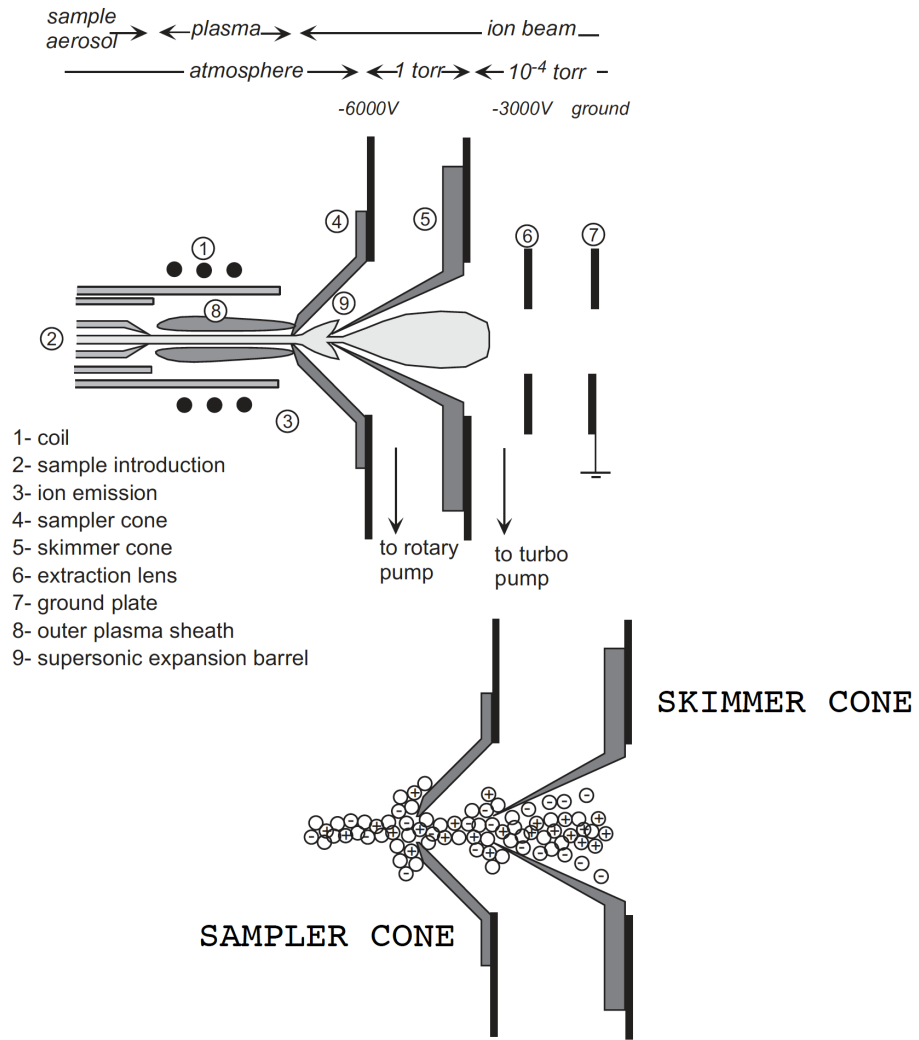


Fig. 11 - The inductively-coupled plasma source (inspired in Niu and Houk, 1996). The original figure has been modified by Albarède and Beard (2004) to show the electrical potentials, the vacuum cascade (top), and the distribution of ions and neutral (bottom) in an MC-ICP-MS similar to the VG Plasma 54. The zone with incipient voltage acceleration right behind the skimmer show maximum space-charge effect with the lighter ions being most efficiently driven off by the strong axial current of positive ions (adapted from Albarède and Beard, 2004).

The plasma discharge is sampled through the MC-ICP-MS interface, which consists of two metal discs with small holes in the center (sampler and skimmer cones, usually made of nickel), through which the plasma and ions travel (**Fig. 11**). The sampler cone has orifice of

approximately 0.8 to 1.2 mm in diameter, where plasma travels through (**Fig. 11**), whereas the skimmer cone (**Fig. 11**), which is behind the sampler cone, has an orifice with a diameter of 0.4 to 0.8 mm ([Albarède and Beard, 2004](#)). The skimmer cone has steeply sloped sides relative to the sampler cone, and the area between them is referred to as the expansion chamber ([Albarède and Beard, 2004](#)). At the torch, there is a pressure drop from that of the atmosphere: first, to a pressure of 1–2 torr after the first disc (sampler cone – **Fig. 11**), and then to a pressure of 10^{-4} torr behind the second disc (skimmer cone – **Fig. 11**, [Albarède and Beard, 2004](#)).

3. POSSIBLE CAUSES FOR FRACTIONATIONS IN THE LABORATORY

To obtain high-precision and accurate isotopic data using MC-ICP-MS, an adequate understanding of instrumental fractionation processes, both mass-dependent and mass-independent, is required, specially because of the complex trajectories of ion beams ([Albarède and Beard, 2004](#)). This means a rigorous assessment of mass bias, combined with standard-sample bracketing method ([Albarède and Beard, 2004](#)).

Mass bias, or the instrumental mass fractionation, is the mass fractionation caused by variable transmission of the ion beam into the equipment, inherent to the mass spectrometer ([Albarède and Beard, 2004](#)). A variety of phenomena may create conditions that lead to this problem, but most fractionation processes take place within the source, either in the area where the analyte is introduced and ionized into the mass spectrometer, or at the interface between the source and the mass analyzer ([Albarède and Beard, 2004](#)). The main reason for this isotopic bias is the very high temperature of the plasma, which generates ions with different initial energies and therefore, complex trajectories in the mass spectrometer ([Albarède et al., 2004](#)).

Bracketing standards are generally used to correct the instrumental mass bias (*e.g.*, [Belshaw et al., 2000](#); [Kehm et al., 2003](#); [Beard et al., 2003a](#); [Albarède and Beard, 2004](#); [Poitrasson et al., 2004](#); [Poitrasson and Freydier, 2005](#); [Poitrasson et al., 2005](#); [Poitrasson and Freydier, 2006](#); [Poitrasson et al., 2006](#); [Fietzke and Eisenhauer, 2006](#); [Poitrasson et al., 2008](#); [Chmeleff et al., 2008](#); [Craddock et al., 2008](#); [Epov et al., 2008](#); [Ikehata et al., 2008](#); [Benkhedda et al., 2008](#)), as well as the comparison of the mass bias inferred from an element spike added to the solution, such as Ni (*e.g.*, [Niu and Houk, 1994](#); [Sharma et al., 2001](#); [Kehm](#)

et al., 2003; Malinovsky *et al.*, 2003; Albarède and Beard, 2004; Poitrasson and Freydier, 2005; Lacan *et al.*, 2008; Estrade *et al.*, 2010; Lacan *et al.*, 2010; dos Santos Pinheiro *et al.*, 2013).

It has been reported that the instrumental mass bias was proportional to the square of the mass difference between isotopes of the analyte (Maréchal *et al.*, 1999). Nonetheless, Albarède and Beard (2004) observed anomalous mass bias when doping a 400 ppb Fe ultra pure standard with varying concentrations of Mg, Al, or La, whereas Carlson *et al.* (2001) noted a similar mass bias of Al on the isotope composition of Mg standard solutions. These studies show that, in general, the Fe isotope composition shifts most strongly as the concentration of the contaminant is increased (Albarède and Beard, 2004). These authors suggested that matrix elements with masses lighter than the analyte are also able to impart changes in instrumental mass bias.

Memory effects are caused by the background from previous runs, which vary daily, according to the instrument and the laboratory (Albarède and Beard, 2004). They are not critical for isotope dilution measurements aiming 2 - 5 per mil precision, but they are also an important issue to any kind of isotopic measurements, as they may have an adverse effect on the accuracy and precision of isotopic compositions in the 100 ppm range (Albarède *et al.*, 2004).

Peak shape effects may occur when isotopic ratios no longer depend only on the mass, but also on the position of the collectors. Although these effects remain hard to detect, as a result of the plasma instabilities, even small deviations from a perfectly flat peak top strongly affect the isotopic ratios, degrading the data quality (Albarède and Beard, 2004).

Residual matrix can cause isotopic shifts of 0.1 - 0.5‰ between samples and standards even for nominally purified iron samples (Arnold *et al.*, 2004; Anbar, 2004). These effects have to be monitored and, at least, partially corrected, either using an ‘element spike’ (Arnold *et al.*, 2004) or high-purity chemical separation (Beard *et al.*, 2003b; Dauphas *et al.*, 2004b). Indeed, if dissociation of the analyte and ionization of the dissociated elements are not complete, mass dependent fractionation may be produced and therefore, an efficient separation and purification chemistry are very important to minimize matrix effects, as well as the elimination of isobars from elements and molecules (Albarède and Beard, 2004).

In the purification of elements by ion exchange chromatography, yields (*i.e.*, recoveries) must be quantitative, as non quantitative yields can generate mass-dependent

laboratory-induced fractionations, effect that was already shown for the elution of Ca (Russell *et al.*, 1978), Cu and Zn (Maréchal *et al.*, 1999; Maréchal and Albarède, 2002), and Fe (Anbar *et al.*, 2000; Roe *et al.*, 2003).

Spectral (or isobaric) type matrix effects are another problem that can deteriorate the data acquired. This type of effect includes: *i*) elemental isobaric interferences such as ^{54}Cr at ^{54}Fe and ^{58}Ni on ^{58}Fe , case in which the mass difference between overlapping species is normally too small to be resolvable; *ii*) molecular interferences such as $^{40}\text{Ca}^{16}\text{OH}$ on ^{57}Fe , $^{40}\text{Ca}^{16}\text{O}$ at ^{56}Fe and $^{40}\text{Ar}^{14}\text{N}$ at ^{54}Fe (**Fig. 9**); *iii*) double charge interferences such as $^{48}\text{Ca}^{2+}$ at ^{24}Mg (Albarède and Beard, 2004). Non-spectral matrix effects are largely associated with the presence of other elements on the analyte (Olivares and Houk, 1986) and can also have a significant impact on the accuracy of isotope measurements, as it changes the sensitivity of an analyte and therefore, the instrumental mass bias (Albarède and Beard, 2004). It appears to be some controls on non-spectral matrix issues (*e.g.*, Olivares and Houk, 1986; Nonose and Kubota, 2001; Albarède and Beard, 2004), but they may also be a result of changes in vaporization position in the plasma (Carlson *et al.*, 2001). There is a strong matrix influence – and hence instrumental mass bias – on the analyte sensitivity associated to matrix elements that have a mass greater than the analyte (*e.g.*, Gillson *et al.*, 1988). Anyhow, as long as these effects, spectral or non-spectral, do not represent a large fraction of the signal, a correction step may resolve the problem.

4. MOST COMMON CORRECTION METHODS: A REVIEW

4.1 Standard bracketing methods

Standard bracketing consists in interpolating the analysis of an unknown sample between the two standard runs, one preceding and one following the sample being analyzed (Albarède and Beard, 2004). This is the most common method to correct the experimental bias during the measurement of the isotopic compositions of H, N, O, C, S (Albarède and Beard, 2004) as well as for isotopic composition of transition elements measured by MC-ICP-MS (Zhu *et al.*, 2002; Beard *et al.*, 2003b, Weyer and Schwieters, 2003; Schoenberg and von Blanckenburg, 2005), which is the case of Fe (**Fig. 12** – note that $\delta^{57}\text{Fe}$ values are expressed in ϵ notation – parts per 10^4 instead of 10^3 –, nomenclature abandoned).

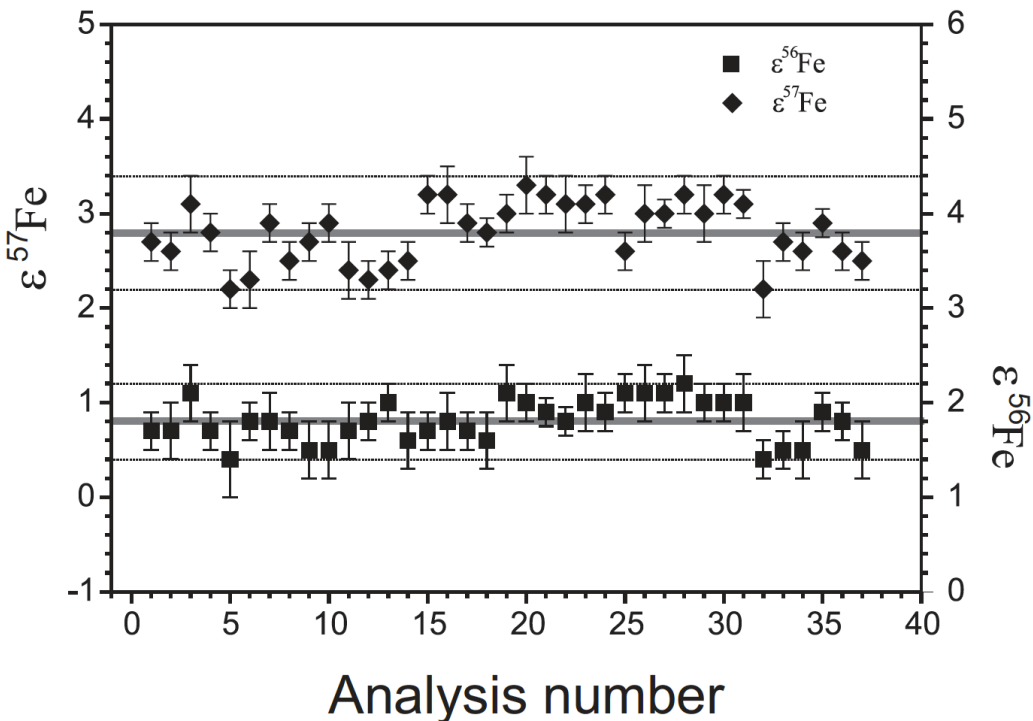


Fig. 12 - Deviations of the $^{56}\text{Fe}/^{54}\text{Fe}$ ratios (right axis) and $^{57}\text{Fe}/^{54}\text{Fe}$ (left axis) in parts per 10.000 of the IRMM-14 Fe standard with respect to an in-house reference solution for a series of 37 runs determined by the standard bracketing technique ([Zhu et al., 2002](#)). A reproducibility of 0.04‰ and 0.06‰ is obtained on each ratio, respectively.

4.2 Ni doping technique

Internal doping techniques ([Malinovsky et al., 2003](#); [Arnold et al., 2004](#); [Poitrasson and Freydier, 2005](#); [Schoenberg and von Blanckenburg, 2005](#); [Lacan et al., 2008](#); [Poitrasson et al., 2008](#); [Lacan et al., 2010](#)) are another common way to correct for mass bias. As nickel isotopic masses are closer to those of iron, the use of ^{60}Ni and ^{61}Ni to correct for iron isotope mass bias seems more appropriate ([Poitrasson and Freydier, 2005](#)). According to these authors, this method permits static MC-ICP-MS measurements, which, besides a potential improvement in analytical precision, can significantly reduce the analysis time and sample consumption.

4.3 Reproducibility issues

A better reproducibility for iron isotope analysis can be achieved by three simple steps ([Poitrasson and Freydier, 2005](#)), which include: 1) the use of the X cones to improve the signal with lower Fe and Ni concentrations in the analytical solutions; 2) a mass bias

correction using ^{60}Ni and ^{61}Ni instead of ^{60}Ni and ^{62}Ni , what allows a simultaneous mass bias correction and monitoring of ^{53}Cr for isobaric interference at mass 54 in the static mode and 3) the use of 0.05M HCl solution as analytical medium instead of higher molarities, which may potentially degrade the precision on the isotope ratio involving ^{57}Fe . The same authors also evaluated the optimum number of replicate analyses required to minimize the uncertainty while maintaining analytical time and cost reasonable. They showed that the reproducibility improves for up to 6 repeat analyses per sample, but at seven repeats or above, there was no noticeable additional benefit. Therefore, the long-term reproducibility is improved if each sample is analyzed six times.

4.4 Correction of the non-mass dependent instrumental bias in static mode

Non-mass dependent biases can be generated due to the imperfect reproducibility on the manufacture of electronic components as well as the imperfect positioning of Faraday cups with respect to the instrument ionic axis ([Albarède and Beard, 2004](#)).

These problems usually involve only a very small fraction of the ion beams in modern mass spectrometers, but they may alter the precision of the measurements in a way that is not a linear function of the mass difference between the beams collected in the Faraday cups ([Albarède and Beard, 2004](#)). This mass-independent isotopic fractionation can be resolved by introducing correction factors (also known as *efficiencies*), which are determined by measuring a standard and comparing its isotopic abundances with the known values ([Albarède and Beard, 2004](#)). Anyhow, these authors demonstrated that these effects may change the measured isotopic compositions, but the slope of the linear alignments is preserved in log-log plots, allowing the isotopic variations among standards to be determined with precision.

5. FINAL CONSIDERATIONS

Natural variations in the isotopic composition of natural materials are a main interest of research and therefore, mass-dependent and mass-independent instrumental fractionations are important issues on isotope analyses of any kind. High mass resolution measurement correction methods have been developed, like the sample-standard bracketing and internal

doping techniques, to correct for the mass bias ([Poitrasson and Freydier, 2005](#)) and deal with the instrumental fractionation processes.

MC-ICP-MS is the most suitable equipment for stable isotope analyses if the signal intensities of samples and standards can be kept within a narrow controlled range ([Albarède and Beard, 2004](#)). The efficient ionization of most elements by the plasma and the possibility of operation of the instrument at steady-state, which allows control of mass fractionation, are some relevant reasons for its choice to acquire iron isotopic data ([Albarède and Beard, 2004](#)). On the other hand, a larger mass fractionation is expected, as well as isobaric interferences and a less-than-perfect peak shape due to the energy spread ([Albarède and Beard, 2004](#)), but these effects that can be, at least in part, corrected.

Iron isotopic measurements at the Geochronology Laboratory of the UnB (Brazil) are made in a Thermo Finnigan Neptune running in static and medium or high-resolution modes. So far, iron isotope measurements have been determined in this laboratory for bulk BIFs, meteorites and suspended matter of rivers. Part of the samples here presented was analyzed at this laboratory, while another part was analyzed at the GET Laboratory (France), using the same equipment, operating in similar conditions.

The standard bracketing and Ni doping techniques described in this chapter were applied to resolve mass biases in both laboratories. Data is presented as delta notation ($\delta^{57}\text{Fe}$, parts per mil) and referred to the international standard IRMM-14. Repeated analyses of the Milhas Hematite were carried out in every session to test the long-term reproducibility and accuracy of the measurements (described in detail in chapters 5 and 7). This hematite standard, also known as ETH hematite, has been analyzed in several laboratories and the values reported internationally agree with values obtained in this work ($\delta^{57}\text{Fe}_{\text{IRMM-14}} = 0.757 \pm 0.067\text{\textperthousand}$; 2SD, n = 20). Further information on the technique applied can also be found on chapters 5 and 7.

CAPÍTULO CINCO

IRON ISOTOPE COMPOSITION OF THE SUSPENDED MATTER ALONG DEPTH AND LATERAL PROFILES IN THE AMAZON RIVER AND ITS TRIBUTARIES

Giana Márcia dos Santos Pinheiro^{a,b}; Franck Poitrasson^{a,b}; Francis Sondag^{a,b}; Lucieth Cruz Vieira^a; Márcio Martins Pimentel^{a,c}

Accepted Article – Journal of South American Earth Sciences – available online August 2012, <http://dx.doi.org/10.1016/j.jsames.2012.08.001>

a. Instituto de Geociências, Universidade de Brasília, 70910-900, Brasília, Brazil

b. Laboratoire Géosciences Environnement Toulouse, Institut de Recherche pour le Développement - Centre National de la Recherche Scientifique - Université de Toulouse III, 14-16, Avenue Edouard Belin, 31400 Toulouse, France

c. Instituto de Geociências, Universidade Federal do Rio Grande do Sul, CP 15001, 91501-970 Porto Alegre, Brazil

Corresponding author: Giana Pinheiro - giana@unb.br

ABSTRACT

Samples of suspended matter were collected at different locations, seasons, depths and lateral profiles in the Amazon River and three of its main tributaries, the Madeira, the Solimões and the Negro rivers. Their iron isotope compositions were studied in order to understand the iron cycle and investigate the level of isotopic homogeneity at the river cross section scale. Samples from four depth profiles and three lateral profiles analyzed show suspended matter $\delta^{57}\text{Fe}$ values (relative to IRMM-14) between $-0.501 \pm 0.075\text{\textperthousand}$ and $0.196 \pm 0.083\text{\textperthousand}$ (2SE). Samples from the Negro River, a black water river, yield the negative values. Samples from other stations (white water rivers, the Madeira, the Solimões and the Amazon) show positive values, which are indistinguishable from the average composition of the continental crust ($\delta^{57}\text{Fe}_{\text{IRMM-14}} \sim 0.1\text{\textperthousand}$). Individual analyses of the depth and lateral profiles show no significant variation in iron isotope signatures, indicating that, in contrast to certain chemical or other isotopic tracers, one individual subsurface sample is representative of river deeper waters. This also suggests that, instead of providing detailed information on the riverine iron cycling, iron isotopes of particulate matter in rivers will rather yield a general picture of the iron sources.

KEYWORDS: iron isotopes; Amazon River Basin; depth profile; lateral profile; suspended matter.

1. INTRODUCTION

Iron is the fourth most abundant element in the Earth's crust (4.3 wt% as Fe - *e.g.*, Wedepohl, 1995). It is found in practically all rocks and soils and is present in a variety of minerals. Rivers are one of the major providers of iron – along with other elements – to oceans (Zhu *et al.*, 2000; Beard *et al.*, 2003b). Other dissolved and particulate iron sources to oceans and rivers are atmospheric deposition, continental run-off, re-suspended sediments, diagenetic pore fluids, underground waters, vegetation, soils, weathering material and hydrothermal fonts (Wells *et al.*, 1995; Elderfield and Schultz, 1996; Johnson *et al.*, 1999; Beard *et al.*, 2003b; Elrod *et al.*, 2004; Jickells *et al.*, 2005; Severmann *et al.*, 2006; Bennett *et al.*, 2008; Rouxel *et al.*, 2008a; Rouxel *et al.*, 2008b; Escoube *et al.*, 2009).

The suspended matter composition of rivers is controlled by several factors, including climate, weathering, erosion and the nature of the geological basement (Bouchez *et al.*, 2010). Its abundances may be directly correlated with water discharge increase (Bouchez *et al.*, 2010), although this was shown not to be the case in larger rivers, like the Amazon at the Óbidos Station (Martinez *et al.*, 2009).

Many trace elements of the Amazon River, including iron, are mobilized between dissolved and particulate forms due to abiotic and biological processes (*e.g.*, redox, adsorption, mineral dissolution, organic complexation, precipitation, erosion and continental run-off – see Beard *et al.*, 1999; Bullen *et al.*, 2001; Skulan *et al.*, 2002; Roe *et al.*, 2003; Fantle and DePaolo, 2004; Rodushkin *et al.*, 2004; Johnson and Beard, 2005; Teutsch *et al.*, 2005; Dauphas and Rouxel, 2006) and they may all have an effect on iron isotope signatures of river born matter.

A number of studies have been carried out on compositional variations and fractionation of iron isotopes in rivers, oceans, lakes and soils (Zhu *et al.*, 2000; Rouxel *et al.*, 2005; Emmanuel *et al.*, 2005; Bergquist and Boyle, 2006; Ingri *et al.*, 2006; Severmann *et al.*, 2006; Staubwasser *et al.*, 2006; Fehr *et al.*, 2008; Poitrasson *et al.*, 2008; Severmann *et al.*, 2008; Zhao *et al.*, 2009; Severmann *et al.*, 2010; Song *et al.*, 2011), but a great deal of work is still needed to successfully use iron isotopes as a tool to understand the biogeochemical cycle of iron (Song *et al.*, 2011).

Riverine inputs to the ocean are described to display $\delta^{57}\text{Fe}$ values from -1.5 to $0.9\text{\textperthousand}$ (Fantle and DePaolo, 2004; Bergquist and Boyle, 2006; Escoube *et al.*, 2009), while atmospheric input yield $\delta^{57}\text{Fe}$ data similar to crustal values (Beard *et al.*, 2003a). Although the particulate load of rivers seemed at first relatively unfractionated with respect to crustal values (Beard *et al.*, 2003a), dissolved Fe in river waters has been reported to exhibit isotopic variability related to the weathering process (Fantle and DePaolo, 2004; Bergquist and Boyle, 2006; Poitrasson *et al.*, 2008). Furthermore, recent reports have shown that Fe isotope compositions of organic and inorganic, dissolved, colloidal and particulate iron forms in rivers may vary (*e.g.*, Bergquist and Boyle, 2006; Escoube *et al.*, 2009). Hence, more detailed studies are required to quantify the various possible sources of iron in rivers, especially during organic and inorganic processes in such environments.

The present study focuses on the iron isotopic composition of suspended matter collected along depth and lateral profiles from the Amazon River and three of its main tributaries: the Solimões River, the Negro River and the Madeira River (Fig. 13). The main objective of this work is to investigate the variability of iron isotope signatures as a function of depth, lateral profiles, seasons and geographic location, to provide a scale of its potential variability and have a better insight into the biogeochemical cycling of iron in the Amazon River and its tributaries.

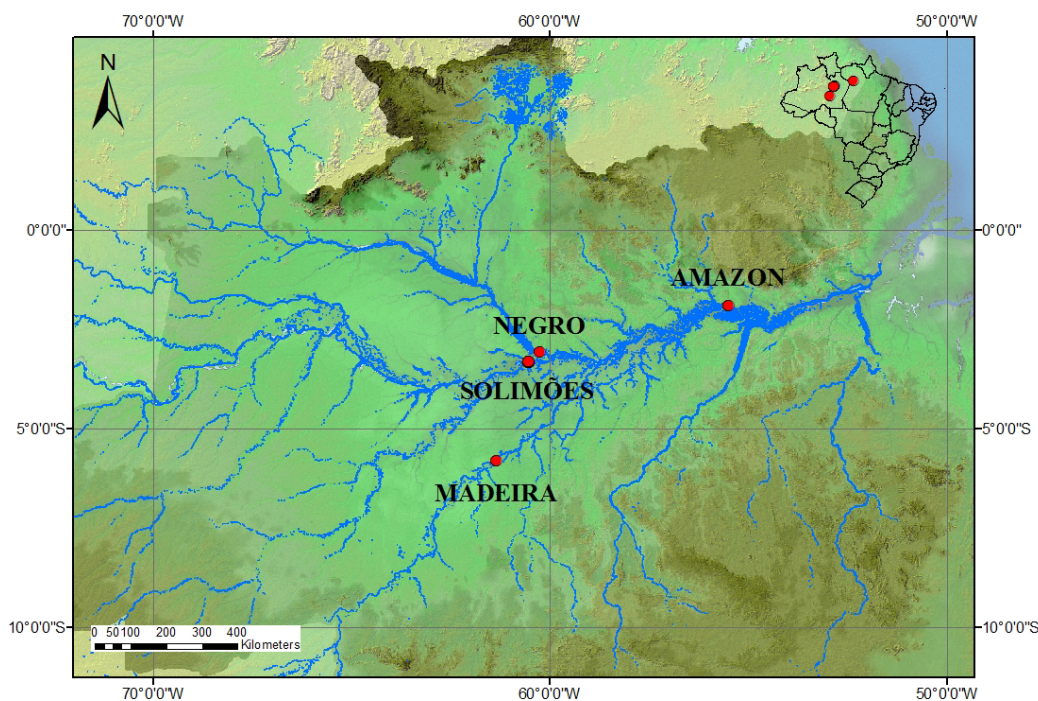


Fig. 13 – Map of sample locations.

2. STUDY AREA, SAMPLING AND METHODS

2.1 Study area

The Amazon River represents approximately 20% of the world riverine fresh waters and, as such, it is an obvious case study of iron transfer from continent to ocean in intertropical zones, where chemical weathering is high. It drains more than 6.4 million km² and has an average water discharge of 209,000 m³s⁻¹. The flux of solids discharged to the ocean by the Amazon River is estimated between 500 and 1,200 million tons yr⁻¹ ([Meade et al., 1979](#); [Dunne et al., 1998](#); [Maurice-Bourgois et al., 2007](#); [Filizola and Guyot, 2009](#)).

The five main inflowing tributaries to the Amazon River in Brazil are the Negro, Solimões, Madeira, Tapajós and Xingu rivers. They display a variety of physical and chemical characteristics that have long been recognized for the rivers of the Amazon basin. Its waters have been classified as white, clear, and black ([Fittkau, 1971](#); [Gibbs, 1972](#); [Sioli, 1984](#); [Lewis et al., 1995](#)).

White water rivers generally flow from the Andes whereas black water rivers drain the central part of the basin, typically covered by the evergreen rainforest ([Seyler and Boaventura, 2003](#)). The first type, which presents a yellow color due to high sediment content, has a pH > 6.25 and alkalinity > 0.2 meq l⁻¹ (e.g., Solimões and Madeira rivers). The latter is tea colored due to high contents of dissolved organic compounds, has very low concentration of suspended solids, a pH lower than 5.5 and alkalinites lower than 0.25 meq l⁻¹ (e.g., Negro River, [Seyler and Boaventura, 2003](#)). Clear water rivers, such as the Tapajós and the Trombetas rivers, have high transparencies due to low concentrations of suspended sediments and usually drain the highly weathered shield areas ([Seyler and Boaventura, 2003](#)). Due to local conditions and seasonal fluctuations, clear water rivers may assume black or white water characteristics, including pH and alkalinites ([Sioli, 1967](#)).

The Andes is the dominant source area for most metals transported by the Amazon River. Trace metals (including Fe) are transported primarily in particulate form, except for the Negro River, where metals are frequently complexed with organic matter, and the iron transport in the dissolved phase is predominant ([McClain, 2001](#)).

Large rivers can be vertically and horizontally heterogeneous in terms of suspended particulate matter concentration, due to processes that are responsible for local transport of material, both in the particulate and dissolved phases. These processes include differential sorting of solids and turbulent mixing ([Bouchez et al., 2010](#); [Bouchez et al., 2011a](#)).

Therefore, sampling suspended sediments as a function of these parameters can help to understand the controls on the distribution of chemical elements throughout a river profile ([Bouchez et al., 2011a](#); [Bouchez et al., 2011b](#)).

Other parameters may also be different in rivers depth and lateral sections, such as temperature, pH, conductivity, water velocity and dissolved oxygen. Thus, mixing and geochemical processes that occur along these kinds of profiles must be considered in order to better understand the dynamics of large rivers, such as the Amazon. Likewise, anthropic activities may as well contribute to a shift in natural conditions of the environments that can lead to distinct isotopic signatures.

2.2 Sampling

The present study focuses on the analysis of 33 samples of suspended matter collected at ([Fig. 13](#)): a) depth profiles in the Amazon River Basin, Northern Brazil, at Óbidos (Amazon River), Manacapuru (Solimões River), Paricatuba (Negro River) and Manicoré (Madeira River) stations; b) lateral profiles collected at Manacapuru (Solimões River) and Paricatuba (Negro River) stations ([Fig. 14](#)).

2.2.1 Depth Profiles (DP)

Five samples were collected in the Amazon River at the Óbidos Station (Pará State, Brazil) on December 06th, 2009. The Óbidos Station in the Amazon River is the last gauging station where the river is still channelized before the delta. At this point, approximately 110 km upstream of Santarém (Pará State, Brazil), the Amazon River narrows to a width of 1.5 km and its depth can reach 100 meters.

The height of the water column along with the water discharge were measured using the Acoustic Doppler Current Profiler – ADCP method ([Filizola and Guyot, 2004](#)) – and five samples were collected in 13 m spaced steps, from the surface down to 52 m deep, a few meters above the river bed.

A similar sampling strategy was adopted for all the depth profiles. In the Madeira River (Amazonas State), five samples were collected at Manicoré Station on November 25th, 2009, with a depth-sampling interval of 3 meters (from surface to 12 meters). The Negro

River samples were collected at the Paricatuba Station (Amazonas State), on October 3rd, 2009, while the Solimões River samples (Manacapuru Station, Amazonas State) were collected on October 6th, 2009. At the Negro River, each sampling step was 5 meters for the first three samples (surface, 5 and 10 meters). From the third to the fourth, and from the fourth to the fifth depths, the sampling steps were 10 meters. Five samples were collected in the Solimões River as well, but only four were analyzed: the first two, closer to the surface, and the last two, closer to the river bed (0.5, 5, 15 and 17 meters).

2.2.2 Lateral Profiles (LP)

Ten samples were collected along two lateral profiles in the Solimões River, at the Manacapuru Station (**Fig. 14**): the first on November 30th, 2009 (dry season), and the second on June 24th, 2010 (flood season). In the Negro River (Paricatuba Station), five samples were collected, but only four of them were analyzed, representing the left and the right banks of the river. These samples were collected on September 28th, 2010.

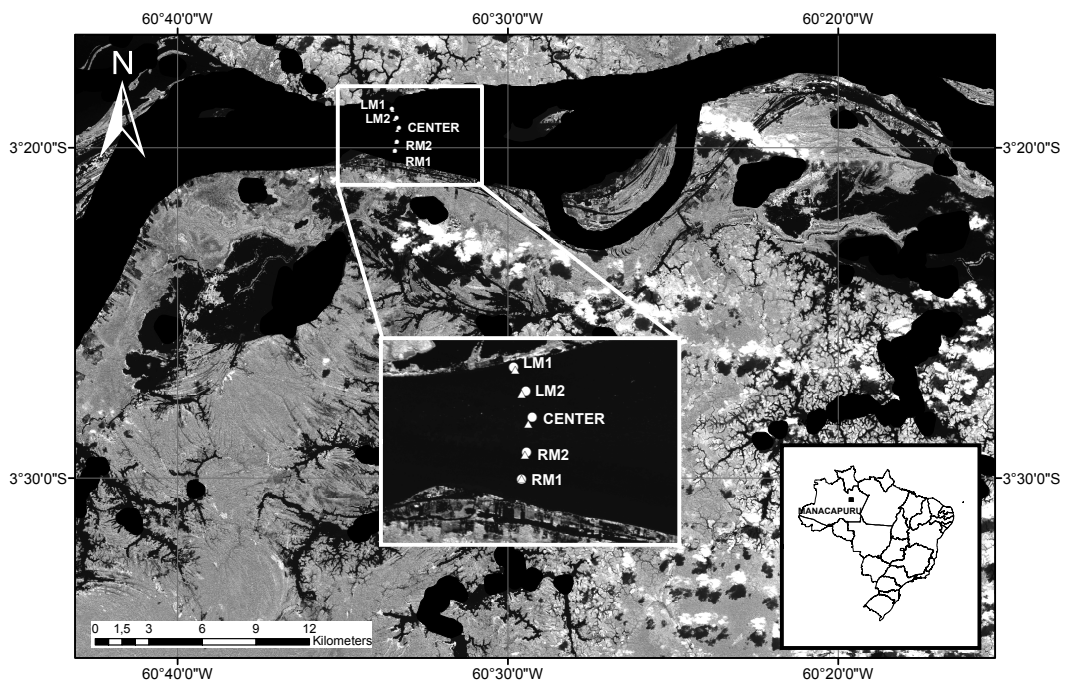


Fig. 14 – SPOT Image showing the collecting strategy for the lateral profile samples at Manacapuru Station.

White triangles represent the location of samples collected during the dry season, and white circles, superimposed to white triangles, represent the location of samples collected during the flood season. RM stands for right margin and LM for left margin.

2.3 Methods

2.3.1 Sample collection and preparation

All material used in the laboratory and in the field was carefully cleaned: polyethylene bottles, tubes and high density polyethylene (HDPE) bottles for sample collections were cleaned with 1N HCl for at least 1 day and then cleaned with nanopure water for another day. Frontal filtration (FF) was performed in the field using Millipore HA mixed cellulose esters, 0.45 µm pore size, 47 mm in diameter. Filters used to collect suspended matter were stored in Petrislide® dishes and dried in an oven for 24 hours at 50°C before weight measurements and analyses. All membrane filters were pre-weighed and then re-weighed after water filtration and drying.

Bottles for sampling were pre-rinsed three times with the corresponding water samples and sample collection was performed using a 300 micrometer net placed at the mouth of the bottle, to avoid sampling of undesirable larger particles that could be floating in the water. Multi-parameter sensors (YSI 6820 V2 and HIDROLAB DS 5X) were used for determining *in situ* parameters. They included pH, electrical conductivity (*cond*, µS/cm), temperature (°C) and turbidity (Nephelometric Turbidity Units - NTU). All water samples were filtered in the field, on the boat, within 12 hours from sampling.

Approximately 1 000 ml of water was collected in each station. The suspended matter analyzed was recovered from the filtration of 380 ml of water for the Negro River at Paricatuba (depth profile - DP); 400 ml for the Solimões River at Manacapuru (DP); 500 ml for the Madeira River at Manicoré (DP) and Amazon River at Óbidos (DP); 500 ml for the Negro River at Paricatuba (lateral profile - LP); and between 500 and 600 ml for the two Solimões River lateral profiles at Manacapuru. After filtration, filtered and unfiltered (bulk) water samples were kept in a freezer at -18°C for future investigations.

2.3.2 Sample dissolution and iron purification

Sample dissolution and chemical purification were carried out in a class 10,000 clean room at the University of Brasília. The method applied consists of successive digestions of samples, followed by purification of iron by anion exchange chromatography. Suspended matter was entirely dissolved (along with the filter membranes) using 8 ml of conc. HNO₃ and 1 ml of H₂O₂ (P.A.). Samples were then taken up in 0.2 ml of conc. HNO₃, 1 ml of conc.

HF and 0.2 ml of conc. 6M HCl. The third step consisted in the addition of 2 ml of 6M HCl. Samples were evaporated and 1 ml 6M HCl was added before centrifugation, which was followed by chromatography. After each of these digestions, samples were left overnight on a hot plate at 120°C and were then evaporated. All acids used were bi-distilled.

Before purification, Teflon thermoretractile columns (internal diameter 4 mm) filled with 0.5 ml of BioRad AG1-X4 200-400 mesh anion exchange resins were cleaned with 5 ml of 6M HCl, followed by approximately 7 ml of 0.05M HCl. Chromatography, as described in [Poitrasson et al. \(2004\)](#), consisted in the preconditioning of the resins with 1 ml of 6M HCl before sample introduction (0.5 ml). Subsequently, 0.5 ml of 6M HCl was added twice. The next step consisted in the addition of 2 ml of 6M HCl, which finished to elute most of the non-desirable matrix elements. Iron was then collected with 2 ml of 0.05M HCl.

After complete evaporation, samples were re-dissolved in 0.05M HCl and analyzed for Fe isotopes with a Finnigan Neptune high mass resolution Multi-Collector Inductively Coupled Plasma Mass Spectrometer (MC-ICP-MS), as presented in more detail in the next section, following the methodology described in [Poitrasson and Freydier \(2005\)](#).

It is noticeable that, after sample purification, the resin used may acquire a brownish color, what was attributed to remains of the membrane that could not be cleaned. The resin was then discarded to avoid possible cross contamination with other samples.

Quantitative recovery from the columns was calculated based on iron analyses made by ICP-OES before the chromatographic separation, and by ICP-MS after chromatography. Columns yielded $90 \pm 10\%$ of iron. According to [Anbar et al. \(2000\)](#) and [Roe et al. \(2003\)](#), isotope fractionation in Fe anion chromatography experiments is absent when this element is eluted with the use of very dilute acids, because FeCl_4 only becomes an important species when the concentration of HCl is higher than 1M. Therefore, elution with dilute acid, *i.e.*, 0.05M HCl in the present study, does not lead to mass-dependent isotopic fractionation during elution, even if the Fe recovery is of *ca.* 90%.

All procedural blanks were <1% of the sample Fe, an insignificant amount for this study, and they included a blank of the 0.45 μm filter membrane used for filtration of the samples. At least 40 μg of iron was processed for each sample.

2.3.3 Iron isotope analyses by mass spectrometry

Iron isotope analyses were performed on a Thermo Finnigan Neptune MC-ICP-MS at the Geochronology Laboratory of the University of Brasília (UnB, Brazil) for the Amazon River samples, and at the Laboratory Géosciences Environnement Toulouse (CNRS, IRD, UPS, France) for the Madeira, the Solimões and the Negro rivers samples. Purified Fe solutions, which ranged in concentration from 2 to 6 ppm depending on the equipment sensitivity, were introduced into the argon plasma in 0.05M HCl medium in the wet plasma mode.

The typical ion beam for 1 ppm Fe solutions of both standards and samples was *ca.* 0.2 to 0.6V on ^{57}Fe . The standard-sample bracketing and Ni doping techniques using the daily regression method were applied to minimize instrumental mass bias (see details in [Poitrasson and Freydier, 2005](#)). Analyses were performed in the medium or high mass resolution mode.

Iron isotope data are generally reported in $\delta^{\text{x}}\text{Fe}$ ($\delta^{56}\text{Fe}$ or $\delta^{57}\text{Fe} = \delta^{57}\text{Fe}/^{54}\text{Fe}$), as parts per thousand (‰) deviations relative to the reference material IRMM-14:

$$\delta^{57}\text{Fe}/^{54}\text{Fe} = (((^{57}\text{Fe}/^{54}\text{Fe})_{\text{sample}} / (^{57}\text{Fe}/^{54}\text{Fe})_{\text{IRMM-14}}) - 1) * 1000$$

The performance of the instrument was assessed by repetitive measurements of a standard (hematite from Milhas, Pyrenees) relative to the Fe isotope reference material IRMM-14. The long-term external reproducibility of the method at the University of Brasília was estimated from replicate analyses of this hematite in every session along four months (from March to July 2010, [Fig. 15](#)). This hematite, also known as ETH hematite, has been analyzed in several laboratories and the values reported by these authors agree well with values obtained in this work ($\delta^{57}\text{Fe}_{\text{IRMM-14}} = 0.757 \pm 0.067\text{‰}$; 2SD, $n = 20$, [Fig. 15](#)). For instance, [Dideriksen *et al.* \(2006\)](#) analyzed this standard 8 times at the Danish Lithosphere Centre, with a VG Axiom MC-ICP-MS, and reported a $\delta^{57}\text{Fe}$ value of $0.87 \pm 0.08\text{‰}$ (2SD), while [Teutsch *et al.* \(2005\)](#), with a Nu Plasma MC-ICP-MS, obtained at ETH Zürich $\delta^{57}\text{Fe}$ values of $0.83 \pm 0.14\text{‰}$ (2SD, $n = 148$). Also, [Fehr *et al.* \(2008\)](#) got $\delta^{57}\text{Fe}$ values of $0.81 \pm 0.13\text{‰}$ at the Swedish Museum of Natural History in Stockholm. High mass resolution measurements at CNRS, Toulouse, France (Finnigan Neptune) yielded $0.744 \pm 0.040\text{‰}$ ($n = 62$)

10; Poitrasson and Freydier, 2005). Literature values reported only in $\delta^{56}\text{Fe}$ were recalculated to $\delta^{57}\text{Fe}$ as $1.5 \times \delta^{56}\text{Fe}$. All data are relative to the IRMM-14 standard.

International rock standards were dissolved, purified and analyzed at the Geochronology Laboratory of Brasília to validate the methodology used in this laboratory. They include the IF-G geostandard, with a $\delta^{57}\text{Fe}$ value of $0.931 \pm 0.082\text{\textperthousand}$ (Vieira *et al.*, 2010), in good agreement with previously published values (see reviews in Craddock and Dauphas, 2011).

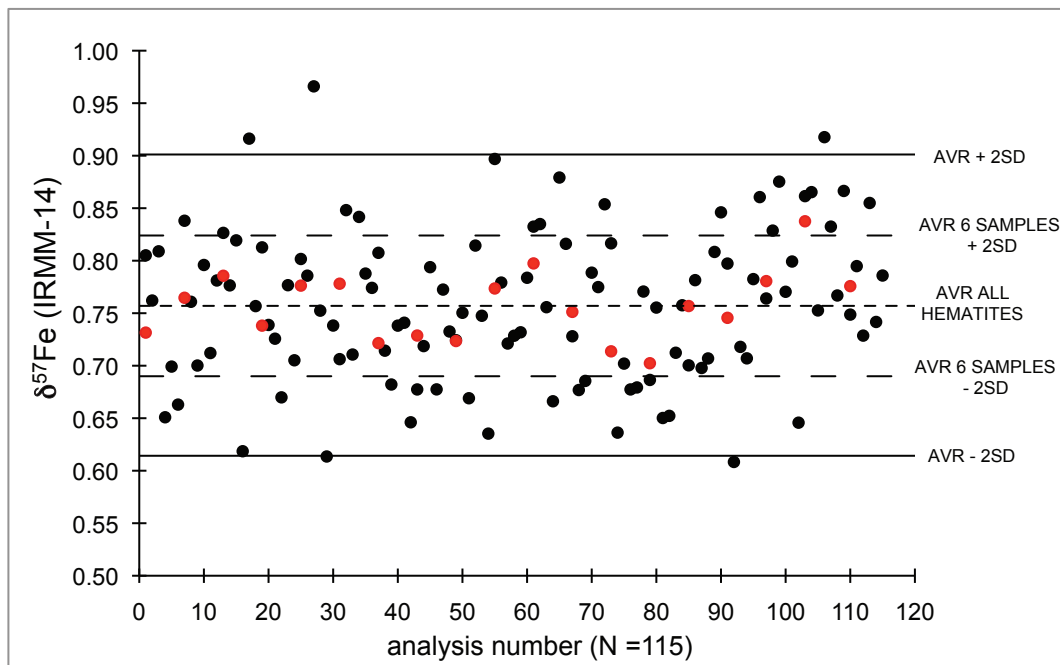


Fig. 15 – The mean $\delta^{57}\text{Fe}$ value of individual measurements (black circles) for the Milhas hematite is $0.758 \pm 0.143\text{\textperthousand}$ (2SD, N=115), whereas pooled data by groups of 6 (red circles) yield a $\delta^{57}\text{Fe}$ of $0.757 \pm 0.067\text{\textperthousand}$ (2SD, N=20).

3. RESULTS

3.1 Environmental parameters

3.1.1 Depth profiles

In both the Madeira River (Manicoré Station) and the Amazon River (Óbidos Station) depth profiles the pH does not show significant variations (**Tabela 1**). The pH was measured only at the surface in the Solimões and Negro rivers depth profiles (respectively Manacapuru and Paricatuba stations). Conductivity values are homogeneous in the water column for the Manicoré (Madeira River), Paricatuba (Negro River) and Óbidos (Amazon River) stations (**Tabela 1**).

The temperature is nearly constant throughout the Madeira (Manicoré) and the Solimões (Manacapuru) rivers depth profiles, whereas at Amazon River (Óbidos Station) there is a hint for cooler temperature in the middle of the water column (**Tabela 1**). The temperature of the Negro River (Paricatuba Station) depth profile is 1°C higher at the surface than at the rest of the profile, and it is also slightly higher than values obtained for white water stations at comparable dates. This could be explained by the darker nature of this kind of water, which better absorbs light to heat.

The turbidity is constant in the Amazon River at Óbidos, with values approximately 3.5 times lower than in the Madeira River at Manicoré. In this last station, turbidity is constant except at 3 m depth, where it decreases drastically (**Tabela 1**). This parameter was not measured in the Negro and Solimões rivers.

3.1.2 Lateral profiles

Individual analyses along lateral profiles show no significant variations in pH from the left to the right bank of the rivers studied (**Tabela 1**). The Negro River (Paricatuba Station) has a lower pH compared to the other two profiles of the Solimões River at the Manacapuru Station. This is in accordance with the different characteristics of black water rivers (Negro) and white water rivers (Solimões).

Conductivity values are nearly constant for both margins of the Negro River (Paricatuba) lateral profile. In contrast, conductivity values for the two lateral profiles at Manacapuru (Solimões River) tend to be lower at the right bank when compared to the center and to the left bank of the river, locations where conductivity values are constant (**Tabela 1**).

Temperature is higher at the right bank of the Negro River (Paricatuba Station) lateral profile. This parameter is nearly constant throughout the Manacapuru (Solimões River) lateral profile collected in June, on the flood season. However, in the lateral profile collected at this river during the dry season (November), samples closer to the right and to the left banks show higher values (**Tabela 1**). Turbidity is higher near the center of the river for both lateral profiles of the Manacapuru Station (Solimões River) and lower close to its left and right margins (**Tabela 1**).

It is important to notice that absolute values of all *in situ* parameters measured (temperature, conductivity, turbidity and pH) for the two Manacapuru lateral profiles

(Solimões River) are always lower in the flood season (June) when compared to the dry season (November, Table 1). This indicates that there is an important shift in the physico-chemical characteristics of this river during these two different hydrological seasons studied and, therefore, other associated (*i.e.*, dependent) parameters may shift as well.

3.2 Comparison between the suspended matter of the rivers studied

Riverine suspended matter shows highly variable concentrations depending on the river studied, varying from 3.2 (Negro River, black water with low pH) to 312 mg L⁻¹ (Madeira River, white water with neutral pH – **Fig. 16** and **Fig. 17, Table 2**). The Amazon and the Solimões rivers show intermediate suspended matter values of 26 to 124 mg L⁻¹. The average suspended matter value of the rivers differentiates the black waters, for which suspended matter is low, from the white waters, where suspended matter is higher. This is in agreement with the strong mechanical erosion inheritance of the white waters (*e.g.*, [Allard et al., 2004](#)), which have their origin in the Andes, from where they transport large amounts of sediments ([Junk and Piedade, 2010](#)).

The Amazon (Óbidos Station) and Negro (Paricatuba Station) depth profiles samples show no significant variation in the suspended matter content (**Fig. 16, Table 2**). For the Solimões River depth profile (Manacapuru Station), a decrease in the suspended matter concentration at the second depth (5 meters) is observed. From this depth on, the quantity of suspended matter increases again, reaching the same value as the surface sample, and stays nearly constant for the rest of the profile (**Fig. 16**). The Madeira River depth samples (Manicoré Station) show an important decrease in the suspended matter content at the second (3 meters) and last (12 meters) depths, while other samples present nearly similar concentrations in this parameter (**Fig. 16**).

The Negro River lateral profile (Paricatuba Station) shows no variations in the content of suspended matter of both river banks (**Fig. 17, Table 2**). On the other hand, the two Manacapuru lateral profiles (Solimões River), collected at two different seasons, show an important increase of suspended matter content near the center of the river, while samples closer to the right and left banks of the river show lower values (**Fig. 17**), in agreement with the observations made for the turbidity. The profile collected during the dry season shows this increase only in the center of the river, whereas the profile collected during the flood season shows this increase on the right and left samples closer to the center as well (**Fig. 17**). Like

other physico-chemical parameters already discussed (*e.g.*, temperature and turbidity), absolute values obtained for suspended matter concentrations are lower in the flood season.

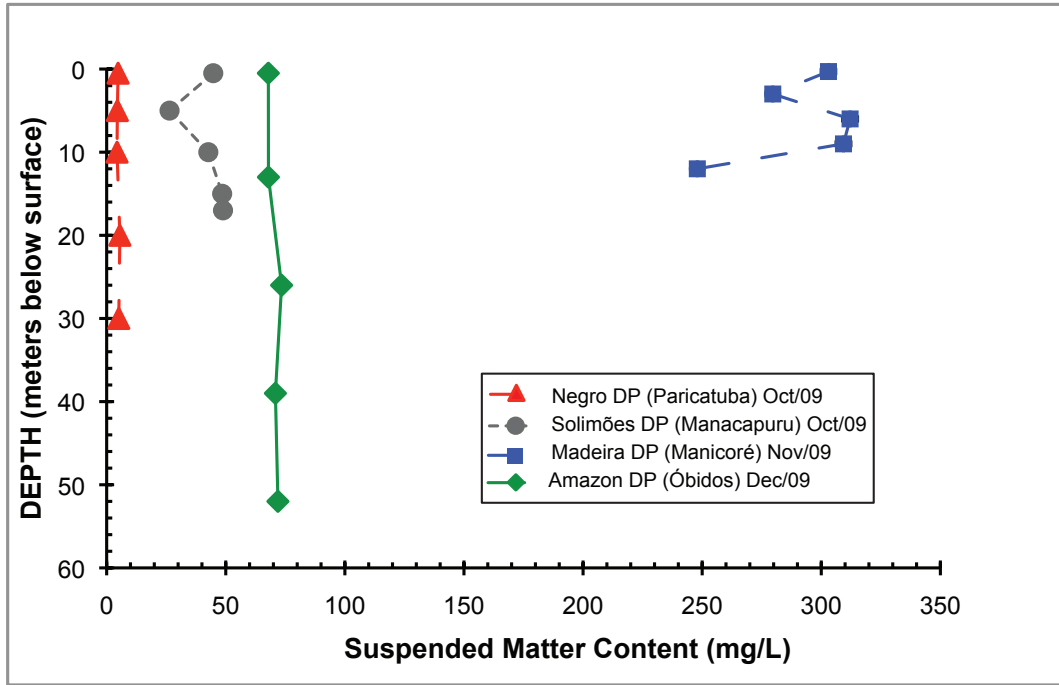


Fig. 16 – Suspended matter concentration in depths profiles - Negro, Madeira, Amazon and Solimões rivers.

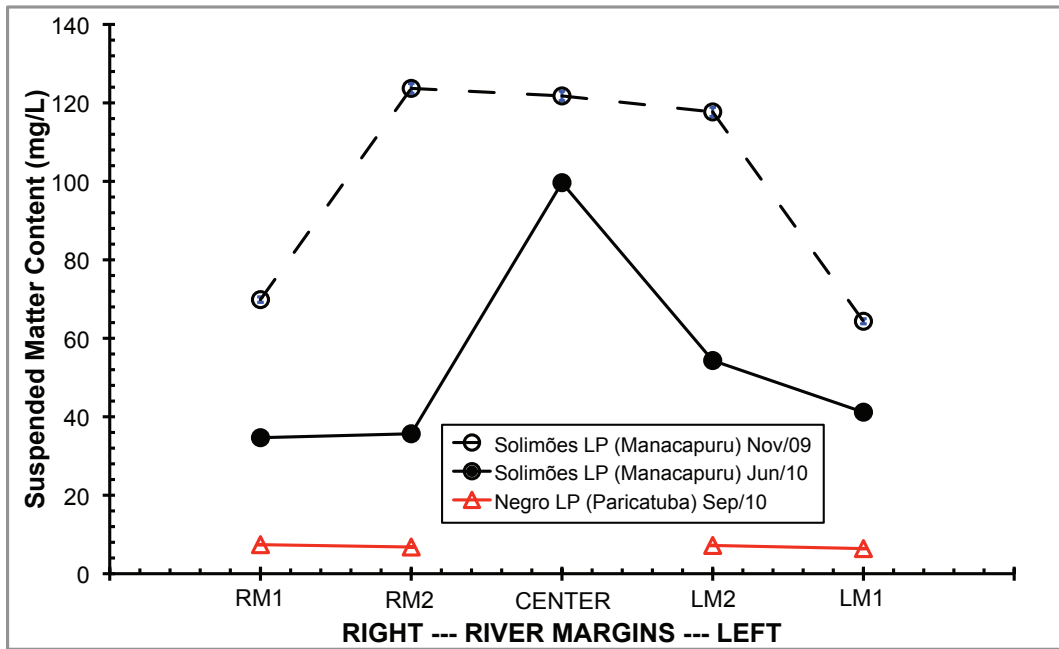


Fig. 17 – Suspended matter concentration in lateral profiles - Negro and Solimões rivers.

3.3 Iron content and isotope composition of suspended matter in the Amazon River and its tributaries

An increase in iron contents of suspended matter is observed from the top to the bottom of depth profiles in all rivers studied, although with some scatter (**Fig. 18**). Lateral profile samples for the Negro (Paricatuba Station) and Solimões (Manacapuru Station collected in November 2009 and June 2010) rivers show no significant variations in iron content from one to the other (**Fig. 19**). Unlike physico-chemical parameters and suspended matter content measured for the two lateral profiles collected at the Solimões River, absolute iron contents of the samples collected during high water levels are higher than those obtained during low water levels (**Fig. 19**).

Suspended particulate matter was analyzed for iron isotope compositions on the four depth profiles (Amazon River at Óbidos, Negro River at Paricatuba, Madeira River at Manicoré and Solimões River at Manacapuru) and three lateral profiles (Solimões at Manacapuru, during flood and dry seasons, and Negro River at Paricatuba). Results are expressed in $\delta^{57}\text{Fe}_{\text{IRMM}-14}$ as parts per mil (‰) and they vary between $-0.501 \pm 0.075\text{‰}$ and $0.196 \pm 0.083\text{‰}$ (**Tabela 2**, **Fig. 20** and **Fig. 21**).

Analyses of depth profiles show negative and homogeneous results for the suspended matter from the Negro River (Paricatuba Station), with $\delta^{57}\text{Fe}_{\text{IRMM}-14}$ values varying between $-0.433 \pm 0.072\text{‰}$ and $-0.501 \pm 0.075\text{‰}$ (**Tabela 2**, **Fig. 20**). In contrast, samples from the Amazon (Óbidos Station), Madeira (Manicoré Station) and Solimões (Manacapuru Station) rivers display similar and also homogenous iron isotope signatures, which are, within analytical uncertainties, nearly indistinguishable from the average composition of the continental crust ($\delta^{57}\text{Fe}_{\text{IRMM}-14} \sim 0.1\text{‰} \pm 0.03$, [Poitrasson, 2006](#) – **Fig. 20**).

Individual analyses of the three lateral profiles (Solimões River at Manacapuru Station, during flood and dry seasons, and the Negro River at Paricatuba Station), collected respectively in November 2009, June 2010 and September 2010, show no significant variations in the Fe isotopic composition of the suspended particulate matter (**Fig. 21**). Results obtained for the Solimões River are also close to the average composition of the continental crust ($\delta^{57}\text{Fe}_{\text{IRMM}-14} \sim 0.1\text{‰} \pm 0.03$, [Poitrasson, 2006](#)), ranging from $-0.001 \pm 0.141\text{‰}$ to $0.196 \pm 0.083\text{‰}$, while results from the Negro River are between $-0.324 \pm 0.150\text{‰}$ and $-0.196 \pm 0.108\text{‰}$. Although lateral variations were not observed in these samples, once more the water nature difference (black *versus* white) is recognized in the results (**Fig. 20** and **Fig. 21**).

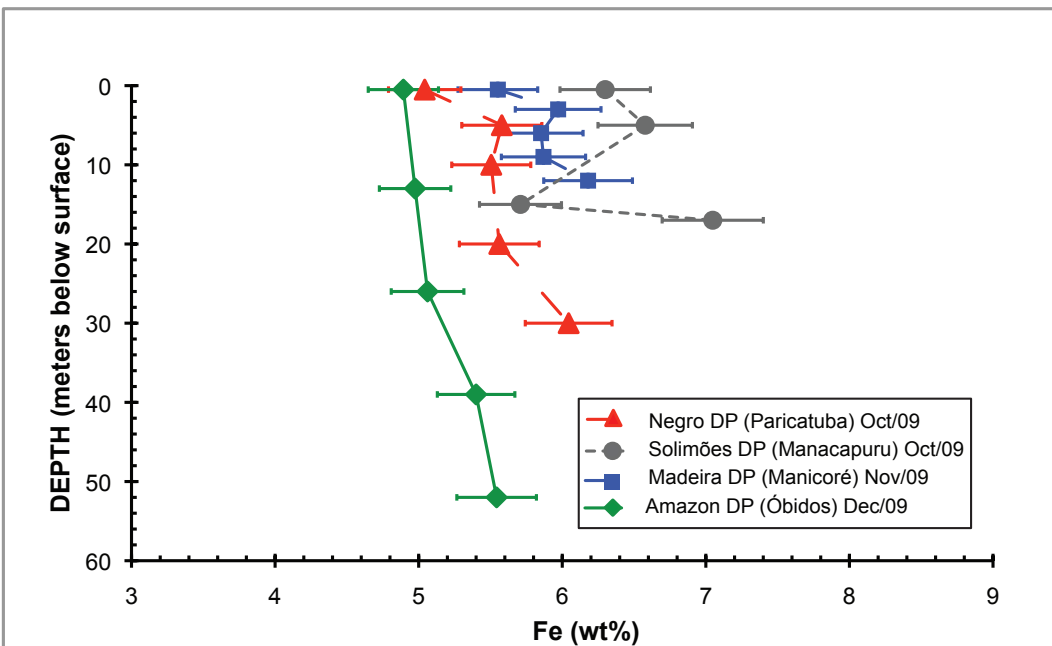


Fig. 18 – Iron concentration variations in suspended matter according to depth (measured with MC-ICP-MS). Negro, Madeira, Amazon and Solimões rivers.

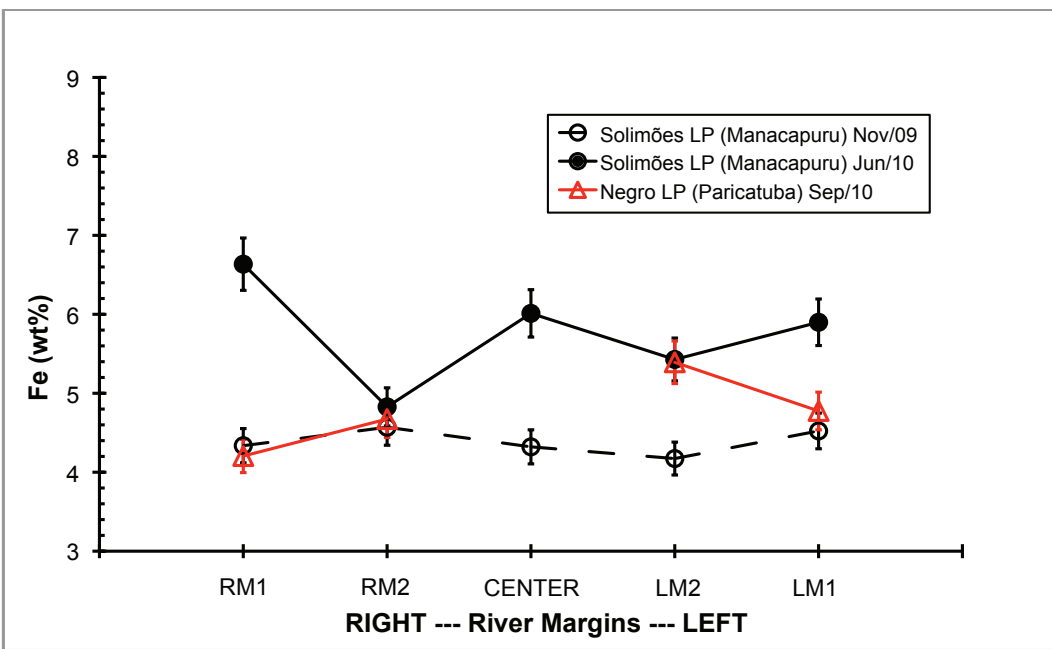


Fig. 19 – Iron concentration variations in suspended matter according to lateral profiles (measured with MC-ICP-MS). Negro and Solimões rivers.

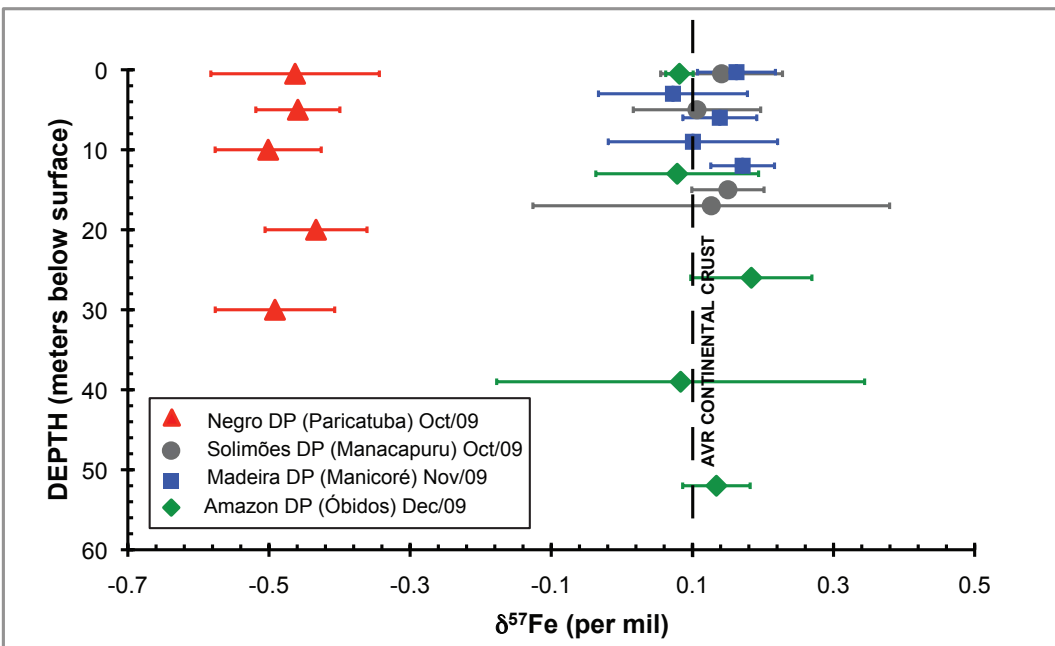


Fig. 20 – $\delta^{57}\text{Fe}$ variations in suspended matter along depth profiles. The average isotopic composition of the continental crust ($\delta^{57}\text{Fe} \sim 0.1 \pm 0.03\text{‰}$; Poitrasson, 2006) is shown for reference.

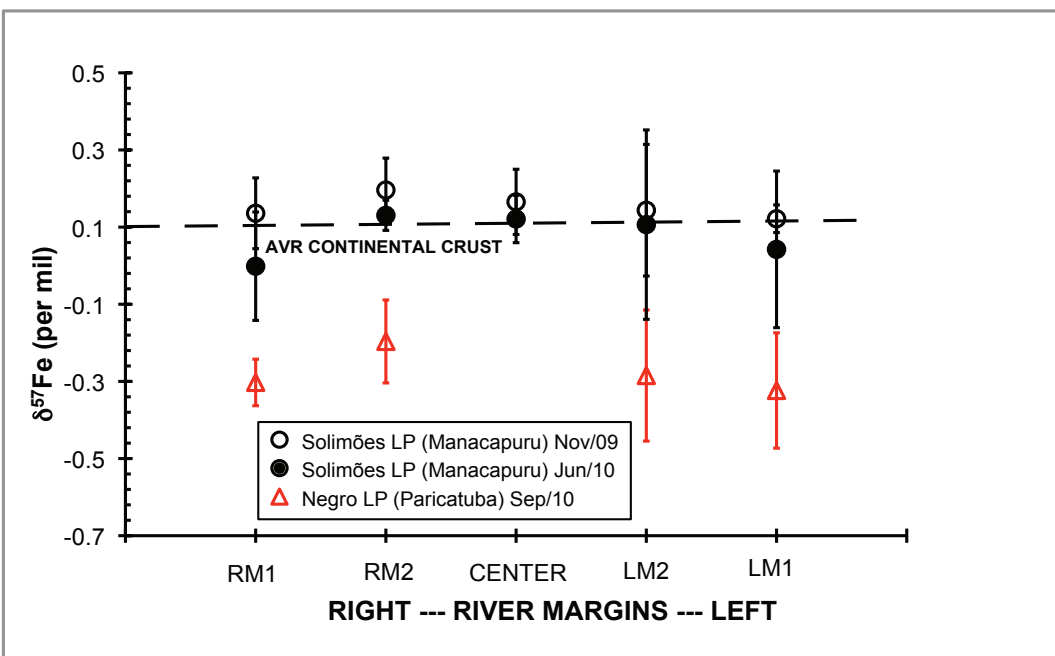


Fig. 21 – $\delta^{57}\text{Fe}$ variations in suspended matter along lateral profiles in the Negro and Solimões rivers. The average isotopic composition of the continental crust ($\delta^{57}\text{Fe} \sim 0.1 \pm 0.03\text{‰}$; Poitrasson, 2006) is shown for reference.

4. DISCUSSION

In contrast to the riverine suspended matter and their Fe concentrations, as well as other *in situ* parameters (**Tabela 1** and **Fig. 16** to **Fig. 19**), the $\delta^{57}\text{Fe}$ values of the seven profiles studied do not vary with depth or lateral cross sections (**Tabela 2** and **Fig. 20** and **Fig. 21**). This suggests that the processes affecting the suspended matter abundances and their Fe concentrations do not modify the iron isotope signatures, which will therefore express the $\delta^{57}\text{Fe}$ of the iron sources. For the Amazon, Madeira and Solimões Rivers, the iron occurring in the suspended matter does not seem to have been through a redox cycle. It thus reflects directly the isotopic composition of its continental crust source, in agreement with the mostly detritic nature of the suspended load of these rivers (e.g., [Guyot et al., 2007](#)).

Results presented here show that the iron isotope signature of subsurface suspended matter samples will be representative of the whole river cross section for the Amazon, the Madeira, the Solimões and the Negro rivers (**Fig. 20** and **Fig. 21**). This is in contrast to recent results for strontium isotopes, as reported by [Bouchez et al. \(2010\)](#), who suggested that suspended sediments in large rivers are not isotopically homogenous. These authors observed significant variations of Strontium isotopes along depth and lateral profiles in the Solimões River at Manacapuru.

The three lateral profiles analyzed also show that, during low and high water levels (respectively dry and flood seasons), there is no isotope fractionation from one riverbank to the other.

Contrasting with the Negro River suspended matter, which has a light isotopic signature (**Fig. 20** and **Fig. 21**), the suspended matter profiles (both depth and lateral) in the Madeira, Solimões and Amazon rivers show values that are very similar to the continental crust $\delta^{57}\text{Fe}$ value ($0.1\text{\textperthousand} \pm 0.03\text{\textperthousand}$; [Poitrasson, 2006](#); **Fig. 20** and **Fig. 21**). Results for the Negro River are in accordance with those discussed by [Bergquist and Boyle \(2006\)](#), who also obtained a light isotope composition for suspended matter from this river. Their results are, however, lighter by approximately 1\textperthousand in $\delta^{57}\text{Fe}$. Given that the data of this study do not suggest a noticeable iron isotope heterogeneity throughout the river cross section, the shift between results presented here and the ones obtained by [Bergquist and Boyle \(2006\)](#) might be attributed to differences in the methodologies employed, such as sample digestion and especially filtration techniques, that are distinct in the respective studies. One more likely

explanation could be related to seasonal variations, as reported in riverine suspended matter by Ingri *et al.* (2006) and Song *et al.* (2011). The sample of Bergquist and Boyle (2006) was collected in March 2002 (a few of months before the flood maximum), whereas the suspended matter samples from the Negro River studied here were collected in October 2009 and September 2010 (close to the dry maximum).

Environmental changes that took place from 2002 to 2010 in the Amazon region, which may have affected the natural conditions of these rivers, might also contribute to the different values reported. Martinez *et al.* (2009) presented a study of 12-year suspended sediment discharge at Óbidos (Amazon River), and observed an increase of about 20% from 1995 to 2007, which suggests a significant shift in the sediment transport regime of the Amazon River, that can probably be attributed to stronger erosion processes. This increase in erosion processes may be due to global change or regional changes, resulting from deforestation for example (Martinez *et al.*, 2009). All these factors may also change the contributions of organic and inorganic matter, leading to distinct isotopic signatures.

Furthermore, the past few years have been very atypical in the Amazon Basin. The hydrological cycle of 2009, for instance, was marked by exceptionally high water levels, while 2010 was very dry. Dry and humid seasons are reaching their peaks over the past few years and that may be an explanation to the difference between results here presented and those of Bergquist and Boyle (2006).

The light isotopic composition found in the Negro River suspended matter may be attributed to the nature of the water studied (black water), that, to a large extent, has different sources than the Madeira, the Solimões and the Amazon rivers (white waters). Its iron signatures most likely reflect iron composition of the reduced horizons in podzols layers of soil that occur in the northern part of the Amazon basin (Allard *et al.*, 2011), which are organic rich and therefore have lighter iron isotope signatures, characteristic of ferrous iron (*e.g.*, Wiederhold *et al.*, 2007b). Iron isotope studies of podzolic soils depth profiles (Fantle and DePaolo, 2004; Wiederhold *et al.*, 2007b) showed that reduced Fe is isotopically lighter (by $\sim -1\text{\textperthousand}$ in $\delta^{57}\text{Fe}$) in shallow organic rich horizons, which may thus explain the lighter isotopic composition of the suspended matter from the Negro River.

The Negro River has low pH and half of its iron is in the dissolved phase (Gaillardet *et al.*, 1997; Bergquist and Boyle, 2006). This soluble reduced form of iron may be heavier isotopically than the particulate phase, according to the Bergquist and Boyle (2006) study of

the Rio Negro and the [Escoube et al. \(2009\)](#) study for the North River (Massachusetts). These authors attribute the results to differences in Fe speciation.

According to [Fantle and DePaolo \(2004\)](#), who studied bulk waters (that represent the total Fe carried by rivers in the suspended and dissolved fractions), rivers with high particle loads, such as the Yukon and Susitna (Alaska), have heavier $\delta^{57}\text{Fe}$, while rivers with lower particle loads, such as the Klamath and Eel (California), have lighter $\delta^{57}\text{Fe}$ values. Results on the suspended matter from both black water rivers and white water rivers from the Amazonian Basin presented here are in agreement with this assumptions, since black water rivers have much lower content of suspended matter than white water rivers.

Results reported here indicate that, after addition of the dissolved and particulate matter of all its tributaries, the iron isotope composition of the Amazon River suspended matter, which represents close to 95% of its total iron ([Gaillardet et al., 1997](#); [Bergquist and Boyle, 2006](#)), is similar to the continental crust ($0.1 \pm 0.03\text{\textperthousand}$, [Poitrasson, 2006](#)). This suggests that, in agreement with previous inferences based on lateritic soil studies ([Poitrasson et al., 2008](#)), large rivers flowing in tropical areas, like the Amazon River, should deliver to the ocean an iron that has an isotopic signature close to that of the continental crust.

5. CONCLUSIONS

This study shows that, in contrast to parameters like water temperature, riverine suspended load or iron concentrations, the suspended matter iron isotope composition of the Amazon River and three of its main tributaries is constant along depth and lateral profiles. This indicates that a subsurface sample might be representative of a whole river cross and lateral sections, at least in a given season, in contrast with other isotopic tracers like strontium. The fact that the Fe isotope composition of a same water type (*i.e.*, white waters) is constant across different locations and depths suggests that these isotopic signatures would likely be a good tracer of the iron sources, instead of providing information on the nature of the processes involving iron in the water column. For instance, the white water suspended load (Amazon, Solimões and Madeira rivers) have $\delta^{57}\text{Fe}$ values that are similar to the continental crust, as expected from their mostly detritic nature that comes from the mechanical erosion of the Andes. In contrast, the light Fe isotopic composition found in the

Negro River black water reflects well the source of its suspended matter, which likely originated from the reduced organic rich layers of podzols from this river basin.

The Negro river suspended matter samples presented here and the datum of [Bergquist and Boyle \(2006\)](#) represent three distinct sampling dates and the differences observed between them may reveal a change in the Fe isotopic composition with time, as previously found in other organic-rich rivers ([Ingrin et al., 2006](#)). A more comprehensive time series study is required to find whether these distinct Fe isotope compositions of the Negro River suspended load reveal seasonal variations, or if they rather record a more global change linked to natural or anthropogenic causes. As the Amazon Basin has one of the greatest biodiversities in the planet, iron and other isotopic systems should be investigated and compared among each other in this area, in order to quantify and qualify possible impacts that can be caused by changes in its environmental conditions.

ACKNOWLEDGEMENTS

The authors would like to thank two anonymous reviewers who significantly helped to improve this manuscript with their constructive comments. Alain Plenecassagne, Alisson Akerman, Bárbara Lima, Celeida Márcia, Daniel Santos, Geraldo Boaventura, Eurides de Oliveira, Gérard Cochonneau, Gwenael Abril, Jean-Loup Guyot, Jean-Michel Martinez, Jérôme Chmeleff, Jonathan Prunier, Marie Paule Bonnet, Myller Sousa, Patrick Seyler, Philippe Besson, Tiago Eli and Valdemar Santos Guimarães are also thanked for discussions, ideas and issues related to analytical techniques. Also, all the crew of the boats is acknowledged for their hard work. The authors wish also to thank the Brazilian National Agency of Water (ANA), CPRM (Brazil Geological Survey), the Coordination for the Improvement of Higher Education-Personnel (CAPES), the National Council of Technological and Scientific Development (CNPq), the Centre National de la Recherche Scientifique (CNRS), the French Committee for the Evaluation of University Cooperation with Brazil (COFECUB), the Institut de Recherche pour le Développement (IRD), the Laboratory of Geochronology of the University of Brasília and the Laboratory Géosciences Environnement Toulouse for their support. They are also indebted to the ORE-HYBAm project for field assistance. This research was partly funded by an EC2CO grant to FP.

Tabela 1 - Physico-chemical parameters of the Amazonian rivers studied.

RIVER	profile type ^a	Station	DEPTH (m)	Temperature (°C ±0.1)	Conductivity (µS/cm±1)	pH (±0.2)	Turbidity (NTU±1)	Sampling Date	Sampling Time	lat ^b	long ^b
NEGRO	DP	PARICATUBA	0.5	32.3	8	4.7	6	03.10.09	21:16		
NEGRO	DP	PARICATUBA	5	31.5	8	-	-	03.10.09	21:26		
NEGRO	DP	PARICATUBA	10	31.3	8	-	-	03.10.09	21:33	-3.07203	-60.26109
NEGRO	DP	PARICATUBA	20	31.2	9	-	-	03.10.09	21:41		
NEGRO	DP	PARICATUBA	30	31.2	8	-	-	03.10.09	21:56		
MADEIRA	DP	MANICORÉ	surface	30.1	66	7.0	342	25.11.09	9:43		
MADEIRA	DP	MANICORÉ	3	30.1	66	7.1	192	25.11.09	9:27		
MADEIRA	DP	MANICORÉ	6	30.1	66	7.1	340	25.11.09	9:18	-5.80992	-61.36462
MADEIRA	DP	MANICORÉ	9	30.1	66	7.1	343	25.11.09	9:06		
MADEIRA	DP	MANICORÉ	12	30.1	66	7.0	339	25.11.09	8:54		
AMAZON	DP	ÓBIDOS	surface	30.4	85	7.2	97	06.12.09	8:08		
AMAZON	DP	ÓBIDOS	13	30.5	80	7.3	99	06.12.09	8:22		
AMAZON	DP	ÓBIDOS	26	30.1	79	7.3	93	06.12.09	8:39	-1.91985	-55.51446
AMAZON	DP	ÓBIDOS	39	30.4	80	7.3	97	06.12.09	8:49		
AMAZON	DP	ÓBIDOS	52	30.6	80	7.3	96	06.12.09	8:53		
SOLIMÕES	DP	MANACAPURU	0.5	30.7	76	6.6	70	05.10.09	21:55		
SOLIMÕES	DP	MANACAPURU	5	-	-	-	-	-	-	-3.33543	-60.51895
SOLIMÕES	DP	MANACAPURU	15	-	-	-	-	-	-		
SOLIMÕES	DP	MANACAPURU	17	-	-	-	-	-	-		
SOLIMÕES	LP	MANACAPURU RM1	0.5	31.4	97	7.3	67	30.11.09	13:14	-3.33521	-60.55701
SOLIMÕES	LP	MANACAPURU RM2	0.5	31.0	101	7.2	106	30.11.09	13:18	-3.33072	-60.55634
SOLIMÕES	LP	MANACAPURU Center	0.5	31.0	104	7.2	102	30.11.09	13:26	-3.32465	-60.55565

Tabela 1 (continued)

RIVER	profile type ^a	Station	DEPTH (m)	Temperature (°C ±0.1)	Conductivity (µS/cm±1)	pH (±0.2)	Turbidity (NTU±1)	Sampling Date	Sampling Time	lat ^b	long ^b
SOLIMÕES	LP	MANACAPURU LM2	0.5	31.0	104	7.2	87	30.11.09	13:31	-3.31901	-60.55703
SOLIMÕES	LP	MANACAPURU LM1	0.5	31.6	103	7.2	67	30.11.09	13:36	-3.31440	-60.55816
SOLIMÕES	LP	MANACAPURU RM1	0.5	28.4	56	6.5	43	24.06.10	18:04	-3.33518	-60.55695
SOLIMÕES	LP	MANACAPURU RM2	0.5	28.4	67	6.7	67	24.06.10	18:19	-3.33009	-60.55604
SOLIMÕES	LP	MANACAPURU Center	0.5	28.4	73	6.8	85	24.06.10	18:29	-3.32333	-60.55495
SOLIMÕES	LP	MANACAPURU LM2	0.5	28.4	74	6.7	70	24.06.10	18:40	-3.31844	-60.55616
SOLIMÕES	LP	MANACAPURU LM1	0.5	28.6	73	6.7	61	24.06.10	18:57	-3.31380	-60.55848
NEGRO	LP	PARICATUBA	0.5	31.9	14	5.3	-	28.09.10	-	-3.06265	-60.26160
NEGRO	LP	PARICATUBA	0.5	32.0	15	4.9	-	28.09.10	-	-3.06532	-60.25885
NEGRO	LP	PARICATUBA	0.5	32.6	9	5.1	-	28.09.10	-	-3.07063	-60.25563
NEGRO	LP	PARICATUBA	0.5	33.0	9	5.2	-	28.09.10	-	-3.07360	-60.25418

^a DP - depth profiles; LP - lateral profiles

^b decimal degrees - WGS-84

Tabela 2 - Suspended matter concentrations and their iron isotope compositions $\delta^{57}\text{Fe}_{\text{IRMM}-14}$ for the Negro, Madeira, Amazon and Solimões rivers lateral and depth profiles.

RIVER	profile type ^a	STATION	DEPTH (m) / POSITION	Date collected	Fe concentration ICP-MS (wt.% \pm 5%)	SPM ^b (mg*L ⁻¹ \pm 1%)	$\delta^{57}\text{Fe}^c$ (‰)	2SE ^d	$\delta^{56}\text{Fe}^c$ (‰)	2SE ^d	number of analysis (n)
NEGRO	DP	PARICATUBA	surface	03.10.09	5.0	4.8	-0.463	0.119	-0.259	0.292	3
NEGRO	DP	PARICATUBA	5	03.10.09	5.6	4.5	-0.459	0.060	-0.324	0.480	3
NEGRO	DP	PARICATUBA	10	03.10.09	5.5	4.4	-0.501	0.075	-0.157	0.388	3
NEGRO	DP	PARICATUBA	20	03.10.09	5.6	5.5	-0.433	0.072	-0.346	0.132	6
NEGRO	DP	PARICATUBA	30	03.10.09	6.0	5.1	-0.492	0.085	-0.336	0.112	6
MADEIRA	DP	MANICORÉ	surface	25.11.09	5.6	303	0.162	0.055	0.118	0.040	6
MADEIRA	DP	MANICORÉ	3	25.11.09	6.0	280	0.072	0.106	0.021	0.152	3
MADEIRA	DP	MANICORÉ	6	25.11.09	5.9	312	0.139	0.052	0.085	0.030	6
MADEIRA	DP	MANICORÉ	9	25.11.09	5.9	309	0.101	0.120	0.057	0.102	3
MADEIRA	DP	MANICORÉ	12	25.11.09	6.2	248	0.171	0.045	0.131	0.077	6
AMAZON	DP	ÓBIDOS	surface	06.12.09	4.9	68	0.082	0.019	0.072	0.019	3
AMAZON	DP	ÓBIDOS	13	06.12.09	5.0	68	0.078	0.115	0.063	0.078	6
AMAZON	DP	ÓBIDOS	26	06.12.09	5.1	73	0.184	0.086	0.101	0.032	6
AMAZON	DP	ÓBIDOS	39	06.12.09	5.4	71	0.083	0.261	0.067	0.207	3
AMAZON	DP	ÓBIDOS	52	06.12.09	5.5	72	0.134	0.048	0.092	0.053	3
SOLIMÕES	DP	MANACAPURU	0.5	06.10.09	6.3	45	0.141	0.086	0.074	0.049	6
SOLIMÕES	DP	MANACAPURU	5	06.10.09	6.6	26	0.106	0.090	0.057	0.076	3
SOLIMÕES	DP	MANACAPURU	15	06.10.09	5.7	48	0.150	0.051	0.084	0.023	3
SOLIMÕES	DP	MANACAPURU	17	06.10.09	7.0	49	0.127	0.253	0.066	0.138	3
SOLIMÕES	LP	MANACAPURU RM1	right margin 1	30.11.09	4.3	70	0.136	0.092	0.105	0.042	3
SOLIMÕES	LP	MANACAPURU RM2	right margin 2	30.11.09	4.6	124	0.196	0.083	0.145	0.055	3
SOLIMÕES	LP	MANACAPURU Center	center	30.11.09	4.3	122	0.165	0.085	0.117	0.068	3

Tabela 2 (continued)

RIVER	profile type ^a	STATION	DEPTH (m) / POSITION	Date collected	Fe concentration ICP-MS (wt.% ± 5%)	SPM ^b (mg*L ⁻¹ ± 1%)	δ ⁵⁷ Fe ^c (‰)	2SE ^d	δ ⁵⁶ Fe ^c (‰)	2SE ^d	number of analysis (n)
SOLIMÕES	LP	MANACAPURU LM2	left margin 2	30.11.09	4.2	118	0.144	0.171	0.078	0.102	3
SOLIMÕES	LP	MANACAPURU LM1	left margin 1	30.11.09	4.5	64	0.122	0.036	0.092	0.007	3
SOLIMÕES	LP	MANACAPURU RM1	right margin 1	24.06.10	6.6	35	-0.001	0.141	-0.009	0.115	3
SOLIMÕES	LP	MANACAPURU RM2	right margin 2	24.06.10	4.8	36	0.131	0.039	0.092	0.031	3
SOLIMÕES	LP	MANACAPURU Center	center	24.06.10	6.0	100	0.121	0.061	0.075	0.072	3
SOLIMÕES	LP	MANACAPURU LM2	left margin 2	24.06.10	5.4	54	0.106	0.246	0.087	0.220	3
SOLIMÕES	LP	MANACAPURU LM1	left margin 1	24.06.10	5.9	41	0.042	0.203	0.035	0.147	3
NEGRO	LP	PARICATUBA	right margin 1	28.09.10	4.2	7.4	-0.303	0.060	-0.253	0.027	3
NEGRO	LP	PARICATUBA	right margin 2	28.09.10	4.7	6.8	-0.196	0.108	-0.167	0.068	3
NEGRO	LP	PARICATUBA	left margin 2	28.09.10	5.4	7.2	-0.285	0.170	-0.245	0.142	6
NEGRO	LP	PARICATUBA	left margin 1	28.09.10	4.8	6.4	-0.324	0.150	-0.269	0.120	6

^a DP - depth profiles; LP - lateral profiles

^b SPM - suspended matter content

^c Iron isotope data relative to IRMM-14

^d 2SE calculated from the number of analyses indicated, using the Student's t-correcting factors ([Platzner, 1997](#)).

CAPÍTULO SEIS

PRELIMINARY IRON ISOTOPIC DATA ON SUSPENDED AND DISSOLVED MATERIAL FROM DISTINCT WATER NATURES IN THE PERUVIAN AND BRAZILIAN AMAZON

1. INTRODUCTION

Some samples of water suspended and dissolved load have been analyzed for iron isotopes in the GET Laboratory, Toulouse, France. Data acquisition needs to be refined before final interpretation, but as the preliminary results bring new insights to the data already in discussion on the scope of this Thesis, this small chapter is offered, focusing only on the presentation of the first data obtained for these waters. Further debate on the results will have place only after this Thesis defense, when new sessions for data acquirement in the Neptune MC-ICP-MS will be available and associated uncertainties might be reduced, leading to a possibly more accurate interpretation.

2. METHODS

Samples were collected during three field campaigns in the Amazon Region: the first on October/November 2009, the second on December 2009 and the third on July 2010 (**Fig. 22, Tabela 3**). Collection strategies are described in chapters 5 and 7, as well as samples digestions and treatments before MC-ICP-MS analyzes. One clear water station, the Alter do Chão at the Tapajós River, was studied for suspended matter collected at December and July, respectively dry and flood seasons.

The dissolved material from each of the Negro River depth profile samples (suspended matter counterparts presented in chapter 5, **Fig. 20**) was recovered after the evaporation of approximately 150 ml of water.

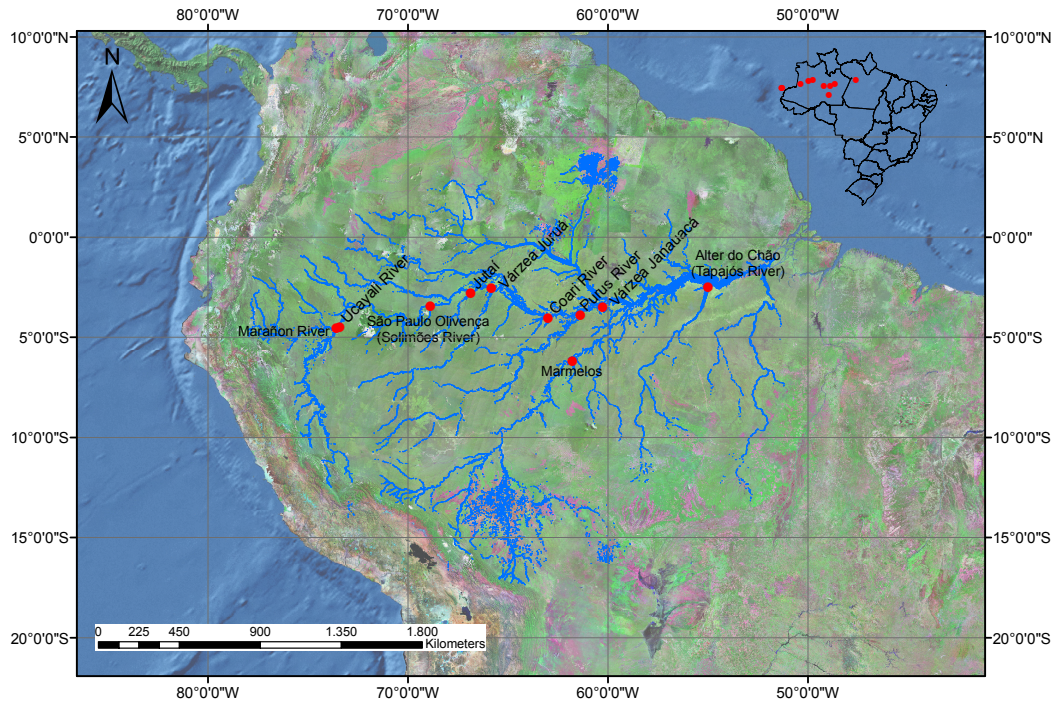


Fig. 22 – Map of sample locations in the Amazon River Basin.

3. RESULTS

3.1 Suspended Matter from White, Black and Clear water rivers

The first set of samples analyzed for suspended matter iron isotopic composition includes three white water rivers (Marañon and Ucayali rivers in Peru – which combine to form the Solimões River in Brazil – and the Solimões River itself, in Brazil, at the São Paulo de Olivença Station). These 3 samples show homogeneous continental crust-like $\delta^{57}\text{Fe}$ values, varying from 0.019 ± 0.16 to 0.160 ± 0.06 , similar to all the other suspended matter from white water rivers analyzed in the scope of this Thesis (**Tabela 3**, **Fig. 20**, **Fig. 21** and **Fig. 23**).

The second group of samples includes the black water rivers Marmelos and Coari, and two distinct rivers: the Purus (white water, [Richey et al., 2004](#), [Junk et al., 2010](#) and [Rios-Villamizar et al., 2011](#)) and Jutaí, both right margin tributaries to the Amazon River. The Jutaí River has been reported to have black water characteristics ([Richey et al., 2004](#)), showing similar parameters to the Negro River, such as significant levels of dissolved organic carbon and low NO_3^- ([Richey et al., 2004](#)).

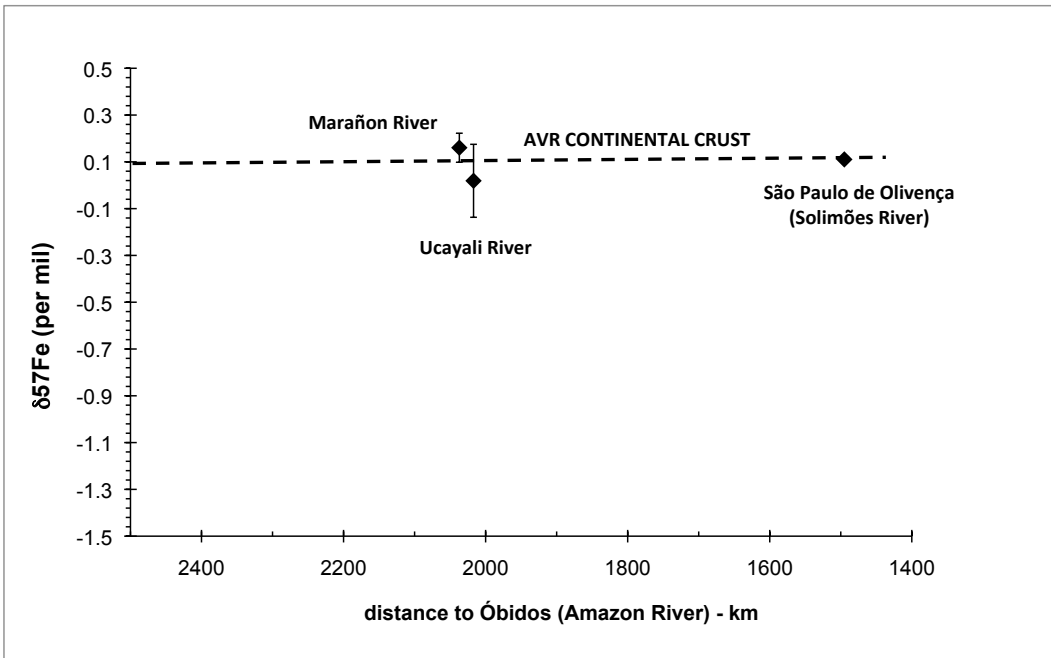


Fig. 23 – $\delta^{57}\text{Fe}$ values from white water rivers in Peru and Brazil. Values in the abscissa represent the average distance (km in straight line) from the collecting station to the Óbidos Station.

Similarly to the Jutaí River, which appears as “black” as the Negro River ([Richey et al., 2004](#)), the Purus River presents visual characteristics similar to the other black water rivers in the region. Despite the high sediment contents, distinctive of white water rivers, the Purus River generally displays a high content of dissolved organic carbon ([Richey et al., 1990](#)) and nitrate levels, similar to black water rivers, besides seasonal fluctuations on physico-chemical parameters ([Rios-Villamizar et al., 2011](#)) and elevated levels of $p\text{CO}_2$ ([Richey et al., 2004](#)).

The water pH, the conductivity values and the suspended matter content of the Jutaí and Purus rivers samples analyzed in this work, collected in June 2010 (**Tabela 3**), confirm their distinction from the classic white water rivers. Hence, these two samples are here considered to be a separate group, due to their not well documented water nature and provenance, and their results are discussed together with the black water rivers group for interpretation purposes. Results on the suspended matter iron isotopic composition for this set of samples are all negative (**Tabela 3** and **Fig. 24**), and vary from -0.432 ± 0.14 (Coari River) and -0.019 ± 0.10 (Marmelos River).

The only clear water river analyzed was the Tapajós River, at the Alter do Chão Station. The two samples, collected in different seasons, show variable suspended matter iron isotopic signatures (**Tabela 3** and **Fig. 24**): in the dry period (December 2009), $\delta^{57}\text{Fe}$ values are negative (-0.538 ± 0.12) and in the flood period, results are positive (0.145 ± 0.28 , July

2010). Anyhow, the uncertainty related to the flood sample, collected in July, is high, and once this data is refined, there is a possibility that the variation on the iron isotopic signature for the Alter do Chão Station (Tapajós River) is weaker than initially thought.

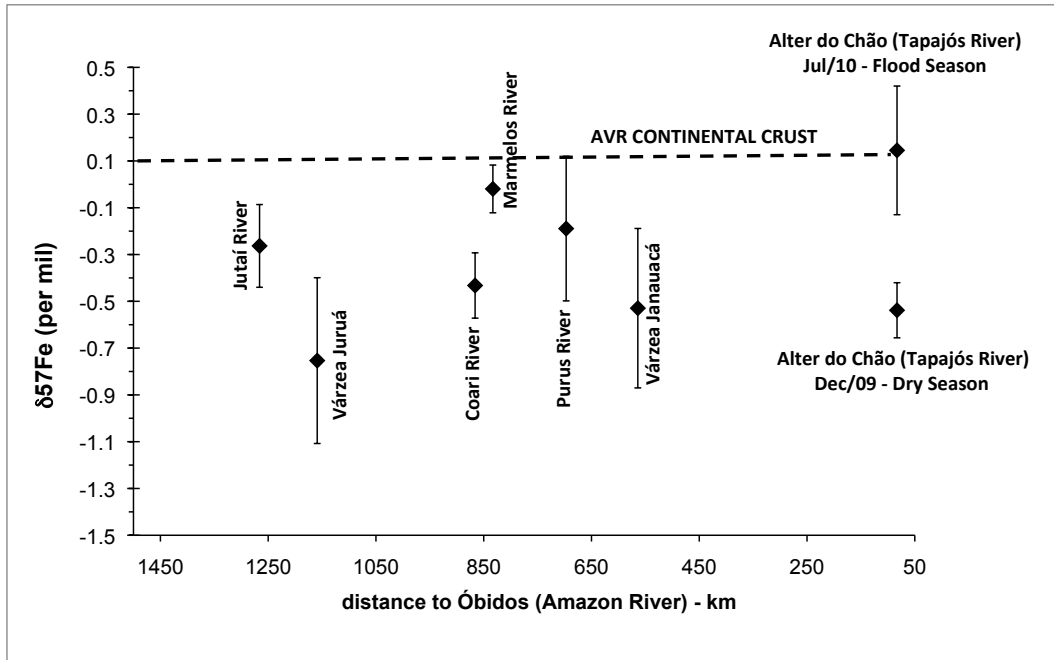


Fig. 24 – $\delta^{57}\text{Fe}$ values from black, clear and differentiated white water rivers in Brazil. Values in the abscissa represent the average distance (km in straight line) from the collecting station to the Óbidos Station (Amazon River).

3.2 Suspended Matter from Várzeas

The term Várzea is used by the Amazonian population to describe periodically flooded areas (Junk *et al.*, 2010), or floodplains, which are associated to nutrient-rich white water rivers. When these regions are related to nutrient-poor black water and clear water rivers, they are called Igapós (Junk and Piedade, 2010). These areas alternate between a terrestrial and an aquatic phase and are considered very productive ecosystems due to the annual deposit of nutrients (Junk *et al.*, 2010).

The suspended matter of the Janauacá (Solimões River) and the Juruá (Juruá River) várzeas were analyzed in this work. The Janauacá sample was collected close to the dry season (October 2009) and the Juruá sample, in the flood season (June 2010). They show the most negative suspended matter iron isotopic results within this set of samples (which includes all the suspended matter samples from the rivers described in this chapter), and

results for this two locations are, respectively, -0.529 ± 0.34 and -0.753 ± 0.35 (**Tabela 3** and **Fig. 24**).

3.3 Negro River Dissolved Fraction

The corresponding dissolved fractions from the Negro River suspended matter depth profile, presented on chapter 5, show that, as expected on the basis of previous studies made in the soluble fraction of this river ([Bergquist and Boyle, 2006](#)), they are isotopically heavy compared to their counterparts (**Fig. 20**, Chapter 5). Results vary from 0.829 ± 0.08 (second depth, 5 meters) to 1.091 ± 0.18 (last depth, 30 meters - **Tabela 3** and **Fig. 25**).

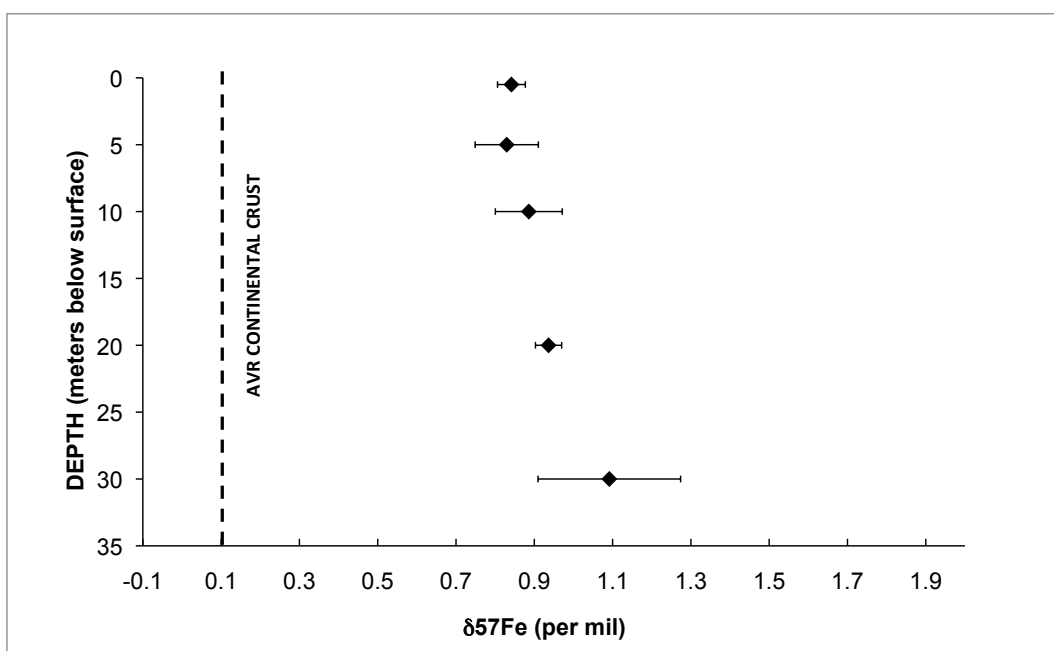


Fig. 25 – $\delta^{57}\text{Fe}$ variations in dissolved fraction along depth profile. The average isotopic composition of the continental crust ($\delta^{57}\text{Fe} \sim 0.1 \pm 0.03\text{‰}$; [Poitrasson, 2006](#)) is shown for reference. Negro River at Paricatuba Station.

4. BRIEF DISCUSSION ON THE PRELIMINARY DATA

The two suspended matter samples from the Tapajós River, at the Alter do Chão Station, collected at different seasons (dry – December – and wet – July) may indicate a temporal variation, where the flood season sample is isotopically heavier than the dry season sample (**Tabela 3** and **Fig. 24**). If confirmed, these results are in accordance to the data obtained for the Negro River suspended matter temporal series further presented (chapter 7). This would indicate that, in contrast to the suspended matter from white water rivers, which

shows homogeneous $\delta^{57}\text{Fe}$ values along the hydrological cycle, the suspended matter from clear water rivers is, similarly to the suspended matter of black water rivers, subject to variations along the hydrological cycle (*cf.* chapter 7).

No variation can be seen, within uncertainties, in the dissolved fraction from the Negro River according to depth (**Tabela 3** and **Fig. 25**), what would be in accordance to the results presented on chapter 5 for the suspended matter depth profiles of different rivers (*cf.* **Fig. 20**). As previously demonstrated by [Bergquist and Boyle \(2006\)](#) the suspended matter in the Negro River is isotopically lighter than the dissolved phase in this river (**Tabela 3** and *cf.* **Fig. 20** and **Fig. 25**). Mass balance calculations based on the results here obtained for the suspended and dissolved phases of this river indicate that the overall iron isotopic signature from the Negro River should be variable along the year, either slightly positive or slightly negative, what is in accordance to assumptions made by [Escoube *et al.* \(2009\)](#).

5. CONCLUDING REMARKS

The preliminary data discussed in this chapter will be further improved and properly interpreted. At this stage, they were used to aid on the interpretation of the more refined data, presented in chapters 5 and 7. The fact that the suspended matter of black / clear water and white water rivers show distinct iron isotopic signatures is well established, as well as the fractionation between dissolved and particulate matter from the Negro River (**Fig. 20** and **Fig. 25**). The new data on the várzeas, which show negative suspended matter $\delta^{57}\text{Fe}$ values, similarly to the black / clear water rivers, and the data on the Jutaí and Purus rivers (which have black water rivers characteristics) constitute an interesting avenue of research. It is also clear from the data here presented and the literature data (*e.g.*, [Bergquist and Boyle, 2006](#); [Ingrin *et al.*, 2006](#); [Escoube *et al.*, 2009](#); [dos Santos Pinheiro *et al.*, 2013](#); [Ilina *et al.*, 2013](#)) that varied iron isotopic signatures will be mainly found in organic reduced, or nutrient-rich environments, rather than in inorganic well-oxygenated systems.

Iron isotopes are known to be sensitive to redox conditions (*e.g.*, [Johnson *et al.*, 2002](#); [Rouxel *et al.*, 2005](#); [Wiederhold *et al.*, 2007b](#), among others) but they can also be effectively used as indicators of biogenic, organic sources, as well as differential weathering. In the next chapter, $\delta^{57}\text{Fe}$ values for two temporal series are provided with the aim of validating the hypothesis that organic environments not only have distinct lighter iron isotopic signatures,

but they are also subject to significant changes due to the variable contribution of suspended material during the hydrological cycles, in opposition to inorganic environments, which seem to have a constant iron isotopic composition during different seasons (*i.e.*, are not affected by changing conditions, such as low and high water levels).

Tabela 3 - Physico-chemical parameters, along with suspended matter concentrations and iron isotope compositions $\delta^{57}\text{Fe}_{\text{IRMM}-14}$. Surface samples from Amazonian rivers in Peru and Brazil, Várzeas (Solimões and Juruá rivers) and dissolved matter (Negro River depth profile).

Sample Identification / DEPTH (m)	Sampling Date	Lat*	Long*	Temperature ($^{\circ}\text{C} \pm 0.1$)	Conductivity ($\mu\text{S}/\text{cm} \pm 1$)	pH (± 0.2)	COD (ppm $\pm 5\%$)	Fe concentration ICP-MS $\pm 5\%$ (wt.% - suspended matter and ng/g - dissolved matter)	SPM ^a ($\text{mg}^*\text{L}^{-1} \pm 1\%$)	$\delta^{57}\text{Fe}$ (‰) ^b	2SE ^c	$\delta^{56}\text{Fe}$ (‰) ^b	2SE ^c	number of analysis (n)
Peruvian and Brazilian white water Rivers														
Marañon	10.06.10	-4.5364	-73.5918	26.4	134	7.6	5.8	5.7	245.4	0.160	0.062	0.107 ^e	0.041	3
Ucayali	10.06.10	-4.4919	-73.4243	27.2	238	7.5	11.7	5.9	98.3	0.019	0.156	0.013 ^e	0.104	3
São Paulo Olivença	15.06.10	-3.4528	-68.8954	27.5	131	7.3	5.3	7.4	142.5	0.110	0.134	0.074	0.102	3
Black water Rivers														
Jutaí	17.06.10	-2.7977	-66.8737	26.9	14	5.7	12.3	7.6	10.8	-0.263 ^d	0.177	-0.175	0.118	6
Marmelos	24.11.09	-6.1617	-61.7897	32.9	6	5.2	n.a.	9.4	2.7	-0.020 ^d	0.102	-0.013	0.068	6
White water Rivers with distinct water characteristics														
Purus	24.06.10	-3.9045	-61.3932	28.5	24	6.0	5.1	11.1	14.5	-0.189	0.309	-0.130	0.166	3
Coari	22.06.10	-4.0358	-63.0048	28.1	77	6.8	4.9	5.3	56.8	-0.432	0.140	-0.100	0.033	3
Clear water Rivers														
Alter dec	08.12.09	-2.4743	-55.0056	30.0	14	7.1	n.a.	3.9	4.2	-0.538	0.118	-0.359	0.079	3
Alter jul	04.07.10			30.2	15	6.9	1.9	3.9	n.a.	0.145 ^d	0.275	0.097	0.183	3

Tabela 3 (continued)

Sample Identification / DEPTH (m)	Sampling Date	Lat*	Long*	Temperature (°C ± 0.1)	Conductivity (µS/cm ± 1)	pH (± 0.2)	COD (ppm ± 5%)	Fe concentration ICP-MS ± 5% (wt.% - suspended matter and ng/g - dissolved matter)	SPM ^a (mg*L ⁻¹ ± 1%)	δ ⁵⁷ Fe (‰) ^b	2SE ^c	δ ⁵⁶ Fe (‰) ^b	2SE ^c	number of analyses (n)
Várzeas														
Várzea Janaúacá	07.10.09	-3.4879	-60.2701	32.5	57	7.7	n.a.	3.9	4.8	-0.529	0.341	-0.350	0.257	3
Várzea Juruá	18.06.10	-2.5614	-65.8464	27.9	34	6.3	6.3	13.0	7.8	-0.753	0.354	-0.360	0.372	3
Dissolved matter Negro River depth profile (Paricatuba Station)														
0.5	03.10.09			32.3	8	4.7	n.a.	32.2	4.8	0.842	0.036	0.521	0.033	3
5	03.10.09			31.5	8	n.a.	n.a.	31.7	4.5	0.830	0.081	0.529	0.030	3
10	03.10.09	-3.0720	-60.2611	31.3	8	n.a.	n.a.	34.0	4.4	0.886	0.086	0.564	0.040	3
20	03.10.09			31.2	9	n.a.	n.a.	35.0	5.5	0.936	0.033	0.588	0.021	3
30	03.10.09			31.2	8	n.a.	n.a.	35.9	5.1	1.092	0.182	0.670	0.103	6

a. SPM - suspended matter content

b. Iron isotope data relative to IRMM-14

c. 2SE calculated from the number of analyses indicated, using the Student's t-correcting factors ([Platzner, 1997](#)).

d. δ⁵⁷Fe calculated from δ⁵⁶Fe value

e. δ⁵⁶Fe calculated from δ⁵⁷Fe value

* decimal degrees - WGS-84

CAPÍTULO SETE

CONTRASTED TEMPORAL IRON ISOTOPIC EVOLUTION OF THE SUSPENDED MATTER FROM THE AMAZON AND NEGRO RIVERS

submitted to Earth and Planetary Science Letters - February, 2013

Giana Márcia dos Santos Pinheiro^{a,b}; Franck Poitrasson^{a,b}; Francis Sondag^{a,b}; Gérard Cochonneau^{b,c}; Lucieth Cruz Vieira^a; Márcio Martins Pimentel^{a,d}

a. Instituto de Geociências, Universidade de Brasília, 70910-900, Brasília, Brazil

b. Laboratoire Géosciences Environnement Toulouse, Institut de Recherche pour le Développement - Centre National de la Recherche Scientifique - Université de Toulouse III, 14-16, Avenue Edouard Belin, 31400 Toulouse, France

c. Agência Nacional das Águas - ANA, Brasília, DF, Brazil

d. Instituto de Geociências, Universidade Federal do Rio Grande do Sul, CP 15001, 91501-970 Porto Alegre, Brazil

Corresponding author: Giana Pinheiro - giana@unb.br

ABSTRACT

With the aim of searching for temporal variations during the hydrological cycles of two major Amazonian Rivers, the Negro and the Amazon (North Brazil), the iron isotope composition of their suspended matter was studied during eleven and twenty one months, respectively. Samples from the Óbidos Station in the Amazon River show homogeneous iron signatures for almost two years. They yield positive $\delta^{57}\text{Fe}$ values for the suspended matter, which are indistinguishable from the average continental crust composition ($\delta^{57}\text{Fe}_{\text{IRMM-14}} \sim 0.1\text{\textperthousand}$). Results for this river are between $-0.002 \pm 0.166\text{\textperthousand}$ and $0.275 \pm 0.175\text{\textperthousand}$ (2SE). On the other hand, samples from the Serrinha Station in the Negro River yield negative and variable values along the hydrological cycle studied. The isotopic range observed for the Negro suspended matter was close to $0.8\text{\textperthousand}$, with $\delta^{57}\text{Fe}$ values ranging from $-0.513 \pm 0.094\text{\textperthousand}$ to $-1.298 \pm 0.036\text{\textperthousand}$. The lack of significant isotopic variations in the Amazon River indicates that one individual subsurface suspended matter sample is representative of the river during the whole hydrological season, in opposition to results obtained for the Negro River. Data presented here suggest that for organic matter poor white water rivers, such as the Amazon, the particulate matter iron isotopic compositions go through little fractionation, reflecting a general picture of the iron sources (*i.e.*, detritic crustal material), whereas for black water rivers like the Negro, characterized by organic-rich and low-pH waters, iron isotopes will rather yield a more detailed information on the iron cycling, which includes biological processes, at the water-soil interface near headwaters.

KEYWORDS: iron isotopes; Amazon and Negro equatorial rivers; temporal series; water suspended matter.

1. INTRODUCTION

Continental weathering is responsible for mechanical and chemical processes that disaggregate rocks and minerals, which may, in their turn, form soils. The weathered material and the soils, together with atmospheric deposition, continental run-off, re-suspended sediments, diagenetic pore fluids, underground waters, vegetation and hydrothermal fluids, among others (Wells *et al.*, 1995; Elderfield and Schultz, 1996; Johnson *et al.*, 1999; Beard *et al.*, 2003b; Elrod *et al.*, 2004; Jickells *et al.*, 2005; Severmann *et al.*, 2006; Bennett *et al.*, 2008; Rouxel *et al.*, 2008a, 2008b; Escoube *et al.*, 2009), are important iron sources – both in the dissolved and the particulate phases – to oceans and rivers. Generally, the particulate phase corresponds to the transport of particles produced during both chemical (*i.e.*, production of secondary minerals) and physical weathering (*i.e.*, mechanical breakdown of rocks – Viers *et al.*, 2007b).

Natural mass-dependent isotopic variations of Fe are small compared to other isotope systems, covering a range of $\sim 11\text{\textperthousand}$ in $\delta^{57}\text{Fe}$ (*e.g.*, Anbar, 2004; Beard and Johnson, 2004a; Fantle and DePaolo, 2004; Bergquist and Boyle, 2006; Dauphas and Rouxel, 2006; Ingrin *et al.*, 2006; Johnson and Beard, 2006; Anbar and Rouxel, 2007; Rouxel *et al.*, 2008b; Escoube *et al.*, 2009; dos Santos Pinheiro *et al.*, 2013; Ilina *et al.*, 2013). Abiotic and biologic redox processes are known to produce some of the most significant Fe isotope variations in nature (Johnson *et al.*, 2004; Beard and Johnson, 2004a). In neutral pH, oxic environments or fluids, iron is essentially under the oxidized and more immobile Fe^{3+} form, which has a very low solubility. Therefore, significant transport of trivalent iron in the aqueous form is excluded (Curie and Briat, 2003; Beard and Johnson, 2004a). Iron becomes mobile only as organo- Fe^{3+} complexes or dissolved Fe^{2+} (Fritsch *et al.*, 2009).

In a reconnaissance study, Bergquist and Boyle (2006) reported distinct $\delta^{57}\text{Fe}_{\text{IRMM-14}}$ values for the dissolved and particulate phases from the Negro, an organic-rich acidic river located in the Amazon region and also studied in this work. The dissolved load was found to be isotopically slightly heavy (+ 0.45‰) while the suspended load was light (- 1.35‰). The light iron isotope composition for the Negro River particulate matter was recently confirmed, however to a lesser extent ($\delta^{57}\text{Fe}_{\text{IRMM-14}} \sim -0.5\text{\textperthousand}$, dos Santos Pinheiro *et al.*, 2013). A similar relation between river dissolved and particulate fractions was also reported by Escoube *et al.* (2009) for the North River, Massachusetts, though to a lower magnitude.

Nonetheless, isotopic $\delta^{57}\text{Fe}_{\text{IRMM}-14}$ variations may also exist among suspended fraction of different types of tributaries of the Amazon River (Bergquist and Boyle, 2006; dos Santos Pinheiro *et al.*, 2013).

Seasonal variations in the iron isotopic composition of the suspended matter (SPM) from rivers and lakes have been observed by Ingri *et al.* (2006) and Song *et al.* (2011). Ingri *et al.* (2006) studied the Kalix, a boreal river in Northern Sweden, along a complete hydrological cycle and attributed the differences observed to the relative abundance of two types of colloidal-particulate matter with different hydrogeochemical origin and, consequently, different Fe-isotope compositions: the Fe-C phase, considered to have a negative $\delta^{57}\text{Fe}_{\text{IRMM}-14}$ value, and the Fe-oxy-hydroxide phase, with a heavier $\delta^{57}\text{Fe}_{\text{IRMM}-14}$ signature. Song *et al.* (2011) found seasonal variations in the suspended matter $\delta^{57}\text{Fe}$ values for both the lake and the rivers studied in China. Lake samples display a range from $-2.04\text{\textperthousand}$ to $-0.15\text{\textperthousand}$ in the summer and from $-0.45\text{\textperthousand}$ to $-0.105\text{\textperthousand}$ in the winter, while river's samples vary from $-1.32\text{\textperthousand}$ to $0.105\text{\textperthousand}$ in the summer and from $-0.525\text{\textperthousand}$ to $-0.045\text{\textperthousand}$ in the winter. In contrast, samples collected during the high and the low water seasons in the Solimões River (Amazon Basin), which is rich in detrital suspended matter, show no such differences in the iron isotope signatures of suspended matter (dos Santos Pinheiro *et al.*, 2013).

According to Fantle and DePaolo (2004), reactions within soils produce both isotopically light and heavy Fe: biological processes, such as the growth of surface vegetation and synthesis of organic ligands, produce a source of isotopically light, relatively mobile Fe, that can more easily be transported. Furthermore, other reports have shown that Fe isotope compositions of organic and inorganic, dissolved, colloidal and particulate iron forms in rivers may vary (*e.g.*, Bergquist and Boyle, 2006; Escoube *et al.*, 2009). Some important processes responsible for Fe chemical fractionation in rivers are equilibrium speciation, precipitation of colloidal Fe^{3+} , and sorption of dissolved Fe onto particle surfaces (de Baar and de Jong, 2001), and these reactions may shift the iron isotopic composition of river materials.

On a global scale, the Amazon River Basin is known to supply the greatest amount of suspended matter to the ocean (Gaillardet *et al.*, 1997), figuring as a very important carrier of iron in all its phases (*i.e.*, dissolved, colloidal and particulate). It is thus an interesting area to study variations on the iron isotopic signature in these different river fractions. Suspended matter samples from two extreme types of water in the Amazon River Basin, the organic-rich Negro River and the suspended mineral-rich Amazon River, were analyzed. The aim was to

investigate the behavior of the suspended matter iron isotopic composition in these rivers during the hydrological cycles, to verify how the distinct processes and sources involved may affect the signatures observed throughout the year.

2. STUDY AREA AND SAMPLE COLLECTION

The variety of physical and chemical characters recognized for the rivers of the Amazon basin lead to the classification of the waters in this region as three different types (Fittkau, 1971; Gibbs, 1972; Sioli, 1984; Lewis *et al.*, 1995): clear and black waters are mostly related to chemical erosion, whereas white waters are associated with mechanical erosion, and consequently contain much stronger sediment loads (Allard *et al.*, 2004).

The Solimões River is relatively cool (*ca.* 29 °C) and has neutral pH (> 6.8). The suspended load of this river consists mainly of materials that are also present in the floodplain sediments, such as quartz and feldspars along with clay minerals (smectites, illite and a minor amount of kaolinite – Irion, 1983; Martinelli *et al.*, 1993, Guyot *et al.*, 2007). Its light brown waters drain the Peruvian Andes, contain high suspended sediment load inherited from physical denudation in the Andes and erosion of alluvial terraces, with Fe mostly exported as Fe-oxides and clay minerals (Gibbs, 1977; Irion, 1991). This river has lower bulk organic carbon concentration (Benedetti *et al.*, 2003a) and carries more than half of both the major ion dissolved load and the water budget of the Amazon River.

By contrast, the black waters of the Negro River drain lowlands that include the most weathered terrains in the Amazon (Stallard, 1980). They are characterized by high phytoplankton production, high concentration of organic matter (dissolved and particulate), low sediment loads and the highest levels of iron complexed to organic matter (Allard *et al.*, 2004, 2011). This element is mainly present as dissolved Fe²⁺ or Fe³⁺ bound to organic colloids (Senesi, 1992; Allard *et al.*, 2002; Benedetti *et al.*, 2003b; Nascimento *et al.*, 2008). It is warmer than the Solimões River by 1-2°C and has a low pH of ~ 4.8 (Bergquist and Boyle, 2006).

The Negro River drainage area is about 600,000 km² and covers parts of Colombia, Venezuela and Brazil. It ranks as the fifth largest river in the world in terms of average water discharge (Meade *et al.*, 1991; Franzinelli and Igreja, 2002). Particulate matter consists in

minor amounts of clays (mainly kaolinite and Fe-oxides, with contributions of gibbsite and particulate organic matter that includes fresh compounds derived from microorganisms and higher plants), residual quartz sands and plant remains (Sioli, 1984; Lewis *et al.*, 1995; Aucour *et al.*, 2003; Allard *et al.*, 2011).

Podzols are an important source of organic matter, although strongly depleted in iron (Allard *et al.*, 2011). They cover 200,000 km² in the high rainfall region of the upper Amazon Basin, and 33% of the Negro River watershed (Radambrasil, 1972–1978). Significant iron chemical and isotopic fractionation is reported in podzolic environments (Fantle and DePaolo, 2004; Ingris *et al.*, 2006; Wiederhold *et al.*, 2007a, b; dos Santos Pinheiro *et al.*, 2013; Ilina *et al.*, 2013). This fractionation contrasts with soils in oxic environments, characterized by limited Fe isotope variations (Emmanuel *et al.*, 2005; Wiederhold *et al.*, 2007b; Poitrasson *et al.*, 2008).

This study focuses on the analyses of suspended matter samples that represent at least one hydrological season from two very different rivers in the Amazon Basin: the Negro (Serrinha Station) and the Amazon (Óbidos Station) rivers (Fig. 26). The first was sampled along almost one year, while the second along almost two years.

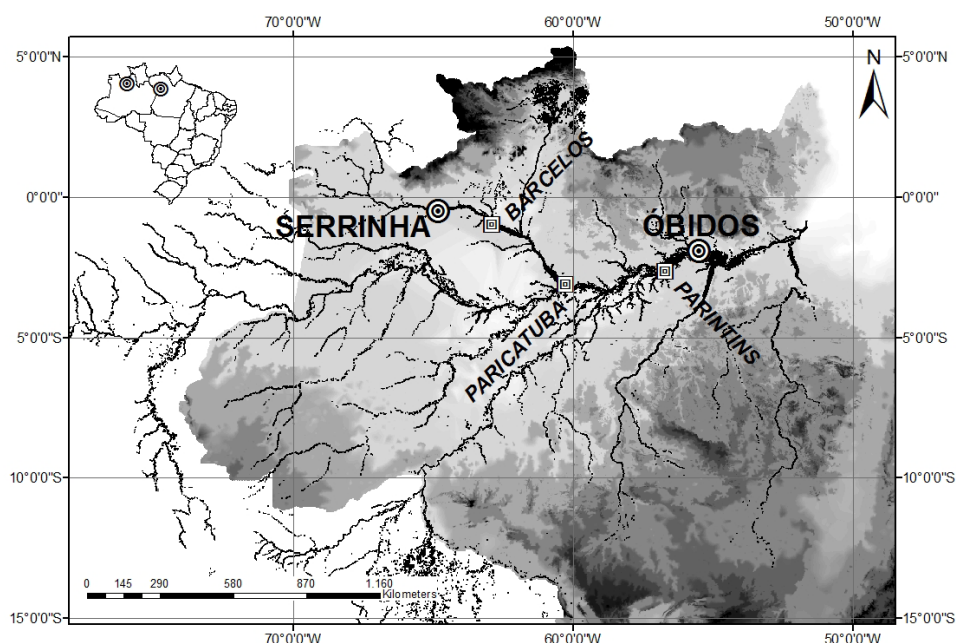


Fig. 26 – Map of temporal series samples locations (circles: Negro River at the Serrinha Station and Amazon River at the Óbidos Station). X-Ray Diffraction and Scanning Electron Microscope studies of the suspended matter were performed in the following locations (squares): Negro River at the Paricatuba Station and Amazon River at the Parintins Station. Precipitation data (available from the INMET - National Institute of Meteorology, Brazil, website in the references list): Negro River at the Barcelos Station (square) and Amazon River at the Óbidos Station (circle).

3. ANALYTICAL METHODS

3.1 Sample collection and preparation

All the studied samples were collected by local observers of the HYdrology of the AMazon Basin (HYBAm) network, who were trained to sample and filter waters from the Amazonian rivers. For further details on sample collection, filtration and analyses techniques, please refer to <http://www.ore-hybam.org/index.php/eng/Tecnicas>.

The suspended matter analyzed was recovered from the filtration of 380 to 530 ml of water for the Negro River at the Serrinha Station and 360 to 500 ml for the Amazon River at the Óbidos Station. The Negro time series comprised 12 samples, from September 2006 to August 2007, while the Amazon time series consists in a set of 22 samples, which starts in April 2009 and finishes in February 2011.

The membrane filters used to collect the suspended matter were stored in Petrislide® dishes and sent from the observers to the Federal University of Amazonas (UFAM) in Manaus. The filters were all pre-weighed and then re-weighed after water filtration and drying, procedures that allowed the calculation of suspended material concentrations in the filtered waters. Before weight measurements and subsequent analyses, the membranes were dried in an oven for 1 hour at 105°C. Temperature and conductivity were measured in field by the observers, with an ECTestr11+ (Eutech Instruments).

Samples used to determine the dissolved organic carbon were provided by the observers as well. Analyses for this parameter were made at the Laboratoire Géosciences Environnement Toulouse (GET, France), with a Shimazu TOC 5000 analyzer, using the high temperature catalytic oxidation method (HTCO). This method combines the dissolved oxygen with the carbon from the sample to form a CO₂ gas, which is measured with an infrared detector. The detected CO₂ generates a peak proportional to the carbon content of the sample. Different ranges (1, 2 and 5 ppm or 2, 5 and 10 ppm) are used according to the sample concentration. The detection limit is 0.15 ppm, whereas the quantification limit is 0.47 ppm. Uncertainties associated with the measurements are between 1.2 and 5%. Standards prepared from a Potassium Biphtalate standard wash solution (1,000 ppm) and the certified reference material BMOOS (soft water lake sample from up-state New York, available by the National Water Research Institute, Canada) were used to validate the analyses.

Scanning Electron Microscopy (SEM) of the suspended matter recovered from the filters was conducted at the GET using a Jeol JSM 6360LV (partial vacuum), coupled to a new generation system of EDS analysis – a "Silicon Drift Detector" (SDD) PGT Sahara. Materials were also analyzed by X-ray diffraction at GET, using an Inel curve sensible diffractometer in type-position CPS 120, equipped with a cobalt anticathode and a graphite monocromator. The acquisition was made simultaneously each 20° in all diffraction angles between 2° to 120°.

Average daily water discharges for the stations covered by the HYBAm network were calculated from the measurements of the water columns heights with the aid of a calibration curve, constructed from regular discharge measurements made over the last 20 years in different periods of the hydrological cycles. In the Amazon Basin, all stations were gauged with Acoustic Doppler Current Profiler (ADCP) localized using the Global Positioning System Fix Data (GGA mode), to measure the water discharges with a 2SD uncertainty better than 2% (see details in [Filizola and Guyot, 2004](#)). Lastly, precipitation data were downloaded from the Brazilian Institute of Meteorology (INMET, <http://www.inmet.gov.br/portal/index.php?r=bdmep/bdmep>).

3.2 Sample dissolution and iron purification

Sample dissolution and chemical purification were carried out in class 10,000 clean rooms, at the Geochronology Laboratory of the University of Brasília (UnB) and the GET Laboratory. The method applied includes successive digestions of samples using bi-distilled acids (see details in [dos Santos Pinheiro et al., 2013](#)). Suspended matter was entirely dissolved (along with the filter membranes), and iron separation was made by anion exchange chromatography, as described in [Poitrasson et al. \(2004\)](#) and [dos Santos Pinheiro et al. \(2013\)](#). Samples were analyzed for their Fe isotope composition in a 0.05M HCl medium, with a Finnigan Neptune High Mass Resolution Multi-Collector Inductively Coupled Plasma Mass Spectrometer (MC-ICP-MS).

Quantitative recovery from the columns was calculated based on iron analyses made by Inductively Coupled Plasma Optical Emission Spectrometry (ICP-OES) before the chromatographic separation, and by MC-ICP-MS after chromatography. The column yields were found to lie between 90 and 100% of iron for most samples. According to [Anbar et al. \(2000\)](#) and [Roe et al. \(2003\)](#), isotope fractionation in Fe anion chromatography experiments is

absent when this element is eluted with the use of dilute hydrochloric acid. Two of the samples analyzed in this study showed low Fe recoveries (Negro River sample from April 2007 and Amazon River sample from December 2010) and their results were therefore discarded. All procedural blanks were below 1% of the sample Fe, an insignificant amount for this study, and they included a blank milli-Q water filtration with a 0.45 µm filter membranes. At least 40 µg of iron was processed for each sample.

3.3 Iron isotope analyses by Mass Spectrometry

Iron isotope analyses were performed at the UnB Geochronology Laboratory for part of the Amazon River samples (Óbidos Station) and the GET Laboratory for the other part of the Amazon (Óbidos Station) and all the Negro River (Serrinha Station) samples. The methods applied are described in detail in [dos Santos Pinheiro *et al.* \(2013\)](#). The standard-sample bracketing and Ni doping techniques using the daily regression method were applied to correct the instrumental mass bias (see [Poitrasson and Freydier, 2005](#)). Analyses were performed in medium or high mass resolution modes. Iron isotope data are here reported as $\delta^{57}\text{Fe}$ ($^{57}\text{Fe}/^{54}\text{Fe}$), as parts per thousand (‰) deviations relative to the reference material IRMM-14:

$$\delta^{57}\text{Fe}/^{54}\text{Fe} = (((^{57}\text{Fe}/^{54}\text{Fe})_{\text{sample}} / (^{57}\text{Fe}/^{54}\text{Fe})_{\text{IRMM-14}}) - 1) * 1000$$

The performance of the instrument at the UnB Geochronology Laboratory was assessed by repeated measurements of a standard (hematite from Milhas, Pyrenees) relative to the Fe isotope reference material IRMM-14. This hematite, also known as ETH hematite, has been analyzed in several laboratories (*e.g.*, [Poitrasson and Freydier, 2005](#); [Dideriksen *et al.*, 2006](#); [Teutsch *et al.*, 2005](#); [Fehr *et al.*, 2008](#)) and the values reported by these authors agree well with values obtained from all the sessions in which samples from the temporal series were analyzed (*i.e.*, results obtained for the Milhas Hematite in both the UnB Geochronology Laboratory and the GET – $\delta^{57}\text{Fe}_{\text{IRMM-14}} = 0.761 \pm 0.064\text{\textperthousand}$; 2SD; n = 25). International rock standards were dissolved, purified and analyzed at the UnB Geochronology Laboratory to validate the methodology. They include the IF-G geostandard, with a $\delta^{57}\text{Fe}$ value of $0.931 \pm$

0.082‰ ([Vieira *et al.*, 2010](#)), also in good agreement with previously published values (see review in [Craddock and Dauphas, 2011](#)).

4. RESULTS

4.1 Characterization of mineral phases and environmental parameters

Suspended matter X-ray diffraction analyses performed in a sample from the Parintins Station (Amazon River, *ca.* 200 km upstream from Óbidos, [Fig. 26](#)), show the presence of biotite, kaolinite, quartz and albite. Scanning electron microscopy of the same sample indicates the occurrence of rutile, pyrite, zircon, chlorite, phosphates (with variable amounts of Sr, La, Ce, Nd, Th, Y), as well as clay minerals (such as montmorillonite) and (Ti, Mn, Fe) oxides. For the Negro River (sample from Paricatuba Station, *ca.* 650 km downstream from Serrinha, [Fig. 26](#)), the X-ray diffraction indicate that the predominant mineral phases are kaolinite and quartz, whereas scanning electron microscopy shows minor amounts of chlorite, albite, phosphates (with variable amounts of La, Ce, Pb, Th, U), clay minerals, (Ti, Fe, Al) oxides and organic material (*e.g.*, fragments of roots, leaves).

Precipitation data from the Negro River area (Barcelos Station, *ca.* 250 km downstream from the Serrinha Station, [Fig. 26](#)) and the Amazon River area (Óbidos Station) are shown in [Fig. 27](#). These data were used to assess how the rainwater may influence the water discharge in the period studied ([Fig. 28](#) and [Fig. 29](#)), as well as the possible role of this parameter on the suspended matter iron isotopic signatures. For the Amazon River, the water discharge response is *ca.* 1-3 months after the precipitation peaks or troughs. On April-May 2009 and 2010 the rains reached their peak maximum, whereas the flood maximum occurred either 2 months later, in July 2009, or 1 month later, in June 2010. The same relation can be seen for the periods of water minimum that occurred in November 2009 and 2010, following the minimum precipitation (August-September 2009 and 2010).

The precipitation values from Barcelos (Negro River, nearest station for which this kind of data was accessible, *ca.* 250 km from the Serrinha Station, [Fig. 26](#)), Parintins Station (Amazon River, data not shown) and Óbidos Station (Amazon River) display similar patterns (peaks and troughs) along the year ([Fig. 27](#)). These relations, added to the fact that the mean annual values for the Negro River at Barcelos are in accordance to the average of the total annual rainfall (both downstream and upstream the Negro River, [Bueno, 2009](#)), were used as

an indication that the data presented in this work represents well the rains in the Negro River Basin.

In the Negro River case, the water discharge response is more immediate, since it happened only one month after the precipitation minimum, which occurred in February 2007. On the other hand, after the precipitation maximum, in March-April 2007, the water discharge took *ca.* 4 months to reach its highest peak, in July 2007, month where the water level finally starts to decrease (**Fig. 29**).

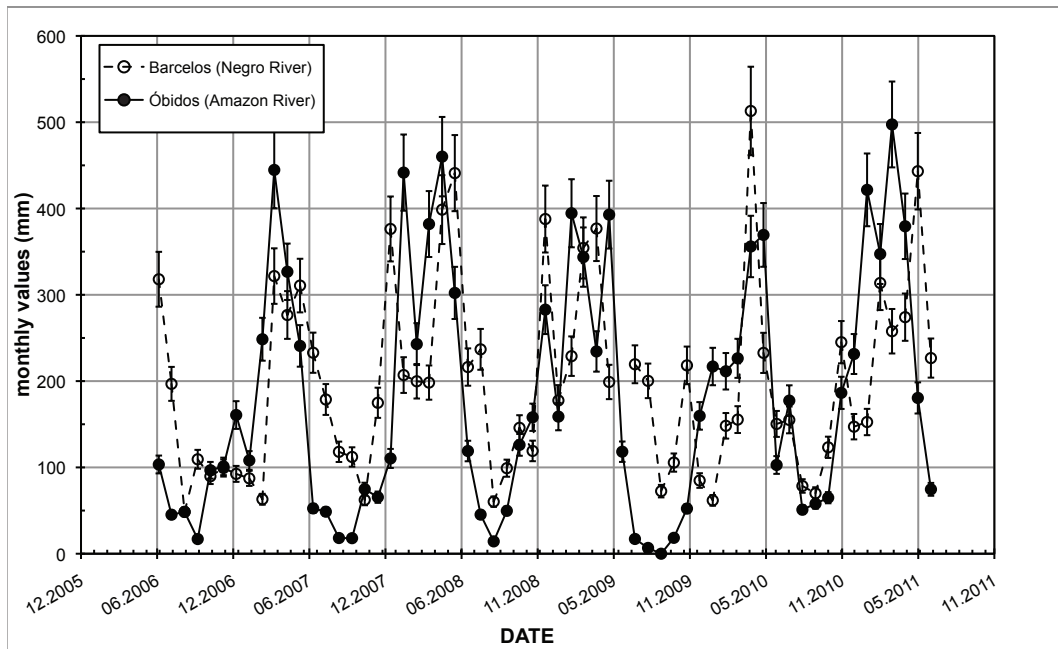


Fig. 27 – Average monthly precipitation along the Negro River area (Barcelos Station) and the Amazon River area (Óbidos Station). Both locations are shown in **Fig. 26**. Data downloaded from the Brazilian Institute of Meteorology (INMET, <http://www.inmet.gov.br/portal/index.php?i=bdmep/bdmep>).

The associations observed indicate that the dynamics of both the Amazon and Negro rivers are complex and relatively variable, in part because the relationship between precipitation and river discharge rate is not well understood and often under debate in the literature (*e.g.*, Getirana *et al.*, 2011 and references therein). In any case, the rivers hydrological regimes have to be considered in order to understand the chemical parameters and the elements transfer in both these rivers.

The suspended matter content in the Amazon River samples show a eightfold variation along the two hydrological cycles studied, responding negatively to the water level with a delay of *ca.* 1-3 months: the lowest water discharges (November 2009 and 2010) are followed by the higher suspended matter contents (January 2010 and February 2011) and vice-versa

(Fig. 28). Also, the iron concentration of the suspended matter shows a rough anticorrelation ($R^2 = 0.43$) with the amount of suspended matter in the water (Fig. 30 – two samples that deviated from the linear trend were taken out of the binary plot – November and December 2009). As a result, the suspended matter iron concentration is higher when the suspended matter content is lower (during high water levels), reaching values above 4 wt% in this time of the year, whereas during the dry season, when the suspended matter content is higher, the percentage of iron in this suspended matter is lower, and below 4 wt% (Fig. 28 and Fig. 30).

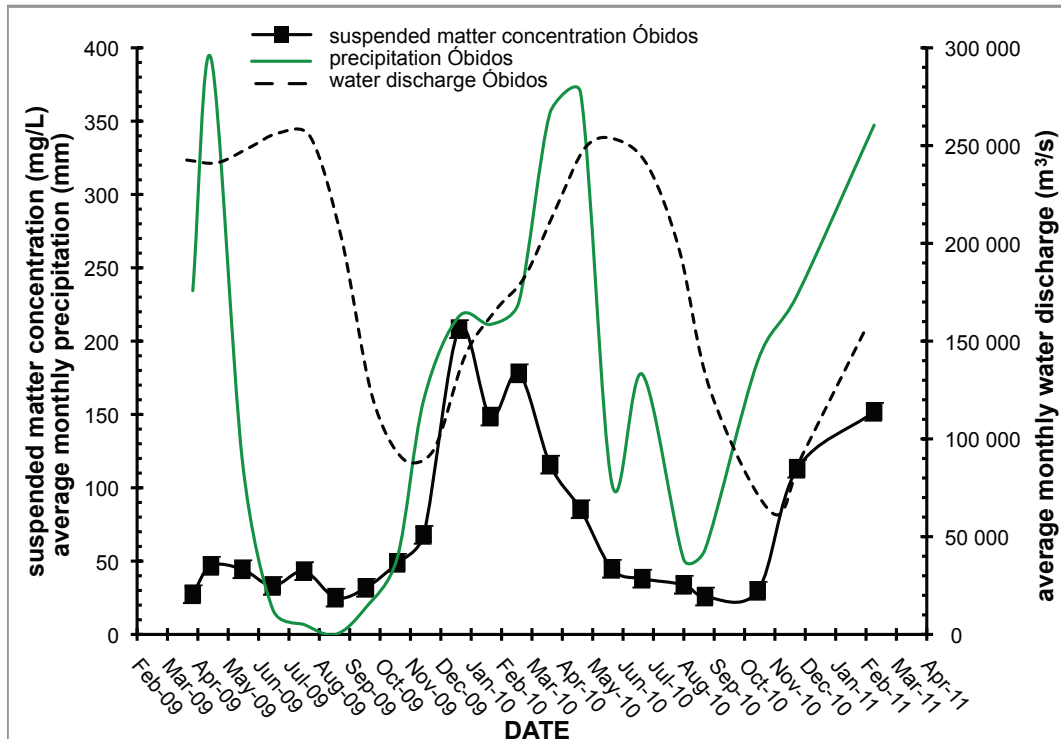


Fig. 28 – Monthly water discharge, suspended matter concentration and precipitation in the Amazon River (Óbidos Station) during the periods studied.

The dissolved organic carbon present in a sample may consist in a mixing of humic and fulvic acids as well as low molecular weight organic acids (Benedetti *et al.*, 2003a, Perez *et al.*, 2011). Values for this parameter show a relation with the water discharge (Fig. 29): as the discharge increases or decreases, dissolved organic carbon values follow this parameter, coinciding one of the lower values with the lowest water discharge, in March 2007. Close to the flood period, the response of this parameter seems to be *ca.* 1-2 months ahead of the water discharge peak, which shows its highest value in July 2007, when the dissolved organic carbon contents are already starting to decrease after reaching their peak in May - June 2007 (Fig. 29).

The suspended matter content in the Negro River shows a very erratic behavior: it doubles or reduces by half from one month to another, with exception of some periods when there is a progressive increase or decrease that lasts more than one month (**Tabela 4**, **Fig. 29**). This specific pattern, which shows great variations in small intervals, was also observed in another set of filter membranes that represent the same time series, but that were weighted by a distinct operator in a different balance. It was therefore assumed that the suspended matter concentration behavior in the Negro River is natural and not caused by artifacts that may have been introduced in the sampling or weighing steps. Like for the Amazon, there is an anticorrelation between the suspended matter content and its Fe concentration in the Negro River at the Serrinha Station (**Fig. 30**), as illustrated by a negative linear correlation ($R^2 = 0.65$, **Fig. 30**).

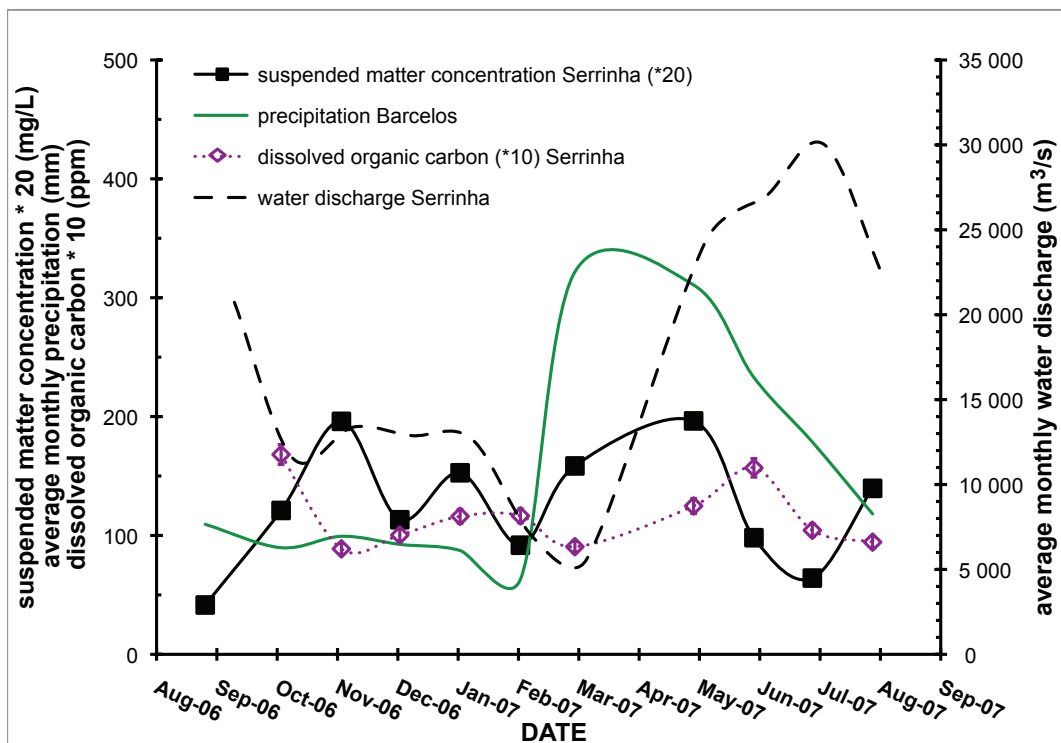


Fig. 29 – Negro River - suspended matter concentration (*20), dissolved organic carbon contents (*10), monthly water discharge (Serrinha Station) and precipitation (Barcelos Station) during the periods studied.

Also similarly to the Amazon River at Óbidos, the water discharge and the suspended matter contents show a negative correspondence, although with a temporal shift, which can be better seen close to the dry and flood periods (**Fig. 29**). In February / March 2007, suspended matter contents start to increase as a response to a decrease in the water discharge levels, which reached its lowest peak in March. Then, from March on, the water discharge increases

whereas the content of suspended matter reaches its highest peak in May and lowest peak in July 2007, the same month where the water discharge reaches its maximum (**Fig. 29**).

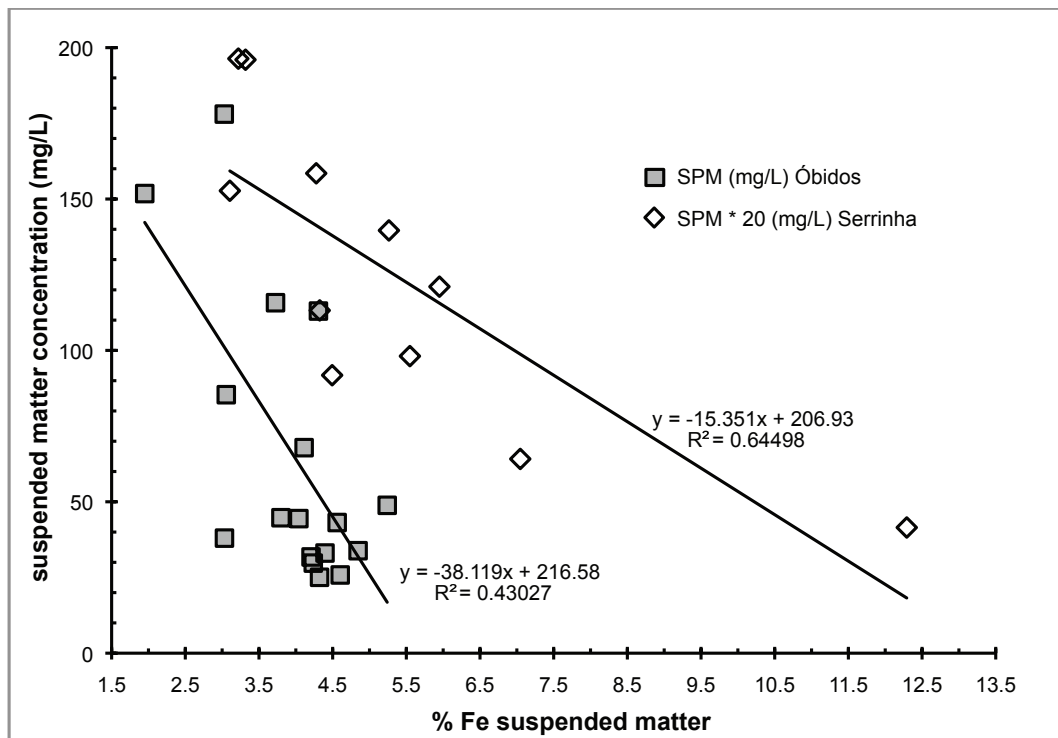


Fig. 30 – Iron concentration variations in suspended matter (SPM), measured with MC-ICP-MS, *versus* suspended matter (SPM) concentration – Amazon River at Óbidos Station (samples from November and December 2009 were taken out of the binary plot) and Negro River at Serrinha Station.

4.2 Iron Isotopes

Samples of suspended matter from the Amazon River at Óbidos show stable Fe isotope compositions within analytical uncertainties. The $\delta^{57}\text{Fe}_{\text{IRMM}-14}$ values range from $-0.002 \pm 0.166\text{\textperthousand}$ to $0.275 \pm 0.175\text{\textperthousand}$ (**Tabela 4**, **Fig. 31**) and scatter around the mean of the continental crust ($0.1 \pm 0.03\text{\textperthousand}$, Poitrasson, 2006). These agree well with the recently reported values for this and other white water rivers along lateral and depth profiles ([dos Santos Pinheiro *et al.*, 2013](#)).

All the suspended matter results from the Negro River are negative (**Tabela 4**, **Fig. 32**), in broad agreement with previously studies ([Bergquist and Boyle, 2006](#); [dos Santos Pinheiro *et al.*, 2013](#)) as further discussed in more detail. Samples show a significant fluctuation along the hydrological cycle studied, with $\delta^{57}\text{Fe}$ values varying from $-1.298 \pm 0.036\text{\textperthousand}$ (February 2007) to $-0.513 \pm 0.094\text{\textperthousand}$ (October, 2006).

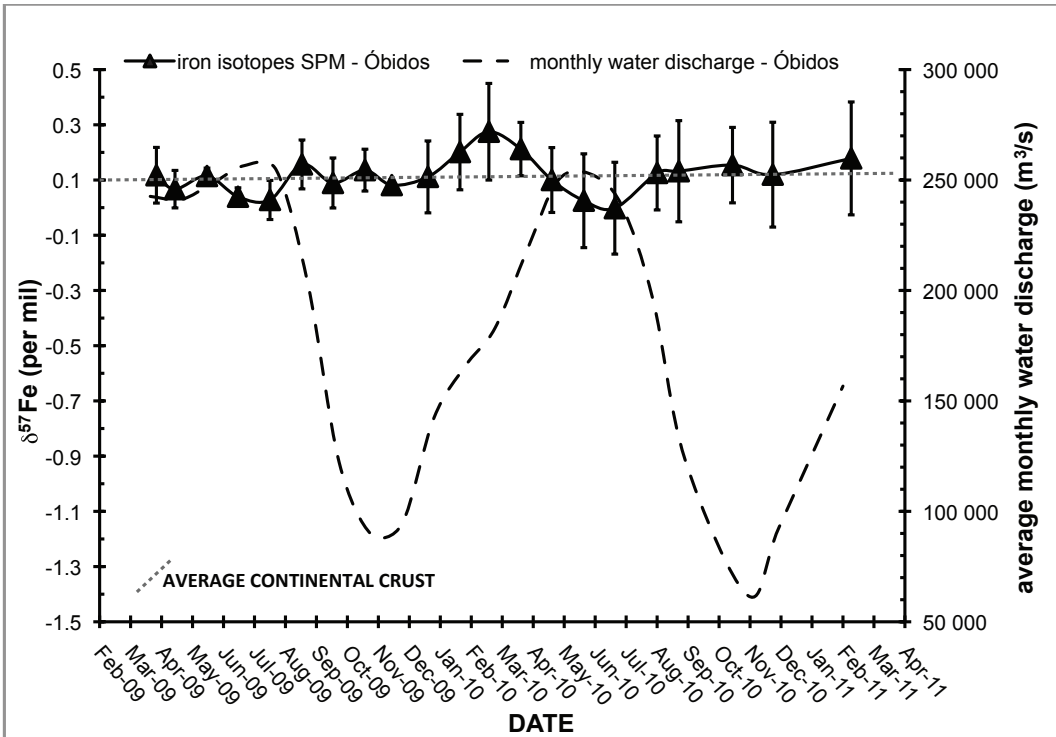


Fig. 31 – $\delta^{57}\text{Fe}$ temporal variations in suspended matter (SPM) along time series in the Amazon River at the Óbidos Station. The average isotopic composition of the continental crust ($\delta^{57}\text{Fe} \sim 0.1 \pm 0.03\text{‰}$; Poitrasson, 2006) is shown for reference.

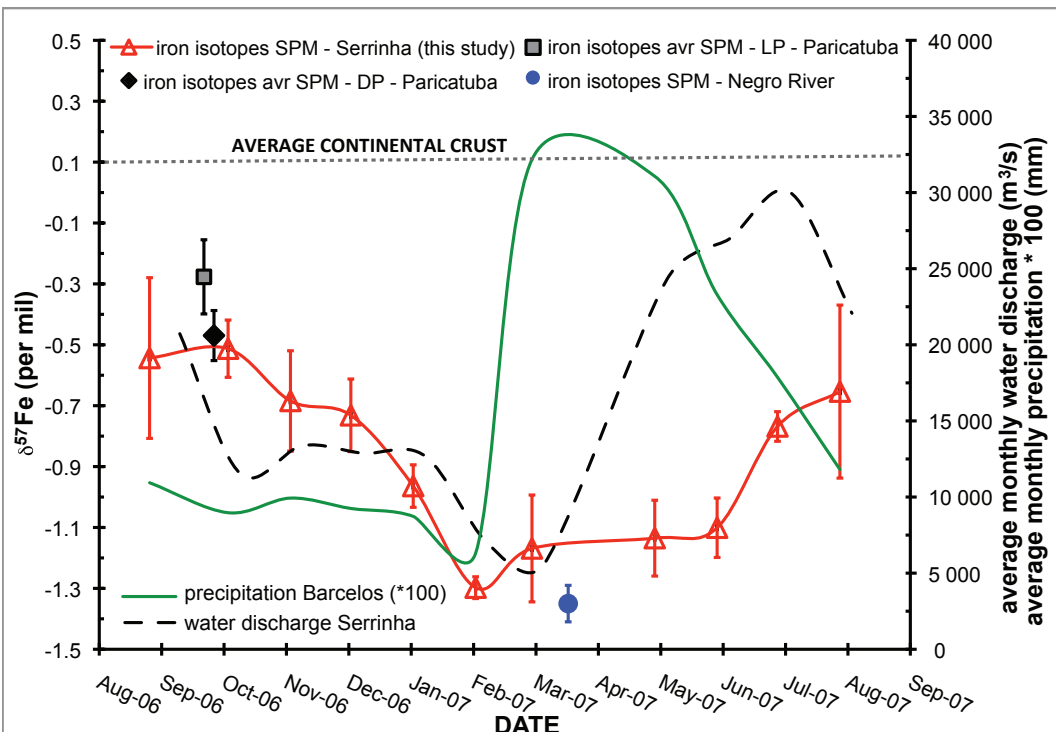


Fig. 32 – $\delta^{57}\text{Fe}$ temporal variations in suspended matter (SPM) along time series in the Negro River at the Serrinha Station. The average isotopic composition of the continental crust ($\delta^{57}\text{Fe} \sim 0.1 \pm 0.03\text{‰}$; Poitrasson, 2006) is shown for reference. Additional data added for comparison: SPM Negro River (circle) from Bergquist and Boyle (2006); average (avr) SPM Negro River (Paricatuba Station) from dos Santos Pinheiro *et al.* (2013), where DP – depth profile; LP – lateral profile).

The most negative result occurs in the same month as the lowest precipitation value (February 2007) and is followed by the lowest water level (March 2007). On the hydrological cycle studied, the iron isotopic composition seems to follow the Negro River water discharge curve, but with a 2-3 months delay for the increase, *i.e.*, higher $\delta^{57}\text{Fe}_{\text{IRMM}-14}$ values seem to be related to waters brought by the end of the flood season (**Fig. 32**).

5. DISCUSSION

5.1 Comparison to previous $\delta^{57}\text{Fe}$ data on the Amazonian rivers

The two years constant time series obtained for the white water Amazon River suspended matter samples (Óbidos Station), with $\delta^{57}\text{Fe}_{\text{IRMM}-14}$ values (from $-0.02 \pm 0.166\text{\textperthousand}$ in July 2010 to $0.275 \pm 0.175\text{\textperthousand}$ in March 2010) undistinguishable from the continental crust signature ($0.1 \pm 0.03\text{\textperthousand}$, [Poitrasson, 2006, Tabela 4, Fig. 31](#)), is in agreement to the recently reported river depth and cross section profiles of the Amazon, Madeira and Solimões rivers ([dos Santos Pinheiro *et al.*, 2013](#)). These data also agree within uncertainties to the values reported by [Bergquist and Boyle \(2006\)](#) for the suspended matter from the mouth of the Amazon River (Macapá Station, $\delta^{57}\text{Fe} = -0.12 \pm 0.23\text{\textperthousand}$). On the other hand, their result for the Solimões River deviates largely from the suspended matter iron isotope measurements of white waters from the present study: they reported a $\delta^{57}\text{Fe}_{\text{IRMM}-14}$ lighter by $0.6\text{\textperthousand}$. There was also a significant shift, of 1\textperthousand , for the particulate matter of the Negro River analyzed by [Bergquist and Boyle \(2006\)](#) and [dos Santos Pinheiro *et al.* \(2013\)](#).

The new Negro River time series here presented (**Fig. 32**) confirms the preferred explanation for the data difference found by [Bergquist and Boyle \(2006\)](#) and [dos Santos Pinheiro *et al.* \(2013\)](#): it is due to contrasted sampling periods in the hydrological cycle. In February and March, close to the low water season, samples show the most negative values (**Fig. 32**), similar to the one obtained by [Bergquist and Boyle \(2006\)](#) for a sample collected in the same month in the Negro River (35 km upstream Manaus), though in a different year (March 2002, **Fig. 32**). September and October show the least negative values (**Fig. 32**), what is in agreement with results published by [dos Santos Pinheiro *et al.* \(2013\)](#) for samples collected in the same months of different years (2009 and 2010).

On the other hand, variations in the hydrological cycle are unlikely an explanation for the negative value obtained by [Bergquist and Boyle \(2006\)](#) on the Solimões River suspended matter they studied in the Amazon region. The evidence here presented on white water rivers point to a constant, undistinguishable from the continental crust $\delta^{57}\text{Fe}_{\text{IRMM}-14}$ value for the suspended matter during the whole hydrological cycle, as observed in the Amazon River temporal series at Óbidos (**Fig. 31**), and in the lateral profiles from the Solimões River, sampled during high and low water levels ([dos Santos Pinheiro *et al.*, 2013](#)). These data confirm that there is little fractionation during the iron transfer from primary sources (*e.g.*, geological basement and soils) to the white water rivers of the Amazon River Basin. Therefore, the divergent results are probably due to differences on the collection methods, filtration techniques and samples treatments.

Overall, the differences found for the Negro, Solimões and the Amazon rivers may be, at least partially, attributed to the percentage of iron carried by each phase: according to [Bergquist and Boyle \(2006\)](#), approximately 95% of the iron in the Solimões and Amazon Rivers is in the suspended fraction, whereas in the Negro River, approximately half of the total Fe is carried in the dissolved load ([Bergquist and Boyle, 2006](#)), which mainly consists in large amounts of humic substances with high molecular weight ([Perez *et al.*, 2011](#)). Another important aspect is the nature of the suspended matter. While the Negro River suspended matter is organic rich, with particulate organic carbon contents around 20% ([Moreira-Turcq *et al.*, 2003](#)), the Solimões River carries mostly detrital minerals arising from mechanical erosion of igneous rocks from the Andes, sediments and lateritic soils. All these components do not show large Fe isotope variations (*e.g.*, [Beard *et al.*, 2003a; Poitrasson, 2006; Poitrasson *et al.*, 2008](#)) and, therefore, a deviation from the continental crust iron isotope signature should not occur in the suspended load of white water rivers like the Solimões and the Amazon.

In the last ten years, the Amazonian region has experienced the two greatest droughts (2005 and 2010) and the two greatest floods (2009 and 2012) over the 110 years of monitoring (measured in the Roadway Station since September 1902, Manaus Port, Amazonas State). The homogeneity in the iron isotopic signatures of the Amazon River samples (Óbidos Station) collected in 2009 (exceptional flood) and 2010 (exceptional drought) and 2011 (no extreme water regime registered) indicates that extraordinary variations on the water discharge do not influence the suspended matter iron isotopic composition. The same statement is applicable to the Negro River, since the comparison of the temporal series (**Fig. 32**, from 2006 to 2007 – no extreme periods registered) with samples

collected in 2002 ([Bergquist and Boyle, 2006](#), no extreme water regime registered) and 2009 (exceptional flood, Negro River depth and lateral profile, [dos Santos Pinheiro et al., 2013](#)) show similar signatures for comparable months, regardless the years these samples were collected.

5.2 Possible sources of iron in the Negro River Basin

The fact that black water rivers show negative and heterogeneous values, in opposition to white water rivers, which show positive homogeneous $\delta^{57}\text{Fe}_{\text{IRMM}-14}$ values, is mainly due to the distinct water characteristics of the two rivers. This arises from the different geological and pedological nature of the areas drained by these rivers.

According to [Sioli \(1991\)](#), the origin of the Rio Negro water properties are largely related to the podzolic soils which cover one third of this basin headwater area ([Fritsch et al., 2009](#)), and this kind of water is associated with the development of reducing and acidic conditions with subsequent accumulation of organic matter in podzolic soils ([Bravard and Righi, 1990](#); [Lucas et al., 1996](#); [Dubroeucq and Volkoff, 1998](#); [Benedetti et al., 2003a](#); [Nascimento et al., 2004](#)). Organic material rapidly undergoes decomposition to humus in these degraded soils and so, is easily transported by the percolating rain water to river surfaces ([Viers et al., 1997](#); [Olivié-Lauquet et al., 1999](#); [Olivié-Lauquet et al., 2000](#); [Franzinelli and Igreja, 2002](#)). The most negative iron isotopic results for the Negro River particulate matter coincide with the highest precipitations (from February to June 2007). Podzols are associated with reduced, isotopically light Fe ([Fantle and DePaolo, 2004](#); [Wiederhold et al., 2007b](#)), and the heavy rain would ease the disaggregation of organic-rich particulate matter from soils. After June 2007, as precipitation values are decreasing, a shift on $\delta^{57}\text{Fe}_{\text{IRMM}-14}$ values towards heavier values can be observed. This could explain, at least in part, the significant fluctuation on the $\delta^{57}\text{Fe}_{\text{IRMM}-14}$ values, which vary from $-0.513 \pm 0.094\text{\textperthousand}$ to $-1.298 \pm 0.036\text{\textperthousand}$, along the hydrological cycle studied ([Fig. 32](#)). Storm events such as these heavy rains can also influence the water discharge and consequently, the heights achieved by the water columns. This would implicate in the leaching of distinct soil horizons that will contribute with iron in variable redox states (and isotopic compositions) along the year ([Ingri et al., 2006](#)).

5.3 The role of weathering and organic substances on the transport of iron

During weathering reactions of most silicate minerals in soils, immobile elements, like Fe under oxidizing conditions, are incorporated into stable secondary products such as clays (*e.g.*, kaolinite) and metallic oxy-hydroxides (*e.g.*, goethite, Viers *et al.*, 2007b). Living organisms (plant roots and microorganisms) release CO₂ and low-molecular-weight organic acids (*e.g.*, acetic acid) in the soil and, therefore, enhance mineral dissolution and chemical weathering (Schlesinger, 1997). Products generated by these processes are preferentially incorporated in the dissolved phase of the waters as colloids. Viers *et al.* (1997); Oliva *et al.* (1999) and Viers *et al.* (2000) have shown that for South Cameroon, Africa, organic matter enhances the weathering rates of silicates by 30%. If the waters are acidic like in the Negro River, the dissolution of minerals will be further enhanced, as the presence of organic colloids is known to increase the dissolution rates and the solubility of silicates and oxy-hydroxides (Viers *et al.*, 2007b), having thus a key role in the transport of elements such as Fe, one of the major constituents of soil minerals (Dupré *et al.*, 1999; Viers *et al.*, 2007b; Olivié-Lauquet *et al.*, 1999).

It is well known that organic Fe is significantly lighter than the mineral Fe in soils (Fantle and DePaolo, 2004; Wiederhold *et al.*, 2007b). Therefore, the divalent iron released in reduced environments (Fritsch *et al.*, 2009), such as the exchangeable Fe from soils and the Fe released from organic leaching and microbial dissolution of minerals (Brantley *et al.*, 2001; Brantley *et al.*, 2004) will be linked to a light isotope signature. The negative iron isotope composition of the Negro River suspended matter (Fig. 32) indicates a preferential incorporation or sorption of this light iron in the suspended material analyzed. Accordingly, Aller *et al.* (2004) estimated that 10 to 50% of the microbially produced Fe²⁺ is lost to authigenic mineral formation.

Further, Allard *et al.* (2011) found that, from the waterlogged podzols to the Negro River tributaries mainstreams (*e.g.*, the Jaú River), there is a decreasing proportion of reduced iron that is correlated with an increase of the trivalent Fe bound to organic matter. If the iron oxidation is close to quantitative, it will result in particulate matter binding ferric iron that will keep the original ferrous light isotope signature (Fig. 32) inherited from fractionation processes within podzols. Supplementary processes – linked to a supposed light photoreduction, or to phytoplankton low molecular weight exometabolites that, due to adsorption, enrich the cell surface in heavy Fe isotopes (Ilina *et al.*, 2013) – could be additional mechanisms favoring the heavy isotopic composition of the dissolved load reported

by Bergquist and Boyle (2006) for the Negro River. Alternatively, following the proposition made by Dauphas and Rouxel (2006) to the fractionation observed in the work of Bullen *et al.* (2001), the isotopic signature found in the Negro River suspended matter may represent two diverse fractionation processes acting in the same system: *i*) the $\text{Fe}^{2+}_{(\text{aq})}$ to $\text{Fe}^{3+}_{(\text{aq})}$ oxidation, which enriches the ferric iron in heavy isotopes (Schauble *et al.*, 2001; Brantley *et al.*, 2004), and *ii*) a subsequent precipitation of $\text{Fe}^{3+}_{(\text{aq})}$ into ferrihydrite, reaction that, due to kinetic processes, enriches the precipitate in light isotopes. Such heavy Fe isotope enrichment, nevertheless, remains much more restricted compared to what is observed in boreal waters by Ilina *et al.* (2013). Ultrafiltration experiments on the Negro River and its tributaries waters would be required to go further in these interpretations.

5.4 Seasonal variations and comparison of suspended matter iron isotopic compositions in boreal, temperate and tropical regions

It was previously inferred (Poitrasson *et al.*, 2008) on the basis of soil and river studies (Fantle and DePaolo, 2004; Ingri *et al.*, 2006) that the iron isotopic signature delivered to oceans will depend on the locality, since the available data show that $\delta^{57}\text{Fe}_{\text{IRMM}-14}$ values are more variable at higher latitudes, but closer to the continental crust signatures in intertropical zones. In their study of temperate and subarctic rivers, Ilina *et al.* (2013) observed a gradual increase of $\delta^{57}\text{Fe}_{\text{IRMM}-14}$ with decreasing pore size (from 100 μm to 1 kDa) and Fe/C ratios. Moreover, these authors showed that temperate rivers are isotopically lighter by approximately 1‰ relative to subarctic rivers and lakes at a given Fe/C ratio.

The time series data obtained in this study allows the verification of such latitudinal dependence. While results for the Amazon River temporal Fe isotope series do not show the seasonal variations reported in previous studies (made in a boreal Swedish river and Chinese temperate rivers and lake, Ingri *et al.*, 2006; Song *et al.*, 2011), the Negro River suspended matter also displays variations in the iron isotope composition according to the hydrological season (**Fig. 32**). Furthermore, whereas the range in the Negro River along one hydrological cycle is only slightly greater than the one found by Ingri *et al.* (2006) for the Kalix River (0.78‰ *versus* 0.62‰ in $\delta^{57}\text{Fe}_{\text{IRMM}-14}$, respectively, **Fig. 33**), their suspended matter $\delta^{57}\text{Fe}_{\text{IRMM}-14}$ values are distinct: the Kalix River exhibits a few slightly negative, but mostly positive data, whereas the Negro River shows a strongly negative iron isotope signature.

Rivers from temperate areas show less contrasted particulate matter iron isotope compositions, with signatures that are closer to the mean continental crust value ([Escoube et al., 2009](#); [Ilina et al., 2013](#)). Hence, it seems that there is a latitudinal gradient for the riverine suspended matter Fe isotope composition possibly linked to climatic context. This does not apply to rivers with high-suspended loads, rich in detritic components and poor in organic material, such as the Amazon River ([dos Santos Pinheiro et al., 2013](#) and **Fig. 31**) and one of its largest tributaries, the Solimões River ([dos Santos Pinheiro et al., 2013](#)), as well as other rivers elsewhere in the world ([Beard et al., 2003a](#)). Available data on the iron isotopic signatures of river-born particles are compiled in **Fig. 34** for comparative purposes.

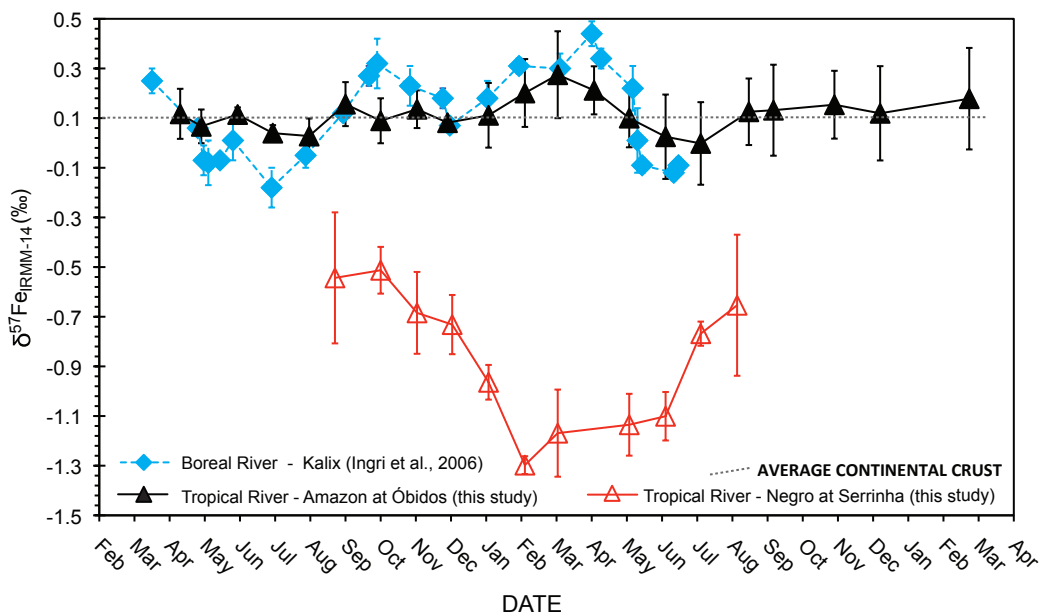


Fig. 33 – Comparison between $\delta^{57}\text{Fe}$ temporal variations in suspended matter along time series in three different rivers: boreal Kalix (Sweden, [Ingri et al., 2006](#)), tropical Amazon River at Óbidos and tropical Negro River at Serrinha Station. The average isotopic composition of the continental crust ($\delta^{57}\text{Fe} \sim 0.1 \pm 0.03\text{‰}$; [Poitrasson, 2006](#)) is shown for reference.

The contrasted results found for the Negro and the Kalix rivers (**Fig. 33**) could be attributed to distinct weathering processes occurring in these areas, but also to other environmental parameters. The water column in the Kalix River is always well oxygenated and the pH is nearly neutral (7 to 7.8, [Widerlund, 1996](#)). During the winter, the water is covered with snow and ice, and during the spring there is a twenty to twenty five-fold volumetric flow raise over a few days ([Dahlqvist et al., 2004](#)). This increase is proportionally several times higher than the water augmentation in the Amazon River and, consequently, the Negro River (*ca.* two fold amplification, [Gibbs, 1972](#); [Martinez et al., 2009](#)). The origin of

the water in the Kalix River also changes from mostly groundwater during winter, to mostly meltwater from the snow cover during peak flood, and finally to water from the mountainous region during the spring flood (Widerlund, 1996).

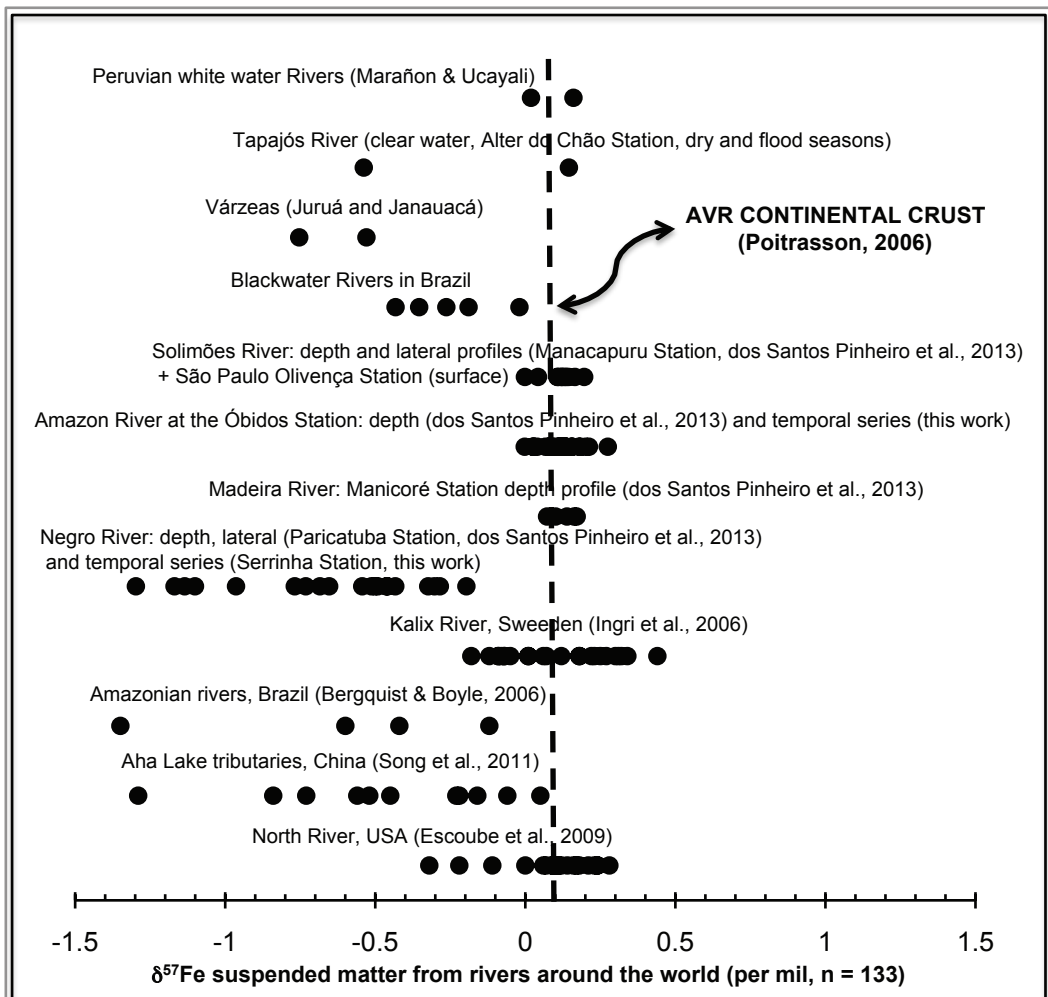


Fig. 34 – Variability on the iron isotopic composition of suspended matter from rivers around the world. Data from Table 1.

Other important differences are the basin area size, the precipitation average, the water discharge values and the depth of the water column (*cf.* Widerlund, 1996 and Dahlqvist *et al.*, 2004). All these parameters have an influence on the soil horizons leached. On the other hand, both rivers – the Negro and the Kalix – have very low concentration of detrital particles, are organic rich and account for podzols as the dominant source of iron to the dissolved and suspended loads. These features seem necessary for the observed $\delta^{57}\text{Fe}$ seasonal variations.

These characteristics indicate that soil processes have a large influence the iron fractionation between the distinct pools involved in rivers systems in a given area. That is,

when well developed podzol profiles are present, like in the region covered by these rivers (Negro River – Brazil, this work –, Kalix River – Sweden, [Ingri and Widerlund, 1994](#); [Ingri et al., 2006](#) –, Senga and Palojoki rivers – Russia, [Ilina et al., 2013](#)), organic and weathering reactions that occur within soils are a major issue affecting the fractionation of iron between phases in these environments. This study shows that such processes can be tracked along the hydrological cycle through the investigation of temporal $\delta^{57}\text{Fe}$ series in suspended matter from rivers.

ACKNOWLEDGEMENTS

The authors would like to thank Alisson Akerman, Bárbara Lima, Carole Causserand, Celeida Márcia, Damien Guillaume, Edi Mendes Guimarães, Elisa Armijos, Geraldo Boaventura, Jean-Michel Martinez, Jérôme Chmeleff, Jonathan Prunier, Myller Sousa, Naziano Filizola, Patrícia Moreira-Turcq, Patrick Seyler, Pauliane Sampaio, Paulo Henrique Junker, Philippe Besson, Rafael Grudka Barroso, Rawaa Ammar, Thierry Aigouy, Tiago Eli and Svetlana Ilina for discussions, ideas and issues related to analytical techniques. Also, the authors wish also to thank the Brazilian National Agency of Water (ANA), Brazilian Coordination for the Improvement of Higher Education-Personnel (CAPES), the National Council of Technological and Scientific Development (CNPq), the Centre National de la Recherche Scientifique (CNRS), the French Committee for the Evaluation of University Cooperation with Brazil (COFECUB), the Institut de Recherche pour le Développement (IRD), the Laboratory of Geochronology of the University of Brasília and the Laboratory Géosciences Environnement Toulouse for their support. They are also indebted to the ORE-HYBAm project for providing the samples to this study. This research was partly funded by an EC2CO grant to FP.

Tabela 4 - Physico-chemical parameters, along with suspended matter concentrations and their iron isotope compositions $\delta^{57}\text{Fe}_{\text{IRMM-14}}$ for the Negro and Amazon rivers time series. Additional (non-refined) data on surface suspended matter samples from variable Amazonian waters are also provided.

Sample Identification	Sampling Date	Temperature ($^{\circ}\text{C} \pm 0.1$)	Conductivity ($\mu\text{S/cm} \pm 1$)	COD (ppm $\pm 5\%$)	Fe concentration ICP-MS (wt.% $\pm 5\%$)	SPM ^a ($\text{mg}^*\text{L}^{-1} \pm 1\%$)	$\delta^{57}\text{Fe}$ (‰) ^b	2SE ^c	$\delta^{56}\text{Fe}$ (‰) ^b	2SE ^c	number of analysis (n)	Lat*	Long*
Negro River at Serrinha Station													
363	01.09.06	n.a.	n.a.	n.a.	12.29	2.1	-0.543	0.264	-0.454	0.064	3		
364	10.10.06	n.a.	n.a.	16.8	5.95	6.1	-0.513	d	0.094	-0.342	0.063	3	
365	10.11.06	29.5	6	8.9	3.32	9.8	-0.684	0.165	-0.365	0.035	3		
366	10.12.06	29.4	6	10.0	4.32	5.7	-0.732	0.119	-0.450	0.123	3		
367	10.01.07	28.6	7	11.6	3.10	7.6	-0.964	0.070	-0.702	0.049	3		
368	10.02.07	29.4	7	11.7	4.49	4.6	-1.298	0.036	-0.824	0.068	3	-0.4850	-64.8289
369	10.03.07	27.5	8	9.1	4.28	7.9	-1.169	0.176	-0.779	0.117	3		
371	10.05.07	26.2	6	12.5	3.22	9.8	-1.135	0.125	-0.682	0.092	3		
372	10.06.07	26.2	4	15.7	5.55	4.9	-1.101	0.098	-0.694	0.107	3		
373	10.07.07	28.5	7	10.4	7.05	3.2	-0.768	0.049	-0.625	0.055	3		
374	10.08.07	27.5	7	9.4	5.26	7.0	-0.654	0.284	-0.512	0.182	6		
Amazon River at Óbidos Station													
Fe1	22.04.09	28.2	40	5.3	4.04	27.4	0.117	0.101	0.076	0.058	9		
Fe2	10.05.09	n.a.	37	5.5	4.40	46.8	0.067	0.068	0.036	0.055	6		
Fe3	10.06.09	n.a.	38	5.0	4.56	44.4	0.115	0.029	0.075	0.030	3	-1.9225	-55.5151
Fe4	10.07.09	n.a.	38	n.a.	4.32	33.1	0.040	0.032	0.029	0.030	6		
Fe5	10.08.09	n.a.	n.a.	4.2	4.21	43.2	0.028	0.071	0.012	0.043	6		

Tabela 4 (continued)

Sample Identification	Sampling Date	Temperature (°C ± 0.1)	Conductivity (µS/cm ± 1)	COD (ppm ± 5%)	Fe concentration ICP-MS (wt.% ± 5%)	SPM ^a (mg*L ⁻¹ ± 1%)	δ ⁵⁷ Fe (‰) ^b	2SE ^c	δ ⁵⁶ Fe (‰) ^b	2SE ^c	number of analysis (n)	Lat*	Long*
Fe6	10.09.09	n.a.	n.a.	5.2	5.24	25.1	0.156	0.089	0.106	0.064	6		
Fe7	10.10.09	n.a.	40	3.6	4.11	31.8	0.065	0.091	0.065	0.057	6		
Fe8	10.11.09	n.a.	55	3.6	6.07	48.8	0.136	0.076	0.094	0.040	9		
ÓBIDOS depth 1	06.12.09	30.4	85.0	14.0	4.94	67.9	0.082	0.019	0.072	0.019	3		
375	10.01.10	n.a.	55	n.a.	3.03	208.2	0.111	0.130	0.094	0.075	3		
376	10.02.10	n.a.	46	n.a.	3.72	148.5	0.201	0.137	0.146	0.092	3		
377	10.03.10	n.a.	n.a.	n.a.	3.06	178.0	0.275	0.175	0.152	0.094	3		
378	10.04.10	n.a.	40	n.a.	3.80	115.8	0.212	0.097	0.137	0.092	3	-1.9225	-55.5151
379	10.05.10	n.a.	33	n.a.	3.03	85.4	0.100	0.118	0.078	0.099	3		
380	10.06.10	n.a.	30	n.a.	4.85	44.7	0.025	0.170	0.013	0.072	3		
381	10.07.10	n.a.	31	6.8	4.60	38.0	-0.002	0.166	-0.001	0.103	3		
382	20.08.10	n.a.	n.a.	n.a.	4.24	33.8	0.126	0.134	0.068	0.088	6		
383	10.09.10	n.a.	29	5.4	4.31	25.8	0.132	0.183	0.055	0.083	3		
385	01.11.10	n.a.	n.a.	n.a.	1.95	29.7	0.154	0.137	0.068	0.077	3		
386	10.12.10	n.a.	58	5.3	1.92	113.0	0.119	0.190	0.059	0.124	3		
387	24.02.11	n.a.	n.a.	n.a.	2.96	151.8	0.178	0.205	0.114	0.111	3		

Tabela 4 (continued)

Sample Identification	Sampling Date	Temperature (°C ± 0.1)	Conductivity (µS/cm ± 1)	COD (ppm ± 5%)	Fe concentration ICP-MS (wt.% ± 5%)	SPM ^a (mg*L ⁻¹ ± 1%)	δ ⁵⁷ Fe (‰) ^b	2SE ^c	δ ⁵⁶ Fe (‰) ^b	2SE ^c	number of analysis (n)	Lat*	Long*
Additional data on Surface Samples from variable Amazonian Rivers													
Peruvian and Brazilian whitewater Rivers													
Marañon	10.06.10	26.4	134	5.8	5.7	245.4	0.160	0.062	0.107	e	0.041	3	-4.5364 -73.5918
Ucayali	10.06.10	27.2	238	11.7	5.9	98.3	0.019	0.156	0.013	e	0.104	3	-4.4919 -73.4243
São Paulo	15.06.10	27.5	131	5.3	7.4	142.5	0.110	0.134	0.074		0.102	3	-3.4528 -68.8954
Olivença													
Blackwater Rivers													
Tefé	20.06.10	28.1	92	5.1	13.4	5.7	-0.354	0.583	-0.232	0.407	3	-3.4639 -64.4504	
Jutaí	17.06.10	26.9	14	12.3	7.6	10.8	-0.263	d	0.177	-0.175	0.118	6	-2.7977 -66.8737
Marmelos	24.11.09	32.9	6	n.a.	9.4	2.7	-0.020	d	0.102	-0.013	0.068	6	-6.1617 -61.7897
Whitewater Rivers with distinct water characteristics													
Purus	24.06.10	28.5	24	5.1	11.1	14.5	-0.189	0.309	-0.130	0.166	3	-3.9045 -61.3932	
Coari	22.06.10	28.1	77	4.9	5.3	56.8	-0.432	0.140	-0.100	0.033	3	-4.0358 -63.0048	
Clearwater Rivers													
Alter dec	08.12.09	30.0	14	n.a.	3.9	4.2	-0.538	0.118	-0.359	0.079	3	-2.4743 -55.0056	
Alter jul	04.07.10	30.2	15	1.9	3.9	n.a.	0.145	d	0.275	0.097	0.183	3	

Tabela 4 (continued)

Sample Identification	Sampling Date	Temperature (°C ± 0.1)	Conductivity ($\mu\text{S}/\text{cm} \pm 1$)	COD (ppm ± 5%)	Fe concentration ICP-MS (wt.% ± 5%)	SPM ^a ($\text{mg}^*\text{L}^{-1} \pm 1\%$)	$\delta^{57}\text{Fe}$ (‰) ^b	2SE ^c	$\delta^{56}\text{Fe}$ (‰) ^b	2SE ^c	number of analyses (n)	Lat*	Long*
Várzeas													
Várzea Janauacá	07.10.09	32.5	57	n.a.	3.9	4.8	-0.529	0.341	-0.350	0.257	3	-3.4879	-60.2701
Várzea Juruá	18.06.10	27.9	34	6.3	13.0	7.8	-0.753	0.354	-0.360	0.372	3	-2.5614	-65.8464

a. SPM - suspended matter content

b. Iron isotope data relative to IRMM-14

c. 2SE calculated from the number of analyses indicated, using the Student's t-correcting factors (Platzner, 1997).

d. $\delta^{57}\text{Fe}$ calculated from $\delta^{56}\text{Fe}$ value

e. $\delta^{56}\text{Fe}$ calculated from $\delta^{57}\text{Fe}$ value

* decimal degrees - WGS-84

CAPÍTULO OITO

CONCLUSÕES GERAIS

Os rios da Amazônia têm sido estudados nos últimos cinqüenta anos pela importante e inigualável contribuição que trazem para o suprimento de água do planeta Terra. Não obstante, devido à vultosa extensão da Bacia Amazônica e à complexa dinâmica dos rios que drenam a área, alguns parâmetros ainda não foram investigados em detalhe e, portanto, ainda não são completamente compreendidos. Este é o caso do sistema isotópico de ferro, que é o principal objeto de estudo da presente investigação.

Tendo em vista que existe uma variedade de processos naturais (*e.g.*, transformações redox, dissolução e precipitação mineral, sorção de Fe e metabolismo biológico, entre outros – ver Beard *et al.*, 1999; Brantley *et al.*, 2001; Skulan *et al.*, 2002; Anbar, 2004; Icopini *et al.*, 2004; Schauble, 2004; Guelke e von Blanckenburg, 2007; Bullen, 2011) que podem afetar a composição isotópica e a concentração de ferro em rios, assinaturas isotópicas deste elemento foram investigadas em amostras coletadas em diferentes localizações geográficas e diferentes tipos de água, de acordo com perfis em profundidade, laterais e temporais, com o objetivo de se estimar possíveis variações de acordo com estes parâmetros. A intenção desta análise foi aportar novas percepções sobre o ciclo biogeoquímico do ferro na Bacia Amazônica, bem como sobre o transporte, especiação e fontes potenciais deste elemento.

Nos três últimos capítulos, dados de $\delta^{57}\text{Fe}$ do material em suspensão de rios Amazônicos foram apresentados e discutidos de acordo com o tipo de amostragem (perfis em profundidade, laterais e temporais, natureza de água e localizações distintas). Este capítulo final constitui uma síntese dos principais resultados e das discussões relacionados ao trabalho como um todo. Embora o Rio Amazonas seja conhecido por suprir aproximadamente um quinto da água doce global que abastece o Oceano Atlântico, poucos estudos sobre a composição isotópica de materiais provenientes destes rios foram publicados (Bergquist e Boyle, 2006; dos Santos Pinheiro *et al.*, 2013). Este trabalho é uma entre muitas contribuições que, estima-se, serão publicadas nos próximos anos e permitirão aprimorar o entendimento e conhecimento que se tem sobre o ciclo de ferro na natureza e, especialmente, em sistemas aquosos. Espera-se que as assinaturas isotópicas aqui reportadas, observadas nos anos de 2006, 2007, 2009, 2010 e 2011 nas águas da Amazônia, possam e sejam utilizadas, posteriormente, como indicadores de mudanças globais e locais.

HOMOGENEIDADE DE PERFIS EM PROFUNDIDADE E LATERAIS

Cinco amostras coletadas ao longo de quatro perfis em profundidade em quatro rios distintos na Bacia Amazônica (Solimões, Madeira, Negro e Amazonas) e ademais, cinco amostras coletadas de uma margem à outra, ao longo de três perfis laterais realizados em dois rios (Solimões e Negro), constituem a base da discussão desta seção. Os resultados demonstram que a composição isotópica de ferro do material em suspensão do Rio Amazonas e destes três importantes tributários é constante ao longo de seções em profundidade e laterais (**Fig. 20** e **Fig. 21**). A estabilidade do ferro contrasta com o fato de que outros parâmetros podem mudar de acordo com a altura na coluna de água ou em seções laterais perpendiculares ao fluxo (e.g., temperatura da água, carga de material fluvial em suspensão, concentrações de ferro – **Tabela 1** e **Fig. 16**, **Fig. 17**, **Fig. 18**, e **Fig. 19**, cf. Meade *et al.*, 1985; Bouchez *et al.*, 2010). Pode-se então concluir que uma amostra de sub-superfície é representativa da assinatura isotópica de ferro de todo o rio, ao menos em uma dada estação do ano, o que contrasta com resultados de outros traçadores isotópicos, como o estrôncio (cf. Bouchez *et al.*, 2011a).

Três dos quatro rios estudados são de água branca (caracterizada por pronunciado conteúdo de material em suspensão, pela natureza inorgânica e pelo pH neutro da água) e mostram, independente das localizações geográficas, composições isotópicas de ferro similares à da media da crosta continental ($\delta^{57}\text{Fe} \sim 0.1 \pm 0.03\text{‰}$; Poitrasson, 2006; **Fig. 20**, **Fig. 21**, **Fig. 31** e **Fig. 32**). Além disso, amostras coletadas no Rio Solimões nas mesmas localidades, porém em diferentes estágios da água (alto em Junho e baixo em Novembro) apresentam valores similares em ambos períodos (**Fig. 21**). Em contraste, os resultados de material em suspensão do único rio de água preta analisado, o Negro (baixa carga particulada, rico em material orgânico e caráter ácido), mostram valores de $\delta^{57}\text{Fe}_{\text{IRMM-14}}$ negativos tanto na estação de Paricatuba quanto na de Serrinha (**Fig. 18**, **Fig. 19**, e **Fig. 32**). Este dado é interpretado como reflexo da assinatura isotópica de camadas reduzidas de espodossolos, ricas em material orgânico (discutido a seguir), que cobrem um terço da Bacia do Rio Negro (Fritsch *et al.*, 2009).

VARIABILIDADES TEMPORAIS CONTRASTADAS

As composições isotópicas de ferro de dois tipos extremos de rios, o Negro (estação de Serrinha) e o Amazonas (estação de Óbidos), foram estudadas ao longo de estações hidrológicas completas. O Rio Amazonas, de água branca, mostrou comportamento similar ao Rio Solimões durante as estações de cheia e de seca, com valores de composição isotópica similares ao da crosta continental ($0.1 \pm 0.03\text{\textperthousand}$, [Poitrasson, 2006](#)) ao longo de aproximadamente dois anos. Por outro lado, o Rio Negro mostra assinaturas negativas e variações consideráveis ao longo do ciclo hidrológico ([Fig. 31](#) e [Fig. 32](#)).

Registrhou-se um impacto significativo e complexo das estações do ano, do volume de precipitações, da vazão de água ([Fig. 32](#)) e da atividade biológica no Rio Negro, de modo que pode-se dizer que estas características, em conjunto, influenciam os resultados de $\delta^{57}\text{Fe}$ do material em suspensão. Tais fatores controlam os conteúdos de carbono orgânico dissolvido e, possivelmente, o pH da água ([Fig. 29](#)). Como todos estes aspectos (*i.e.*, pH da água, carbono orgânico dissolvido, volume de precipitações) têm um importante papel no sistema deste rio, mudanças associadas a eles podem contribuir para variações na composição isotópica de ferro do material em suspensão do Rio Negro, como verificado nos resultados da série temporal deste rio ([Fig. 32](#)).

A origem da diferença de 1‰ entre os resultados de $\delta^{57}\text{Fe}_{\text{IRMM-14}}$ obtidos e os resultados de [Bergquist e Boyle \(2006\)](#) para o Rio Negro foi questionada no capítulo cinco. Para resolver esta questão, dados do Rio Negro apresentados nos capítulos 5 e 7 foram comparados às observações de [Bergquist e Boyle \(2006\)](#), dados mostrados na [Fig. 32](#)). As assinaturas isotópicas de ferro das três amostras, coletadas em março de 2002 ([Bergquist e Boyle, 2006](#)), outubro de 2009 e setembro de 2010 ([dos Santos Pinheiro *et al.*, 2013](#)), equivalem, dentro das incertezas analíticas, ao $\delta^{57}\text{Fe}_{\text{IRMM-14}}$ dos períodos correspondentes estudados na série temporal do Rio Negro ([Fig. 32](#)).

Variações temporais já foram observadas por [Ingri *et al.* \(2006\)](#) para o rio boreal Kalix, na Suécia. Os resultados apresentados por estes autores apontam, entretanto, para uma assinatura leve dos colóides de Fe-C, o que está em oposição às observações feitas para o Rio Negro, para o qual os colóides orgânicos (presentes na fração $< 0.45 \mu\text{m}$) mostram assinaturas positivas. Pode-se atribuir este contraste à incorporação preferencial de ferro isotopicamente mais pesado (Fe^{3+}) na fração coloidal / dissolvida em ambientes reduzidos (*e.g.*, [Allard *et al.*,](#)

2011). Dados do estudo de Bergquist e Boyle (2006) também apontam para uma fase Fe-C coloidal pesada, o que está de acordo com os resultados positivos aqui reportados para o material dissolvido do Rio Negro (capítulo 6, **Fig. 25**).

No estudo de Ingri *et al.* (2006), oxi-hidróxidos de Fe são enriquecidos em isótopos pesados, o que leva à assinatura positiva do material em suspensão. As flutuações na composição isotópica de ferro ao longo do ano foram atribuídas à contribuição variável de partículas / colóides de Fe-C, que mudariam a composição isotópica pra assinaturas mais leves, especialmente durante eventos de tempestade (**Fig. 33**). No trabalho apresentado nesta Tese, a composição isotópica do material em suspensão é essencialmente leve e mostra valores de $\delta^{57}\text{Fe}$ negativos (**Fig. 33**), o que pode ser explicado pela incorporação / sorção preferencial de ferro leve nas partículas deste rio. Seguindo a explicação dada por Ingri *et al.* (2006) para as variações sazonais encontradas no Rio Kalix, eventos de tempestade (no caso, fortes chuvas que aumentam a vazão dos rios) permitem que o nível de água suba e lixivie horizontes de solo distintos, os quais contribuem com materiais que têm diferentes naturezas e portanto, diferentes composições isotópicas.

INFLUÊNCIA DA NATUREZA DA ÁGUA

O fato do material em suspensão de rios de água preta mostrar valores negativos e heterogêneos durante o ciclo hidrológico está, em oposição ao material particulado de rios de água branca (que mostram $\delta^{57}\text{Fe}_{\text{IRMM-14}}$ positivos e homogêneos, **Fig. 32**), fortemente relacionado às distintas características destes dois rios. Estas diferenças ocorrem especialmente devido ao embasamento geológico e à natureza dos solos tipicamente drenados por estes sistemas de rios. As assinaturas negativas encontradas para o material em suspensão de águas ácidas do Rio Negro sugerem que o fracionamento que ocorre nos solos segregaria o ferro leve, que vai estar mais ou menos disponível de acordo com as estações do ano. Desta forma, a altura atingida pela coluna de água depende significativamente da vazão e das precipitações anuais (**Fig. 32**). Com efeito, pode-se dizer que os conteúdos de carbono orgânico (**Fig. 29**), a atividade biológica e o pH da água são afetados por – e que reciprocamente afetam – outros parâmetros físico-químicos. Como consequência, a composição isotópica deste sistema fluvial registra uma mistura de todas as possíveis fontes e processos envolvidos no ciclo do ferro neste ambiente.

De acordo com [Skulan et al. \(2002\)](#), em soluções com pH próximo ao neutro, quando dissolução é também acompanhada por precipitação, um contraste isotópico deve ser esperado entre sólido total e o Fe em solução. Neste estudo, a rápida precipitação de hematita não permitiu o equilíbrio isotópico entre cristais e líquido. Efeitos isotópicos cinéticos seriam possivelmente responsáveis pelo fracionamento observado, o que é também a explicação proposta pelo estudo de [Bullen et al. \(2001\)](#), no qual a precipitação de ferrihidrita em escalas de tempo curtas produz ferrihidrita isotopicamente pesada, se comparada ao Fe aquoso. Este último estudo está, contudo, em oposição aos resultados apresentados para o Rio Negro, para o qual o precipitado (*i.e.*, o material em suspensão) é isotopicamente mais leve. Neste caso, uma presumida completa oxidação do $\text{Fe}^{2+}_{(\text{aq})}$ para o $\text{Fe}^{3+}_{(\text{aq})}$ enriqueceria o ferro férrico em isótopos pesados ([Schauble et al., 2001](#); [Brantley et al., 2004](#)), e uma subsequente precipitação de Fe^{3+} em ferrihidrita enriqueceria o precipitado em isótopos leves, devido à processos cinéticos ([Dauphas e Rouxel, 2006](#)).

Ferrihidrita é a fase oxi-hidróxido predominante a se formar em sistemas aquáticos com pH maior que 4, e em pH maior que 5 todo o $\text{Fe}^{3+}_{(\text{aq})}$ produzido pela oxidação do Fe^{2+} e seus produtos intermediários são imediatamente precipitados como ferrihidrita ([Bullen et al., 2001](#)). Além disso, é fato notório que a taxa de oxidação se vê aumentada pela presença de CO_2 e de material orgânico ([Viers et al., 1997](#); [Viers et al., 2000](#); [Oliva et al., 1999](#) e [Bullen et al., 2001](#)), que são característicos no Rio Negro. Em adição à possíveis efeitos cinéticos, esta pode ser, ao menos em parte, uma explicação para o contraste isotópico verificado entre fases sólidas e dissolvidas, tal como para o Rio Negro.

Outra possibilidade é uma completa oxidação do Fe^{2+} derivado de espodossolos presentes na área, processo que concorre para a assinatura isotópica negativa do material em suspensão encontrado no Rio Negro. Assumindo-se que este foi o caso, a falta de dois reservatórios distintos de ferro impede a troca isotópica e, consequentemente, o fracionamento do ferro. Os compostos recém-formados de Fe^{3+} manteriam sua composição isotópica inicialmente leve, herdada de processos no interior de solos. Não obstante, uma explicação não exclui a outra e em cada caso (ou em ambos os casos), a assinatura isotópica do material em suspensão foi adquirida antes da precipitação do material em suspensão.

No presente estágio, a variabilidade anual na composição isotópica do Rio Negro não pode ser especificamente definida como efeito cinético ou em equilíbrio, e a oxidação de Fe^{2+} para Fe^{3+} não pode ser claramente atribuída a processos biológicos ou abióticos. As diferenças no $\delta^{57}\text{Fe}_{\text{IRMM-14}}$ encontradas para o material dissolvido e em suspensão refletem, desta

maneira, todas as reações de troca que envolvem o ferro neste complexo e dinâmico sistema de rio.

Resultados para o Rio Amazonas estão de acordo com a suposição de que água bruta (*i.e.*, não filtrada) de rios com altas cargas de material em suspensão (*e.g.*, rios Solimões, Madeira e Amazonas) tendem a ter $\delta^{57}\text{Fe}_{\text{IRMM-14}}$ similares à média da crosta continental, enquanto os resultados do Rio Negro parecem confirmar a relação oposta, *i.e.*, água bruta de rios com pequenas quantidades de carga em suspensão terão assinaturas isotópicas mais leves se comparadas à crosta continental ([Fantle e DePaolo, 2004](#)).

FONTES DE FERRO PARA OS RIOS AMAZÔNICOS

Os valores $\delta^{57}\text{Fe}_{\text{IRMM-14}}$ similares ao da crosta encontrados para o material em suspensão de rios de água branca (Solimões, Madeira e Amazonas, [Fig. 20](#), [Fig. 21](#), [Fig. 31](#) e [Fig. 32](#)) refletem a assinatura de material detritico, que consiste em fragmentos mecanicamente intemperizados e erodidos da rocha primária, representados pelo conteúdo de material em suspensão, altamente carregado, que é característico destes rios. O material em questão é erodido da principal fonte de metais para estes rios, os Andes. Os resultados de material em suspensão observados confirmam que existe pequeno ou nenhum fracionamento isotópico durante o transporte de ferro a partir de fontes primárias (principalmente de rochas ígneas e sedimentos) para os rios de água branca da Bacia Amazônica. Eles ainda indicam que as assinaturas isotópicas de ferro podem ser utilizadas como traçadores de fontes de ferro, ao invés de trazerem informações sobre a natureza de processos que envolvem a ciclagem geoquímica / isotópica de ferro em rios inorgânicos de água branca.

Por outro lado, os valores negativos e variáveis de $\delta^{57}\text{Fe}$ do material em suspensão do Rio Negro ([Fig. 20](#), [Fig. 21](#) e [Fig. 32](#)) estão fortemente relacionados com as camadas superiores de espodossolos que cobrem um terço da Bacia deste rio. Este reservatório de ferro reduzido e leve, segregado durante a pedogênese, é transportado de solos para a corrente principal dos rios, onde é oxidado por vários processos, que podem incluir, como sugerido por [Allard *et al.* \(2011\)](#), atividade biológica, como a ação de bactérias ativas em meio ácido ([Kappler e Straub, 2005](#)), ou a produção fotoquímica de H_2O_2 ([Pullin e Cabaniss, 2003](#)). A oxidação quantitativa previamente mencionada de Fe^{2+} derivado de espodossolos, para Fe^{3+} , contribui para manter a assinatura isotópica originalmente leve, herdada durante a

pedogênese. Assim, o material em suspensão mostra composições distintas devido à incorporação deste ferro leve, como observado nos resultados do Rio Negro.

Ainda que o Rio Kalix, estudado por [Ingri et al. \(2006\)](#), mostre composições do material em suspensão mais pesadas se comparadas ao Rio Negro ([Fig. 33](#)), a variabilidade temporal deste rio sueco foi igualmente associada aos espodossolos drenados por este rio, em menor extensão. As distinções entre estes dois rios – Kalix e Negro – podem ser atribuídas à vários fatores: como discutido no capítulo 7, de acordo com [Widerlund \(1996\)](#) a origem da água do Rio Kalix muda drasticamente durante o ciclo hidrológico (passa de águas subterrâneas para águas de degelo e, posteriormente, para águas de regiões montanhosas). Ademais, são bastante diferentes as áreas das bacias, as médias de precipitação e os valores de vazão de água dos dois rios (*cf.* [Widerlund, 1996](#) e [Dahlqvist et al., 2004](#)) e estas feições podem explicar, ao menos parcialmente, as discrepâncias observadas entre as assinaturas isotópicas do material em suspensão de cada um dos rios comentados.

De acordo com as observações feitas por [Ingri et al. \(2006\)](#), como as colunas de água são fortemente influenciadas pelo volume de precipitação e pela vazão de água, cada um destes rios alcança níveis distintos de horizontes de solo durante o ciclo hidrológico e, consequentemente, os materiais lixiviados e incorporados à suas águas são representativos dos compartimentos fracionados que existem nos espodossolos drenados por ambos os rios.

Os isótopos leves provenientes das camadas superiores de solos ricos em matéria orgânica são incorporados nas águas do Rio Negro especialmente durante altos níveis de água (enchentes e períodos de fortes chuvas). Isto é demonstrado pela relação inversa entre, de um lado, as composições isotópicas de ferro e, de outro lado, a vazão de água ou precipitações (*i.e.*, em períodos chuvosos e de cheias, a composição isotópica de ferro é mais negativa – ou mais leve – [Fig. 32](#)). A coluna de água alcança diferentes horizontes de solo ao longo do ano e isso determinaria a contribuição dos diversos reservatórios de ferro.

O ferro leve pode ser tanto precipitado sob a forma de oxi-hidróxidos, ou absorvido / incorporado em partículas carregadas pelo Rio Negro, enquanto o ferro pesado permanece disponível para se ligar a substâncias orgânicas, especialmente na forma de colóides (que estão, neste estudo, incluídos na fração dissolvida). Este fracionamento leva, finalmente, ao enriquecimento de isótopos leves na fase particulada – como confirmado pelo presente estudo ([Fig. 20](#), [Fig. 21](#) e [Fig. 32](#)) e por [Bergquist e Boyle \(2006\)](#), – e a uma assinatura isotópica pesada da fração dissolvida do Negro, como observado na [Fig. 25](#) e em [Bergquist e Boyle \(2006\)](#).

Na zona de mistura entre os rios Negro e Solimões, em Manaus, onde o Rio Amazonas é formado, as características contrastantes da água geram uma frente onde diversas reações ocorrem, tais como possíveis perdas de elementos e de carbono orgânico total, bem como a coagulação e a dissolução de minerais ([Aucour et al., 2003](#); [Benedetti et al., 2003a](#)). Um estudo detalhado de isótopos de ferro na zona de mistura entre os rios Negro e Solimões é necessária para que se possa entender adequadamente a sistemática envolvida na combinação destes dois tipos extremos de água, bem como para a compreensão de como a referida mistura afeta o comportamento dos isótopos de ferro. De todas as formas, pode ser concluído, com base nas assinaturas encontradas para o material em suspensão do Rio Amazonas na Estação de Óbidos ($\delta^{57}\text{Fe} \sim 0.1\text{\textperthousand}$, [Fig. 20](#) e [Fig. 31](#)), que a contribuição do material em suspensão do Rio Amazonas para o Oceano Atlântico é próxima ao valor médio da crosta continental. Tal afirmação é ainda reforçada pelo fato de que os rios Solimões (na Estação de Manacapuru) e Madeira (na Estação de Manicoré) – que são os principais contribuintes de material em suspensão para o Rio Amazonas, somando aproximadamente 90% da carga sedimentar ([Gibbs, 1967](#); [Meade et al., 1985](#)) – também mostram assinaturas isotópicas similares às da media da crosta continental ([Fig. 20](#) e [Fig. 21](#)).

Em síntese, os resultados apresentados indicam que assinaturas isotópicas de sedimentos em suspensão de rios, assim como de outras fases (e.g., coloidal, dissolvida), podem variar ao longo do ano, devido às particularidades de cada ambiente estudado. Ao mesmo tempo, eles podem oferecer importantes indicações sobre os regimes de intemperismo que atuam em cada cenário, bem como (e especialmente) sobre o papel da atividade biológica na ciclagem do ferro. De forma similar, isótopos de ferro podem ser utilizados para estimar possíveis transformações / perdas deste elemento quando da mistura de diferentes corpos de água presentes na região Amazônica. Este traçador isotópico pode, portanto, ser valioso no esclarecimento e diferenciação dos compartimentos que resultam das reações que envolvem ferro, assim como permite fazer inferências sobre o transporte e ciclo deste elemento, particularmente em ambientes que dividem fontes orgânicas e inorgânicas.

CAPÍTULO NOVE

PERSPECTIVAS

A discussão com os membros da banca examinadora foi, por ocasião da defesa de Tese, bastante produtiva e, neste sentido, faz-se oportuno explorar, ainda que sucintamente, alguns dos comentários e sugestões relativos a este trabalho. O intuito da inclusão deste capítulo é registrar linhas de desenvolvimento que podem contribuir para a continuidade deste estudo, bem como para futuras pesquisas na área de isótopos de ferro de materiais provenientes de rios. Aproveito para agradecer novamente a todos os membros da banca pelo aporte que trouxeram.

1) É conveniente fazer uso de técnicas disponíveis para a determinação, quantitativa e qualitativa, da mineralogia, de forma que se possa estimar a influência que cada fase identificada exerce nas assinaturas do material em suspensão. Análises de oligoelementos (como Al, Ca, Mg) também são adequadas, visto que as composições isotópicas de ferro poderiam ser atribuídas mais especificamente a minerais encontrados em maior ou menor quantidade nas amostras coletadas em diferentes localidades ou períodos do ciclo hidrológico.

2) É importante proceder a determinação do Eh (potencial de redução) para maiores esclarecimentos sobre o ferro existente no Rio Negro (se Fe^{2+} ou Fe^{3+}), de forma a viabilizar a utilização de diagramas Eh *versus* pH, os quais permitiriam verificar as fases estáveis nos distintos compartimentos estudados. Contudo, a medição deste parâmetro exige equipamento específico, com calibragem também específica. Tal fator não pode ser considerado no âmbito deste trabalho, entretanto, fica clara a utilidade do emprego desta ferramenta para melhor avaliação e interpretação dos resultados.

3) Sugere-se a análise de isótopos de ferro em águas de poros de solos que ocorrem na Bacia do Rio Negro, além do estudo do tempo de residência do ferro neste sistema e da velocidade de transferência deste elemento de reservatórios para os rios. Desta forma, pode-se confirmar se as assinaturas negativas do material em suspensão do Rio Negro e demais rios de água preta se relacionam apenas aos espodossolos ou se consistem na mistura de ferros provenientes de outros tipos de solos e/ou coberturas (*e.g.*, vegetal, embasamento geológico) presentes na região.

4) É oportuno empregar de técnicas de ultrafiltração e filtração em cascata, para que sejam separadas as frações particulada, coloidal e dissolvida. Todavia, o presente trabalho se ateve à coleta e ao estudo das frações particulada e dissolvida, e a menção aos colóides se deu por extração dos resultados, com base na literatura consultada. Seria conveniente, ainda, que as diferentes frações separadas fossem divididas em sub-frações de acordo com os tamanhos e pesos moleculares das partículas. Desta maneira, as assinaturas isotópicas de ferro (especialmente no caso do Rio Negro) poderiam ser atribuídas, mais especificamente, a um determinado grupo de partículas, uma vez que a fração particulada poderia conter colóides mais pesados e a fração dissolvida, colóides mais leves. Esta última fração (*i.e.*, colóides) pode ainda conter diversos tamanhos de material que permitem individualização (*e.g.*, 0.1, 0.046, 0.0066 (100 kDa), 0.0031 (10 kDa) e 0.0014 μm (1 kDa)). Por outro lado, no caso do Rio Negro, que apresenta baixo conteúdo de material em suspensão, a probabilidade de que partículas menores do que 0,45 μm tenham sido retidas no filtro utilizado é pequena. Não obstante, é necessário especificar a fração que controla a assinatura da fase dissolvida.

Os comentários dos membros são muito pertinentes, porém, seguir tais recomendações exige planejamento prévio de estudo (uma vez que requer quantidades extra de amostras e uma logística ainda mais refinada de materiais a serem levados para o barco em missões de campo). Procedimentos distintos de tratamento após as coletas também devem ser antecipados (*i.e.*, para que os tamanhos desejados possam ser estudados, devem estar disponíveis aparatos de filtração diferentes dos que foram utilizados neste trabalho).

CAPÍTULO DEZ

REFERÊNCIAS

- Albarède, F. & Beard, B. (2004). "Analytical Methods for Non-Traditional Isotopes." *Reviews in Mineralogy & Geochemistry*(55): 113-152.
- Albarède, F., Télouk, P., Blichert-Toft, J., Boyet, M., Agranier, A., Nelson, B. (2004). "Precise and accurate isotopic measurements using multiple-collector ICPMS." *Geochimica et Cosmochimica Acta* **68**: 2725-2744.
- Allard, T., Ponthieu, M., Weber, T., Filizola, N., Guyot, J. L., Benedetti, M. (2002). "Nature and properties of suspended solids in the Amazon Basin." *Bull. Soc. Géol. France* **173**: 67-75.
- Allard, T., Menguy, N., Salomon, J., Calligaro, T., Weber, T., Calas, G., Benedetti, M. F. (2004). "Revealing forms of iron in river-borne material from major tropical rivers of the Amazon Basin (Brazil)." *Geochimica et Cosmochimica Acta* **68**(14): 3079-3094.
- Allard, T., Webe, T., Bellot, C., Damblans, C., Bardy, M., Bueno, G., Nascimento, N. R., Fritsch, E., Benedetti, M. F. (2011). "Tracing source and evolution of suspended particles in the Rio Negro Basin (Brazil) using chemical species of iron." *Chemical Geology* **280**: 79-88.
- Aller, R. C., Heilbrun, C., Panzeca, C., Zhu, Z., Baltzer, F. (2004). *Marine Geology* **208**(2-4): 331-360.
- Anbar, A. D. (2004). "Iron stable isotopes: beyond biosignatures." *Earth and Planetary Science Letters* **217**: 223-236.
- Anbar, A. D. & Rouxel, O. (2007). "Metal Stable Isotopes in Paleoceanography." *Annual Review of Earth and Planetary Sciences* **35**: 717-746.
- Anbar, A. D., Roe, J. E., Nealson, K. H. (2000). "Nonbiological Fractionation of Iron Isotopes." *Science* **288**(5463): 126-128.
- Arnold, G. L., Weyer, S., Anbar, A. D. (2004). "Fe isotope variations in natural materials measured using high mass resolution multiple collector ICPMS." *Analytical Chemistry* **76**: 322-327.
- Aucour, A. M., Tao, F. A., Moreira-Turcq, P., Seyler, P., Sheppard, S., Benedetti, M. F. (2003). "The Amazon River: behaviour of metals (Fe, Al, Mn) and dissolved organic matter in the initial mixing at the Rio Negro/Solimoes confluence." *Chemical Geology* **197**(1-4): 271-285.
- Basu, A. R., Sharma, M., DeCelles, P. G. (1990). "Nd, Sr-isotopic provenance and trace element geochemistry of Amazonian foreland basin fluvial sands, Bolivia and Peru: implications for ensialic Andean orogeny." *Earth and Planetary Science Letters* **100** 1-17.
- Beard, B. L. & Johnson, C. M. (1999). "High precision iron isotope measurements of terrestrial and lunar materials." *Geochimica et Cosmochimica Acta* **63**: 1653-1660.
- Beard, B. L. & Johnson, C. M. (2003). "High Temperature inter mineral Fe isotope fractionation." *Geochimica et Cosmochimica Acta* **67**(18): A35-A35.
- Beard, B. L. & Johnson, C. M. (2004a). "Inter-mineral Fe isotope variations in mantle-derived rocks and implications for the Fe geochemical cycle." *Geochimica et Cosmochimica Acta* **68**: 4727-4743.
- Beard, B. L. & Johnson, C. M. (2004b). Fe isotope variations in the modern and ancient Earth and other planetary bodies. In: *Geochemistry of non-traditional stable isotopes*. C. M. Johnson , B. L. Beard and F. Albarède. Washington, Mineralogical Society of America. **55**: 319-357.
- Beard, B. L. & Johnson, C. M. (2007). "Comment on "Iron isotope fractionation during planetary differentiation" by S. Weyer et al., Earth Planet. Sci. Lett. V240, pages 251-264." *Earth and Planetary Science Letters* **256**(3-4): 633-637.

- Beard, B. L., Johnson, C. M., Cox, L., Sun, H., Nealson, K. H., Aguilar, C. (1999). "Iron Isotope Biosignatures." *Science* **285**(5435): 1889-1892.
- Beard, B. L., Johnson, C. M., Skulan, J. L., Nealson, K. H., Cox, L., Sun, H. (2003a). "Application of Fe isotopes to tracing the geochemical and biological cycling of Fe." *Chemical Geology* **195**: 87-117.
- Beard, B. L., Johnson, C. M., Von Damm, K. L., Poulsen, R. L. (2003b). "Iron isotope constraints of Fe cycling and mass balance in the oxygenated Earth oceans." *Geology* **31**: 629-632.
- Belshaw, N. S., Zhu, X. K., O'Nions, R. K. (2000). "High precision measurement of iron isotopes by plasma source mass spectrometry." *International Journal of Mass Spectrometry* **197**: 191-195.
- Benedetti, M. F., Mounier, S., Filizola, N., Benaim, J., Seyler, P. (2003a). "Carbon and metal concentrations, size distributions and fluxes in major rivers of the Amazon basin." *Hydrological Processes* **17**(7): 1363-1377.
- Benedetti, M. F., Ranville, J. F., Allard, T., Bednar, A. J., Menguy, N. (2003b). "The iron status in colloidal matter from the Rio Negro, Brasil." *Colloids and Surfaces A - Physicochemical and Engineering Aspects* **217**: 1-9.
- Benkhedda, K., Chen, H., Dabeka, R., Cockell, K. (2008). "Isotope ratio measurements of iron in blood samples by multi-collector ICP-MS to support nutritional investigations in humans." *Biological Trace Element Research* **122**(2): 179-192.
- Bennett, S. A., Achterberg, E. P., Connelly, D. P., Statham, P. J., Fones, G. R., German, C. R. (2008). "The distribution and stabilisation of dissolved Fe in deep-sea hydrothermal plumes." *Earth and Planetary Science Letters* **270**: 157-167.
- Bergquist, B. A. & Boyle, E. A. (2006). "Iron isotopes in the Amazon River system: Weathering and transport signatures." *Earth and Planetary Science Letters* **248**(1-2): 54-68.
- Bouchez, J., Lajeunesse, E., Gaillardet, J., France-Lanord, C., Dutra-Maia, P., Maurice, L. (2010). "Turbulent mixing in the Amazon River: The isotopic memory of confluences." *Earth and Planetary Science Letters* **290**(1-2): 37-43.
- Bouchez, J., Gaillardet, J., France-Lanord, C., Maurice, L., Dutra-Maia, P. (2011a). "Grain size control of river suspended sediment geochemistry: Clues from Amazon River depth profiles." *Geochem. Geophys. Geosyst.* **12**, Q03008, doi:10.1029/2010GC003380.
- Bouchez, J., Métivier, F., Lupker, M., Maurice, L., Gaillardet, J., France-Lanord, C., Filizola, N. (2011b). "Prediction of depth-integrated fluxes of suspended sediment in the Amazon River: particle aggregation is a complicating factor." *Hydrological Processes* **25**(5): 778-794.
- Brantley, S. L., Liermann, L., Bullen, T. D. (2001). "Fractionation of Fe isotopes by soil microbes and organic acids." *Geology* **29**: 535-538.
- Brantley, S. L., Liermann, L. J., Guynn, R. L., Anbar, A., Icopini, G. A., Barling, J. (2004). "Fe isotopic fractionation during mineral dissolution with and without bacteria." *Geochimica et Cosmochimica Acta* **68**: 3189-3204.
- Bravard, S. & Righi, D. (1990). "Podzols in Amazonia." *Catena* **17**: 461-475.
- Briat, J. F. & Lobreaux, S. (1997). "Iron transport and storage in plants." *Trends in Plant Science* **2**(5): 187-193.
- Bruland, K. W., Donat, J. R., Hutchins, D. A. (1991). "Interactive Influences of Bioactive Trace-Metals on biological production in Oceanic Waters." *Limnology and Oceanography* **36**(8): 1555-1577.
- Bueno, G. T. (2009). Appauvrissement et podzolisation des latérites du bassin du Rio Negro et genèse des podzols dans le haut bassin amazonien. PhD Thesis. Institut de Physique du Globe de Paris and Universidade Estadual Paulista "Julio de Mesquita Filho" (UNESP).
- Buffle, J., Wilkinson, K. J., Stoll, S., Filella, M., Zhang, J. W. (1998). "A generalized description of aquatic colloidal interactions: The three-colloidal component approach." *Environmental Science & Technology* **32**(19): 2887-2899.

- Bullen, T. D. (2011). Stable Isotopes of Transition and Post-Transition Metals as Tracers in Environmental Studies. In: Handbook of Environmental Isotope Geochemistry, Advances in Isotope Geochemistry. M. Baskaran (ed.), Springer-Verlag, Berlin Heidelberg. 177-203.
- Bullen, T. D., White, A. F., Childs, C. W., Vivit, D. V., Schultz, M. S. (2001). "Demonstration of significant abiotic iron isotope fractionation in nature." Geology **29**: 699-702.
- Callède, J., Ronchail, J., Guyot, J.-L., de Oliveira, E. (2008). "Amazonian deforestation: its influence on the Amazon discharge at Óbidos (Brasil)." Revue des Sciences de l'Eau **21**(1): 59-72.
- Callède, J., Cochonneau, G., Ronchail, J., Vieira Alves, F., Guyot, J.-L., Guimarães, V. S., de Oliveira, E. (2010). "The River Amazon water contribution to the Atlantic Ocean." Revue des Sciences de l'Eau **23**(3): 247-273.
- Canfield, D. E. (1997). "The geochemistry of river particulates from the continental USA: Major elements." Geochimica et Cosmochimica Acta **61**(16): 3349-3365.
- Carlson, R. W., Hauri, E. H., Alexander, C. M. O. D. (2001). Matrix induced isotopic mass fractionation in the ICP-MS. In: Plasma source mass spectrometry: The new Millennium. T. S. Holand G. Cambridge, Royal Society of Chemistry 288-297.
- Chmeleff, J., Horn, I., Steinhöfel, G., von Blanckenburg, F. (2008). "In situ determination of precise stable Si isotope ratios by UV-femtosecond laser ablation high-resolution multi-collector ICP-MS." Chemical Geology **249**(1-2): 155-166.
- Cornell, R. M. & Schwertmann, U. (2003). The Iron Oxides: Structure, Properties, Reactions, Occurrences and Uses. 2nd ed. Weinheim, Germany. Wiley- VCH Verlag GmbH & Co. KGaA, 664 pp.
- Craddock, P. R. & Dauphas, N. (2011). "Iron Isotopic Compositions of Geological Reference Materials and Chondrites." Geostandards and Geoanalytical Research **35**(1): 101-123.
- Craddock, P. R., Rouxel, O. J., Ball, L. A., Bach, W. (2008). "Sulfur isotope measurement of sulfate and sulfide by high-resolution MC-ICP-MS." Chemical Geology **253**(3-4): 102-113.
- Craddock, P. R., Dauphas, N., Clayton, R. E. (2010). Mineralogical control on iron isotopic fractionation during lunar differentiation and magmatism. LPSC XXXXI, Houston. 1230.pdf
- Craig, H. (1954). "Geochemical implications of the isotopic composition of carbon in ancient rocks." Geochimica et Cosmochimica Acta **6**: 186 to 196.
- Curie, C. & Briat, J. F. (2003). "Iron transport and signaling in plants." Annual Review of Plant Biology **54**: 183-206.
- Dahlqvist, R., Benedetti, M., Andersson, K., Turner, D., Larsson, T., Stolpe, B., Ingri, J. (2004). "Association of calcium with colloidal particles and speciation of calcium in the Kalix and Amazon rivers." Geochimica et Cosmochimica Acta **68**(20): 4059-4075.
- Dauphas, N. & Rouxel, O. (2006). "Mass spectrometry and natural variations of iron isotopes." Mass Spectrometry reviews **25**: 515-550.
- Dauphas, N., van Zuilen, M., Wadhwa, M., Davis, A. M., Marty, B., Janney, P. E. (2004a). "Clues from Fe isotope variations on the origin of Early Archean BIFs from Greenland." Science **306**: 2077-2080.
- Dauphas, N., Janney, P. E., Mendybaev, R. A., Wadhwa, M., Richter, F. M., Davis, A. M., van Zuilen, M., Hines, R., Foley, C. N. (2004b). "Chromatographic separation and multicollection-ICPMS analysis of iron. Investigating mass-dependent and independent isotope effects." Analytical Chemistry **76**: 5855-5863.
- Dauphas, N., Van Zuilen, M., Busigny, V., Lepland, A., Wadhwa, M., Janney, P. (2007a). "Iron isotope, major and trace element characterization of early Archean supracrustal rocks from SW Greenland: Protolith identification and metamorphic overprint." Geochimica et Cosmochimica Acta **71**(19): 4745-4770.
- Dauphas, N., Cates, N., Mojzsis, S., Busigny, V. (2007b). "Identification of chemical sedimentary protoliths using iron isotopes in the >3750 Ma Nuvvuagittuq supracrustal belt, Canada." Earth and Planetary Science Letters **254**(3-4): 358-376.

- Dauphas, N., Craddock, P. R., Asimow, P. D., Bennett, V. C., Nutman, A. P., Ohnenstetter, D. (2009). "Iron isotopes may reveal the redox conditions of mantle melting from Archean to Present." *Earth and Planetary Science Letters* **288**(1-2): 255-267.
- Dauphas, N., Teng, F. Z., Arndt, N. T. (2010). "Magnesium and iron isotopes in 2.7 Ga Alexo komatiites: Mantle signatures, no evidence for Soret diffusion, and identification of diffusive transport in zoned olivine." *Geochimica et Cosmochimica Acta* **74**(11): 3274-3291.
- de Baar, H. J. W. & de Jong, J. T. M. (2001). Distributions, sources and sinks of iron in seawater. In: *The Biogeochemistry of Iron in Seawater*. D. R. Turner and K. A. Hunter. Chichester, NY, IUPAC Series on Analytical and Physical Chemistry of Environmental Systems. **7**: 123–253.
- Dideriksen, K., Baker, J. A., Stipp, S. L. S. (2006). "Iron isotopes in natural carbonate minerals determined by MC-ICP-MS with a Fe-58-Fe-54 double spike." *Geochimica et Cosmochimica Acta* **70**(1): 118-132.
- Dideriksen, K., Baker, J. A., Stipp, S. L. S. (2008). "Equilibrium Fe isotope fractionation between inorganic aqueous Fe(III) and the siderophore complex, Fe(III)-desferrioxamine B." *Earth and Planetary Science Letters* **269**: 280-290.
- Dixon, P. R., Perrin, R. E., Rokop, D. J., Maeck, R., Janecky, D. R., Banar, J. P. (1993). "Measurement of Iron Isotopes (^{54}Fe , ^{56}Fe , ^{57}Fe , and ^{58}Fe) Submicrogram Quantities of Iron." *Analytical Chemistry* **65**: 2125-2130.
- dos Santos Pinheiro, G. M., Poitrasson, F., Sondag, F., Vieira, L. C., Pimentel, M. M. (2013). "Iron isotope composition of the suspended matter along depth and lateral profiles in the Amazon River and its tributaries." *Journal of South American Earth Sciences* **44**: 35-44. <http://dx.doi.org/10.1016/j.jsames.2012.08.001>.
- Dubroeucq, D. & Volkoff, B. (1998). "From Oxisols to Spodosols and Histosols: evolution of the soil mantles in the Rio Negro basin (Amazonia)." *Catena* **32**: 245–280.
- Dunne, T., Mertes, L. A. K., Meade, R. H., Richey, J. E., Forsberg, B. R. (1998). "Exchanges of sediment between the flood plain and channel of the Amazon River in Brazil." *Geological Society of America Bulletin* **110**(4): 450-467.
- Dupré, B., Viers, J., Durand, J.-L., Polvé, M., Bénézeth, P., Vervier, P., Braun, J.-J. (1999). "Major and trace elements associated with colloids in organic-rich river waters: ultrafiltration of natural and spiked solutions." *Chemical Geology* **160**: 63–80.
- Elderfield, H. & Schultz, A. (1996). "Mid-ocean ridge hydrothermal fluxes and the chemical composition of the ocean." *Annu. Rev. Earth Planet. Sci.* **24**: 191–224.
- Elrod, V. A., Berelson, W. M., Coale, K. H., Johnson, K. S. (2004). "The flux of iron from continental shelf sediments: A missing source for global budgets." *Geophysical Research Letters* **31**, L12307, doi:10.1029/2004GL020216: 4 pp.
- Emmanuel, S., Erel, Y., Matthews, A., Teutsch, N. (2005). "A preliminary mixing model for Fe isotopes in soils." *Chemical Geology* **222**(1-2): 23-34.
- Epov, V. N., Rodriguez-Gonzalez, P., Sonke, J. E., Tessier, E., Amouroux, D., Bourgoin, L. M., Donard, O. F. X. (2008). "Simultaneous determination of species-specific isotopic composition of Hg by gas chromatography coupled to multicollector ICPMS." *Analytical Chemistry* **80**(10): 3530-3538.
- Escoube, R., Rouxel, O. J., Sholkovitz, E., Donard, O. F. X. (2009). "Iron isotope systematics in estuaries: The case of North River, Massachusetts (USA)." *Geochimica et Cosmochimica Acta* **73**: 4045-4059.
- Estrade, N., Carignan, J., Sonke, J. E., Donard, O. F. X. (2010). "Measuring Hg Isotopes in Bio-Geo-Environmental Reference Materials." *Geostandards and Geoanalytical Research* **34**(1): 79-93.
- Eyrolle, F., Benedetti, M. F., Benaim, J. Y., Février, D. (1996). "The distributions of colloidal and dissolved organic carbon, major elements, and trace elements in small tropical catchments." *Geochimica et Cosmochimica Acta* **60**(19): 3643-3656.
- Fantle, M. S. & DePaolo, D. J. (2004). "Iron isotopic fractionation during continental weathering." *Earth and Planetary Science Letters* **228**: 547-562.

Fantle, M. S. & Bullen, T. D. (2009). "Essentials of iron, chromium, and calcium isotope analysis of natural materials by thermal ionization mass spectrometry." *Chemical Geology* **258**: 50-64.

Faure, G. (1986). *Principles of isotope geology*. 2nd ed. New-York. John Wiley & Sons. 589 pp.

Fehr, M. A., Andersson, P. S., Halenius, U., Morth, C.-M. (2008). "Iron isotope variations in Holocene sediments of the Gotland Deep, Baltic Sea." *Geochimica et Cosmochimica Acta* **72**: 807-826.

Fietzke, J. & Eisenhauer, A. (2006). "Determination of temperature-dependent stable strontium isotope (Sr-88/Sr-86) fractionation via bracketing standard MC-ICP-MS." *Geochemistry Geophysics Geosystems* **7**, Q08009, doi:10.1029/2006GC001243.

Filizola, N. & Guyot, J. L. (2004). "The use of Doppler technology for suspended sediment discharge determination in the River Amazon." *Hydrological Sciences Journal-Journal Des Sciences Hydrologiques* **49**(1): 143-153.

Filizola, N. P. & Guyot, J. L. (2009). "Suspended sediment yields in the Amazon basin: an assessment using the Brazilian national data set." *Hydrological Processes* **23**(22): 3207-3215.

Fittkau, E. J. (1971). "Distribution and Ecology of Amazonian Chironomids (Diptera)." *Canadian Entomologist* **103**(3): 407-413.

Franzinelli, E. & Igreja, H. (2002). "Modern sedimentation in the Lower Negro River, Amazonas State, Brazil." *Geomorphology* **44**: 259-271.

Frei, R. & Polat, A. (2007). "Source heterogeneity for the major components of similar to 3.7 Ga Banded Iron Formations (Isua Greenstone Belt, Western Greenland): Tracing the nature of interacting water masses in BIF formation." *Earth and Planetary Science Letters* **253**(1-2): 266-281.

Fritsch, E., Allard, T., Benedetti, M. F., Bardy, M., do Nascimento, N. R., Li, Y., Calas, G. (2009). "Organic complexation and translocation of ferric iron in podzols of the Negro River watershed. Separation of secondary Fe species from Al species." *Geochimica et Cosmochimica Acta* **73**(7): 1813-1825.

Gaillardet, J., Dupré, B., Allbarède, C. J., Négrel, P. (1997). "Chemical and physical denudation in the Amazon River Basin." *Chemical Geology* **142** 141-173.

Getirana, A. C. V., Espinoza, J. C. V., Ronchail, J., Rotunno Filho, O. C. (2011). "Assessment of different precipitation datasets and their impacts on the water balance of the Negro River basin." *Journal of Hydrology* **404**(3-4): 304-322.

Gibbs, R. J. (1967). "Amazon River: Environmental Factors that control its dissolved and suspended load." *Science* **156**: 1734-1736.

Gibbs, R. J. (1972). "Water chemistry of the Amazon River." *Geochimica et Cosmochimica Acta* **36**: 1061-1066.

Gibbs, R. J. (1973). "Mechanisms of Trace Metal Transport in Rivers." *Science* **180**(4081): 71-73.

Gibbs, R. J. (1977). "Transport phases of transition-metals in Amazon and Yukon Rivers" *Geological Society of America Bulletin* **88**(6): 829-843.

Gillson, G. R., Douglas, D. J., Fulford, J. E., Halligan, K. W., Tanner, S. D. (1988). "Nonspectroscopic Interelement Interferences in Inductively Coupled Plasma Mass Spectrometry." *Analytical Chemistry* **60**: 1472-1474.

Guelke, M. & von Blanckenburg, F. (2007). "Fractionation of stable iron isotopes in higher plants." *Environmental Science & Technology* **41**(6): 1896-1901.

Guelke, M., von Blanckenburg, F., Schoenberg, R., Staubwasser, M., Stuetzel, H. (2010). "Determining the stable Fe isotope signature of plant-available iron in soils." *Chemical Geology* **277**(3-4): 269-280.

Guyot, J., Jouanneau, J., Soares, L., Boaventura, G., Maillet, N., Lagane, C. (2007). "Clay mineral composition of river sediments in the Amazon Basin." *Catena* **71**(2): 340-356.

- Halliday, A. N., Lee, D.-C., Christensen, J. N., Walder, A. J., Freedman, P. A., Jones, C. E., Hall, C. M., Yi, W., Teagle, D. (1995). "Recent developments in inductively coupled plasma magnetic sector multiple collector mass spectrometry." *International Journal of Mass Spectrometry and Ion Processes* **146/147**: 21 -33.
- Hakanson, L. & Peters, R. H. (1995). *Predictive Limnology Methods for Predictive Modelling*. Amsterdam. SPC Academic Publishing. 464 pp.
- Hezel, D. C., Needham, A. W., Armytage, R., Georg, B., Abel, R. L., Kurahashi, E., Coles, B. J., Rehkamper, M., Russell, S. S. (2010). "A nebula setting as the origin for bulk chondrule Fe isotope variations in CV chondrites." *Earth and Planetary Science Letters* **296**(3-4): 423-433.
- Hutcheon, I. D., Armstrong, J. T., Wasserburg, G. J. (1987). "Isotopic studies of Mg, Fe, Mo, Ru and W in freemdinge from Allende Refractory Inclusions" *Geochimica et Cosmochimica Acta* **51**(12): 3175-3192.
- Icopini, G. A., Anbar, A. D., Ruebush, S. S., Tien, M., Brantley, S. L. (2004). "Iron isotope fractionation during microbial reduction of iron: The importance of adsorption." *Geology* **32**: 205-208.
- Ikehata, K., Notsu, K., Hirata, T. (2008). "In situ determination of Cu isotope ratios in copper-rich materials by NIR femtosecond LA-MC-ICP-MS." *Journal of Analytical Atomic Spectrometry* **23**(7): 1003-1008.
- Ilina, S. M., Poitrasson, F., Lapitskiy, S. A., Alekhin, Y. V., Viers, J., Pokrovsky, O. S. (2013). "Extreme iron isotope fractionation between colloids and particles of boreal and temperate organic-rich waters." *Geochimica et Cosmochimica Acta*, **101**: 96-111.
- Ingri, J. & Widerlund, A. (1994). "Uptake of alkali and alkaline-earth elements on suspended iron and manganese in the Kalix River, northern Sweden." *Geochimica et Cosmochimica Acta* **58**: 5433–5442.
- Ingri, J., Malinovsky, D., Rodushkin, I., Baxter, D. C., Widerlund, A., Andersson, P., Gustafsson, Ö., Forsling, W., Öhlander, B. (2006). "Iron isotope fractionation in river colloidal matter." *Earth and Planetary Science Letters* **245**(3-4): 792-798.
- Irion, G. (1983). Clay mineralogy of the suspended load of the Amazon and of rivers in the Papua New Guinea Mainland. In: *Transport of Carbon and Minerals in Major World Rivers*. E. T. Degens, S. Kempe and H. Soliman, Mitt. Geol.-Paleontol. Inst. Univ. Hamb., SCOPE/UNED Sonderb: 482– 504.
- Irion, G. (1991). Minerals in rivers. In: *Biogeochemistry of Major World Rivers*. E. Degens , S. Kempe and J. E. Richey. Chichester, John Wiley & Sons: 265–281.
- Jickells, T. D., An, Z. S., Andersen, K. K., Baker, A. R., Bergametti, G., Brooks, N., Cao, J. J., Boyd, P. W., Duce, R. A., Hunter, K. A., Kawahata, H., Kubilay, N., laRoche, J., Liss, P. S., Mahowald, N., Prospero, J. M., Ridgwell, A. J., Tegen, I., Torres, R. (2005). "Global iron connections between desert dust, ocean biogeochemistry, and climate." *Science* **308**(5718): 67-71.
- John, S. G. & Adkins, J. F. (2010). "Analysis of dissolved iron isotopes in seawater." *Marine Chemistry* **119**(1-4): 65-76.
- Johnson, C. M. & Beard, B. L. (1999). "Correction of instrumentally produced mass fractionation during isotopic analysis of Fe by thermal ionization mass spectrometry." *International Journal of Mass Spectrometry* **193**: 87-99.
- Johnson, C. M. & Beard, B. L. (2005). "Biogeochemical Cycling of Iron Isotopes." *Science* **309**: 1025-1027.
- Johnson, C. M. & Beard, B. L. (2006). "Fe isotopes: An emerging technique for understanding modern and ancient biogeochemical cycles." *GSA Today* **16**(11): 4-10.
- Johnson, K. S., Gordon, R. M., Coale, K. H. (1997). "What controls dissolved iron concentrations in the world ocean?" *Marine Chemistry* **57**(3-4): 137-161.
- Johnson, K. S., Chavez, F. P., Friederich, G. E. (1999). "Continental-shelf sediment as a primary source of iron for coastal phytoplankton." *Nature* **398**: 697–700.
- Johnson, C. M., Skulan, J. L., Beard, B. L., Sun, H., Nealson, K. H., Brateman, P. S. (2002). "Isotopic fractionation between Fe(III) and Fe(II) in aqueous solutions." *Earth and Planetary Science Letters* **195**: 141-153.

- Johnson, C. M., Beard, B. L., Beukes, N. J., Klein, C., O'Leary, J. M. (2003). "Ancient geochemical cycling in the Earth as inferred from Fe isotope studies of banded iron formations from the Transvaal Craton." *Contributions to Mineralogy and Petrology* **144**(5): 523-547.
- Johnson, C. M., Beard, B. L., Roden, E. E., Newman, D. K., Nealson, K. H. (2004). Isotopic constraints on the biogeochemical cycling of Fe. In: *Geochemistry of non-traditional stable isotopes*. C. M. Johnson , B. L. Beard and F. Albarède. Washington, Mineralogical Society of America. **55**: 359-408.
- Johnson, C. M., Beard, B. L., Roden, E. E. (2008). "The iron isotope fingerprints of redox and biogeochemical cycling in the modern and ancient Earth." *Annual Review of Earth and Planetary Sciences* **36**: 457-493.
- Johnson, C. M., Bell, K., Beard, B. L., Shultz, A. I. (2009). "Iron isotope compositions of carbonatites record melt generation, crystallization, and late-stage volatile-transport processes." *Mineralogy and Petrology* **98**(1-4): 91-110.
- Junk, W. J. & Piedade, M. T. F. (2010). An introduction to South American wetland forests: distribution, definitions and general characterization. In: *Amazonian Floodplain Forests - Ecophysiology, Biodiversity and Sustainable Management*. W. J. Junk , M. T. F. Piedade , F. Wittmann , J. Schöngart and P. Parolin. New York, Springer Dordrecht Heidelberg London. *Ecological Studies* vol. **210**.
- Junk, W. J., Piedade, M. T. F., Wittmann, F., Scöngart, J., Parolin, P. (2010). *Amazonian Floodplain Forests - Ecophysiology, Biodiversity and Sustainable Management*. Springer. 615 pp.
- Kappler, A. & Straub, K. L. (2005). "Geomicrobiological cycling of iron." *Molecular Geomicrobiology* **59**: 85-108.
- Kappler, A., Johnson, C. M., Crosby, H. A., Beard, B. L., Newman, D. K. (2010). "Evidence for equilibrium iron isotope fractionation by nitrate-reducing iron(II)-oxidizing bacteria." *Geochimica et Cosmochimica Acta* **74**(10): 2826-2842.
- Kehm, K., Hauri, E. H., Alexander, C. M. O., Carlson, R. W. (2003). "High precision iron isotope measurements of meteoritic material by cold plasma ICP-MS." *Geochimica et Cosmochimica Acta* **67**(15): 2879-2891.
- Krayenbuehl, P. A., Walczyk, T., Schoenberg, R., von Blanckenburg, F., Schulthess, G. (2005). "Hereditary hemochromatosis is reflected in the iron isotope composition of blood." *Blood* **105**(10): 3812-3816.
- Lacan, F., Radic, A., Jeandel, C., Poitrasson, F., Sarthou, G., Pradoux, C., Freydier, R. (2008). "Measurement of the isotopic composition of dissolved iron in the open ocean." *Geophysical Research Letters* **35**(24): L24610, doi:10.1029/2008GL035841.
- Lacan, F., Radic, A., Labatut, M., Jeandel, C., Poitrasson, F., Sarthou, G., Pradoux, C., Chmeleff, J., Freydier, R. (2010). "High-Precision Determination of the Isotopic Composition of Dissolved Iron in Iron Depleted Seawater by Double Spike Multicollector-ICPMS." *Analytical Chemistry* **82**(17): 7103-7111.
- Leppard, G. G. (1992). "Size, morphology and composition of particulates in aquatic ecosystems - solving speciation problems by correlative electron-microscopy." *Analyst* **117**(3): 595-603.
- Levasseur, S., Frank, M., Hein, J. R., Halliday, A. N. (2004). "The global variation in the iron isotope composition of marine hydrogenetic ferromanganese deposits: implications for seawater chemistry?" *Earth and Planetary Science Letters* **224**: 91-105.
- Lewis , W. M. J., Hamilton, S. K., Saunders III, J. F. (1995). Rivers of Northern South America. In: *River and Stream Ecosystems*. C. E. Cushing, Elsevier. **22**: 219–256.
- Lucas, Y., Nahon, D., Cornu, S., Eyrolle, F. (1996). "Genèse et fonctionnement des sols en milieu équatorial." *C.R. Acad. Sci., Paris*, **322** (IIa): 1–16.
- Malinovsky, D., Stenberg, A., Rodushkin, I., Andren, H., Ingri, J., Öhlander, B., Baxter, D. C. (2003). "Performance of high-resolution MC-ICP-MS for Fe isotope ratio measurements in sedimentary geological materials." *Journal of Analytical Atomic Spectrometry* **18**(7): 687-695.
- Malmaeus, J. M. & Hakanson, L. (2003). "A dynamic model to predict suspended particulate matter in lakes." *Ecological Modelling* **167**(3): 247-262.

- Mandernack, K. W. (1999). "Oxygen and Iron Isotope Studies of Magnetite Produced by Magnetotactic Bacteria." *Science* **285**(5435): 1892-1896.
- Maréchal, C. & Albarède, F. (2002). "Ion-exchange fractionation of copper and zinc isotopes." *Geochimica et Cosmochimica Acta* **66**(9): 1499-1509.
- Maréchal, C. N., Télouk, P., Albarède, F. (1999). "Precise analysis of copper and zinc isotopic composition by plasma source mass spectrometry." *Chemical Geology* **156**: 251-273.
- Martin, J. H. (1992). Iron as a limiting factor in oceanic productivity. In: *Primary productivity and biogeochemical cycles in the sea*. Falkowski, P. G., Woodhead, A. D. (Eds.). New York, Plenum Publishing Corporation: 123-137.
- Martin, J. M. & Whitfield, M. (1983). The significance of the river input of chemical elements to the ocean. In: *Trace Metals in Sea Water*. C. S. Wong, E. Boyle, K. W. Bruland, J. D. Burton, E. D. Goldberg (Eds). New York, Plenum Publishing Corporation. 265-96.
- Martin, J. H. & Fitzwater, S. E. (1988). "Iron deficiency limits phytoplankton growth in the Northeast Pacific Subarctic." *Nature* **331**(6154): 341-343.
- Martin, J. H. & Gordon, R. M. (1988). "Northeast Pacific iron distributions in relation to phytoplankton productivity." *Deep-Sea Research* **34**: 267-285.
- Martin, J. H., Gordon, R. M., Fitzwater, S., Broenkow, W. W. (1989). "Vertex - Phytoplanton iron studies in the Gulf of Alaska." *Deep-Sea Research Part A - Oceanographic Research Papers* **36**(5): 649-680.
- Martin, J. H., Coale, K. H., Johnson, K. S., Fitzwater, S. E., Gordon, R. M., Tanner, S. J., Hunter, C. N., Elrod, V. A., Nowicki, J. L., Coley, T. L., Barber, R. T., Lindley, S., Watson, A. J., Vanscoy, K., Law, C. S., Liddicoat, M. I., Ling, R., Stanton, T., Stockel, J., Collins, C., Anderson, A., Bidigare, R., Ondrussek, M., Latasa, M., Millero, F. J., Lee, K., Yao, W., Zhang, J. Z., Friederich, G., Sakamoto, C., Chavez, F., Buck, K., Kolber, Z., Greene, R., Falkowski, P., Chisholm, S. W., Hoge, F., Swift, R., Yungel, J., Turner, S., Nightingale, P., Hatton, A., Liss, P., Tindale, N. W. (1994). "Testing the iron hypothesis in ecosystems of the equatorial Pacific-Ocean." *Nature* **371**(6493): 123-129.
- Martinelli, L. A., Victoria, R. L., Dematte, J. L. I., Richey, J. E., Devol, A. H. (1993). "Chemical and mineralogical composition of Amazon River floodplain sediment, Brazil." *Applied Geochemistry* **9**: 391-402.
- Martinez, J. M., Guyot, J. L., Filizola, N., Sondag, F. (2009). "Increase in suspended sediment discharge of the Amazon River assessed by monitoring network and satellite data." *Catena* **79**(3): 257-264.
- Matthews, A., Morgans-Bell, H. S., Emmanuel, S., Jenkyns, H. C., Erel, Y., Halicz, L. (2004). "Controls on iron-isotope fractionation in organic-rich sediments (Kimmeridge Clay, Upper Jurassic, Southern England)." *Geochimica et Cosmochimica Acta* **68**(14): 3107-3123.
- Maurice-Bourgoin, L., Quemarais, B., Moreira-Turcq, P., Seyler, P. (2007). "Transport, distribution and speciation of mercury in the Amazon River at the confluence of black and white waters of the Negro and Solimões Rivers." *Hydrol. Processes* **17**: 1405-1417.
- McClain, M. E. (2001). The Relevance of Biogeochemistry to Amazon Development and Conservation. In: *The Biogeochemistry of the Amazon Basin*. M. E. McClain, R. Victoria and J. E. Richey (Eds.), Cambridge University Press: 3-17.
- Meade, R. H., Nordin, J. C. F., Curtis, W. F., Costa Rodrigues, F. M., Do Vale, C. M., Edmond, J. M. (1979). "Sediments load in the Amazon River." *Nature* **278**: 161-163.
- Meade, R. H., Dunne, T., Richey, J. E., Santos, U. D., Salati, E. (1985). "Storage and remobilization of suspended sediment in the lower amazon river of Brazil." *Science* **228**(4698): 488-490.
- Meade, R. H., Raiol, J. M., Conceição, S. C., Natividade, J. R. G. (1991). "Back water effects in the Amazon River Basin." *Environ. Geol. Water Sci.* **18**(2): 105-114.
- Molinier, M., Guyot, J. L., Oliveira, E., Guimarães, V. (1996). Les régimes hydrologiques de l'Amazone et de ses affluents. In: *L'hydrologie tropicale: géoscience et outil pour le développement*. Paris, AIHS: 209-222.

- Montaser, A., Minnich, M. G., Liu, H., Gustavsson, A. G. T., Browner, R. F. (1998a). Fundamental aspects of sample introduction in ICP spectrometry. In: *Inductively Coupled Plasma Mass Spectrometry*. A. Montaser. New York, Wiley-VCH: 335-420.
- Montaser, A., Minnich, M. G., McLean, J. A., Liu, H., Caruso, J. A., McLeod, C. W. (1998b). Sample introduction in ICPMS. In: *Inductively Coupled Plasma Mass Spectrometry*. New York, Wiley-VCH: 83-264.
- Moreira-Turcq, M.F., Seyler, P., Guyot, J-L., Etcheber, H. (2003). Exportation of organic carbon from the Amazon River and its main tributaries. *Hydrological Process* **17**, 1329-1344.
- Mullane, E., Russell, S. S., Gounelle, M. (2002). Iron isotope fractionation within a differentiated asteroidal sample suite. 65th Annual Meteoritical Society Meeting. *Meteoritics & Planetary Science*, **37**, Supplement, p. A105.
- Mullane, E., Russell, S. S., Gounelle, M., Mason, T. F. D. (2003a). "Iron isotope composition of Allende and Chainpur chondrules: effects of equilibration and thermal history." *Lunar and Planetary Science Conference XXXIV*, League City, Texas. Abstract 1027.pdf.
- Mullane, E., Russell, S. S., Gounelle, M., Mason, T. F. D. (2003b). "Iron isotope composition of Allende matrix, CAIs and chondrules." *66th Annual Meteoritical Society Meeting*: abstract number 5117.
- Nabelek, P. I., Russ-Nabelek, C., Haeussler, G. T. (1992). "Stable isotope evidence for the petrogenesis and fluid evolution in the Proterozoic Harney Peak leucogranite, Black Hills, South Dakota." *Geochimica et Cosmochimica Acta* **56**(1): 403-417.
- Nascimento, N. R., Bueno, G. T., Fritsch, E., Herbillon, A. J., Allard, T., Melfi, A. J., Astolfo, R., Boucher, H., Li, Y. (2004). "Podzolisation as a deferralitization process: a study of an Acrisol-Podzol sequence derived from Palaeozoic sandstones in the northern upper Amazon Basin." *Eur. J. Soil Sci.* **55**(523–538).
- Nascimento, N. R., Fritsch, E., Bueno, G. T., Bardy, M., Grimaldi, C., Melfi, A. J. (2008). "Podzolization as a deferralitization process: dynamics and chemistry of ground and surface waters in an Acrisol - Podzol sequence of the upper Amazon Basin." *European Journal of Soil Science* **59**(5): 911-924.
- Nielsen, J. M. (1960). "The Radiochemistry of Iron." National Academy of Sciences/National Research Council. 46 pp.
- Niu, H. & Houk, R. S. (1994). "Langmuir probe measurements of the ion extraction process in inductively coupled plasma mass spectrometry-I. Spatially resolved determination of electron density and electron temperature." *Spectrochim Acta* **49B**: 1283-1303.
- Niu, H. & Houk, R. S. (1996). "Fundamental aspects of ion extraction in inductively coupled plasma mass spectrometry." *Spectrochimica Acta* **51** (Part B): 779-815.
- Nonose, N. & Kubota, M. (2001). "Non-spectral and spectral interferences in inductively coupled plasma high-resolution mass spectrometry - Part 2. Comparison of interferences in quadrupole and high-resolution inductively coupled plasma mass spectrometries." *Journal of Analytical Atomic Spectrometry* **16**(6): 560-566.
- Oliva, P., Viers, J., Dupre, B., Fortune, J. P., Martin, F., Braun, J. J., Nahon, D., Robain, H. (1999). "The effect of organic matter on chemical weathering: Study of a small tropical watershed: Nsimi-Zoetele site, Cameroon." *Geochimica et Cosmochimica Acta* **63**(23-24): 4013-4035.
- Olivares, J. A. & Houk, R. S. (1986). "Suppression of Analyte Signal by Various Concomitant Salts in Inductively Coupled Plasma Mass Spectrometry." *Analytical Chemistry* **58**: 20-25.
- Olivié-Lauquet, G., Allard, T., Benedetti, M., Muller, J. (1999). "Chemical distribution of trivalent iron in riverine material from a tropical ecosystem: a quantitative EPR study." *Water Resources Research* **33**(11): 2726-2734.
- Olivié-Lauquet, G., Allard, T., Bertaux, J., Muller, J. (2000). "Crystal chemistry of suspended matter in a tropical hydro system, Nyon Basin (Cameroon, Africa)." *Chemical Geology* **170**: 113-131.

Perez, M.A.P., Moreira-Turcq, P., Gallard, H., Allard, T., Benedetti, M. (2011). Dissolved organic matter dynamic in the Amazon basin: Sorption by mineral surfaces." *Chemical Geology* **286**: 158-168.

Perret, D., Gaillard, J. F., Dominik, J., Atteia, O. (2000). "The diversity of natural hydrous iron oxides." *Environmental Science & Technology* **34**(17): 3540-3546.

Platzner, I. T. (1997). *Modern isotope ratio mass spectrometry*. Chichester. John Wiley & Sons. 514 pp.

Poitrasson, F. (2006). "On the iron isotope homogeneity level of the continental crust." *Chemical Geology* **235**: 195-200.

Poitrasson, F. (2007). "Does planetary differentiation really fractionate iron isotopes?" *Earth and Planetary Science Letters* **256**: 484-492.

Poitrasson, F. & Freydier, R. (2005). "Heavy iron isotope composition of granites determined by high-resolution MC-ICP-MS." *Chemical Geology* **222**(1-2): 132-147.

Poitrasson, F. & Freydier, R. (2006). "Search for Fe-58 anomalies in Orgueil and Allende meteorites." *Meteoritics & Planetary Science* **41**(8): A141-A141.

Poitrasson, F., Halliday, A. N., Lee, D. C., Levasseur, S., Teutsch, N. (2003). "Iron isotope evidence for formation of the Moon through partial vaporisation." *Lunar and Planetary Science XXXIV*, League City, Texas. Abstract 1433.pdf., 2 pp.

Poitrasson, F., Halliday, A. N., Lee, D.-C., Levasseur, S., Teutsch, N. (2004). "Iron isotope differences between Earth, Moon, Mars and Vesta as possible records of contrasted accretion mechanisms." *Earth and Planetary Science Letters* **223**(3-4): 253-266.

Poitrasson, F., Levasseur, S., Teutsch, N. (2005). "Significance of iron isotope mineral fractionation in pallasites and iron meteorites for the core–mantle differentiation of terrestrial planets." *Earth and Planetary Science Letters* **234**(1-2): 151-164.

Poitrasson, F., Roskosz, M., Delpech, G., Grégoire, M., Moine, B. N. (2006). "Iron isotopes track planetary accretion or differentiation?" *Geochimica et Cosmochimica Acta* **70** (18): A498.

Poitrasson, F., Viers, J., Martin, F., Braun, J. J. (2008). "Limited iron isotope variations in recent lateritic soils from Nsimi, Cameroon: Implications for the global Fe geochemical cycle." *Chemical Geology* **253**: 54-63.

Poulton, S. W. & Raiswell, R. (2002). "The low-temperature geochemical cycle of iron: From continental fluxes to marine sediment deposition." *American Journal of Science* **302**(9): 774-805.

Pullin, M. J. & Cabaniss, S. E. (2003). "The effects of pH, ionic strength, and iron–fulvic acid interactions on the kinetics of non-photochemical iron transformations. I. Iron(II) oxidation and iron(III) colloid formation." *Geochimica et Cosmochimica Acta* **67**(21): 4067–4077.

Radambrasil (1972–1978). Levantamento de recursos naturais. Vols. 1–15. Rio de Janeiro, Departamento Nacional de Produção Mineral (DNPM), Ministério de Minas & Energia.

Richey, J., Hedges, J. I., Devol, A. H., Quay, P. D., Victoria, R., Martinelli, L., Forsberg, B. R. (1990). "Biogeochemistry of carbon in the Amazon River." *Limnol. Oceanogr.* **35**: 352–371.

Richey, J., Victoria, R., Mayorga, E., Martinelli, L., Meade, R. (2004). Integrated Analysis in a Humid Tropical Region - The Amazon Basin. In: *Vegetation, Water, Humans, and the Climate*. P. Kabat, M. Claussen, P. A. Dirmeyer, J. H. C. Gash, L. Bravo de Guenni, M. Meybeck, R. Pielke, C. J. Vörösmarty, R.W.A. Hutjes, S. Lütkemeier (Eds.). Berlin, Springer: 415-428.

Rios-Villamizar, E. A., Junior, A. F. M., Waichman, A. V. (2011). "Caracterização físico-química das águas e desmatamento na Bacia do Rio Purus, Amazônia Brasileira Ocidental " *Rev. Geogr. Acadêmica* **5**(2): 54-65.

Rodushkin, I., Stenberg, A., Andrén, H., Malinovsky, D., Baxter, D. C. (2004). "Isotopic Fractionation during Diffusion of Transition Metal Ions in Solution." *Analytical Chemistry* **76**: 2148-2151.

Roe, J., Anbar, A. D., Barling, J. (2003). "Nonbiological fractionation of Fe isotopes: evidence of an equilibrium isotope effect." *Chemical Geology* **195**(1-4): 69-85.

- Roussel, O. J. & Auro, M. (2009). "Iron Isotope Variations in Coastal Seawater Determined by Multicollector ICP-MS." *Geostandards and Geoanalytical Research* **34**(2): 135-144.
- Roussel, O., Dobbek, N., Ludden, J., Fouquet, Y. (2003). "Iron isotope fractionation during oceanic crust alteration." *Chemical Geology* **202**: 155-182.
- Roussel, O. J., Bekker, A., Edwards, K. J. (2005). "Iron isotope constraints on the Archean and Paleoproterozoic ocean redox state." *Science* **307**(5712): 1088-1091.
- Roussel, O., Shanks, W. C., Bach, W., Edwards, K. (2008a). "Integrated Fe and S isotope study of seafloor hydrothermal vents at East Pacific Rise 9-10N." *Chemical Geology* **252**: 214-227.
- Roussel, O., Sholkovitz, E., Charette, M., Edwards, K. J. (2008b). "Iron isotope fractionation in subterranean estuaries." *Geochimica et Cosmochimica Acta* **72**(14): 3413-3430.
- Russell, W. A., Papanastassiou, D. A., Tombrello, T. A. (1978). "Ca isotope fractionation on the Earth and other solar system materials." *Geochimica et Cosmochimica Acta* **42**: 1075-1090.
- Schauble, E. A. (2004). Applying stable isotope fractionation theory to new systems. In: *Geochemistry of Non-Traditional Stable Isotopes*. **55**: 65-111.
- Schauble, E. A., Rossman, G. R., Taylor Jr, H. P. (2001). "Theoretical estimates of equilibrium Fe-isotope fractionations from vibrational spectroscopy." *Geochimica et Cosmochimica Acta* **65**: 2487-2497.
- Schlesinger, W. H. (1997). *Biogeochemistry: An Analysis of Global Change*. 2nd Ed. New York, Academic Press. 588 pp.
- Schoenberg, R. & von Blanckenburg, F. (2005). "An assessment of the accuracy of stable Fe isotope ratio measurements on samples with organic and inorganic matrices by high-resolution multicollector ICP-MS." *International Journal of Mass Spectrometry* **242**(2-3): 257-272.
- Schoenberg, R. & von Blanckenburg, F. (2006). "Modes of planetary-scale Fe isotope fractionation." *Earth and Planetary Science Letters* **252**(3-4): 342-359.
- Schuessler, J., Schoenberg, R., Sigmarsdóttir, O. (2009). "Iron and lithium isotope systematics of the Hekla volcano, Iceland – Evidence for Fe isotope fractionation during magma differentiation." *Chemical Geology* **258**: 78-91.
- Senesi, N. (1992). Metal-humic substance complexes in the environment. Molecular and mechanistic aspects by multiple spectroscopic approach. In: *Biogeochemistry of Trace Metals*. D. C. Adriano (Ed.), Lewis Publishers, Boca Raton, FL, 429-496.
- Severmann, S., Johnson, C., Beard, B., McManus, J. (2006). "The effect of early diagenesis on the Fe isotope compositions of porewaters and authigenic minerals in continental margin sediments." *Geochimica et Cosmochimica Acta* **70**(8): 2006-2022.
- Severmann, S., Lyons, T. W., Anbar, A., McManus, J., Gordon, G. (2008). "Modern iron isotope perspective on the benthic iron shuttle and the redox evolution of ancient oceans." *Geology* **36**(6): 487-490.
- Severmann, S., McManus, J., Berelson, W. M., Hammond, D. E. (2010). "The continental shelf benthic iron flux and its isotope composition." *Geochimica et Cosmochimica Acta* **74**(14): 3984-4004.
- Seyler, P. T. & Boaventura, G. R. (2001). Trace elements in the mainstream Amazon River. In: *The Biogeochemistry of the Amazon Basin*. M. E. McClain, R. Victoria and J. E. Richey (Eds.), Oxford University Press: 307-327.
- Seyler, P. T. & Boaventura, G. R. (2003). "Distribution and partition of trace metals in the Amazon basin." *Hydrological Processes* **17**(7): 1345-1361.
- Sharma, M., Polizzotto, M., Anbar, A. D. (2001). "Iron isotopes in hot springs along the Juan de Fuca Ridge." *Earth and Planetary Science Letters* **194**: 39-51.
- Shreeve, W. W. (2007). "Use of isotopes in the diagnosis of hematopoietic disorders." *Experimental Hematology* **35**(4 - Suppl. 1): 173-179.

- Sioli, H. (1967). Studies in Amazonian waters. *Atlas do Simpósio sobre "Biota Amazônica"*, Rio de Janeiro. *Limnologia* **3**, 9-50
- Sioli, H. (1984). *The Amazon: Limnology and landscape ecology of a mighty tropical river and its basin*. Monographiae Biologicae **56**. H. Sioli H., J. Dumont (Eds.) Dordrecht/Boston/Lancaster. Dr. W. Junk Publishers. 763 pp.
- Sioli, H. (1991). *Amazônia: Fundamentos da Ecologia da Maior Região de Florestas Tropicais*. 3rd Ed. Petrópolis, Ed. Vozes. 74 pp.
- Skulan, J. L., Beard, B. L., Johnson, C. M. (2002). "Kinetic and equilibrium Fe isotope fractionation between aqueous Fe(III) and hematite." *Geochimica et Cosmochimica Acta* **66**: 2995-3015.
- Song, L., Liu, C.-Q., Wang, Z.-L., Zhu, X., Teng, Y., Liang, L., Tang, S., Li, J. (2011). "Iron isotope fractionation during biogeochemical cycle: Information from suspended particulate matter (SPM) in Aha Lake and its tributaries, Guizhou, China." *Chemical Geology* **280**(1-2): 170-179.
- Stallard, R. F. (1980). Major element chemistry of the Amazon River system. *Massachusetts Institute of Technology/WHOI Joint Program in Oceanography*. MA, Cambridge. PhD Thesis. 365 pp.
- Staubwasser, M., von Blanckenburg, F., Schoenberg, R. (2006). "Iron isotopes in the early marine diagenetic iron cycle." *Geology* **34**(8): 629-632.
- Tangalos, G. E., Beard, B. L., Johnson, C. M., Alpers, C. N., Shelobolina, E. S., Xu, H., Konishi, H., Roden, E. E. (2010). "Microbial production of isotopically light iron(II) in a modern chemically precipitated sediment and implications for isotopic variations in ancient rocks." *Geobiology* **8**(3): 197-208.
- Taylor, P. D. P., Maeck, R., De Bièvre, P. (1992). "Determination of the absolute isotopic composition and atomic weight of a reference sample of natural iron." *International Journal of Mass Spectrometry and Ion Processes* **121**(1-2): 111-125.
- Taylor, P. D. P., Maeck, R., Hendrickx, F., De Bikvre, P. (1993). "The gravimetric preparation of synthetic mixtures of iron isotopes." *International Journal of Mass Spectrometry and Ion Processes* **128**: 91-97.
- Teng, F. Z., Dauphas, N., Helz, R. T. (2008). "Iron isotope fractionation during magmatic differentiation in Kilauea Iki Lava Lake." *Science* **320**(5883): 1620-1622.
- Teutsch, N., von Gunten, U., Porcelli, D., Cirpka, O. A., Halliday, A. N. (2005). "Adsorption as a cause for iron isotope fractionation in reduced groundwater." *Geochimica et Cosmochimica Acta* **69**(17): 4175-4185.
- Teutsch, N., Schmid, M., Müller, B., Halliday, A. N., Bürgmann, H., Wehrli, B. (2009). "Large iron isotope fractionation at the oxic-anoxic boundary in Lake Nyos." *Earth and Planetary Science Letters* **285**(1-2): 52-60.
- Thompson, A., Ruiz, J., Chadwick, O., Titus, M., Chorover, J. (2007). "Rayleigh fractionation of iron isotopes during pedogenesis along a climate sequence of Hawaiian basalt." *Chemical Geology* **238**(1-2): 72-83.
- Turnlund, J. R. & Keyes, W. R. (1990). "Automated-analysis of stable isotopes of zinc, copper, iron, calcium and magnesium by Thermal Ionization Mass Spectrometry using double isotope-dilution for tracer studies in humans." *Journal of Micronutrient Analysis* **7**(2): 117-145.
- Vieira, L. C., Poitrasson, F., Trindade, R. I. F., Alkimim, F. F. (2010). *Iron Isotope Signature of Paleoproterozoic Banded Iron Formation from Quadrilátero Ferrífero, Minas Gerais, Brazil*. VII South American Symposium on Isotope Geology (SSAGI), Brasília, Brasil.
- Viers, J., Dupré, B., Polve, M., Schott, J., Dandurand, J. L., Braun, J. J. (1997). "Chemical weathering in the drainage basin of a tropical watershed (Nsimi-Zoetele site, Cameroon): Comparison between organic-poor and organic-rich waters." *Chemical Geology* **140**(3-4): 181-206.
- Viers, J., Dupré, B., Braun, J.-J., Deberdt, S., Angelett, B., Ndam Ngoupayou, J., Michard, A. (2000). "Major and trace element abundances, and strontium isotopes in the Nyong basin rivers Cameroon: constraints on chemical weathering processes and elements transport mechanisms in humid tropical environments." *Chemical Geology* **169**(1-2): 211-241.

- Viers, J., Oliva, P., Nonell, A., Gelabert, A., Sonke, J., Freydier, R., Gainville, R., Dupré, B. (2007a). "Evidence of Zn isotopic fractionation in a soil–plant system of a pristine tropical watershed (Nsimi, Cameroon)." *Chemical Geology* **239**(1-2): 124-137.
- Viers, J., Oliva, P., Dandurand, J.-L., Dupré, B. (2007b). "Chemical Weathering Rates, CO₂ Consumption, and Control Parameters Deduced from the Chemical Composition of Rivers." *Treatise On Geochemistry*: 1-25.
- von Blanckenburg, F. (2000). Iron isotope fractionation in soils. Goldschmidt Conference, Journal of Conference Abstracts, **5**(2): 1057. Oxford, Cambridge Publications.
- Walczyk, T. (1997). "Iron isotope ratio measurements by negative thermal ionisation mass spectrometry using FeF₄- molecular ions." *International Journal of Mass Spectrometry and Ion Processes* **161**(1-3): 217-227.
- Walczyk, T. (2004). "TIMS *versus* multicollector-ICP-MS: coexistence or struggle for survival?" *Analytical and Bioanalytical Chemistry* **378**(2): 229-231.
- Walczyk, T. & von Blanckenburg, F. (2002). "Natural iron isotope variations in human blood." *Science* **295**(5562): 2065-2066.
- Weber, K. A., Achenbach, L. A., Coates, J. D. (2006). "Microorganisms pumping iron: anaerobic microbial iron oxidation and reduction." *Nature Reviews Microbiology* **4**(10): 752-764.
- Wedepohl, K. H. (1995). "The composition of the continental crust." *Geochimica et Cosmochimica Acta* **59**(7): 1217-1232.
- Welch, S. A., Beard, B. L., Johnson, C. M., Brateman, P. S. (2003). "Kinetic and equilibrium Fe isotope fractionation between aqueous Fe(II) and Fe(III)." *Geochimica et Cosmochimica Acta* **67**(22): 4231-4250.
- Wells, M. L., Price, N. M., Bruland, K. W. (1995). "Iron chemistry in seawater and its relationship to phytoplankton: a workshop report." *Marine Chemistry* **48**: 157-182.
- Weyer, S. & Schwieters, J. B. (2003). "High precision Fe isotope measurements with high mass resolution MC-ICPMS." *International Journal of Mass Spectrometry* **226**: 355-368.
- Weyer, S. & Ionov, D. (2007). "Partial melting and melt percolation in the mantle: The message from Fe isotopes." *Earth and Planetary Science Letters* **259**(1-2): 119-133.
- Weyer, S., Anbar, A., Brey, G., Munker, C., Mezger, K., Woodland, A. (2005). "Iron isotope fractionation during planetary differentiation." *Earth and Planetary Science Letters* **240**(2): 251-264.
- Weyer, S., Anbar, A. D., Brey, G. P., Munker, C., Mezger, K., Woodland, A. B. (2007). "Fe-isotope fractionation during partial melting on Earth and the current view on the Fe-isotope budgets of the planets - (reply to the comment of F. Poitrasson and to the comment of B.L. Beard and C.M. Johnson on "Iron isotope fractionation during planetary differentiation" by S. Weyer, A.D. Anbar, G.P. Brey, C. Munker, K. Mezger and A.B. Woodland)." *Earth and Planetary Science Letters* **256**(3-4): 638-646.
- White, A. F. & Brantley, S. L. (1995). *Chemical Weathering Rates of Silicate Minerals*. A. F. White & S. L. Brantley (Eds.). P. H. Ribbe (Series Ed.). Reviews in mineralogy **31**, Mineralogical Society of America. 583 pp.
- Widerlund, A. (1996). Suspended particulate matter, sedimentation and early diagenetic processes in the Kalix River estuary, northern Sweden. Division of Applied Geology, Department of Environmental Planning and Design. Lulea, Sweden, Lulea University of Technology. PhD Thesis. 25 pp.
- Wiederhold, J. G., Teutsch, N., Kraemer, S. M., Halliday, A. N., Kretzschmar, R. (2007a). "Iron isotope fractionation in oxic soils by mineral weathering and podzolization." *Geochimica et Cosmochimica Acta* **71**(23): 5821-5833.
- Wiederhold, J. G., Teutsch, N., Kraemer, S. M., Halliday, A. N., Kretzschmar, R. (2007b). "Iron isotope fractionation during pedogenesis in redoximorphic soils." *Soil Science Society of America Journal* **71**(6): 1840-1850.
- Wiesli, R. A., Beard, B. L., Taylor, L. A., Johnson, C. M. (2003). "Space weathering processes on airless bodies: Fe isotope fractionation in the lunar regolith." *Earth and Planetary Science Letters* **216**(4): 457-465.

Williams, H. M., McCammon, C., Peslier, A. H., Halliday, A. N., Teutsch, N., Levasseur, S., Burg, J. (2004). "Iron isotope fractionation and the oxygen fugacity of the mantle." *Science* **304**: 1656-1659.

Williams, H., Peslier, A., McCammon, C., Halliday, A., Levasseur, S., Teutsch, N., Burg, J. (2005). "Systematic iron isotope variations in mantle rocks and minerals: The effects of partial melting and oxygen fugacity." *Earth and Planetary Science Letters* **235**(1-2): 435-452.

Yamaguchi, K. E., Beard, B. L., Johnson, C. M., Ohkouchi, N., Ohmoto, H. (2003). "Iron isotope evidence for redox stratification of the Archean oceans." *Geochimica et Cosmochimica Acta* **67**(18): A550-A550.

Zhao, X., Zhang, H., Zhu, X., Tang, S., Tang, Y. (2009). "Iron isotope variations in spinel peridotite xenoliths from North China Craton: implications for mantle metasomatism." *Contributions to Mineralogy and Petrology* **160**(1): 1-14.

Zhu, X. K., O'Nions, R. K., Guo, Y., Reynolds, B. C. (2000). "Secular Variation of Iron Isotopes in North Atlantic Deep Water." *Science* **287**(5460): 2000-2002.

Zhu, X. K., Guo, Y., O'Nions, R. K., Young, E. D., Ash, R. D. (2001). "Isotopic homogeneity of iron in the early solar nebula." *Nature* **412**: 311-313.

Zhu, X. K., Guo, Y., Williams, R. J. P., O'Nions, R. K., Matthews, A., Belshaw, N. S., Canters, G. W., de Waal, E. C., Weser, U., Burgess, B. K., Salvato, B. (2002). "Mass fractionation processes of transition metal isotopes." *Earth and Planetary Science Letters* **200**: 47-62.

MATERIAL ONLINE

Environmental Research Observatory (ORE) HYBAm (2012). Geodynamical, hydrological and biogeochemical control of erosion/alteration and material transport in the Amazon basin - Data on samples collection, methods and laboratory analyzes. <http://www.ore-hybam.org/index.php/eng/Tecnicas>.

Instituto Nacional de Meteorologia (2012). Banco de Dados Meteorológicos para Ensino e Pesquisa - Ministério da Agricultura, Pecuária e Abastecimento. Pluviometry data for Óbidos and Barcelos (Amazonas State). <http://www.inmet.gov.br/portal/index.php?r=bdmep/bdmep>.

ANEXOS

*Parâmetros físico-químicos e localização de amostras não
analisadas coletadas na região amazônica*

Station	lat	long	DEPTH (m)	Dates	Temp (°C ± 0.1)	Cond (µS/cm ± 1)	pH	Turbidity (NTU)	SPM (mg*L-1 ± 1%)
VÁRZEA MANACAPURU	-3.1909	-60.7728	0.5	05-10-09	31.3	10	5.0	5	7
VÁRZEA JANAUACÁ 0,45 mm ACID RINSED	-3.4879	-60.2701	0.5	07-10-09	32.8	59	7.7	15	4
VÁRZEA JANAUACÁ 0,22 mm ACID RINSED	-3.4879	-60.2701	0.5	07-10-09	32.8	59	7.7	15	10
VÁRZEA JANAUACÁ 0,22 mm NON-ACID RINSED	-3.4879	-60.2701	0.5	07-10-09	32.8	59	7.7	15	4
FOZ MADEIRA	-3.4076	-58.7849	0.5	09-10-09	31.9	77	7.2	80	36
ITACOATIARA DEPTH 1	-3.1723	-58.4074	0.5	10-10-09	30.9	61	6.8	58	31
ITACOATIARA DEPTH 2	-3.1723	-58.4074	8	10-10-09	30.3	61	6.7	n.a.	13
ITACOATIARA DEPTH 3	-3.1723	-58.4074	16	10-10-09	30.4	60	6.8	n.a.	41
ITACOATIARA DEPTH 4	-3.1723	-58.4074	24	10-10-09	30.0	61	6.9	n.a.	50
ITACOATIARA DEPTH 5	-3.1723	-58.4074	32	10-10-09	30.0	60	7.1	n.a.	46
PORTO VELHO	-8.7804	-63.9198	0.5	20-11-09	28.8	72	7.2	460	367
HUMAITÁ	-7.5263	-63.0059	0.5	22-11-09	29.5	74	7.1	320	324
BORBA	-4.3668	-59.6501	0.5	28-11-09	30.9	71	7.1	199	196
ITACOATIARA	-3.1743	-58.4060	0.5	03-12-09	30.9	80	7.3	110	104
PARINTINS	-2.5931	-56.6628	0.5	04-12-09	31.1	73	7.3	84	76
SANTARÉM DEPTH 1	-2.4438	-54.5598	0.5	07-12-09	30.6	42	7.4	92	56
SANTARÉM DEPTH 2	-2.4438	-54.5598	9	07-12-09	30.5	80	7.5	94	66
SANTARÉM DEPTH 3	-2.4438	-54.5598	18	07-12-09	30.3	79	7.4	96	64
SANTARÉM DEPTH 4	-2.4438	-54.5598	27	07-12-09	30.4	80	7.4	93	62
SANTARÉM DEPTH 5	-2.4438	-54.5598	36	07-12-09	30.6	86	7.4	93	63
Tamshyiaco RM1	-4.0099	-73.1576	0.5	10-06-10	26.7	170	7.5	263	236
Tamshyiaco RM2	-4.0104	-73.1584	0.5	10-06-10	26.7	168	7.6	268	236
Tamshyiaco center	-4.0102	-73.1593	0.5	10-06-10	26.7	168	7.6	277	226
Tamshyiaco LM2	-4.0105	-73.1609	0.5	10-06-10	26.7	168	7.6	265	224

Station	lat	long	DEPTH (m)	Dates	Temp (°C ± 0.1)	Cond (µS/cm ± 1)	pH	Turbidity NTU	SPM (mg*L-1 ± 1%)
Tamshiyaco LM1	-4.0119	-73.1622	0.5	10-06-10	26.7	166	7.6	226	149
Napo	-3.9964	-73.1695	0.5	11-06-10	26.5	41	7.1	172	159
Tabatinga	-4.2606	-69.9485	0.5	13-06-10	27.0	148	7.5	231	197
Javari	-4.3245	-70.0521	0.5	13-06-10	26.0	16	6.2	120	95
Içá	-3.1351	-68.0588	0.5	16-06-10	27.4	16	5.9	18	17
Fonte Boa	-2.4889	-66.0917	0.5	18-06-10	27.5	99	7.0	142	128
Juruá	-2.6265	-65.7981	0.5	18-06-10	27.5	63	6.7	188	139
Japurá	-3.1409	-64.7844	0.5	19-06-10	28.1	60	6.6	65	47
Tefé RM1	-3.4628	-64.4608	0.5	20-06-10	28.1	71	6.7	70	42
Tefé RM2	-3.4631	-64.4557	0.5	20-06-10	27.8	90	6.9	104	72
Tefé center	-3.4639	-64.4504	0.5	20-06-10	28.1	92	6.9	96	60
Tefé LM2	-3.4631	-64.4461	0.5	20-06-10	27.9	79	6.8	79	66
Tefé LM1	-3.4626	-64.4415	0.5	20-06-10	28.0	62	6.6	55	68
Rio Tefé	-3.3420	-64.7386	0.5	20-06-10	31.29	8	6.3	0	5
Coari Lake	-4.0544	-63.1769	0.5	21-06-10	32.9	7	6.9	0	4
Negro - Paricatuba	-3.0736	-60.2723	0.5	27-06-10	29.4	10	4.9	1	4
Foz Madeira	-3.4102	-58.7875	0.5	28-06-10	29.3	47	6.7	125	64
Itacoatiara	-3.1576	-58.4474	0.5	29-06-10	29.1	53	6.5	77	42
Parintins	-2.5926	-56.6610	0.5	30-06-10	29.5	47	6.5	43	33
Óbidos DEPTH 1	-1.9359	-55.5019	0.5	02-07-10	29.1	47	6.6	60	50
Óbidos DEPTH 2	-1.9359	-55.5019	14	02-07-10	29.2	45	6.4	92	53
Óbidos DEPTH 3	-1.9359	-55.5019	28	02-07-10	29.1	46	6.4	89	57
Óbidos DEPTH 4	-1.9359	-55.5019	42	02-07-10	29.1	46	6.4	98	43
Óbidos DEPTH 5	-1.9359	-55.5019	56	02-07-10	29.1	46	6.3	101	61

Latitude and Longitude in decimal degrees – WGS-84; SPM – suspended matter content.

Protocolos pra tratamento e análise de amostras

Laboratório de Geocronologia – UnB

LIMPEZA DE SAVILEX

(após colunas cromatográficas para purificação de Fe ou
após ataques para abertura de amostras)

Em becker de vidro:

- 1) 1 volume de água régia (= 1 volume HNO₃ + 2 volumes HCl) + 3 volumes de H₂O nanopura (obs: ácidos comerciais);
- 2) 12 h de exposição em placa aquecedora 120°C;
- 3) enxaguar com H₂O nanopura;
- 4) completar becker com H₂O nanopura;
- 5) 12 h placa 120°C;
- 6) 1 volume HCl + 3 volumes H₂O nanopura (obs: ácido comercial);
- 7) 12 h placa 120°C;
- 8) enxaguar com H₂O nanopura;
- 9) completar becker com H₂O nanopura;
- 10) 12 h placa 120°C;
- 11) secar savilex.

LIMPEZA DE TUBOS DE CENTRÍFUGA

- 1) 24h HCl 1N (obs: ácido comercial);
- 2) 24h H₂O nanopura;
- 3) secagem dos tubos.

ABERTURA DOS FILTROS DE MATERIAL EM SUSPENSÃO OU MATERIAL DISSOLVIDO

Em Savilex de 60 ml:

1) 8 ml HNO₃** + 1 ml H₂O₂ P.A. ou H₂O₂ suprapure (nesta ordem - filtro por baixo)

- Atenção: a reação pode ser forte, principalmente com H₂O₂ suprapure, portanto, seguir o passo 2;

2) descanso com tampa aberta até fim da reação;

3) 1 noite 100°C (tampa SEMI-fechada);

4) evaporar (120°C);

5) 0,2 ml HNO₃** + 1 ml HF** + 0,2 ml HCl 6M**;

6) 1 noite 100°C (tampa SEMI-fechada);

7) evaporar (120°C);

8) mudar de frascos (de 60 ml para 12 ou 7 ml, por exemplo);

9) 2 ml HCl 6M**;

10) 1 noite 100°C (tampa SEMI-fechada);

11) evaporar (120°C);

12) PARA A LEITURA ICP-MS DE MATERIAL DISSOLVIDO:

MATRIZ = 0,5 A 1 ml HCl 6M** (0,5 ml para ICP-MS e 0,5 ml para química – ICP-OES)

OU

12) PARA A LEITURA ICP-MS DE MATERIAL EM SUSPENSÃO (FILTROS):

MATRIZ = 5 ml HCl 6M** (1 ml para ICP-MS e 4 ml para química – ICP-OES)

13) fechar frascos

PURIFICAÇÃO DE FERRO EM COLUNAS CROMATOGRÁFICAS

- 1) pilar resinas das colunas gentilmente;
- 2) pipetá-las até homogeneização;
- 3) aguardar resina assentar / verificar nível correto da resina;
- 4) adicionar 5 ml HCl 6M** (~1h15);
- 5) reciclar HCl 6M dentro pote comercial descartado (para lixo – a ser reutilizado ou não pelo laboratório);
- 6) completar colunas com HCl 0,05M** (utilizar pipeta precisa, ~1h15);
- 7) 1 ml HCl 6M** (utilizar pipeta precisa, ~20min);
- 8) adicionar 0,5 ml amostra em matriz 0,5 ml HCl 6M** (proveniente da abertura dos filtros de material em suspensão ou do material dissolvido);

- 9) amostras de material dissolvido e rochas – enxaguar mais 2x o frasco de onde a amostra veio com 0,5 ml HCl 6M**;

OU

- 9) amostras de filtros de material em suspensão – acrescentar 2x 0,5 ml HCl 6M** diretamente na coluna;

- 10) 0,5 ml HCl 6M** (esperar eluir) + 1,5 ml HCl 6M ** (total 2 ml HCl 6M)
- 11) colocar savilex abaixo das colunas para coleta de Fe;
- 12) 0,5 HCl 0,05M (esperar eluir, ~10min);
- 13) 0,5 ml HCl 0,05M + 1 ml HCl 0,05N (total 1,5 ml HCl 0,05N, ~30min);
- 14) caso haja suspeita de que ainda resta ferro preso nas colunas, pode-se adicionar mais 0,5 ml HCl 0,05M para carrear o restante deste elemento;
- 15) Evaporar produto da etapa 14.

OBSERVAÇÃO IMPORTANTE: amostras de filtros de material em suspensão devem ser centrifugadas antes da etapa de colunas cromatográficas para que possíveis sólidos não sejam introduzidos nas colunas.

LIMPEZA DAS COLUNAS APÓS SUA UTILIZAÇÃO PARA PURIFICAÇÃO DE FERRO
(esperar a eluição de cada uma das etapas)

- 1) 5 ml HCl 6M**;
- 2) completar coluna com HCl 0,05M**;
- 3) lavar com H₂O nanopura;
- 4) armazenar no frasco HCl 0,05M**;

OU

- 1) retirar resina para descarte com ajuda H₂O nanopura;
- 2) armazenar colunas vazias no frasco HCl 0,05M**.

MATRIZ DAS AMOSTRAS PARA LEITURA NO MC-ICP-MS

(tratamento das amostras após evaporação final = após etapa 15 do protocolo “purificação de ferro em colunas cromatográficas”):

MATRIZ DE FILTROS DE MATERIAL EM SUSPENSÃO:

5 ml HCl 0,05M** (pipeta precisa - 4 ml para química – ICP-OES – e 1 ml para ICP-MS);

MATRIZ DE MATERIAL EM SUSPENSÃO:

0,5 ou 1 ml HCl 0,05M** (pipeta precisa. 0,5 ml para química e 0,5 ml para ICP-MS)

MATRIZ DE BRANCOS DE LABORATÓRIO E BRANCOS DE CAMPO:

0,5 ou 1 ml HCl 0,05M** (pipeta precisa. 0,5 ml para química e 0,5 ml para ICP-MS)

ATENÇÃO: o símbolo (**) indica ácidos BIDESTILADOS;

Esta seção é apresentada com a notação brasileira de numeração (1/2 = 0,5).

Lista de Comunicações, Artigos Submetidos e Publicados

2012 and 2013:

1. Submitted, February 2013: DOS SANTOS PINHEIRO, G.M., Poitrasson, F., Sondag, F., Cochonneau, G., Viera, L. C., Pimentel, M. M. **CONTRASTED TEMPORAL IRON ISOTOPIC EVOLUTION OF THE SUSPENDED MATTER FROM THE AMAZON AND NEGRO RIVERS.** *Earth and Planetary Science Letters*, Under review.
2. Accepted August 2012, **Published** 2013: DOS SANTOS PINHEIRO, G.M., Poitrasson, F., Sondag, F., Viera, L. C., Pimentel, M. M. **IRON ISOTOPE COMPOSITION OF THE SUSPENDED MATTER ALONG DEPTH AND LATERAL PROFILES IN THE AMAZON RIVER BASIN.** Special Issue on Hydrology, Geochemistry and Dynamic of South American Great River Systems, *Journal of South American Earth Sciences* **44** :35-44.
<http://dx.doi.org/10.1016/j.jsames.2012.08.001>.

Other years:

3. DOS SANTOS PINHEIRO, G.M., Poitrasson, F., Sondag, F., Viera, L. C., Martinez, J. M., Pimentel, M. M.; Distribution in space and time of iron isotopes in particulate matter from the Amazon River and its main tributaries. **4ème Réunion scientifique de l'ORE HYBAM - Hydrologie et géodynamique actuelle des bassins fluviaux sud-américains, Lima, Peru, September 2011, conference proceedings.**
4. Poitrasson, F., Viera, L. C., Seyler, P., PINHEIRO, G. M. S., Mulholland, D., Lima, B. A. F., Bonnet, M. P., Martinez, J. M., Prunier, J.; Isotope composition of iron delivered to the oceans by intertropical rivers: The Amazon River case. **Goldschmidt Conference, Prague, Czech Republic, August 2011. Mineral. Mag., 75, 1653.pdf**
5. DOS SANTOS PINHEIRO, G.M., Poitrasson, F., Sondag, F., Pimentel, M.M., Martinez, J.M., Lima, Vieira, L.C.; Composition isotopique du fer de la matière suspendue du fleuve Amazone, Brésil: méthodologie pour les mesures MC-ICP-MS et premiers résultats. **Colloque de restitution du Programme National EC2CO, CNRS-INSU, bilan quadriennal et perspectives, Toulouse, November 2010.**
6. DOS SANTOS PINHEIRO, G.M., Poitrasson, F., Sondag, F., Pimentel, M. M., Martinez, J. M., LIMA, B. A. F., Viera, L. C.; Análise isotópica de Fe em fração particulada proveniente do Rio Amazonas, região de Óbidos, Pará. **45º Congresso Brasileiro de Geologia, Belém, Brazil, October 2010, conference proceedings.**
7. DOS SANTOS PINHEIRO, G.M., Poitrasson, F., Sondag, F., Pimentel, M.M., Martinez, J.M., Lima, Vieira, L.C.; Composition isotopique du fer de la fraction particulière de l'Amazone : premiers résultats. **Journées scientifiques de l'Observatoire Midi-Pyrénées : Les isotopes non-traditionnels, nouvelle frontière en géochimie, October 2010.**
8. DOS SANTOS PINHEIRO, G.M., Poitrasson, F., Sondag, F., Viera, L. C., Pimentel, M. M., Martinez, J. M., LIMA, B. A. F. An iron isotope study of suspended matter at Óbidos, Amazon river, Brazil. **AGU Joint Assembly 10, Meeting of the Americas, Foz do Iguaçu, Brazil, August 2010, Abstract V24A-03.**
9. DOS SANTOS PINHEIRO, G.M., Poitrasson, F., Sondag, F., Pimentel, M.M., Martinez, J.M., Lima, Vieira, L.C.. Iron isotopes of suspended matter from the Amazon River, Brazil : sample preparation for MC-ICPMS and first results. **VII South American Symposium on Isotope Geology, Brasilia, July 2010, conference proceedings.**

Space and time variations on the iron isotopic composition of water suspended matter from the intertropical Amazon River and its main tributaries

Abstract

Suspended matter samples were collected during field campaigns on the Amazon, the Negro, the Solimões and the Madeira rivers. They were investigated for their iron isotope composition in order to verify the possible sources of iron and relate them to different physico-chemical parameters. The samples were collected in different locations and seasons, along depth and lateral profiles.

In white water rivers little or no fractionation occurs during the transport of iron from clastic sources (rock fragments) to the mainstream of these rivers. On the other hand, the Negro River presents negative results and the main source of organic matter and reduced iron for the Negro River black waters are podzols characteristic of this area.

It is inferred, on the basis of this study, that the Amazon River delivers to the Atlantic Ocean a slightly heavy and similar to the continental crust suspended matter iron isotopic composition ($\delta^{57}\text{Fe}_{\text{IRMM-14}} \sim 0.1\text{\textperthousand}$).

Keywords: iron isotopes, suspended matter, Amazonian rivers, intertropical zones, Amazon River.

Balanço espaço-temporal do ciclo dos isótopos de Fe no material em suspensão de águas da Bacia Intertropical do Rio Amazonas e de seus afluentes

Resumo

Amostras de material em suspensão foram coletadas em campanhas de campo nos rios Amazonas, Negro, Solimões e Madeira. Estes rios foram investigados quanto à composição isotópica de ferro, a fim de verificar as possíveis fontes deste elemento e relacioná-las com diferentes parâmetros físico-químicos. As amostras foram coletadas em diferentes locais e estações climáticas, ao longo de perfis em profundidade e laterais.

Em rios de água branca pouco ou nenhum fracionamento ocorre durante o transporte de ferro de fontes clásticas (fragmentos de rocha) para a corrente principal destes rios. Por outro lado, o Rio Negro apresenta resultados negativos e a principal fonte de matéria orgânica e ferro reduzido para as águas pretas do Rio Negro são espodossolos característicos desta área.

Infere-se, com base neste estudo, que o Rio Amazonas descarrega no Oceano Atlântico material em suspensão com composição isotópica de ferro levemente pesada, semelhante à da crosta continental ($\delta^{57}\text{Fe}_{\text{IRMM-14}} \sim 0.1\text{\textperthousand}$).

Palavras-chave: isótopos de ferro, material em suspensão, rios amazônicos, zonas intertropicais, Rio Amazonas.
